LEVEL II

12

SSI 7719-4

January 1979

BLAST UPGRADING OF EXISTING STRUCTURES

AD A066998

FINAL REPORT

DDC FILE COPY

Approved for public release;
distribution unlimited

Contract No. DCPA01-77-C-0205
Work Unit 1127G

SCIENTIFIC SERVICE INC.

79 04 ... 4

SSI

BLAST UPGRADING OF EXISTING STRUCTURES

DCPA Work Unit 1127G

SSI 7719-4

(12)

7719-4 Final Report January 1979

BLAST UPGRADING OF EXISTING STRUCTURES

Approved for public release;
distribution unlimited

This report has been reviewed in the Defense Civil Preparedness Agency and approved for publication. Approval does not signify that the contents necessarily reflect the views and policies of the Defense Civil Preparedness Agency.

prepared for

Defense Civil Preparedness Agency
Washington, D.C. 20301

Contract No. DCPA01-77-C-0205
Work Unit 1127G

Dr. Michael A. Pachuta COTR

by

B.L. Gabrielsen, G. Cuzner, R. Lindskog

Scientific Service, Inc.
1536 Maple Street
Redwood City, CA 94063

Unclassified

SECURITY CLASSIFICATION OF THIS PAGE (When Data Entered)

REPORT DOCUMENTATION PAGE	READ INSTRUCTIONS BEFORE COMPLETING FORM
1. REPORT NUMBER / 2. GOVT ACCESSION NO. 9	3. RECIPIENT'S CATALOG NUMBER
4. TITLE (and Subtitle) 6 BLAST UPGRADING OF EXISTING STRUCTURES.	5. [redacted] & PERIOD COVERED Final rep[redacted]- Aug[redacted]77-Jan[redacted]79.
	6. [redacted] 14 SSI-7719-4
7. [redacted] 10 B.L./Gabrielsen, G./Cuzner R./Lindskog	8. [redacted] NUMBER(s) 15 DCPA01-77-C-0205
9. [redacted] NAME AND ADDRESS Scientific Service, Inc./ 1536 Maple Street Redwood City, CA 94063	10. PROGRAM ELEMENT, PROJECT, TASK AREA & WORK UNIT NUMBERS Work Unit No. 1127G
11. CONTROLLING OFFICE NAME AND ADDRESS Defense Civil Preparedness Agency Washington, D.C. 20301	12. [redacted] 11 Jan[redacted]79
	13. [redacted] 278
14. MONITORING AGENCY NAME & ADDRESS(if different from Controlling Office) 12 279p.	15. SECURITY CLASS. (of this report) Unclassified
	15a. DECLASSIFICATION/DOWNGRADING SCHEDULE

16. DISTRIBUTION STATEMENT (of this Report)

Approved for public release; distribution unlimited

17. DISTRIBUTION STATEMENT (of the abstract entered in Block 20, if different from Report)

18. SUPPLEMENTARY NOTES

19. KEY WORDS (Continue on reverse side if necessary and identify by block number)

Civil Defense; concrete slab; construction; dynamic loading; prediction methodology; shoring; static loadings; structural elements; structural failure; upgrading; wood structures

20. ABSTRACT (Continue on reverse side if necessary and identify by block number)

A major facet of preparedness is the upgrading of structures to provide shelter from nuclear weapons effects. This report describes some upgrading concepts, develops practical techniques for predicting structural failure, and verifies the failure prediction methodology by comparing the analysis with structural failure/test data developed under this program and available in the literature. (over)

DD FORM 1473 1 JAN 73 EDITION OF 1 NOV 65 IS OBSOLETE

Unclassified

SECURITY CLASSIFICATION OF THIS PAGE (When Data Entered)

392 925

20 (contd)

The analyses and prediction techniques were applied to wood, steel, and concrete roof and floor specimens; and to static, dynamic, and combined loadings. The prediction methodology is founded on engineering mechanics, limit theory, and a statistical approach to failure analysis that enables realistic assessment to be made of failure probabilities based on the combined effects of statistical variation in materials, structural elements, and construction processes.

The failure prediction methodology is demonstrated experimentally for wood and reinforced concrete floor structures. Because wood systems are the most technically demanding, the wood structure examples are analyzed in "cookbook" style, with the source data reproduced in tables, and the governing probability distribution functions developed in detail for each of the various elements. The impact of significant changes in design procedures, steel grading and properties, and building codes over the years are discussed.

Wood, steel-reinforced concrete, and open-web joist floor systems were analyzed to demonstrate the failure prediction methodology for standard and upgraded systems. These were then compared with experimental data from failure tests conducted during this program and with data in the literature on open-web joist structures. Test procedures were used to develop loads equivalent to blast overpressures.

The upgrading techniques tested improved structural resistance to failure by factors of 2 to 10. The greatest improvement was developed by simple shoring. In a wood structure shored at the third points, the improvement was ten fold, and in the single shored reinforced concrete slab, the improvement was three fold. Failure loads of two concrete test specimens were predicted within 10% by the analytical techniques. Further, the concrete tests clearly indicate potential for achieving 30 to 40 psi shelter spaces in risk areas with standard concrete floor systems.

7719-4 Summary Report January 1979

BLAST UPGRADING
OF
EXISTING STRUCTURES

prepared for

Defense Civil Preparedness Agency
Washington, D.C. 20301

Contract No. DCPA01-77-C-0205
Work Unit 1127G

Dr. Michael A. Pachuta COTR

by

B.L. Gabrielsen, G. Cuzner, R. Lindskog

Scientific Service, Inc.
1536 Maple Street
Redwood City, CA 94063

SUMMARY REPORT

A major facet of preparedness is the upgrading of structures to provide shelter from nuclear weapons effects. This report describes some upgrading concepts, develops practical techniques for predicting structural failure, and verifies the failure prediction methodology by comparing the analysis with structural failure test data developed under this program and available in the literature.

The analyses and prediction techniques are applied to wood, steel, and concrete roof and floor specimens; and to static, dynamic, and combined loadings. The prediction methodology is founded on engineering mechanics, limit theory, and a statistical approach to failure analysis that enables realistic assessment to be made of failure probabilities based on the combined effects of statistical variation in materials, structural elements, and construction processes.

The failure prediction methodology is demonstrated experimentally for wood and reinforced concrete floor structures. Because wood systems are the most technically demanding, the wood structure examples are analyzed in "cookbook" style, with the source data reproduced in tables, and the governing probability distribution functions developed in detail for each of the various elements. Little appreciated practical problems that face the professional structural analyst with responsibility for developing rating and upgrading techniques for structures are discussed. These include the impact of significant changes in design procedures, steel grading and properties, and building codes over the years, and analytical techniques to combine time-dependent static load resistance of a wood structure (e.g., covered with dirt for fallout protection) with the dynamic overpressure resistance.

Wood, steel-reinforced concrete, and open-web joist floor systems were analyzed to demonstrate the failure prediction methodology for standard and upgraded systems. These were then compared with experimental data from failure tests on 4 ft x 16 ft specimens of wood floors and steel reinforced concrete slab specimens tested during this program, and with data in the literature on open-web joist structures. Test procedures were used to develop loads equivalent to blast overpressures.

The upgrading techniques that were tested improved structural resistance-to-failure by factors of 2 to 10 over the base case. The greatest improvement was developed by simple shoring. In a wood structure shored at the third points, the improvement was ten-fold and in the single shored reinforced concrete slab, the improvement was three-fold. Failure loads of two concrete test specimens were predicted by the analytical techniques within 10%.

The methodology developed promises to provide a potent analytical tool for quantitative assessment of failure loads before and after upgrading. Hence it will provide a means for ranking upgrading techniques for experimental evaluation and incorporation into a manual.

Further, the concrete tests clearly indicate potential of achieving 30 to 40 psi shelter spaces in risk areas with standard concrete floor systems.

Table of Contents

Table of Contents (contd)

List of Figures

List of Figures (contd)

List of Figures (contd)

List of Figures (contd)

List of Tables

List of Tables (contd)

Conversion Factors for U.S. Customary
to Metric (SI) Units of Measurement

To convert from:	To:	Multiply by:
inch	meter (m)	2.540×10^{-2}
foot	meter (m)	0.3048
yard	meter (m)	0.9144
square inch	meter^2 (m^2)	6.452×10^{-4}
square foot	meter^2 (m^2)	9.290×10^{-2}
pound	kilogram (kg)	0.4536
pounds per linear foot (PLF)	newtons per meter (N/m)	14.5939
kip	newton (N)	4.448×10^3
kips per foot	kilonewtons per meter	14.5932
pressure (psi)	pascal (Pa)	6.894×10^3
pounds per square foot (psf)	pascal (Pa)	47.88
ksi	pascal (Pa)	6.894×10^6
kips per square foot (KSF)	pascal (Pa)	4.788×10^3
inch-pounds	meter-newtons	0.1129848
inch-pounds per foot	meter-newtons/meter	0.370682
degrees Fahrenheit	degrees Celsius	$(t_{°F} - 32)/1.8$

Acknowledgements

This report describes some upgrading concepts designed to provide shelter from nuclear weapons effects, develops practical techniques for structural failure prediction and attempts to substantiate the concepts and prediction by test. The authors wish to take this opportunity to thank all those involved in completing this project. We particularly want to thank Mr. Chuck Wilton for his contributions to overall project direction; Messrs Malcolm Koch, Don McCarter, and Fred Ehat for their tireless efforts during the testing; and the secretarial staff, Mmes Larue Wilton, Evelyn Kaplan, and Maureen Ineich for their patience as well as their talents. A special thanks to Mr. Andy Longinow of IITRI for his thorough and helpful technical review.

The aid and assistance of Dr. Michael A. Pachuta and Mr. George Sisson of the Defense Civil Preparedness Agency is also gratefully acknowledged.

Section 1
INTRODUCTION

Current Defense Civil Preparedness Agency policy for protection of the population from combined nuclear weapons effects involves: 1) Evacuation of the major portion of the population to low risk areas where only fallout protection would be required, and 2) Protection of a much smaller contingent of key workers, who would remain behind, from blast, fire, and fallout. This policy, termed "Crisis Relocation," presumes that a period of crisis buildup will precede any future conflict, allowing a brief period of a few days for evacuation and upgrading of existing shelter spaces.

The objective of this research program was to develop analytical techniques for predicting the upgraded strengths of structural elements while developing and testing upgrading techniques. Primary emphasis in this program was on wood floors and roof systems with effort also devoted to concrete floors and steel open web joist supported roof systems.

The overall objective of the DCPA-sponsored research in this area, of which this program was a part, is to supply data for a manual* which will allow personnel (who are not normally skilled in structural dynamics and blast effects) to quickly analyze existing structures for suitability as shelters and to implement the necessary upgrading measures.

Previous work in this area has concentrated heavily on wall systems (Ref. 1) and has led to the development of the wall failure matrix shown in Figs. 1-1 and 1-2 and the survival pressure matrix in Table 1-1. With

* Now being developed at SSI under Contract No. DCPA01-78-C-0215.

the exception of work at Stanford Research International (Refs. 2 and 3) and work conducted at Waterways Experiment Station (Refs. 4 and 5) and this program, very little has been done in the area of failure prediction and upgrading of existing floor and roof systems.

To give an indication of the magnitude of the problem, a candidate list of floor systems* which could be of interest as key worker and host area shelters is presented in Table 1-2. It should be noted that almost any of the floor systems listed in this table can also be a roof system, which would be of interest for host area fallout shelter purposes. A brief listing of other roof systems which may be of interest is presented in Table 1-3. To indicate the status of preliminary work which has been done on both these floor and roof systems, the references included on these tables indicate either failure analysis or upgrading work. Items marked with an "X" indicate work which has been conducted during this program. It is obvious, however, that a number of cases still need to be investigated.

The remainder of the report is organized as follows:

Section 2 - Discussion of wood floor test program.
Section 3 - Discussion of concrete floor test program.
Section 4 - Development of production methods matrix for wood structures and comparison with test data.
Section 5 - Analysis work on open-web joist systems.
Section 6 - Summary and conclusions.
Appendix A - Presents the construction details, test geometries, and data for the basic wood floor tests.

* This list was developed principally by Dr. Michael Pachuta of DCPA.

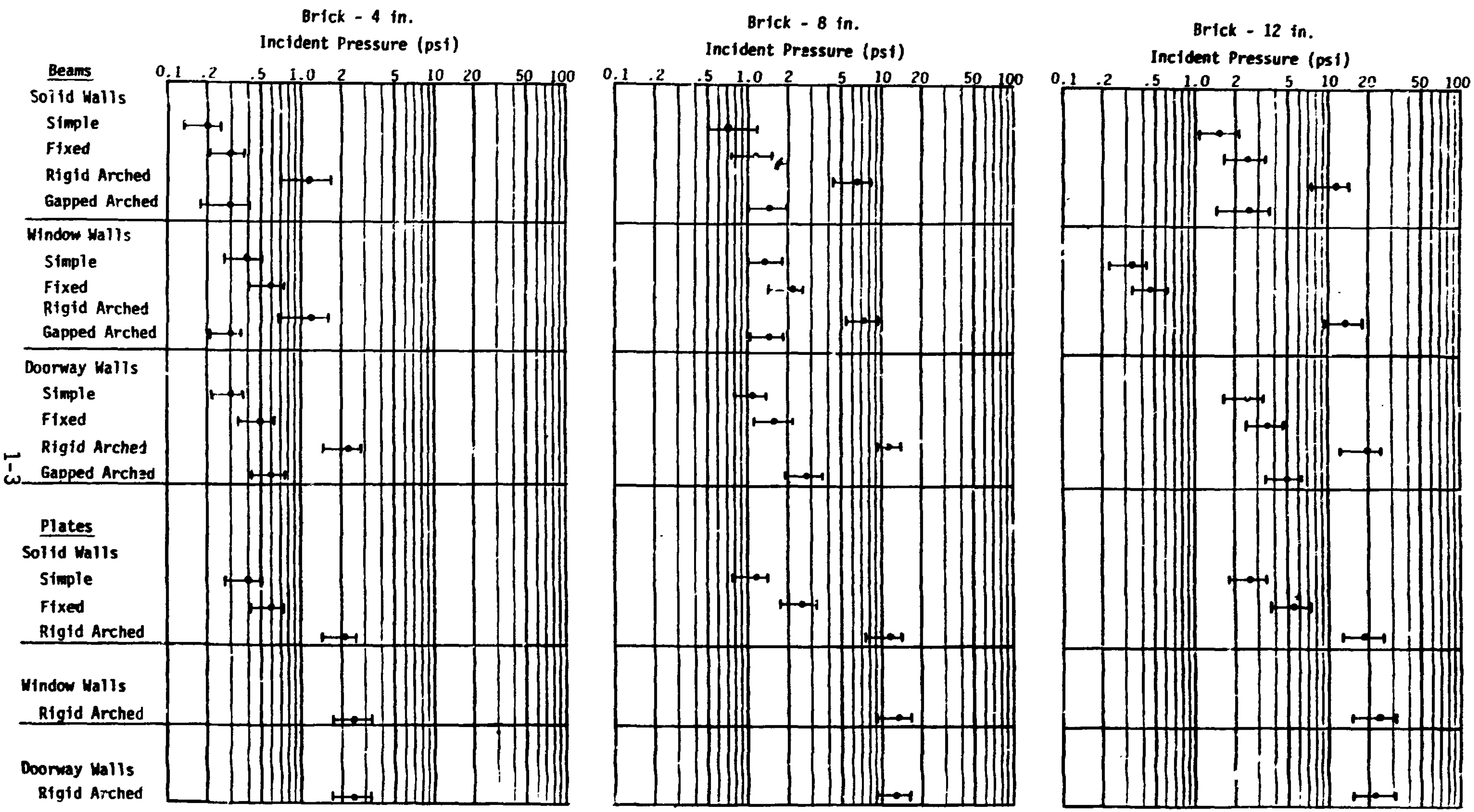

Fig. 1-1. Failure Pressure Chart —— Brick Walls.

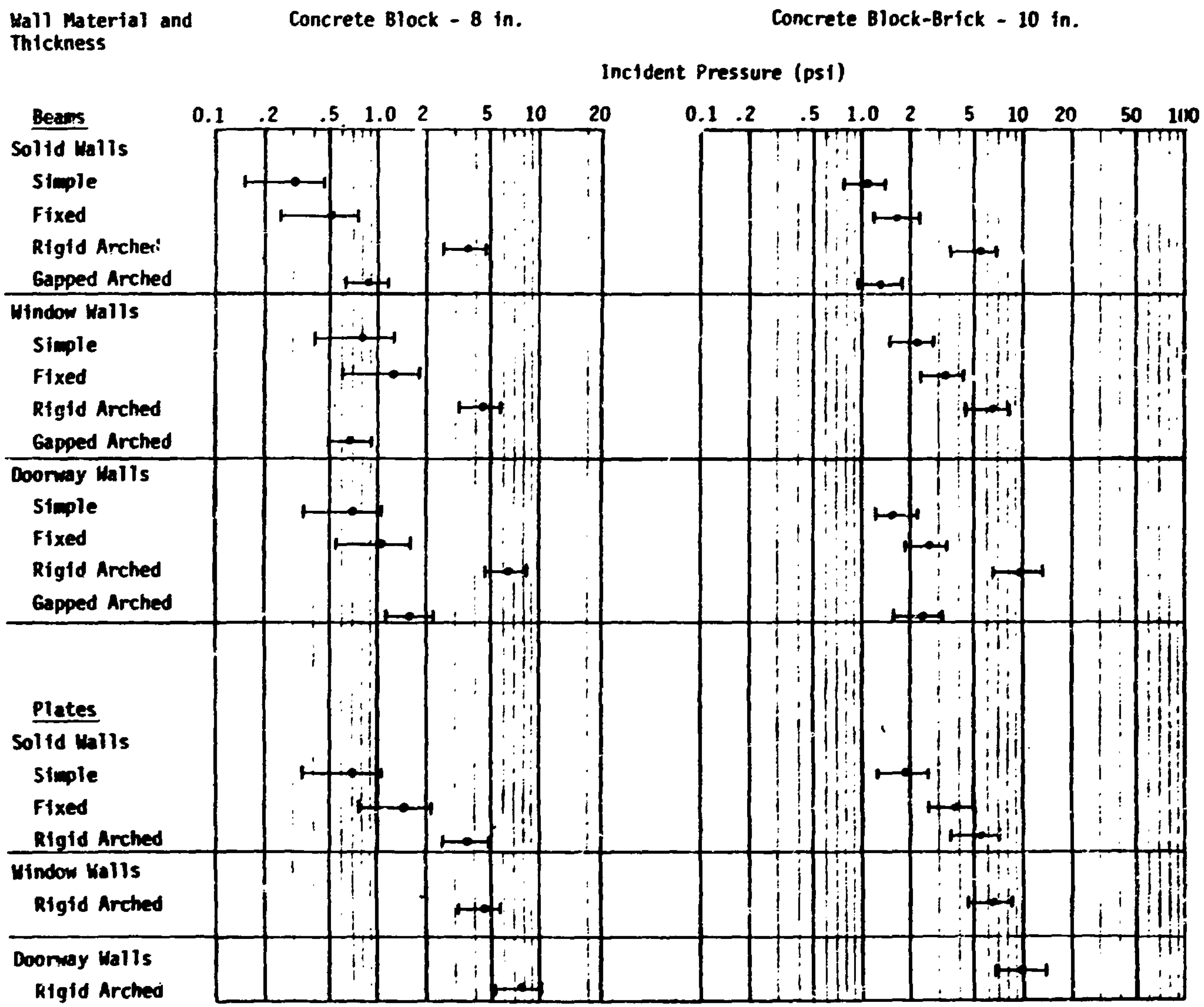

Fig. 1-2. Failure Pressure Chart —— Concrete Block and Composite Brick-Concrete Block Walls.

Table 1-1. Survival Pressure Matrix

Incident Overpressures at which 90% of Walls Will Survive
(all tabulated values are in psi)

Wall Material and Thickness / BEAMS	Brick			Concrete Block	Composite Concrete Block/ Brick
	4-in.	8-in.	12-in.	8-in.	10-in.
Solid Walls					
Simple	0.1	0.4	1.0	0.1	0.7
Fixed	0.2	0.7	1.4	0.2	1.0
Rigid Arched	0.8	4.3	7.7	2.6	3.7
Gapped Arched	0.2	1.1	1.9	0.6	0.9
Window Walls					
Simple	0.2	0.8	1.9	0.4	1.3
Fixed	0.4	1.3	2.9	0.5	2.0
Rigid Arched	0.8	5.3	9.8	3.2	4.5
Gapped Arched	0.3	0.6	2.5	0.8	1.3
Doorway Walls					
Simple	0.2	0.7	1.5	0.3	1.0
Fixed	0.3	0.4	2.3	0.5	1.6
Rigid Arched	1.5	7.7	14.0	4.6	6.7
Gapped Arched	0.4	2.0	3.5	1.2	1.7
PLATES					
Solid Walls					
Simple	0.2	0.7	1.6	0.3	1.1
Fixed	0.4	1.5	3.4	0.6	2.3
Rigid Arched	1.5	7.7	13.3	2.6	3.7
Window Walls					
Rigid Arched	1.8	9.3	17.1	3.2	4.5
Doorway Walls					
Rigid Arched	1.8	9.2	16.8	4.6	6.7

Table 1-2. List of Floor Systems

	Failure[1)]	Upgrading[2)]
1. Wood Floor Systems		
A. Joist with plywood or board subflooring	X	X
B. Post and beam with plywood or tongue and groove board subflooring	X	
C. Open web steel joists with plywood or board subflooring	X (Ref. 4)	X (Ref. 4)
2. Concrete Floor Systems		
A. Flat plate - concrete frame	Ref. 5	
B. Flat plate - steel frame		
C. Flat slab - concrete frame	Ref. 5	
D. Flat slab - steel frame		
E. Two-way slab - concrete frame	Ref. 5	
F. Two-way slab - steel frame		
G. One-way slab - concrete frame	X	X
H. One-way slab - steel frame		
I. Pan slab (one-way and two-way) - concrete frame		
J. Pan slab (one-way and two-way) - steel frame		
K. Pre-cast slab (one-way and two-way) - steel frame		
L. Pre-cast slab - steel frame		
M. Prestressed slab - concrete frame		
N. Prestressed slab - steel frame		
O. Slab on steel decking - steel beam support		
P. Slab on steel decking - open-web joist support		
Q. Post-tensioned concrete slab - concrete frame		
R. Post-tensioned concrete slab - steel frame		

1) Refer to reports that contain failure analysis.
2) Refer to reports that contain upgrading analysis.

Table 1-3. List of Additional Roof Systems

		Failure[1]	Upgrading[2]
1.	Wood truss with plywood or board decking	Ref. 4	
2.	Steel truss with plywood or board decking		
3.	Laminated wood with plywood or tongue and groove decking		
4.	Wood truss with corrugated steel roofing		
5.	Steel truss with corrugated steel roofing		
6.	Wood beam with corrugated steel roofing.		
7.	Steel beam with corrugated steel roofing.		
8.	Space steel truss with plywood decking		
9.	Space steel truss with metal deck		
10.	Space steel truss with metal deck and concrete slab		

1) Refer to reports that contain failure analysis.

2) Refer to reports that contain upgrading analysis.

Section 2
WOOD FLOOR TESTS

INTRODUCTION

The wood floor test series conducted at San Jose State by Scientific Service were intended to accomplish several goals. These goals were: first to establish base-line data to correlate tests conducted by the Waterways Experiment Station (Ref.1) ; second, to provide data to help establish a failure prediction theory for timber structures; and third, to demonstrate several upgrading options. Another item of major importance in this program was to provide a test loading sufficiently rapid to avoid the necessity of blast testing every form of structural upgrading technique. The test data indicate simulation of very rapid loading nearly equivalent to blast loading has been accomplished, because the responses of the floor systems tested were within 5% of those for the most rapid loading achievable: a step loading from a blast itself. In Section 4, considerable effort was made to demonstrate that the time effects of loading were approached semi-logarithmically. Hence, typical static loading tests conducted over a period of 5 to 8 min show a strength increase of 1.6 as compared with the upper bound increase in strength of 2.0 for the fastest possible loading. For the test loadings used in this program, typical failure, or peak load, times were a few seconds and resulted in a 1.95 strength increase, or 95% of the potential strength increase indicative of very rapid loadings such as blast loading. These results compare favorably with data found in Ref. 6 (Technical Report 573, "Dynamic Properties of Small Clear Specimens of Structural Grade Timber," by the Naval Civil Engineering Laboratory at Port Hueneme, California). Since the tests indeed approximate a blast load, it is felt that it is perfectly justified in putting an overpressure equivalent on the test values for the various test specimens.

A series of eleven tests on base case and upgraded floor systems were conducted. The wood floor systems used in this program were typical of floor systems found in residential and commercial structures throughout the U.S. and were 16 ft long, 4 ft wide and were constructed of three 2-in. x 10-in. joists covered with 3/4 in. plywood and 3/8 in. particle board underlayment. Construction details of the basic floor are presented in Figs. 2-1 through 2-3.

Table 2-1 is a summary of the eleven tests performed on the various floor systems and the actual measured loads and equivalent overpressures. Table 2-2 presents the average values from Table 2-1. A brief description of the test program and the dynamic response data are presented at the end of this section. The basic data including pre- and post-test photograpns for each of the tests are presented in Appendix A.

From the work in Section 4, it was found that the Group 1 (base case specimens Nos. 1 and 4) and Group 2 (specimens 3 and 6, with 2 x 6 flanges glued to the bottom of the joists) had average values very near the predicted or theoretical average value for the basic material. This is implicit in Table 2-1, if the averages are calculated for each particular grouping. That is, Group 1, the base case consisting of floors Nos. 1 and 4 had an average load of 195 lb/sq ft, which is an equivalent overpressure of 1.35 psi. Group 2, the 2 x 10 joist with 2 x 6 flanges glued to the bottom, had an average load of 391 psf, or a blast equivalent of 2.72 psi. Group 3, consisting of specimens 5 and 9, had an average strength of 467 lb/sq ft or 3.25 psi. Group 4 (specimen 10), the base case floor system with a single shoring spaced at the center, had an average of 1,130 lb/sq ft, or an equivalent 7.85 psi overpressure resistance. It is noted that this value is 5.81 times the base case with no shores. Theoretically one would expect a maximum of 6 times the force in a completely plastic system. Based on this one would expect the double shore situation, Group 5 representing specimen No. 2, would have an increase in strength of approximately 12-fold over the base case, or a load of 2,333 lbs/sq ft, which is equivalent to 16.2 psi. As can be seen in

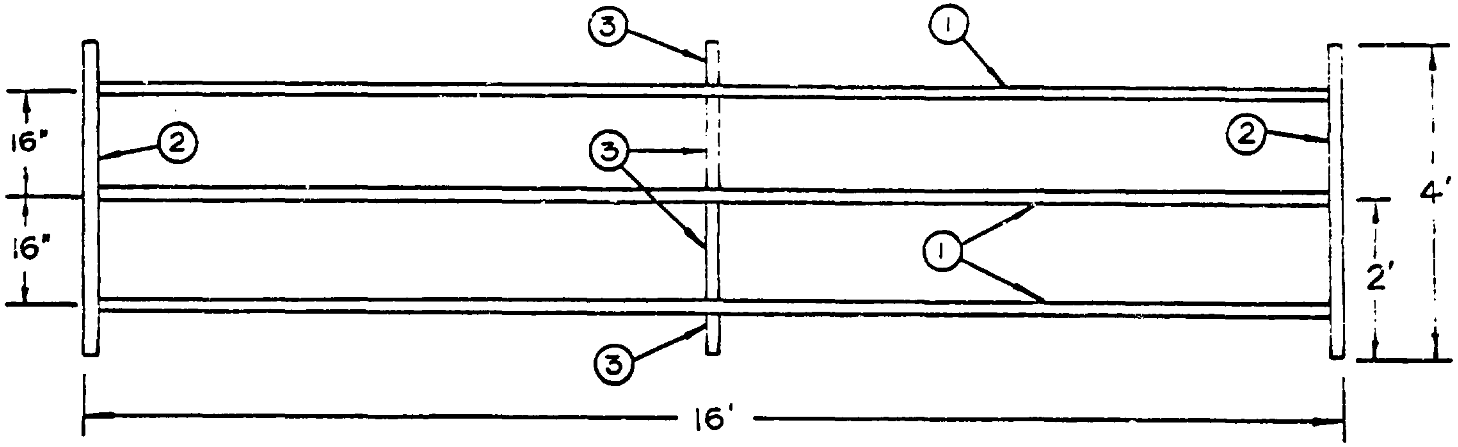

(1) 2" x 10" x 15'9" JOIST ON 16" CENTERS

(2) 2" x 10" x 4' HEADER

(3) 2" x 10" BLOCKING

ALL FRAMING MATERIAL IS:
- DOUGLAS FIR
- SELECT STRUCTURAL

HEADERS NAILED TO JOISTS WITH 3 16-d COMMON NAILS / JOIST

BLOCKING NAILED TO JOISTS WITH EITHER:
(a) 2-16-d COMMON NAILS (if nailed)
(b) 3-16-d COMMON NAILS (if toenailed)

Fig. 2-1. Framing Detail for All Floor Panels.

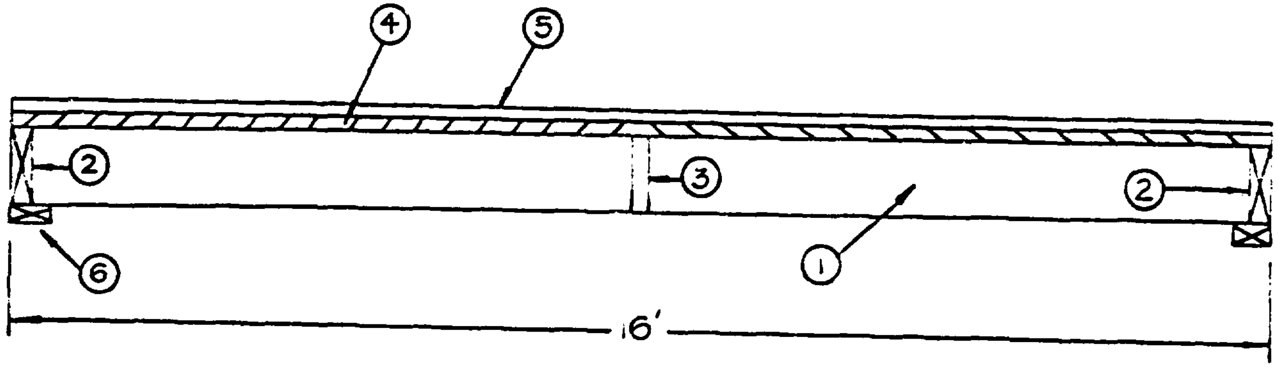

1. 2" x 10" x 15'9" JOIST
2. 2" x 10" x 4' END BLOCK
3. 2" x 10" BLOCKING
4. 3/4" 4'x8' PLYWOOD SUBFLOOR (C-D EXT)
5. 3/8" PARTICLE BOARD
6. 2" x 4" x 4' SILL

Fig. 2-2. Construction Details for Floor Panels 1 and 4.

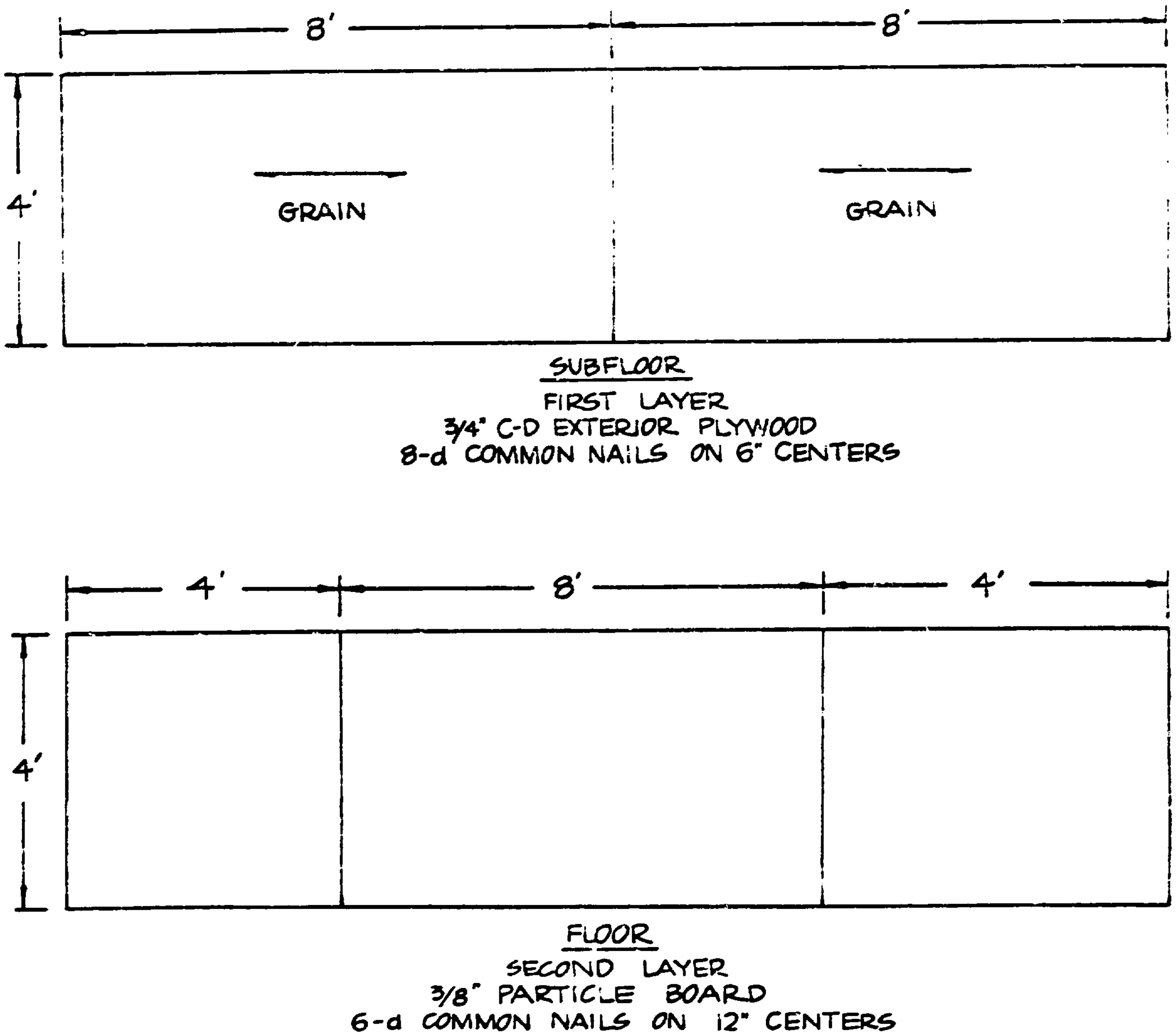

Fig. 2-3. Flooring Detail for All Floor Panels.

Table 2-1. Wood Floors - Summary of Test Data

Group	Specimen No.	Hardening Technique	W_{Peak} (KSF)	t_{Peak} (seconds)	F_b (psi)	P (psi)
1	1	None	0.166	0.8	3,973	1.15
	4		0.224	1.28	5,362	1.56
2	3	2 x 6 glued to bottom of joists	0.310	2.9	4,210	2.15
	6		0.472	3.0	6,410	3.28
3	5	2 layers of plywood on bottom	0.479	20.0	--	3.33
	9		0.456	8.5	--	3.17
4	10	Shores (single)	1.13	4.5	--	7.85
5	2	Shores (double)	1.47	2.25	--	10.21
6	7	King-Post	0.411	6.0	--	2.85
	8	"	0.636	26.0	--	4.42
	11	"	0.527	8.5	--	3.66

Note: Dynamic response curves for each of these tests are at the end of this chapter.

Table 2-2. Overpressure Capability (Average Value)

Group	Case	Load (Average)	Equivalent O.P.
1	Base Case - 1 and 4	195 psf	1.35 psi
2	2 x 6 Glued - 3 and 5	391 psf	2.72 psi
3	Plywood - 5 and 9	467 psf	3.25 psi
4	Single Shore - 10	1,130 psf	7.85 psi
5	Double Shore* - 2	2,333 psf	16.20 psi
6	King-Post - 7, 8, and 11	525 psf	3.64 psi

* Estimated on a first cycle failure mode.

Table 2-1, specimen 2 had an actual test load of 1,470 lb/sq ft or 10.2 psi equivalent overpressure. It is interesting to note that specimen 2 was loaded to a level of approximately 10 psi six times. On the sixth loading there was considerable crushing near the supports and eventually one joist failed on the first span. This repeated loading occurred because original programming of the load controller did not allow for sufficient load to fail the structure. The sixth group, the king post truss group, exhibited an average strength of 525 psf, or 6.64 psi overpressure equivalent. Based on the consistency of the test data , it appears that these values represent the average to be expected from a floor system of this type, i.e., Douglas Fir Select Structural 2 x 10's at 16 inches center- to-center and 16 ft spans.

In the DCPA Crisis Relocation philosophy where people move to host areas, it will be necessary to upgrade the fallout protection of basements covered with floor systems such as described in the previous two tables. When floor systems are covered with soil, the response is different from that when subjected to a blast load. Table 2-3 is a summary of the maximum load bearing capabilities (based on the averages) for each of the floor systems tested in groups 1 through 6 under an assumed load duration of two weeks (e.g., a soil loading). In Section 4 it is shown that timber displays a strength twice as great for response to a blast type load than for a long-term load (10 years). A two-week load, of course, falls between these time limits. In particular, for a two-week loading, timber displays strengths that are 1.2 times as great as the ten-year (normal) loading. In other words, the floor systems subjected to a loading for two weeks would appear only 60% as strong as those tested at blast equivalence. This is implicit in Table 2-3. For example, the base case (Group 1, Table 2-1) would have an average strength of only 117 psf when subjected to a two-week soil type loading, instead of 195 psf. Table 2-4 is an illustration of a combined situation, that is, where the building would have 1 foot of soil placed on the floor for fallout protection and, in addition, be subjected to a blast load. In this case, soil loads must be less than the strengths shown in Table 2-3, and the difference between Table 2-2 and

Table 2-3. Soil Load Capability (Average Value)
(Two Week Loading)

Group	Soil Load	Depth*
1	117 psf	14 inches
2	234 psf	28 inches
3	280 psf	34 inches
4	678 psf	81 inches
5	1,300 psf	168 inches
6	315 psf	38 inches

* Assumes 100 lb/ft^3 soil.

Table 2-4. Soil Load Plus Blast

Group	Soil Load (psf)	Blast Load (psf)	(psi)
1	100	95	0.7
2	100	291	2.0
3	100	367	2.5
4	100	1,030	7.2
5	100	2,233	15.2
6	100	425	3.0

Table 2-4 values define the initial capability to resist blast loads, while the differences between Table 2-3 and 2-4 values define the capability to resist blast loads at two weeks. For example, for Case 1, there is a blast resistance of 95 psf left "immediately" after placing a 100 lb soil load on it, while two weeks later it will be 34 psf. An additional observation is that if one were to put 200 psf on this floor system, it would have, in all probability, collapsed, as it has a soil resistance of only 117 psf. Note that all other floor systems, however, would have some residual strength. A soil load requirement of 300 psf would eliminate case 1, 2, 3, and leave only 4, 5, and 6 with any ability to resist blast. In fact, the first three would , in all likelihood, collapse with a 300 psf soil load, even though Nos. 2 and 3 could resist a 300 psf blast load.

The goal of this section and Section 4 is to evolve a very simple, straightforward method to be put in a manual from which a practicing engineer, or possible even a shelter manager, could determine upgrading schemes. To illustrate, Table 2-5, extracted from Ref. 7(1976 Uniform Building Code) gives the allowable spans in floor systems. For example, the floor system considered in this report was designed for a 40 lb/sq ft live load, 10 psf dead load, and if the table is consulted (for 2 x 10's, 16 in. centers, and a 16-ft span), it is noted that the material is at least 1,200 psi in strength and has a modulus of elasticity of better than 1.5 million. Hence, by merely inspecting a building, that is, measuring the depth of the joist and the spans and their spacing, the minimum material specifications could be determined. Then it is envisioned that another table, similar in nature, would tell the engineer or shelter manager the strength developed by placing a shore at the mid-point or third-point, etc. Of course, before these tables can be constructed, it is necessary to establish reasonable criteria; that is, acceptable probabilities of failure for systems and further, all the various fixes must be evaluated and carefully designed so that they are easy to install properly and effectively.

Table 2-5. Allowable Spans for Floor Joists, 40 lbs per sq ft Live Load
(from 1976 Uniform Building Code, Table No. 25-T-J-1)

DESIGN CRITERIA: Deflection - For 40 lbs. per sq. ft. live load. Limited to span in inches divided by 360. Strength - Live load of 40 lbs. per sq. ft. plus dead load of 10 lbs. per sq. ft. determines the required fiber stress value.

JOIST SIZE (IN)	SPACING (IN)	Modulus of Elasticity, "E", in 1,000,000 psi													
		0.8	0.9	1.0	1.1	1.2	1.3	1.4	1.5	1.6	1.7	1.8	1.9	2.0	2.2
2x6	12.0	8-6 720	8-10 780	9-2 830	9-6 890	9-9 940	10-0 990	10-3 1040	10-6 1090	10-9 1140	10-11 1190	11-2 1230	11-4 1280	11-7 1320	11-11 1410
	16.0	7-9 790	8-0 860	8-4 920	8-7 980	8-10 1040	9-1 1090	9-4 1150	9-6 1200	9-9 1250	9-11 1310	10-2 1360	10-4 1410	10-6 1460	10-10 1550
	24.0	6-9 900	7-0 980	7-3 1050	7-6 1120	7-9 1190	7-11 1250	8-2 1310	8-4 1380	8-6 1440	8-8 1500	8-10 1550	9-0 1610	9-2 1670	9-6 1760
2x8	12.0	11-3 720	11-8 780	12-1 830	12-6 890	12-10 940	13-2 990	13-6 1040	13-10 1090	14-2 1140	14-5 1190	14-8 1230	15-0 1280	15-3 1320	15-9 1410
	16.0	10-2 790	10-7 850	11-0 920	11-4 980	11-8 1040	12-0 1090	12-3 1150	12-7 1200	12-10 1250	13-1 1310	13-4 1360	13-7 1410	13-10 1460	14-3 1550
	24.0	8-11 900	9-3 980	9-7 1050	9-11 1120	10-2 1190	10-6 1250	10-9 1310	11-0 1380	11-3 1440	11-5 1500	11-8 1550	11-11 1610	12-1 1670	12-6 1780
2x10	12.0	14-4 720	14-11 780	15-5 830	15-11 890	16-5 940	16-10 990	17-3 1040	17-8 1090	18-0 1140	18-5 1190	18-9 1230	19-[illegible] 1280	19-5 1320	20-1 1410
	16.0	13-0 790	13-6 850	14-0 920	14-5 980	14-11 1040	15-3 1090	15-8 1150	16-0 1200	16-5 1250	16-9 1310	17-0 1360	17-4 1410	17-8 1460	18-3 1550
	24.0	11-4 900	11-10 9[illegible]0	12-3 1050	12-8 1120	13-0 1190	13-4 1250	13-8 1310	14-0 1380	14-4 1440	14-7 1500	14-11 1550	15-2 1610	15-5 1670	15-11 1780
2x12	12.0	17-5 720	18-1 780	18-9 830	19-4 890	19-11 940	20-5 990	21-0 1040	21-6 1090	21-11 1140	22-5 1190	22-10 1230	23-3 1280	23-7 1320	24-5 1410
	16.0	15-10 790	16-5 860	17-0 920	17-7 980	18-1 1040	18-7 1090	19-1 1150	19-6 1200	19-11 1250	20-4 1310	20-9 1360	21-1 1410	21-6 1460	22-2 1550
	24.0	13-10 900	14-4 980	14-11 1050	15-4 1120	15-10 1190	16-3 1250	16-8 1310	17-0 1380	17-5 1440	17-9 1500	18-1 1550	18-5 1610	18-9 1670	19-4 1780

✱

NOTES:
(1) The required extreme fiber stress in bending, F_b, in pounds per square inch is shown below each span.
(2) Use single or repetitive member bending stress values (F_b) and modulus of elasticity values (E), from Tables Nos. 25-A-1, and 25-A-2.
(3) For more comprehensive tables covering a broader range of bending stress values (F_b) and Modulus of Elasticity values (E), other spacing of members and other conditions of loading, see U. B. C. Standard No. 25-21.
(4) The spans in these tables are intended for use in covered structures or where moisture content in use does not exceed 19 percent.

TEST RESULTS

For all specimens except the first base case, a six-point load system was used with the load points symmetrically spaced along the span to approximate a uniform load (Fig. A-10, Appendix A). (A three-point loading was used in the first test as shown in Fig. A-6.)

As the load increased, a continuous recording of the applied force from each hydraulic actuator was obtained. The recording was graduated with time lines spaced 0.1 seconds apart. At the same time, the output from an LVDT monitoring the deflection of the floor was recorded alongside the applied force trace.

At each 0.1 second time interval, the actuator loads were read and averaged and an equivalent uniform load was calculated. The calculation is based on the assumption that failure occurs in bending. Thus, the equivalent uniform load can be obtained simply by dividing the center span loading by the total beam area. Thus, for the 4 ft wide beam:

$$W = \frac{P}{4\ell}$$

where P = Load from actuator (lbs)
ℓ = Span (ft)
W = Uniform load/unit width beam

Group 1

For the Group 1 floor systems, Fig. 2-4 shows the applied uniform load versus time for floor No. 1 with the curve shown in Fig. 2-4 approximating the plotted data.

For floor No. 4, the dynamic uniform load versus time graph is shown in Fig. 2-5. This specimen was tested using a six-point loading system and the equivalent uniform load determined in the same manner described previously. The maximum load resisted was 225 psf (at 1.0 seconds). The results for floor No. 1 are similar with a maximum load of 165 psf (at 0.8 seconds).

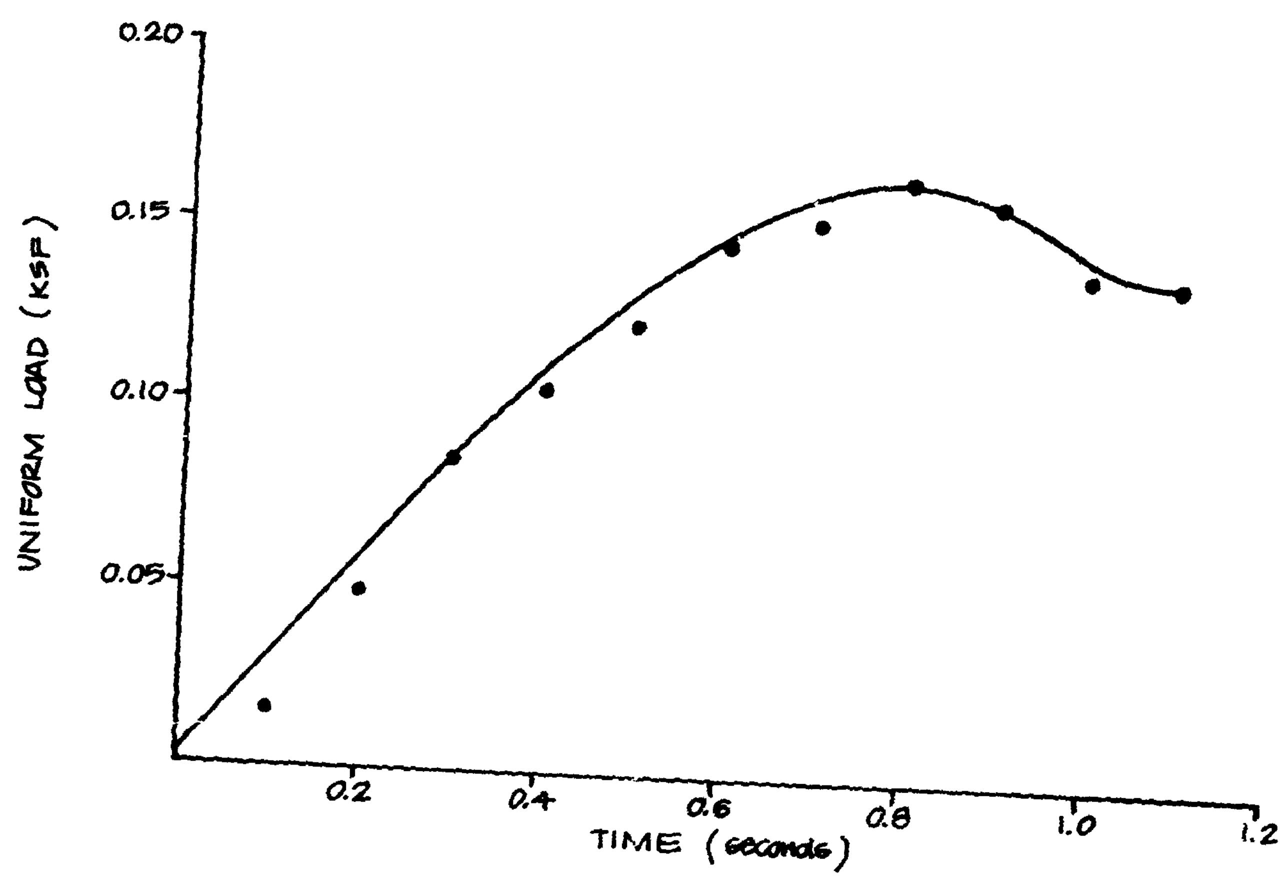

Fig. 2-4. Group 1 - Floor No. 1 - Load Versus Time.

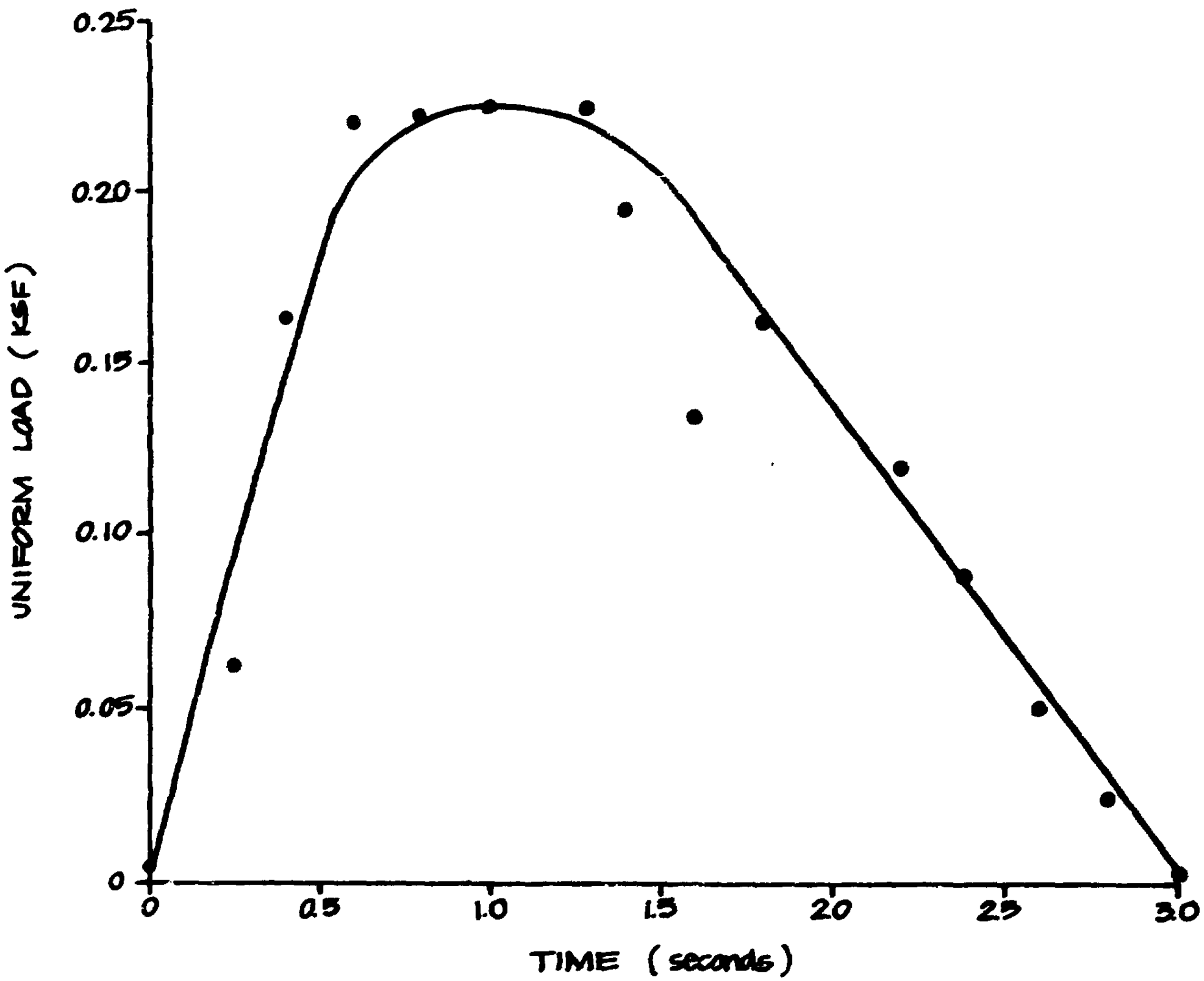

Fig. 2-5. Group 1 - Floor No. 4 - Load Versus Time.

Group 2

Group 2 investigated an upgrading technique designed to increase the moment resistance of the floor system by adding a 2 x 6 flange at the bottom of each joist. Fig. 2-6 shows the results for floor No. 3 indicating a maximum uniform load restraint of 305 psf at 2.9 seconds. For floor No. 6, an LVDT monitored the center deflection and these data are shown in Fig. 2-7. The graph in Fig. 2-8 is the equivalent uniform pressure time history.

The data from Figs. 2-7 and 2-8 can be combined to obtain a dynamic uniform load versus deflection relationship. This has been done in Fig. 2-9 which shows a maximum pressure of 456 psf at 1.95 inches of deflection. This graph can also be used to determine the energy absorption potential for this type of floor upgrading by calculating the area under the curve.

Group 3

This floor system used plywood attached to the bottom edge of the floor joists (creating a box beam) to provide a greater section modulus for more bending resistance. Fig. 2-10 shows the dynamic load history for specimen 5 indicating a maximum load resistance of 479 psf. The load history for another Group 3 specimen, floor No. 9, is shown in Fig. 2-11 and indicates a maximum load of 458 psf. Fig. 2-12 is the corresponding deflection record and Fig. 2-13 shows the dynamic load deflection relationship for floor No. 9. The sharp changes (discontinuities) visible in the curve of Fig. 2-13 represent a significant structural crack and sudden increase in deflection causing the load to drop off.

Group 4

This group contains one specimen, floor No. 10, which consisted of a floor similar to Group 1 with an additional support placed at the center of the span. Fig. 2-14 shows the uniform pressure time history failure at 1,020 psf after 11 seconds. The floor deflection was measured at the midpoint between the end support and center shoring and is shown in Fig. 2-15.

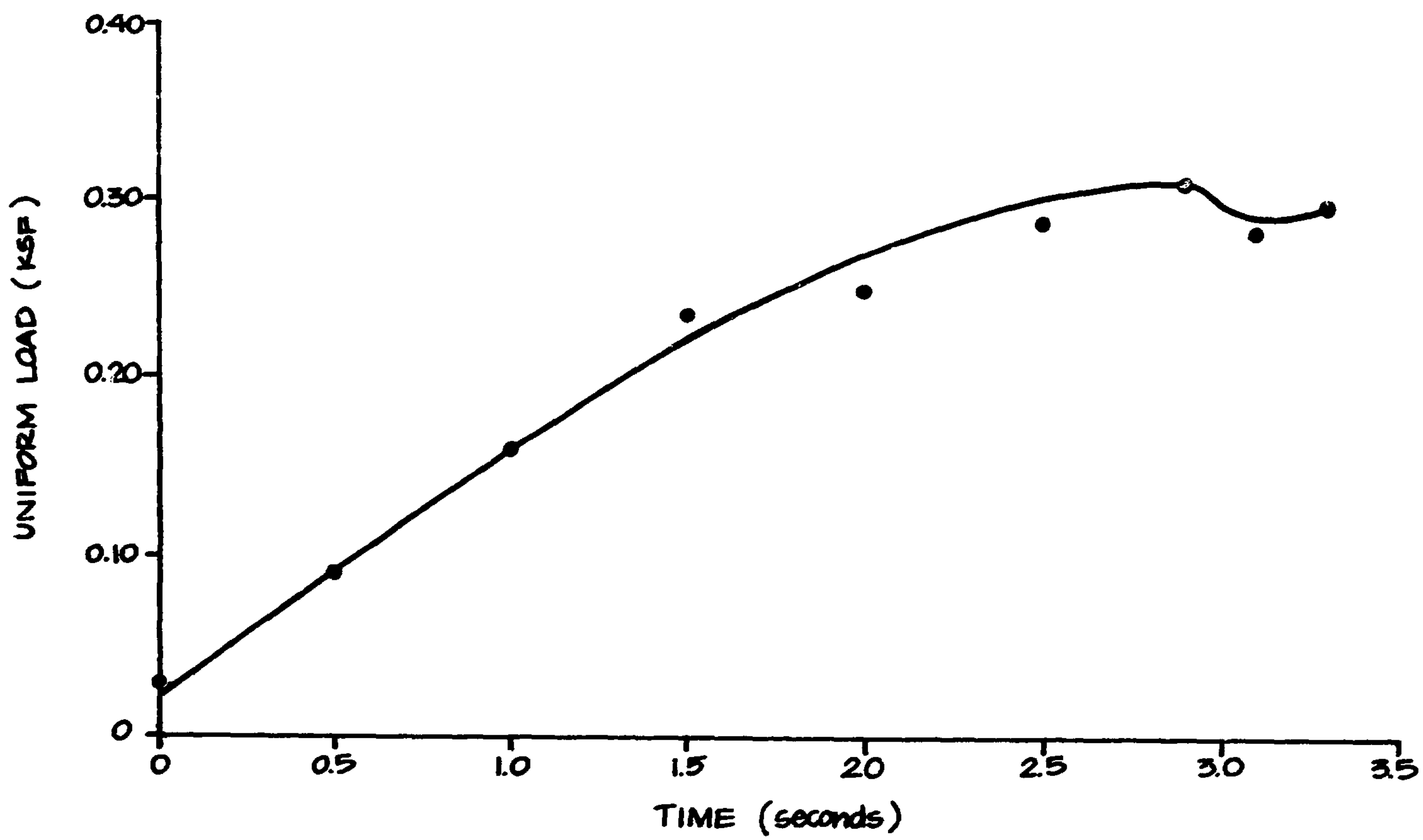

Fig. 2-6. Group 2 - Floor No. 3 - Load Versus Time.

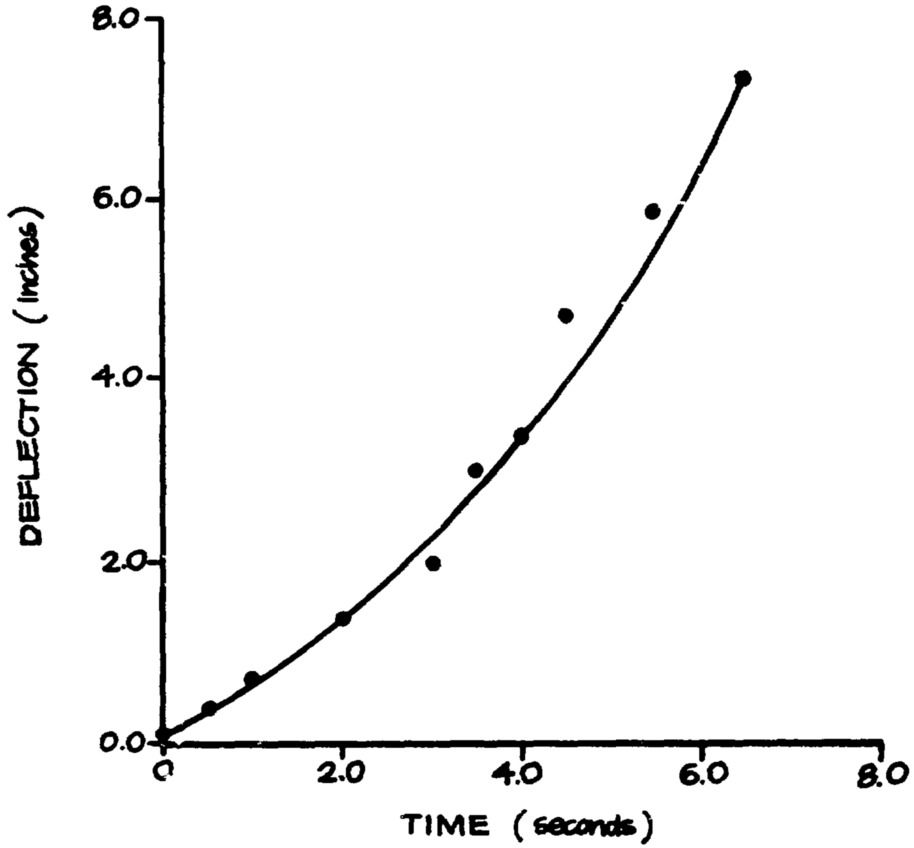

Fig. 2-7. Group 2 - Floor No. 6 - Deflection Versus Time.

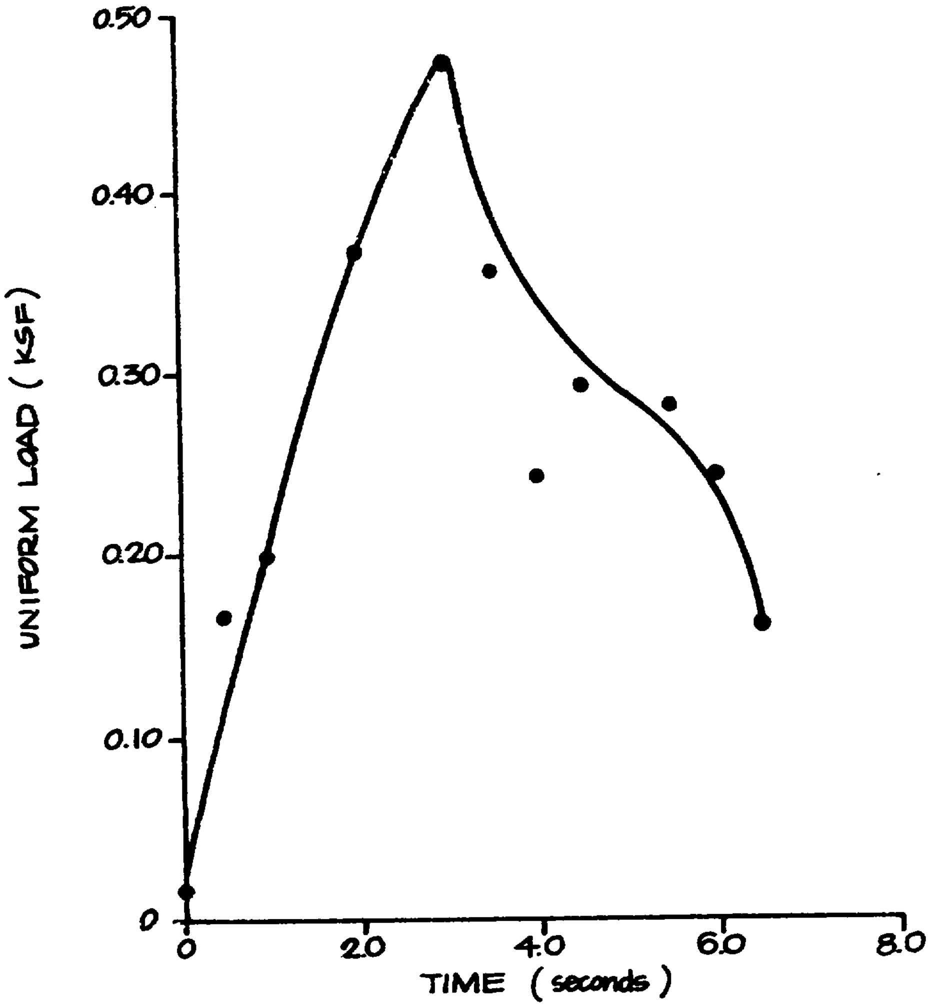

Fig. 2-8. Group 2 - Floor No. 6 - Load Versus Time.

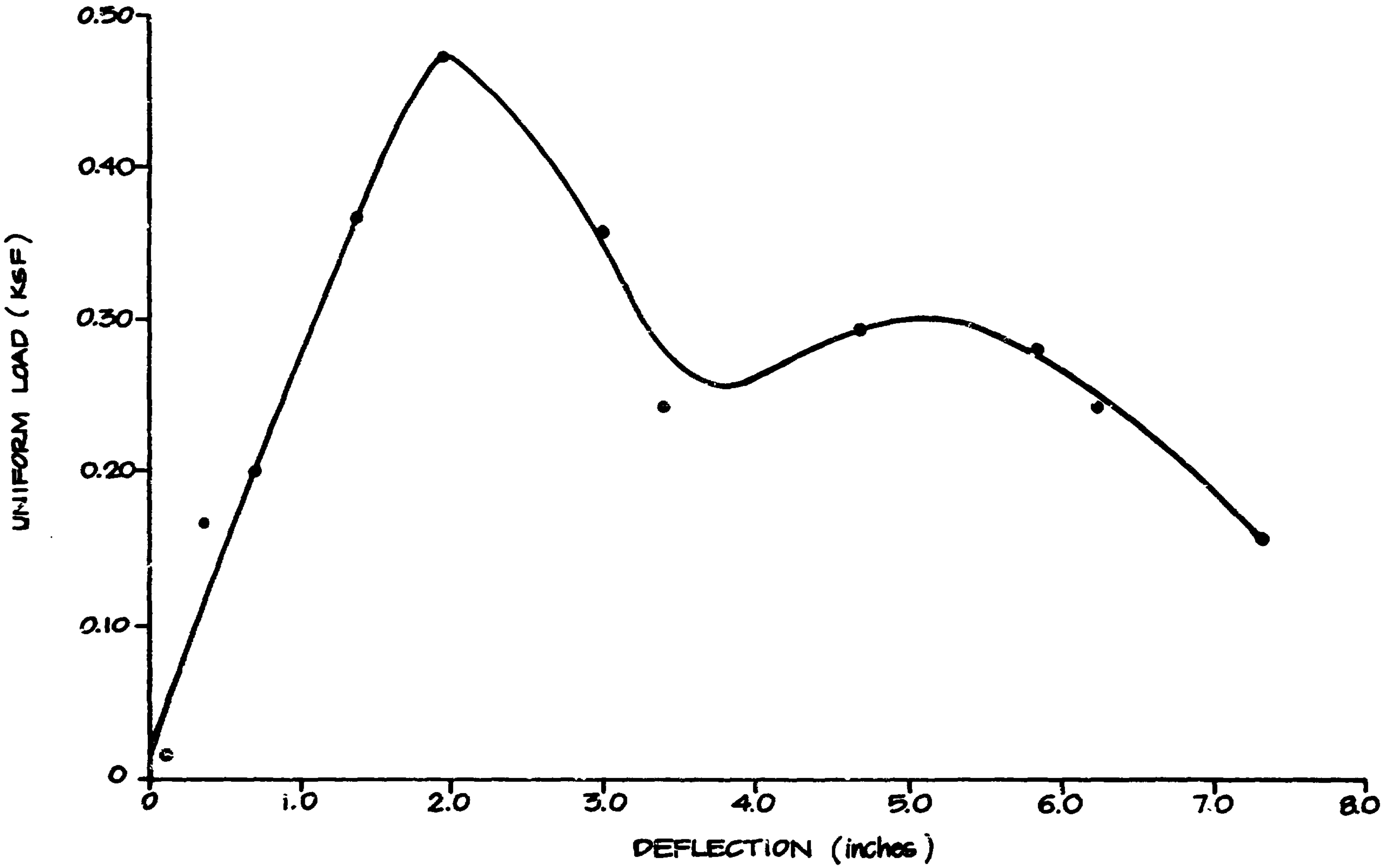

Fig. 2-9. Group 2 - Floor No. 6 - Load Versus Deflection.

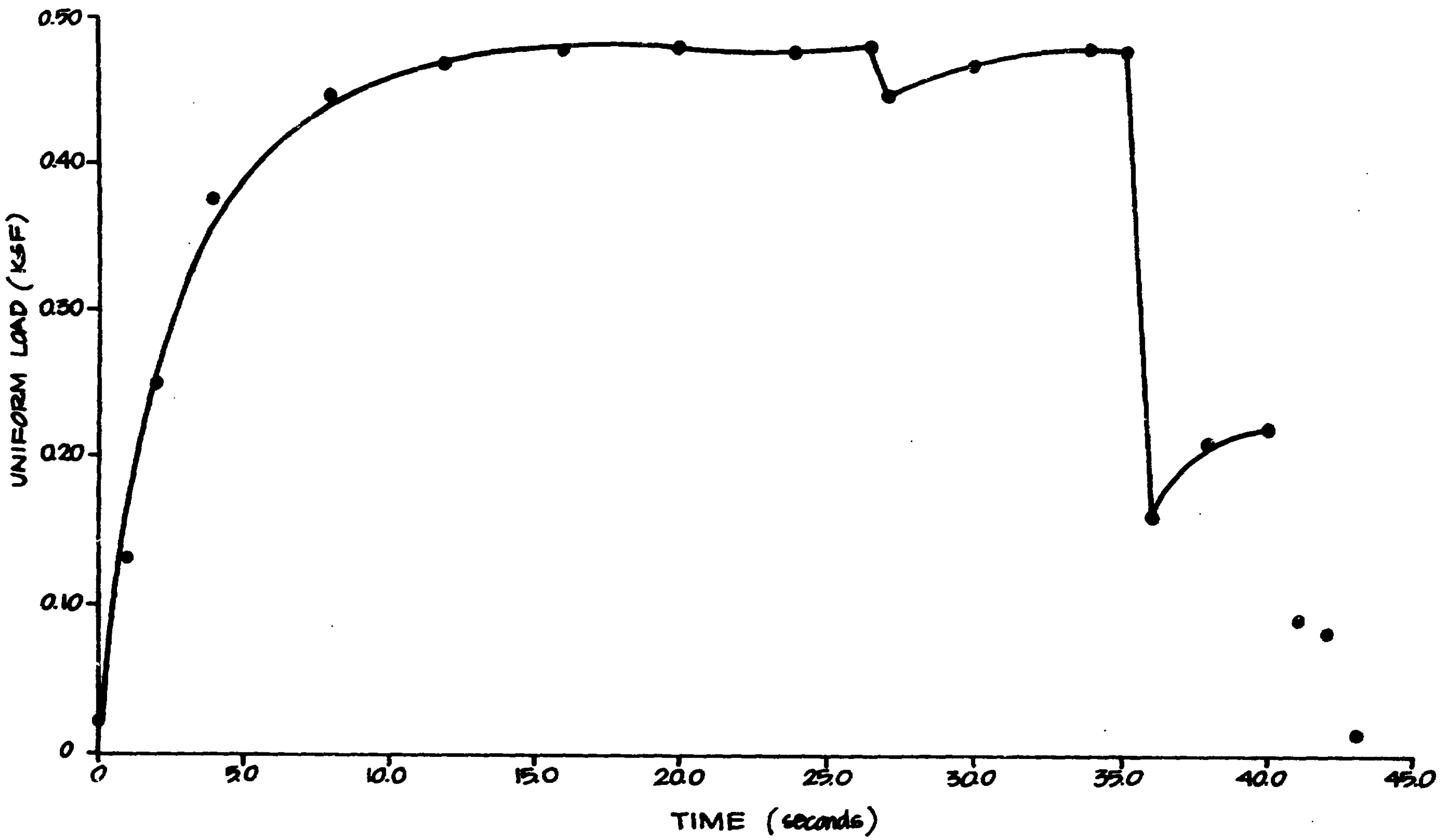

Fig. 2-10. Group 3 - Floor No. 5 - Load Versus Time.

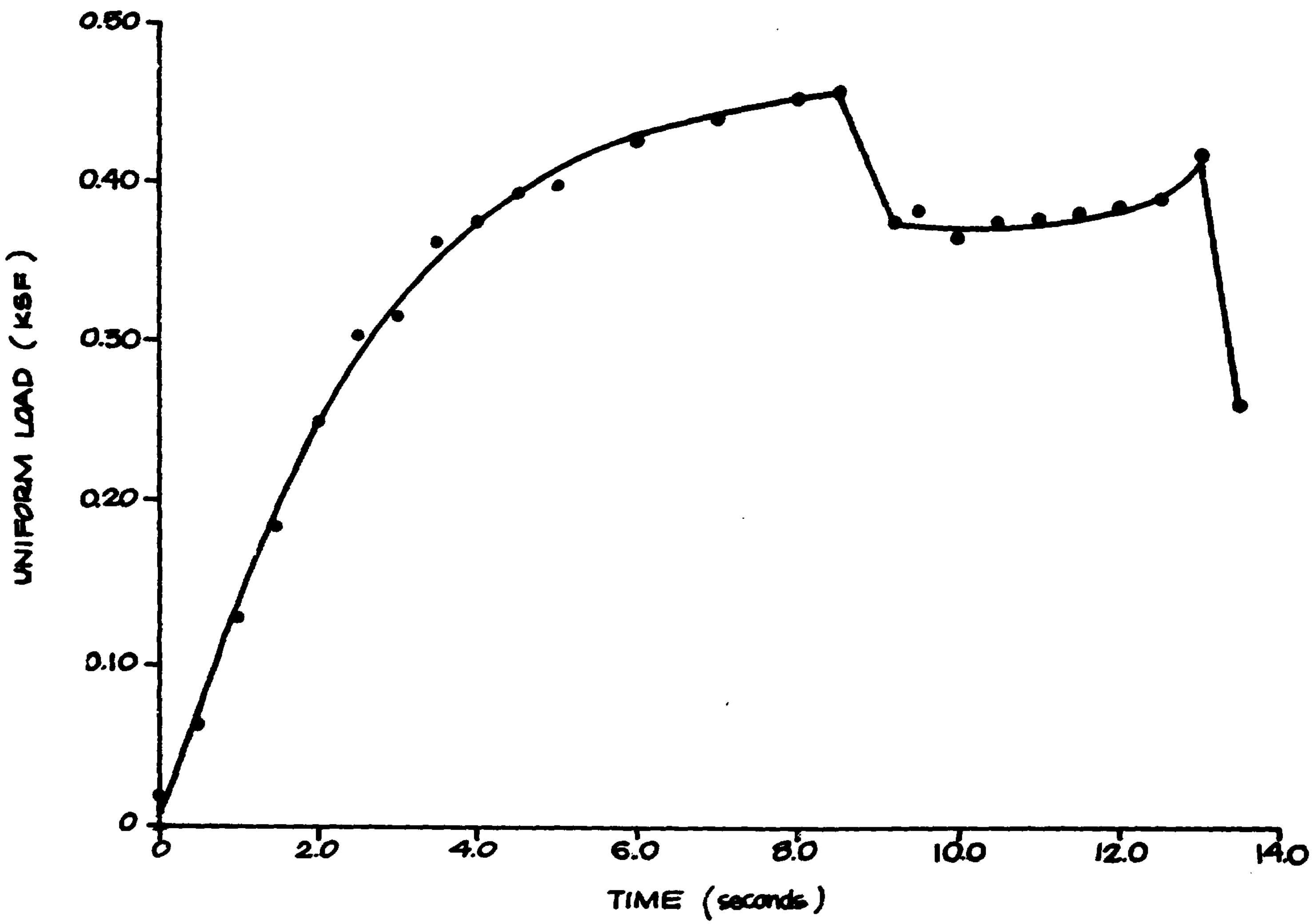

Fig. 2-11. Group 3 - Floor No. 9 - Load Versus Time.

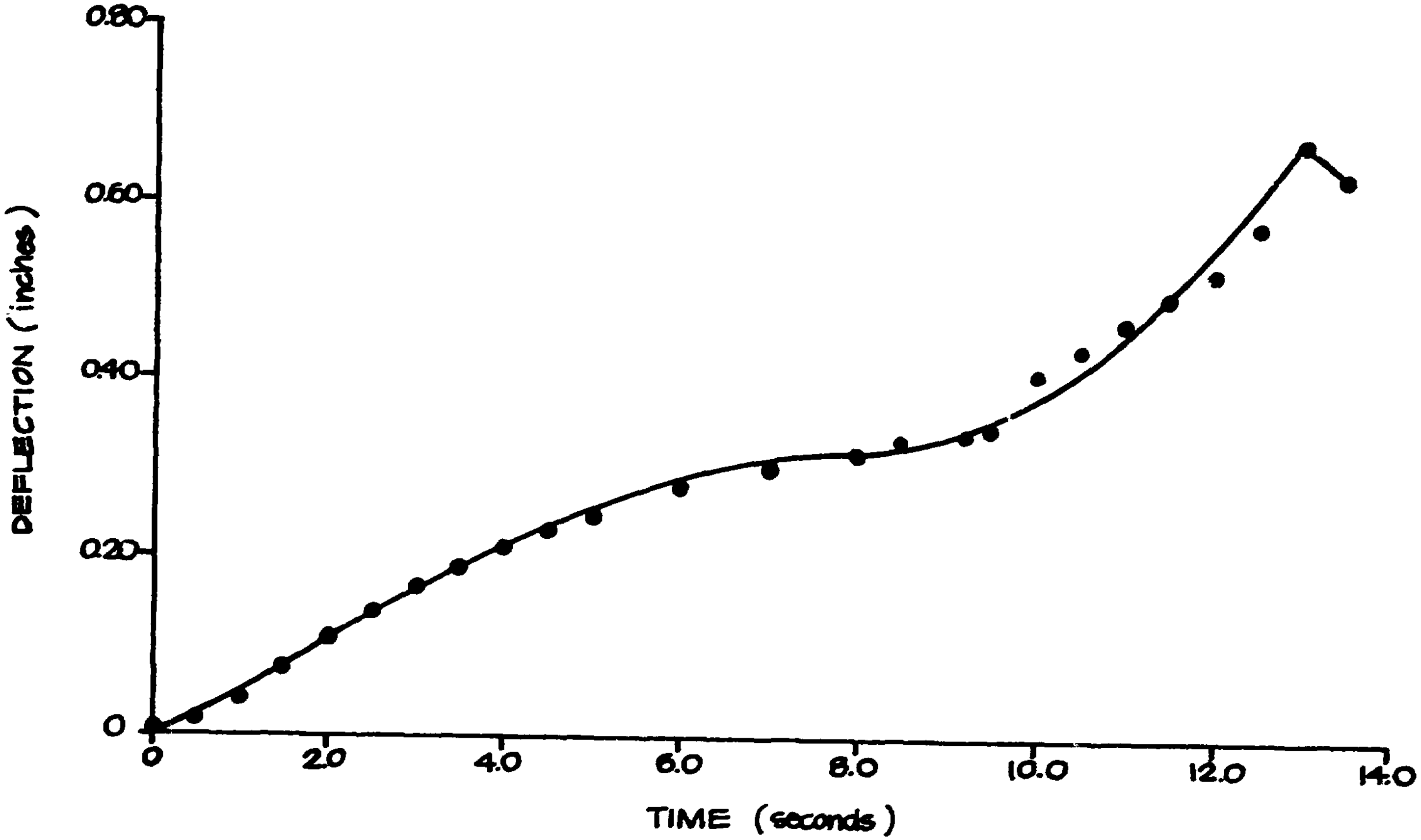

Fig. 2-12. Group 3 - Floor No. 9 - Deflection Versus Time.

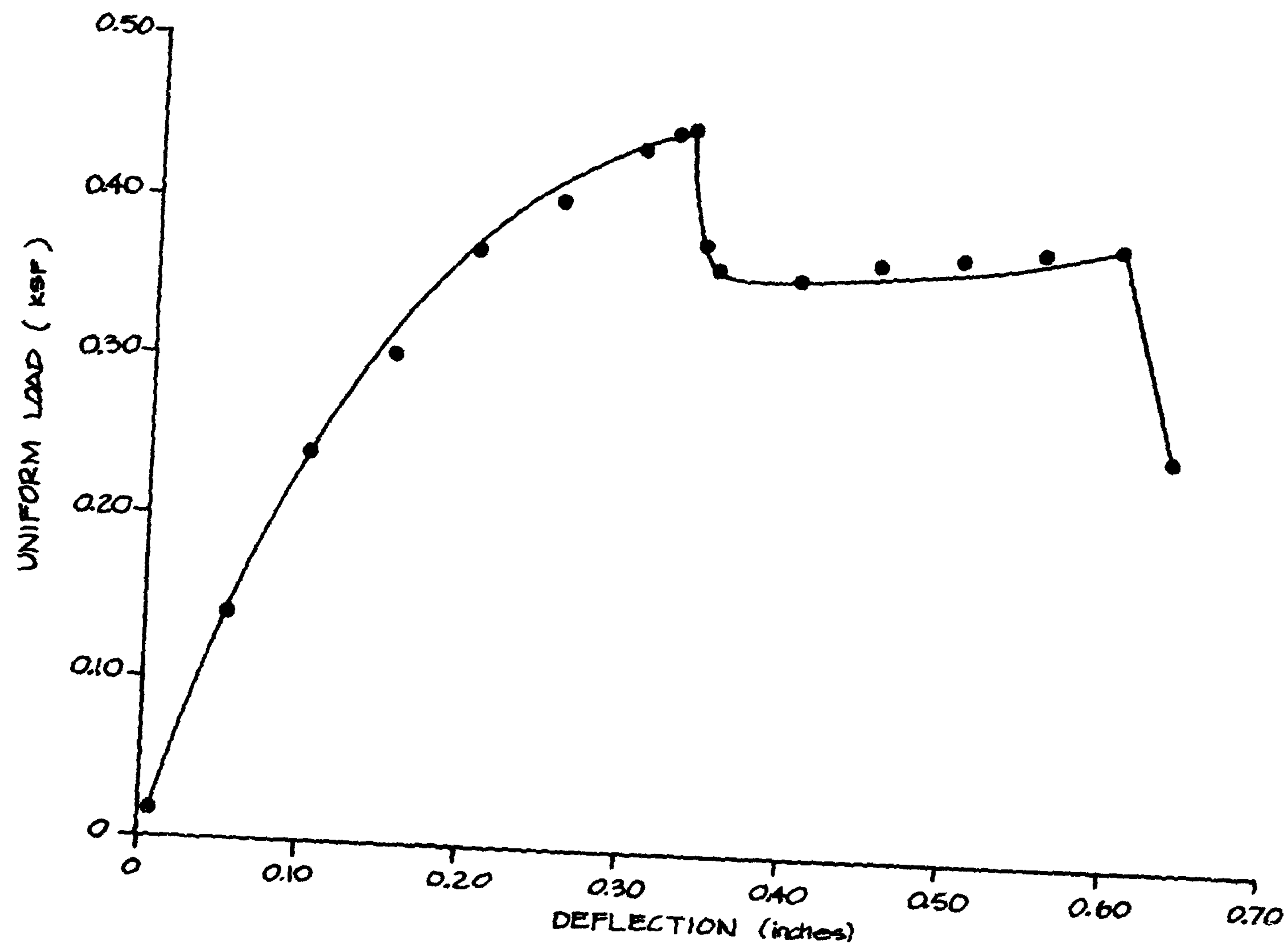

Fig. 2-13. Group 3 - Floor No. 9 - Load Versus Deflection.

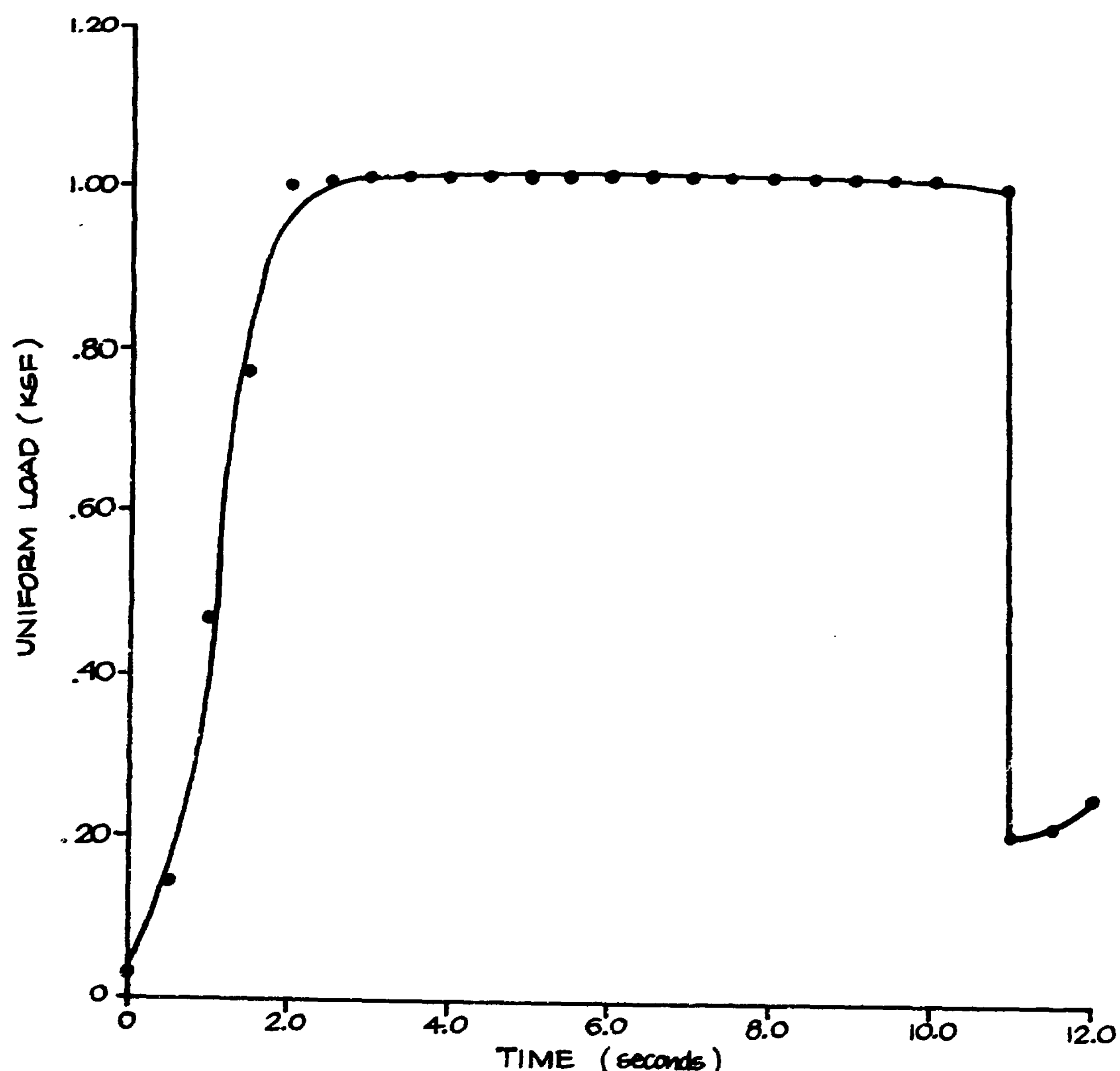

Fig. 2-14. Group 4 - Floor No. 10 - Load Versus Time.

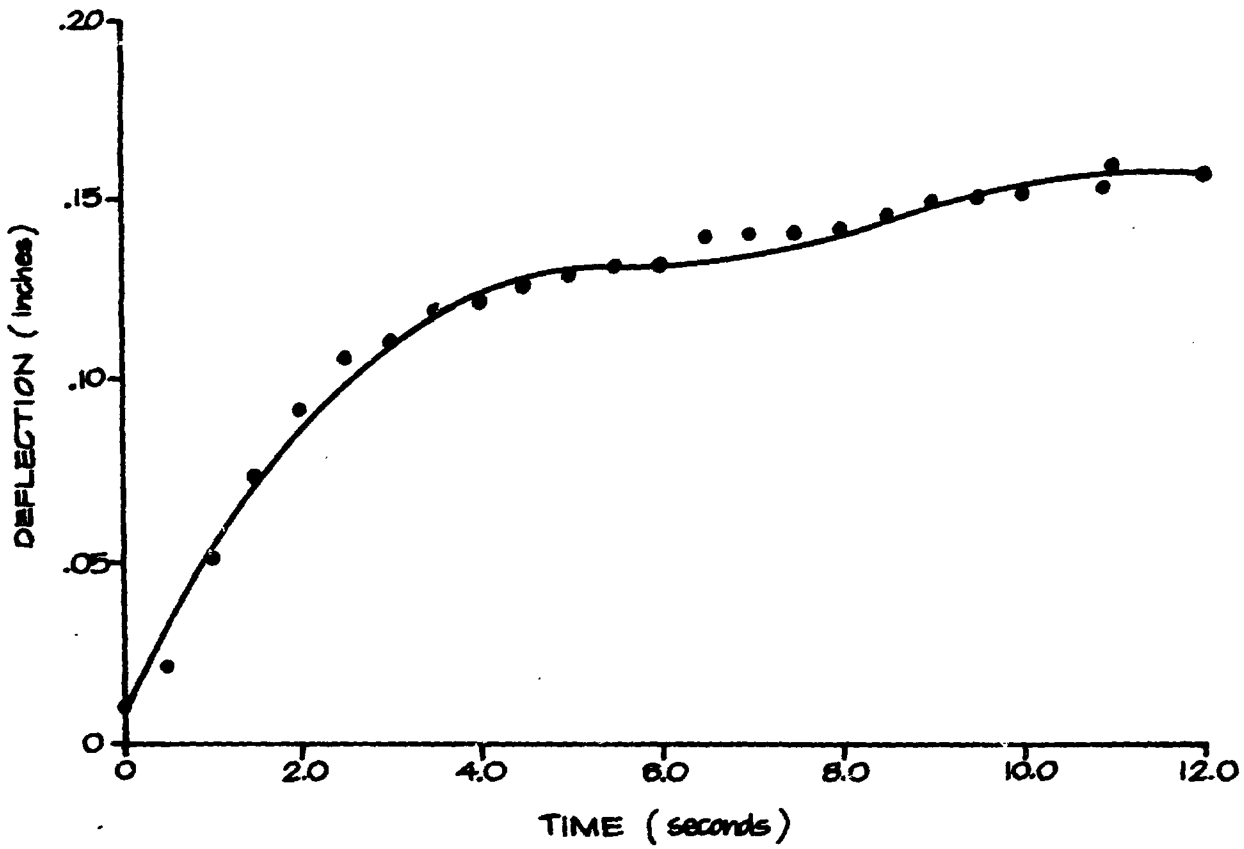

Fig. 2-15. Group 4 - Floor No. 10 - Deflection Versus Time.

Combining the results of Fig. 2-14 and 2-15, the dynamic load versus deflection graph is obtained (Fig. 2-16). This figure shows the greatly increased stiffness of the structure and the higher load carrying capacity. Note, however, the energy absorbed has not increased significantly.

Group 5

This group also consisted of one specimen (floor No. 2) and was shored at the third points. Fig. 2-17 shows the load time history for the three load actuators to failure. Fig. 2-18 represents the average of those three loadings.

Group 6

This group consists of floors Nos. 7, 8, and 11, each of which used a king post and various tensioning techniques to provide greater moment resistance. Figs. 2-19 and 2-20 present the load and deflection time histories for floor No. 7. The load-deflection relationship for floor No. 7 is shown in Fig. 2-21 and demonstrates the ability of this upgrading technique to absorb much greater energy than the other upgrading techniques. Also, note there is no sudden change or discontinuity in the curve which indicates efficient usage of the available strength in all elements.

Figs. 2-22 and 2-23 contain the load and deflection time histories for floor No. 8. The maximum load restrained by the specimen was 40 psf. The load versus deflection graph can be seen in Fig. 2-24. The test results for floor No. 11 can be seen in Figs. 2-25 through 2-27.

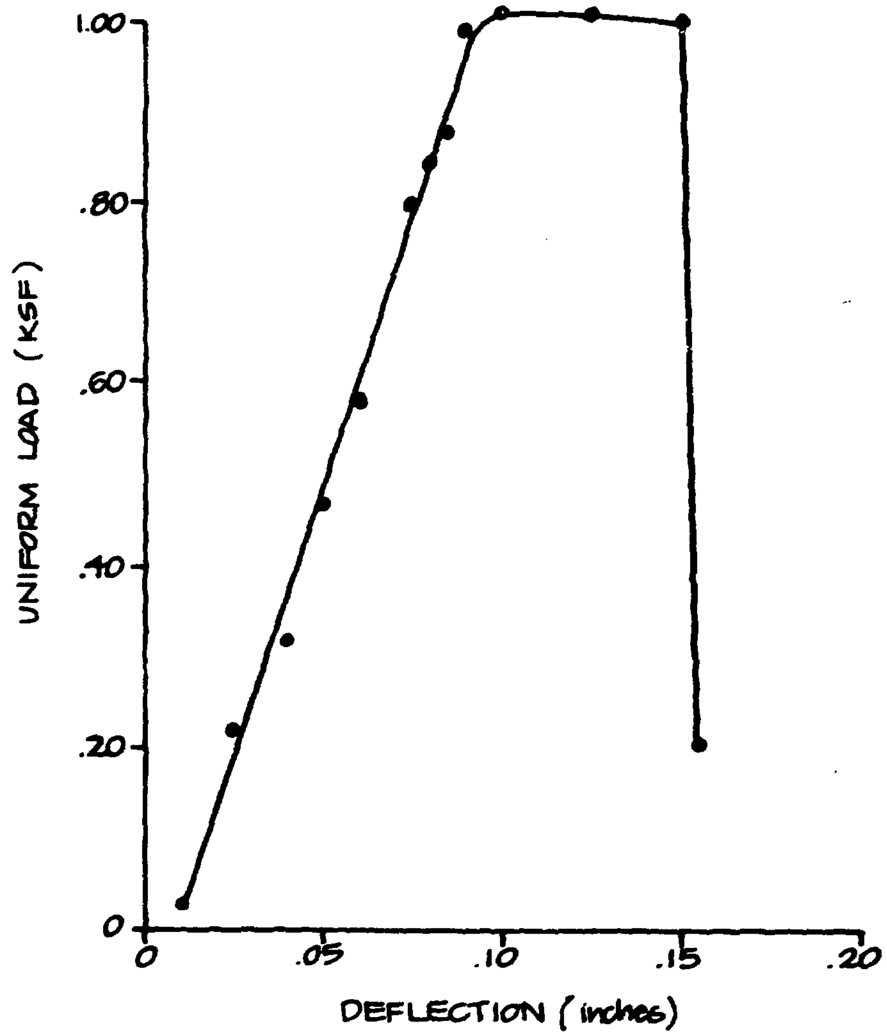

Fig. 2-16. Group 4 - Floor No. 10 - Load Versus Deflection.

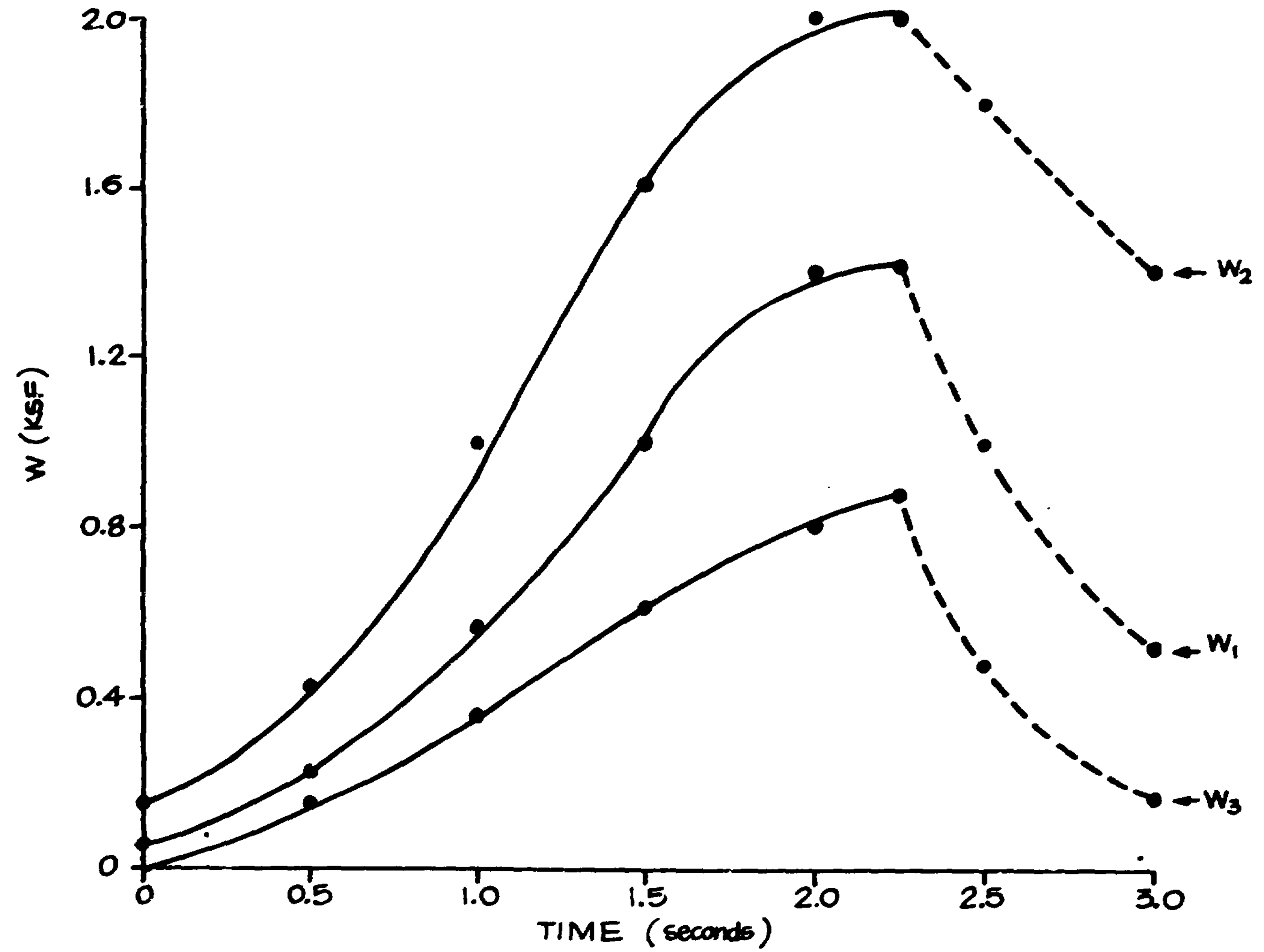

Fig. 2-17. Group 5 - Floor No. 2 - Load Versus Time For the Three Load Actuators (see Fig. A-36).

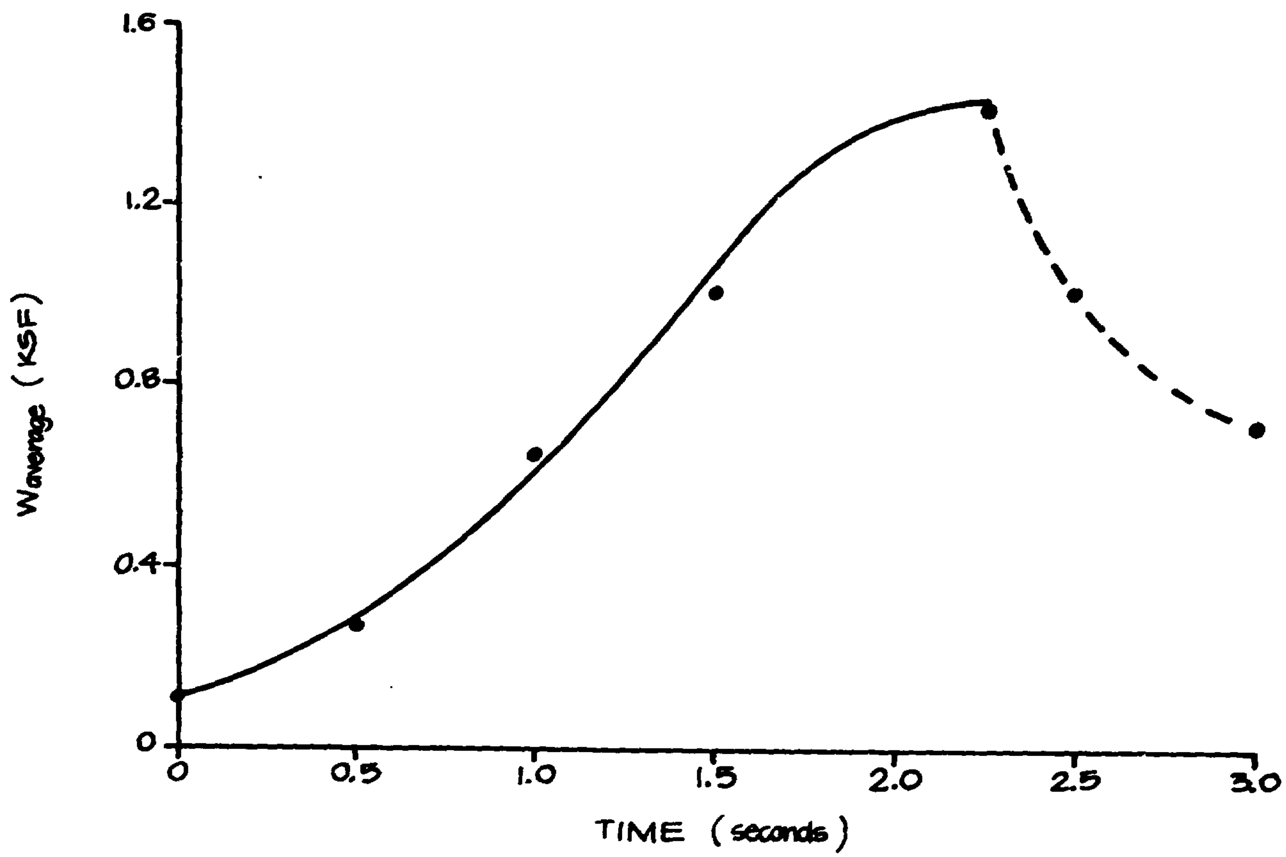

Fig. 2-18. Group 5 - Floor No. 2 - Average Load Versus Time.

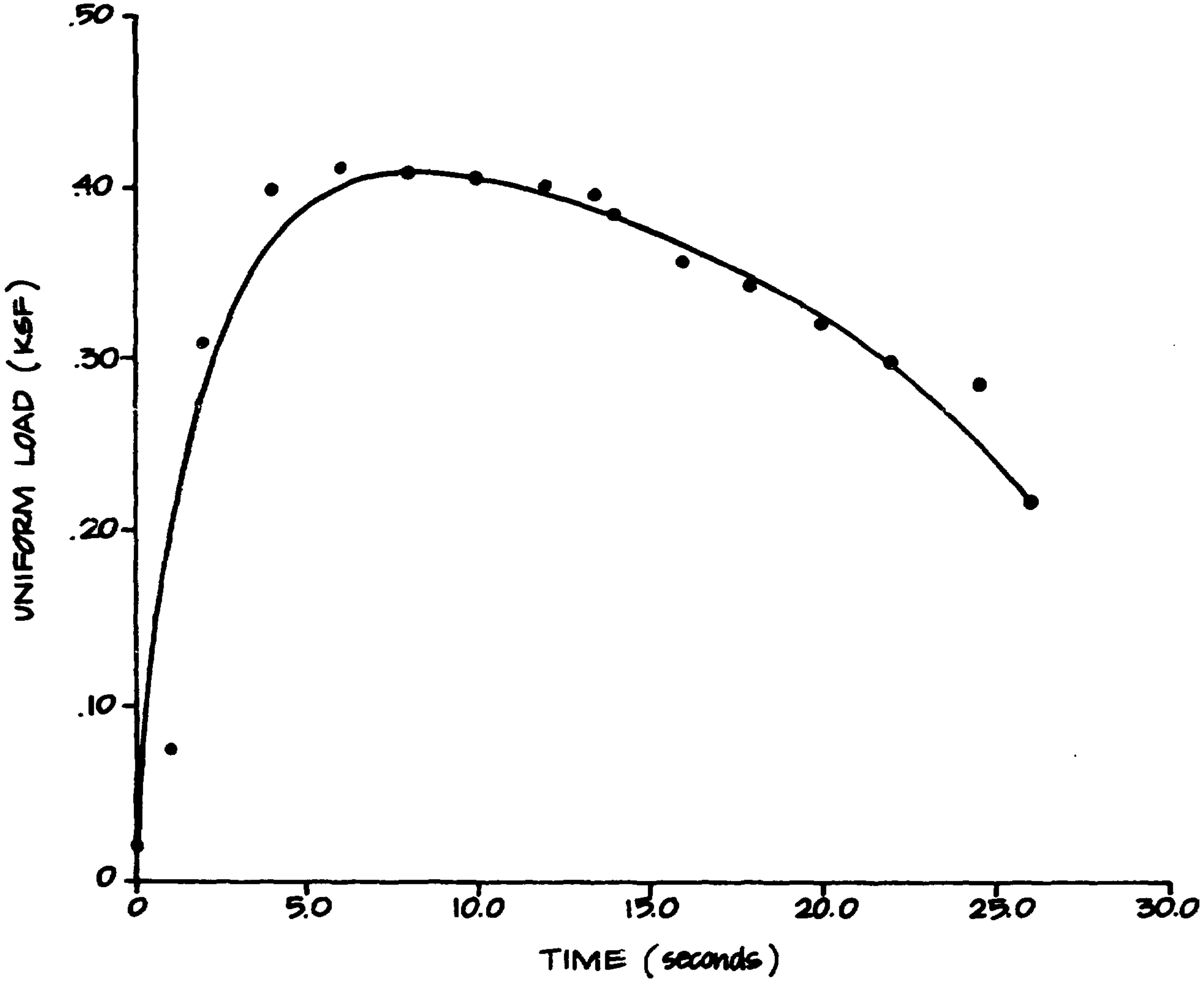

Fig. 2-19. Group 6 - Floor No. 7 - Load Versus Time.

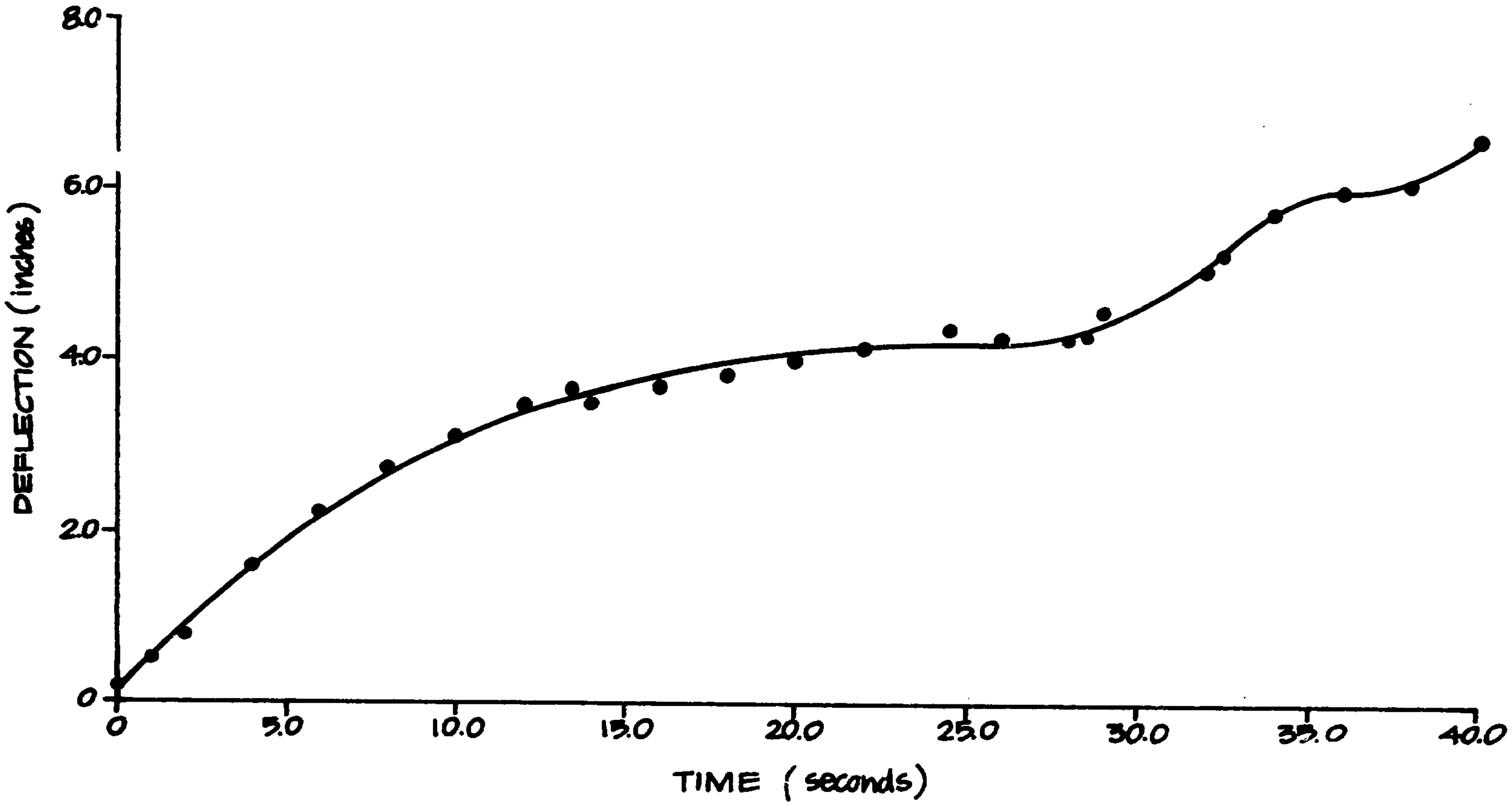

Fig. 2-20. Group 6 - Floor No. 7 - Deflection Versus Time.

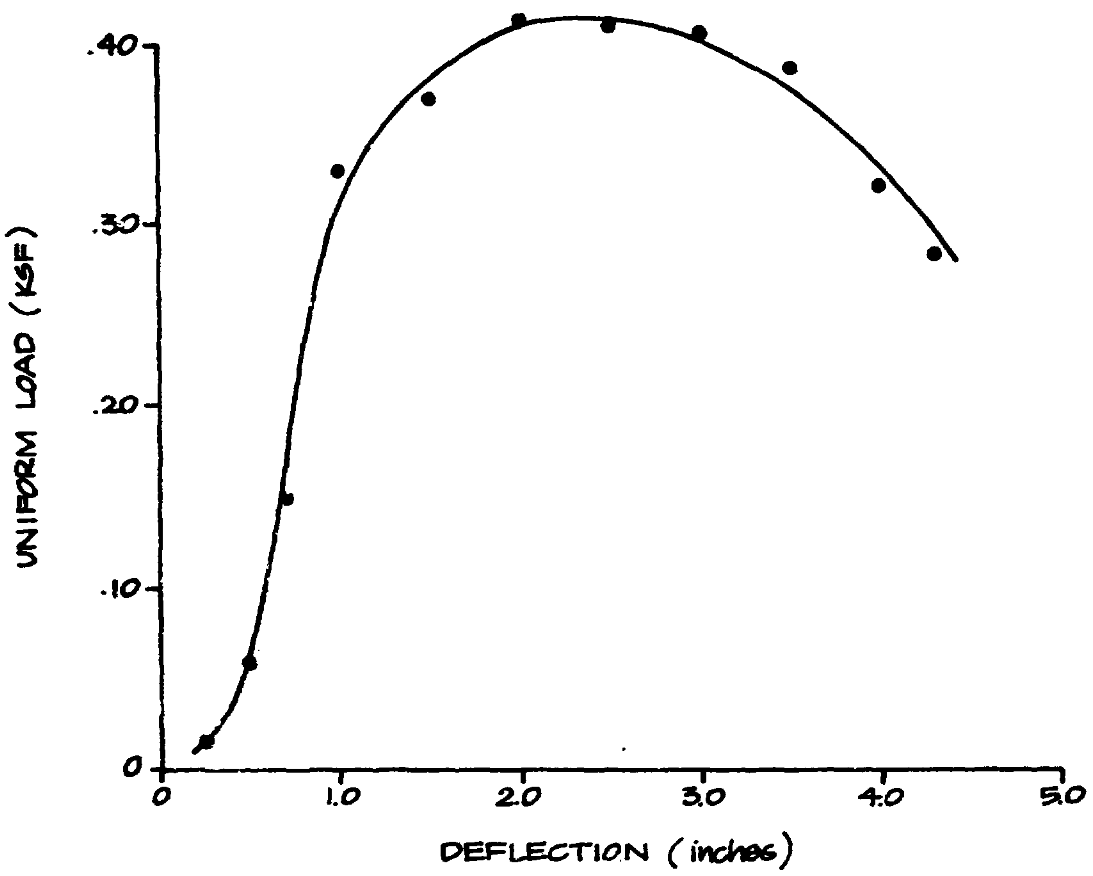

Fig. 2-21. Group 6 - Floor No. 7 - Load Versus Deflection.

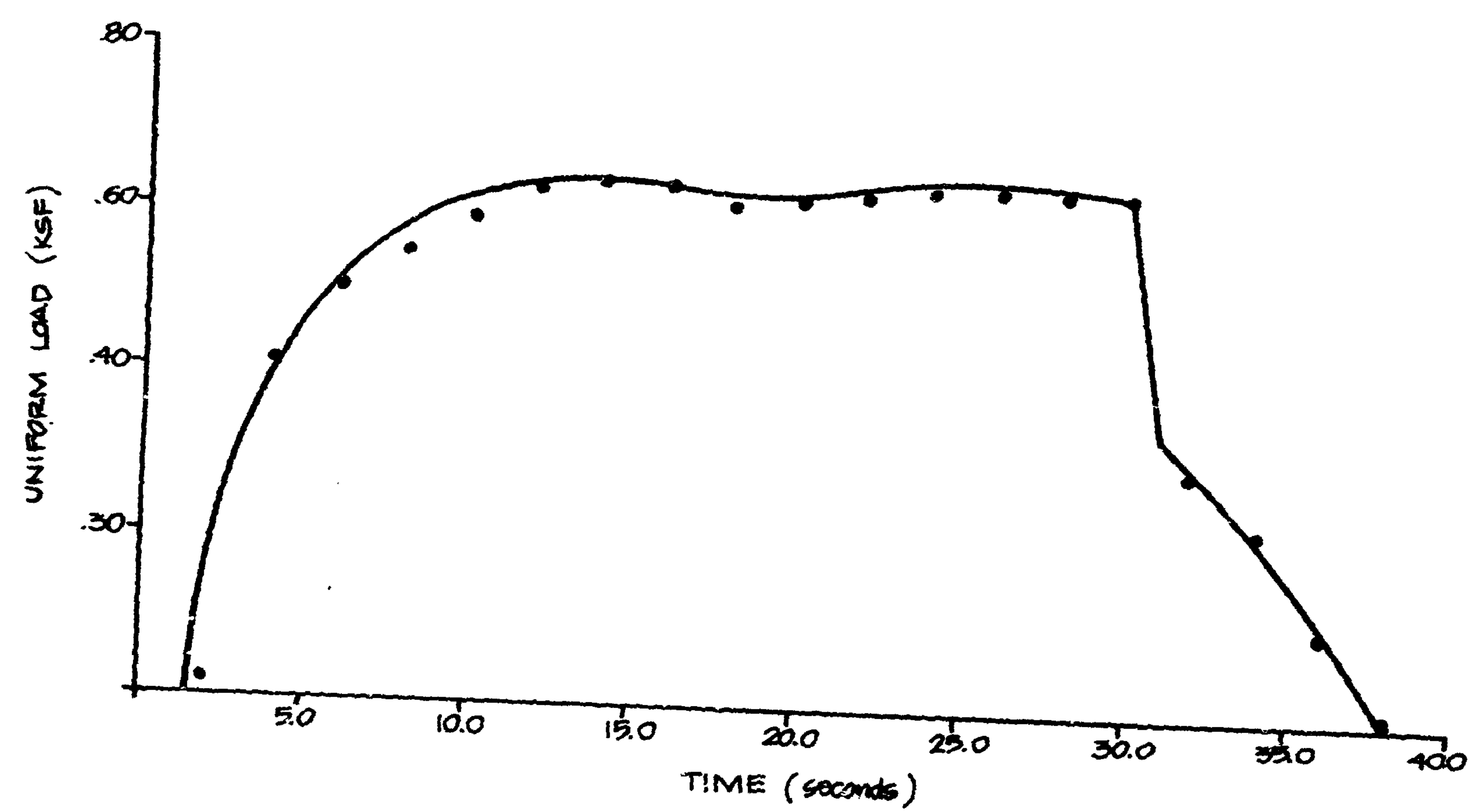

Fig. 2-22. Group 6 - Floor No. 8 - Load Versus Time.

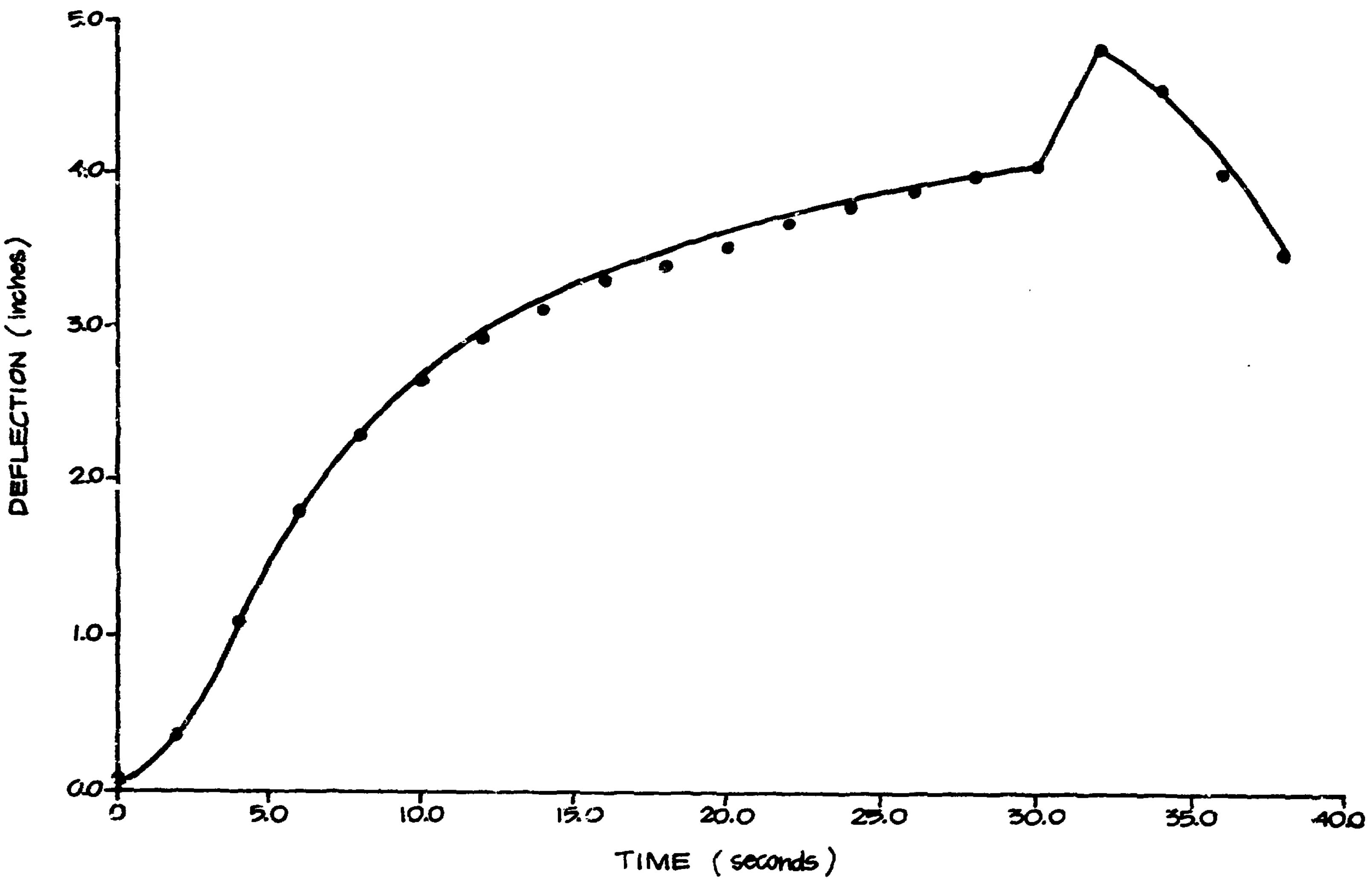

Fig. 2-23. Group 6 - Floor No. 8 - Deflection Versus Time.

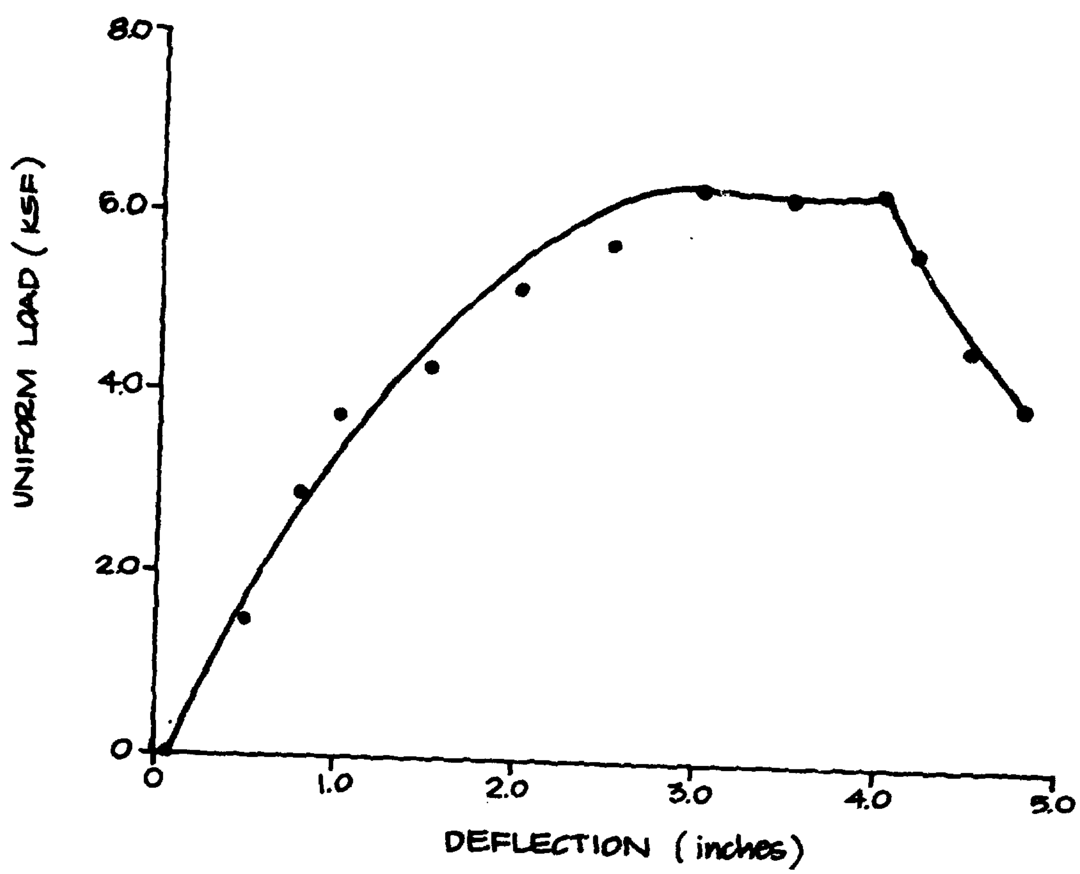

Fig. 2-24. Group 6 - Floor No. 8 - Load Versus Deflection.

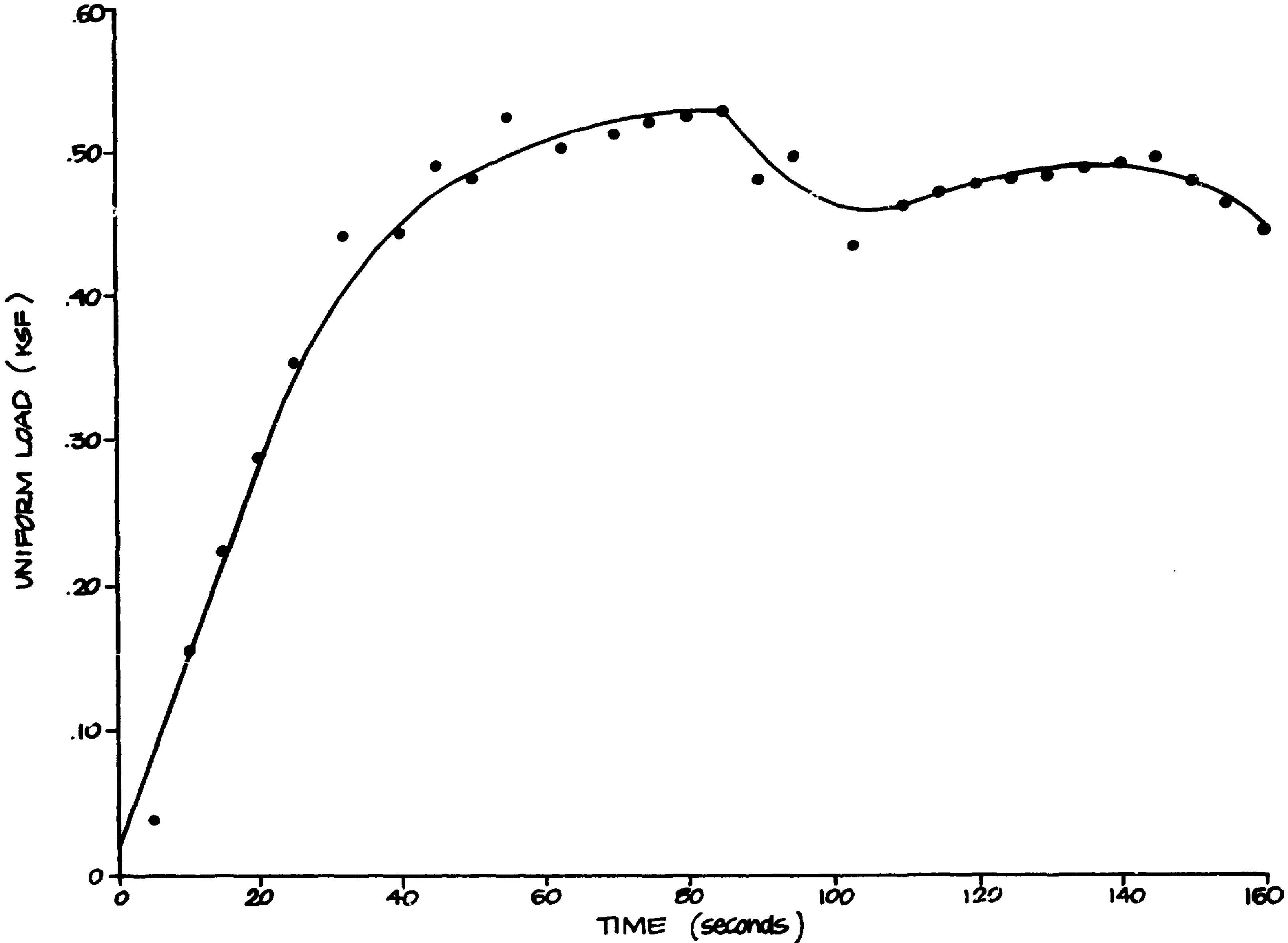

Fig. 2-25. Group 6 - Floor No. 11 - Load Versus Time.

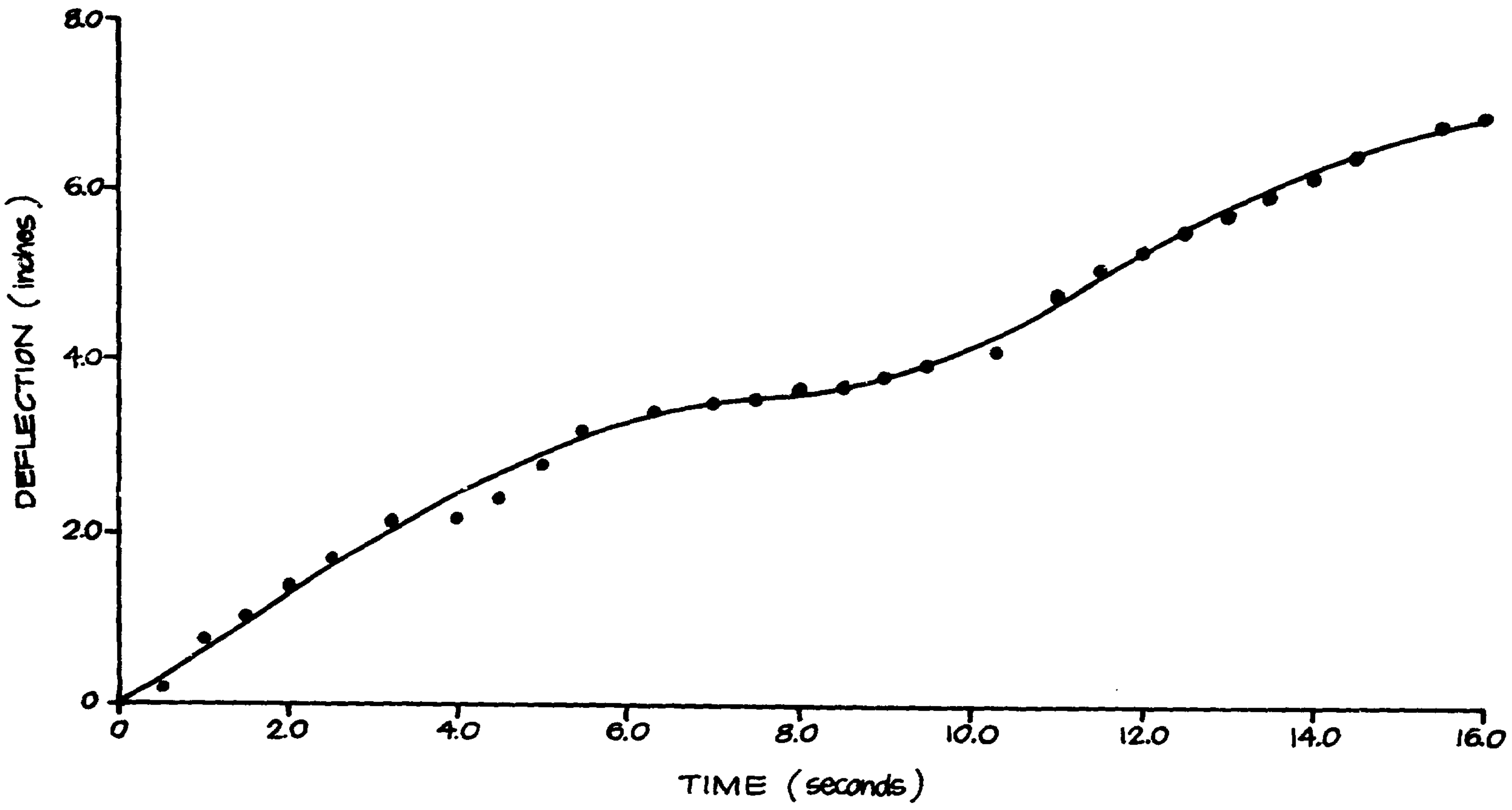

Fig. 2-26. Group 6 - Floor No. 11 - Deflection Versus Time.

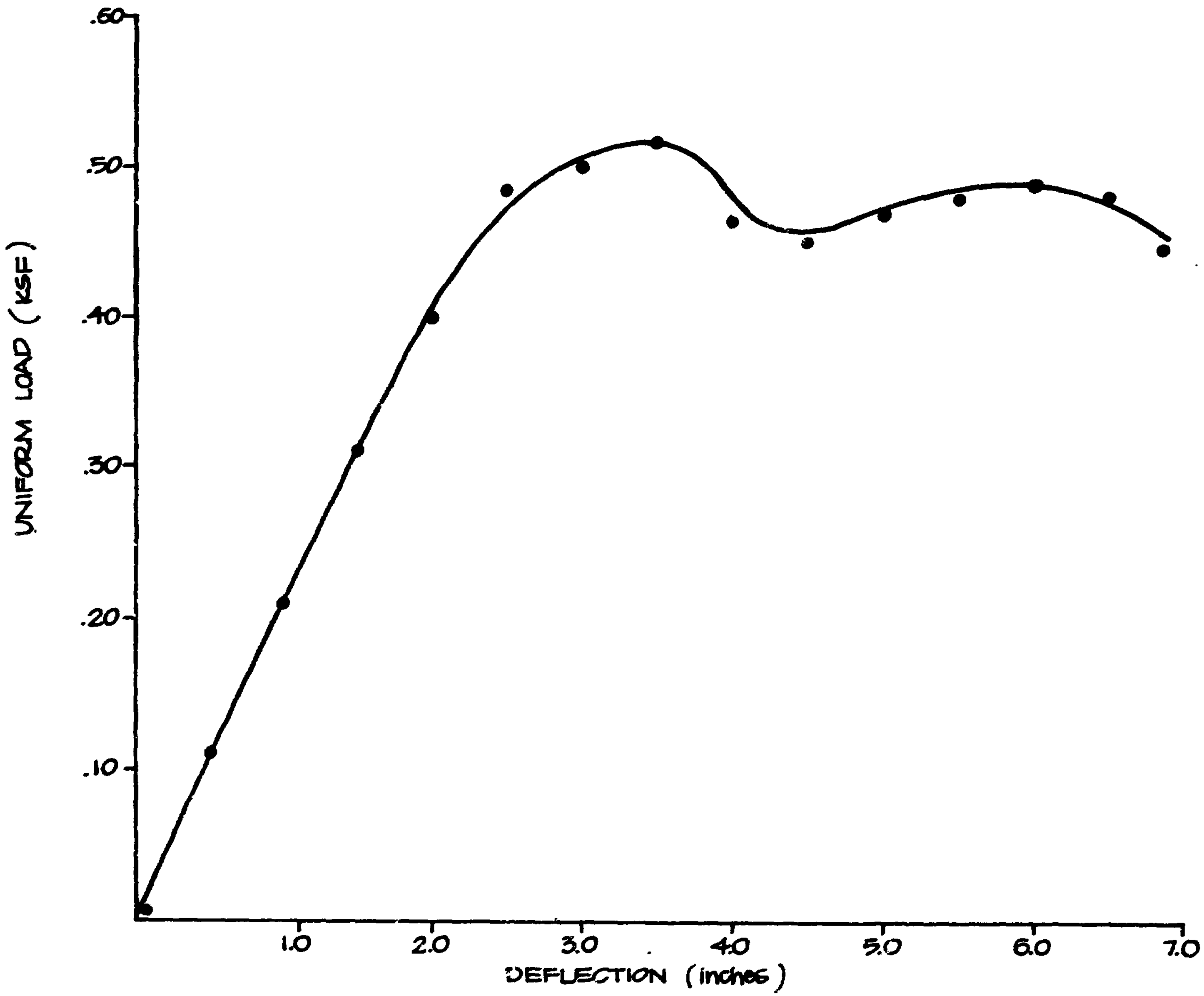

Fig. 2-27. Group 6 - Floor No. 11 - Load Versus Deflection.

Section 3
CONCRETE

INTRODUCTION

Prior to 1963 the design of reinforced concrete structures used a simple extension of elastic theory based on the strength of materials. Thus, design of concrete structures with the elastic theory was based on allowable stress levels in the concrete and steel reinforcement components. These allowables were assumed to be the maximum stresses encountered in the materials at service or design loads. Concrete, however, is not a simple elastic material and in reality the so-called working stress design (WSD) was actually a set of satisfactory approximations that provided a reliable design. Note that the actual stresses were never really known because concrete shrinks, creeps, and cracks, all of which change the stresses in both the steel and concrete throughout the structure.

In 1963 a notable step forward was taken when the ACI building code brought forth the ultimate strength design concepts (USD). These concepts provided the designer with an accurate method of predicting the actual strength of a member at a point or zone. That is, an engineer could accurately predict the bending moment resistance of a beam at a point (perhaps as close as 5%) assuming that the properties of the beam were known. During the time frame from 1963 to 1971, most design work still used the working stress approach with the ultimate strength approach slowly working its way into the profession. With the advent of the 1971 ACI code, the use of working stress design was virtually eliminated as far as sizing members, predicting allowable loads, etc.

The effect of this evolution on DCPA, or engineers involved in DCPA work, is that they are faced with buildings of all vintages. From this brief discussion, one could deduce that reinforced concrete buildings constructed prior to 1963 are most likely working stress designed. Buildings constructed in the era from 1963 to 1967 are probably a mixture of working stress and ultimate stress designed. By 1971, however, most designers in the field had become familiar with USD methods and from 1971 to the present, USD is almost universally used throughout the profession. The motivation, of course, was not strictly analytical but primarily economic since it allows the use of smaller member sizes and less material.

The present codes do not allow for true limit design. By limit design it is generally meant that elastic techniques are used for solving the bending moments, shears, and axial forces on members in a structure and the ultimate strength concepts are used for sizing the members based on the local elastic values. True limit design, however, allows the engineer to treat the entire structure as an inelastic body, to determine the collapse mechanisms, and then to size the members, such as beams and columns. In general, the elastic procedure approach currently used to establish design moments, loads, shear, etc. is conservative, and limit design would allow still further reductions in size of members in a structure. A major benefit of the limit design approach is that it enables failures of concrete systems, such as slabs, to be predicted. Limit concepts are used in this section of the report to predict slab failures. Membrane behavior is present only for specific boundary conditions, which are not present in this particular test arrangement.

The concrete specimens designed, constructed, and tested at San Jose State under this program were slabs or portions of slabs taken from an imaginary beam, slab, and girder building that could have represented all of the above eras. The test slab was a 4-ft strip approximately 22 ft long and 6½ in. thick. The slab span, beam-to-beam, was 16 ft, with a clear span of 15 ft. The reinforcing pattern could have been from any design era, i.e., governed by 1956 and earlier codes, the 1963 codes, or perhaps 1971 code, with different allowable loads being represented by the different eras. The ACI code moment coefficients were used to establish the steel requirements over the supports in mid-span, and ACI recommended steel was used. The thickness was established by the ACI deflection criteria, or maximum depth to span ratio, which is very common in slab structures. Fig. 3-1A and 3-1B are sketches of the test specimen. Note that 4,000 psi concrete and 60,000 psi steel were selected for the design. There are 13 number 4 bars in the top of the slab for negative moment over the beam supports and 7 number 4 bars in the bottom of the slab for the positive mid-span moment. Table 3-1 illustrates the difference in eras of concrete design. The upper portion of the table is for grade 40 steel and the lower portion is for grade 60. The dead load was assumed to be 100 lbs, 80 lbs for the slab itself and 20 lbs for partitions, which is common in design codes throughout the nation. Note that the slab shown in Fig. 3-1, when designed by working stress design, has a live load capacity of 100 psf with 40 ksi steel in it and 140 psf with 60 ksi steel. These respective ratings would apply anytime from the early 1930's to the present day. In the table, observe that prior to the 1956 code, USD is not applicable, since the allowable load by ultimate strength design was not recognized. By 1963 the allowable load is 138 psf and by 1971 the allowable load is 152 psf. Keep in mind that the slab is identical in all six cases; i.e., had the slab existed in 1956 (rated at 100 psf by working design) it could be reanalyzed in 1971 and be found safe to use at 152 psf. This same slab with a grade 60 steel would have been rated at 140 psf by working stress, regardless of the era, and rerated by the 1963 code ultimate strength to 240 psf, and again in 1971 to 260 psf. Nominally, the slab would have been at 150 psf under working stress design and 250 psf under ultimate stress design. At a 150 psf rating it might be used for a light duty warehouse and at 250 psf it could be used for heavy warehousing, or manufacturing. This makes a complex problem for an engineer interested in upgrading, because the slab in all 12 cases looks identical with no exterior markings to indicate whether it is a 100 psf or 263 psf floor. In fact, the number of bars of steel are identical, only the steel grade and rating method changed in going from a 100 psf service load to a 263 psf service load. Note also that all the slabs listed under the grade 40 table, that is, in all 6 cases, the slab would fail at the same ultimate load, independent of the rated allowable load. This vast difference in ratings and

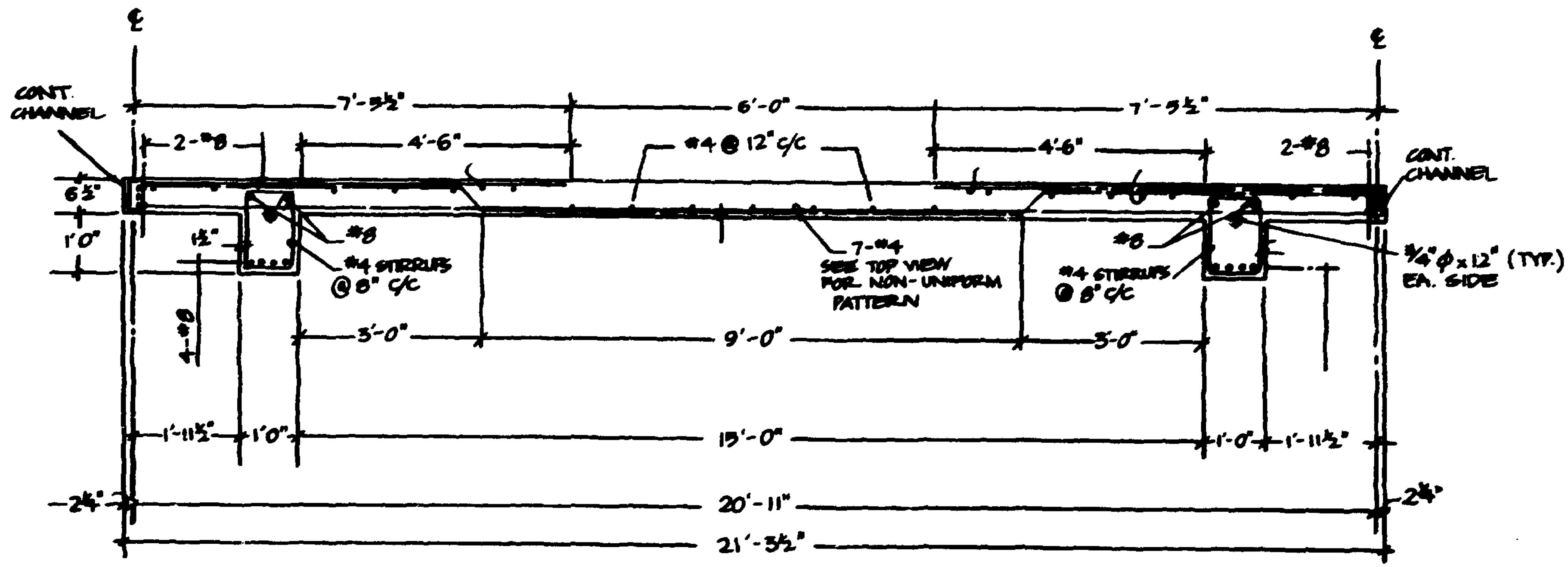

Fig. 3-1A. Sketch of Concrete Test Specimen.

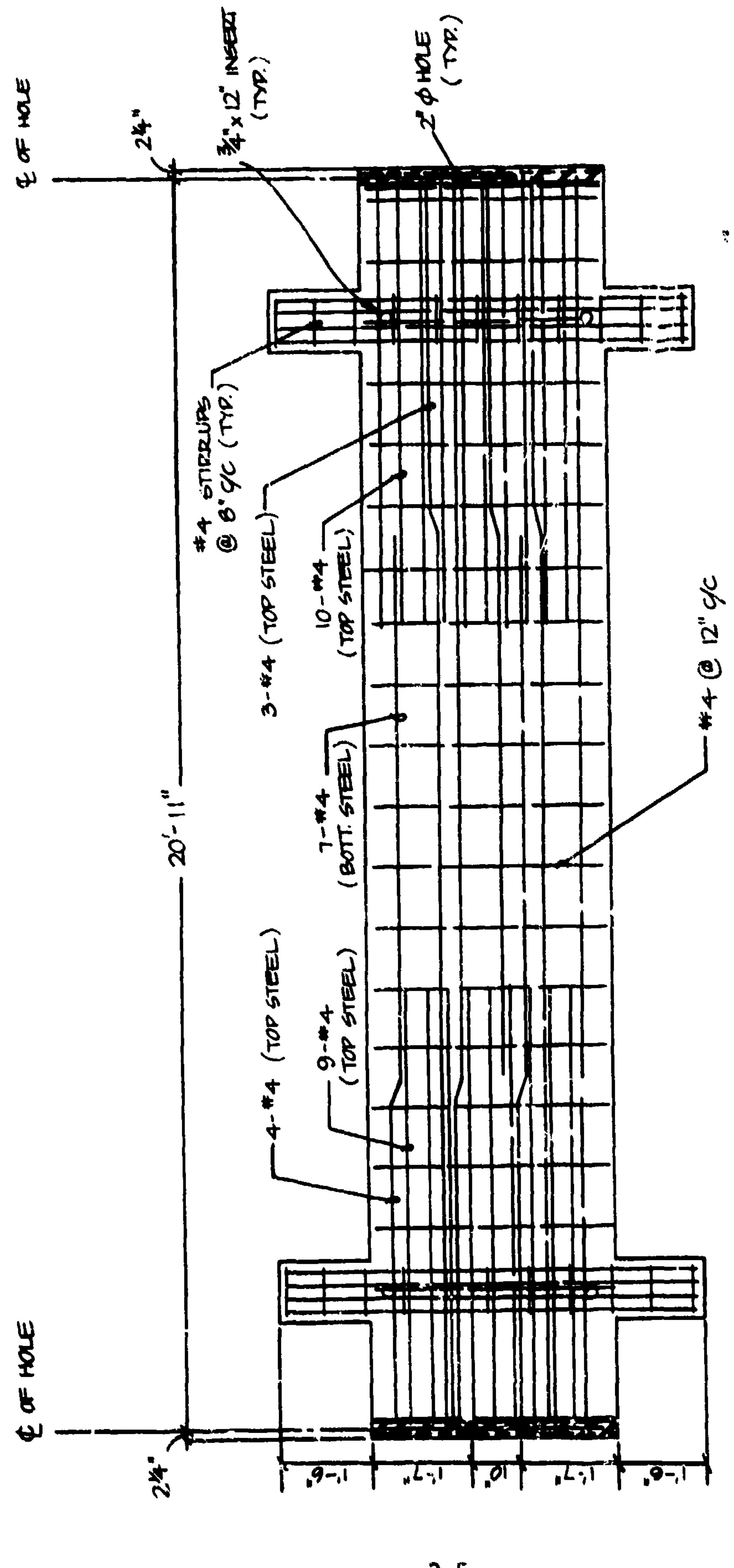

Fig. 3-1B. Sketch of Concrete Test Specimen.

Table 3-1. Live Load Floor Capacities

ACI Code	(Period)	WSD	USD
		WITH GRADE 40 STEEL	
1956 and Earlier	Before 1973	100 psf*	N/A
1963	1963 - 1971	100 psf	138 psf
1971	After 1971	N/A (optional)**	152 psf
		WITH GRADE 60 STEEL	
1956 and Earlier	Before 1963	140 psf	N/A
1963	1963 - 1971	140 psf	240 psf
1971	After 1971	N/A (optional)**	263 psf

* Dead load = 80 lb slab + 20 lb partitions.
** Rarely used unless deflections are a critical question -- loads would be same as 63 WSD.

allowables in safety factors makes it almost mandatory to resort to so-called limit design techniques to predict failure of the entire slab. This failure prediction for slabs is fairly well developed and is known as yield line theory. For the particular slab tested, it becomes a very simple problem in that the yield lines are merely hinge points and then it behaves much like the limit design concept used in steel.

An interesting problem occurred during the design, construction, and testing period of the slab specimens used in the SSI experimental program. The slab specimens were contracted out to a small pre-casting yard that specializes in custom pre-casting. The drawings were prepared and submitted to the contractor specifying 60,000 psi or grade 60 steel, 4,000 psi concrete, etc. After the slabs had been constructed, it was discovered that the contractor's purchasing agent had ordered grade 40 steel. Based on steel grade, this appeared to be a 50% change, but based on yield strength, the change was not significant. Fig. 3-2 is a stress strain curve developed from testing the actual bars used in the SSI test specimens. Although the grade 60 was called out, the figure shows that the grade 40 steel ordered has a yield stress of 56,000 psi, or only about 6% below the yield stress specified. This points up two important changes that have occurred in the re-bar industry since the early to mid-1960's. First, note the very short yield domain, perhaps less than one-half the total deformation to yield. This short yield domain is not harmful in itself, but it does change the character of the flexural specimen. Two things can happen. If the slab or concrete structure is under-reinforced, that is, if it contains much less steel than would cause a failure to occur in the concrete, then one will get a greater performance out of it than ultimate strength design would predict (i.e., one would no longer assume that when the steel yields, the structure ceases to pick up load, the cracks enlarge, deformations increase, and collapse becomes imminent). With a short yield domain, often the slab has sufficient ductility to deform and allow the steel to strain harden so that despite the steel yielding at 60,000 psi, the structure may indeed perform like a 70,000 to 75,000 psi steel-reinforced structure. If the concrete member is fairly heavily reinforced, which is more common in beams but not so common in slabs,

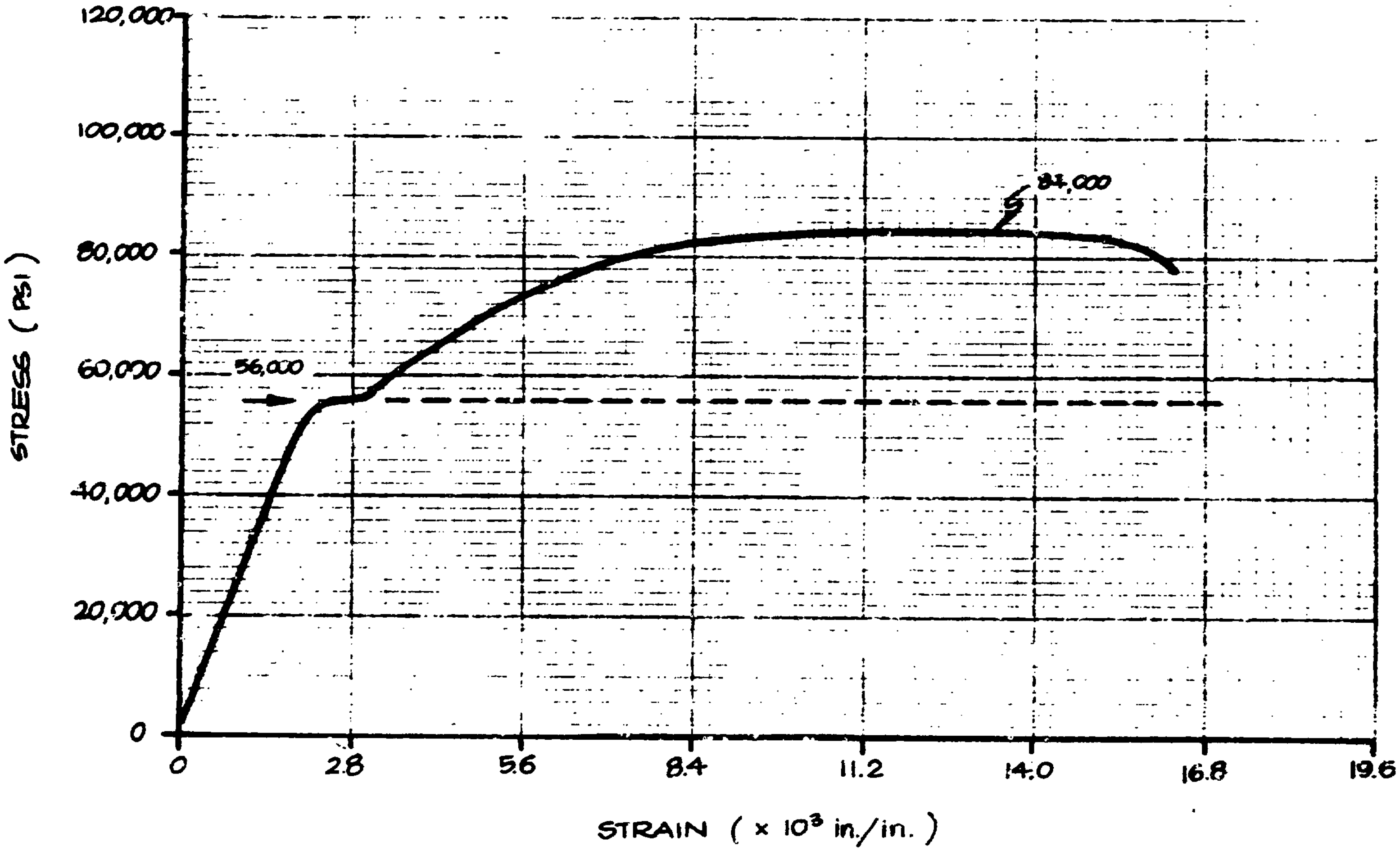

Fig. 3-2. Stress-Strain Curve for Rebar in Concrete Test Specimens.

one may get a brittle failure. Here, the steel begins to strain harden, the member is unable to take additional stresses in the concrete, and the structure will fail with a small deflection, after reaching an ultimate load. This ultimate load will, of course, be as large as predicted.

For blast resistance, ductility has always been a key factor. The more ductility the more energy that the structural system can absorb before it collapses. Concrete structures constructed in the "old days," that is, prior to the decade of the 70's, perhaps from 1960 backwards, contained steels that were produced to yield at very close to the specification, so that a grade 40 would typically yield at 40 to 45 ksi. The yield domain would be at least 10 yield deformations (rather than the one-half deformation yield currently seen), and structures did indeed behave very much like an ideally plastic material, as strain hardening seldom entered into the structural behavior. Hence, looking at the limit design concepts for structures built prior to 1970, one is very apt to encounter a very nearly ideally elasto-plastic material, like the dotted lines shown in Fig. 3-2.

Today, a grade 40 steel is entirely different, as evidenced by the solid stress-strain curve in the figure; it no longer signifies that the engineer has no better than 40,000 psi steel. In the current process of manufacturing re-bar, the steel is graded as it is manufactured—as grade 60 if it has a 60 ksi yield strength or more, and grade 40 if it has less than 60 ksi yield strength. The point is that material properties can no longer be related to grade as far as the actual structural performance and prediction go. This is clearly evident from our experience with a grade 40 steel that is virtually a grade 60 steel. As a consequence, the entire program was designed as if a grade 60 steel had been used and a design criterion of 150 psf WSD, or nominally a 250 psf allowable load as per USD. No additional adjustments were made for dynamic strength increases as the loading is not that fast.

TEST PROGRAM

The Base Case, Specimen 1

The concrete test specimen was loaded into a test frame and turnbuckles at the end were tightened sufficiently to represent the end moment that would have been induced by the dead load of the slab only — that is, if this is a chunk of a slab out of a large building floor, the slab would have continuity over the beam section and there would be a dead load moment induced such that the slope would be zero. The short cantilever section that the turnbuckle bolts are connected to is very stiff relative to the long 16-ft span between the beams; hence, as the slab is loaded with the three rams at six loading points, the moment will develop relatively equally on both sides and develop hinges, as shown in Fig. 3-3. Fig. 3-3 also shows a moment diagram with a maximum positive moment in the mid-span center of 36.72 kip/ft and a maximum negative moment at the supports or beams of minus 36.72 kip/ft. These moments are calculated theoretical moments using ultimate strength concepts. The limit design assumption is that until all three hinges (or five, looking at both sides of the support) develop, collapse cannot occur. With this assumption and limit design computation, the predicted ultimate failure strength of this slab was 826 psf, or 3,306 lbs per linear foot of slab. The actual peak load, shown in Fig. 3-4, is 875 lbs/sq ft or 3,500 lbs/linear ft. Figs. 3-4, 3-5, and 3-6 show load-versus-time, deflection-versus-time, and load-versus-deflection curves, respectively. From the load-versus-deflection curve, it can be seen that the total ductility of the slab was actually on the order of 12 to 13, which is very high, indicating that the slab is lightly or moderately reinforced and no brittle failures can occur.

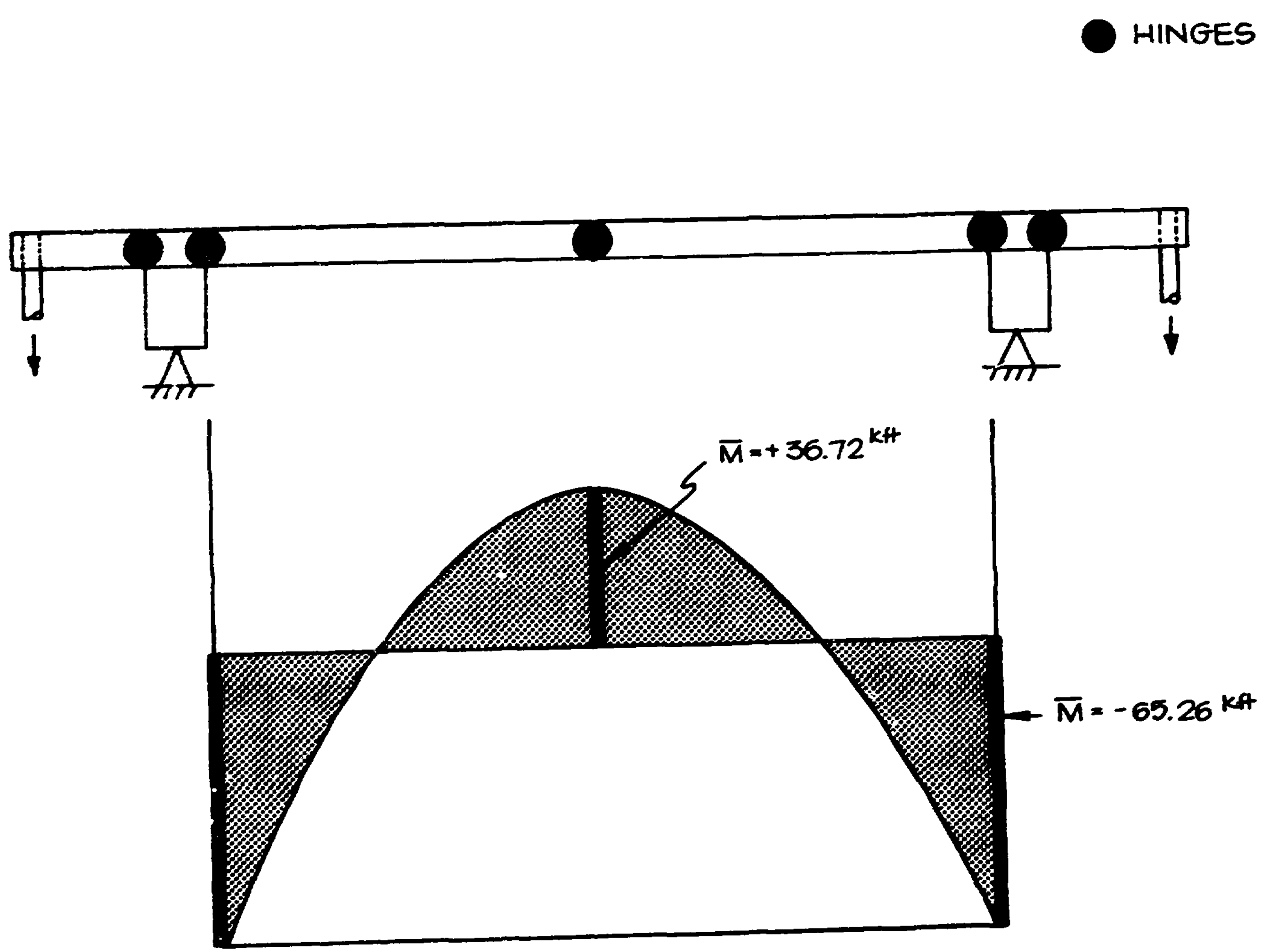

Fig. 3-3. Predicted Failure Moments for Bad Case.

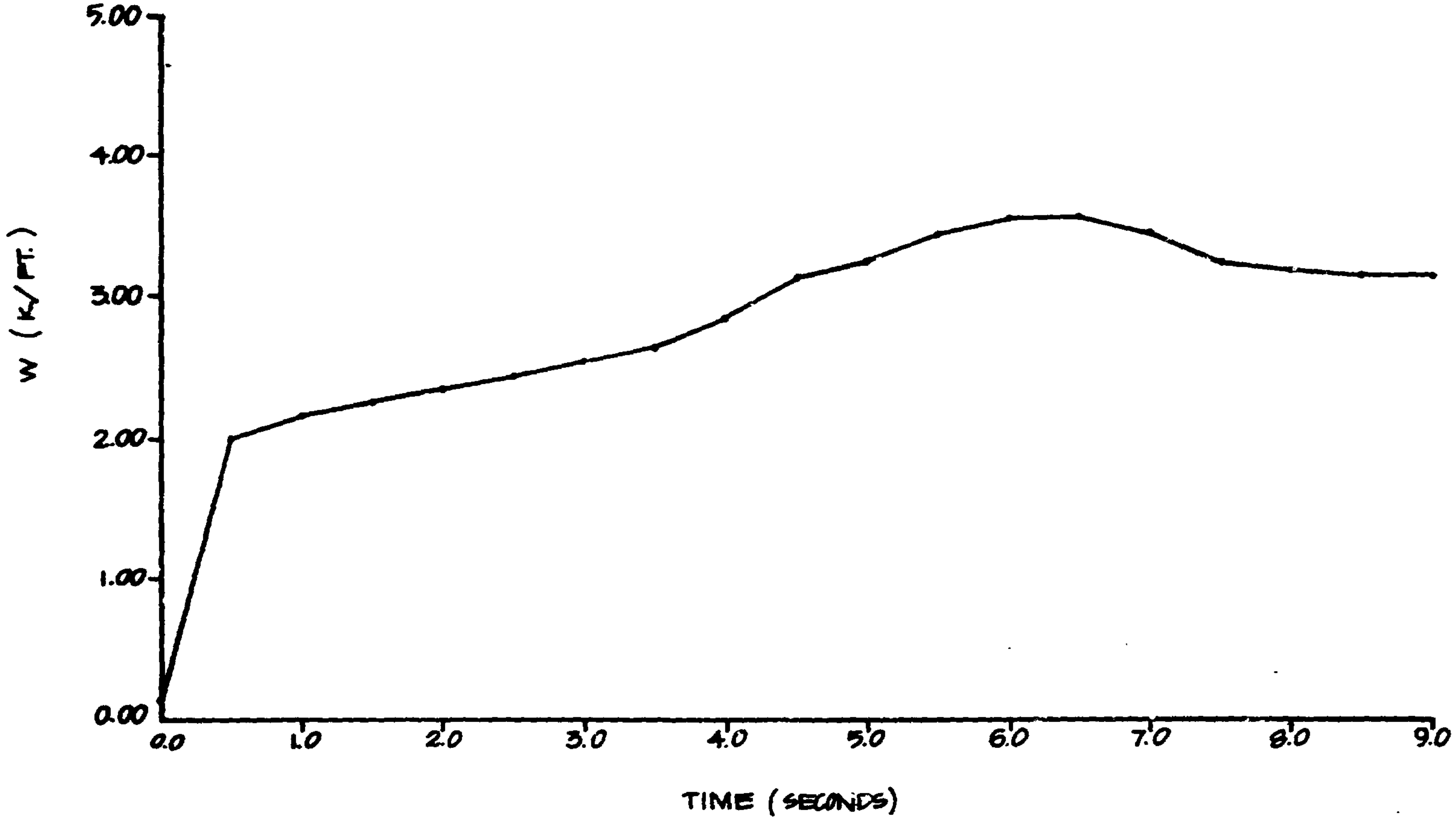

Fig. 3-4. Load vs Time, Specimen No. 1.

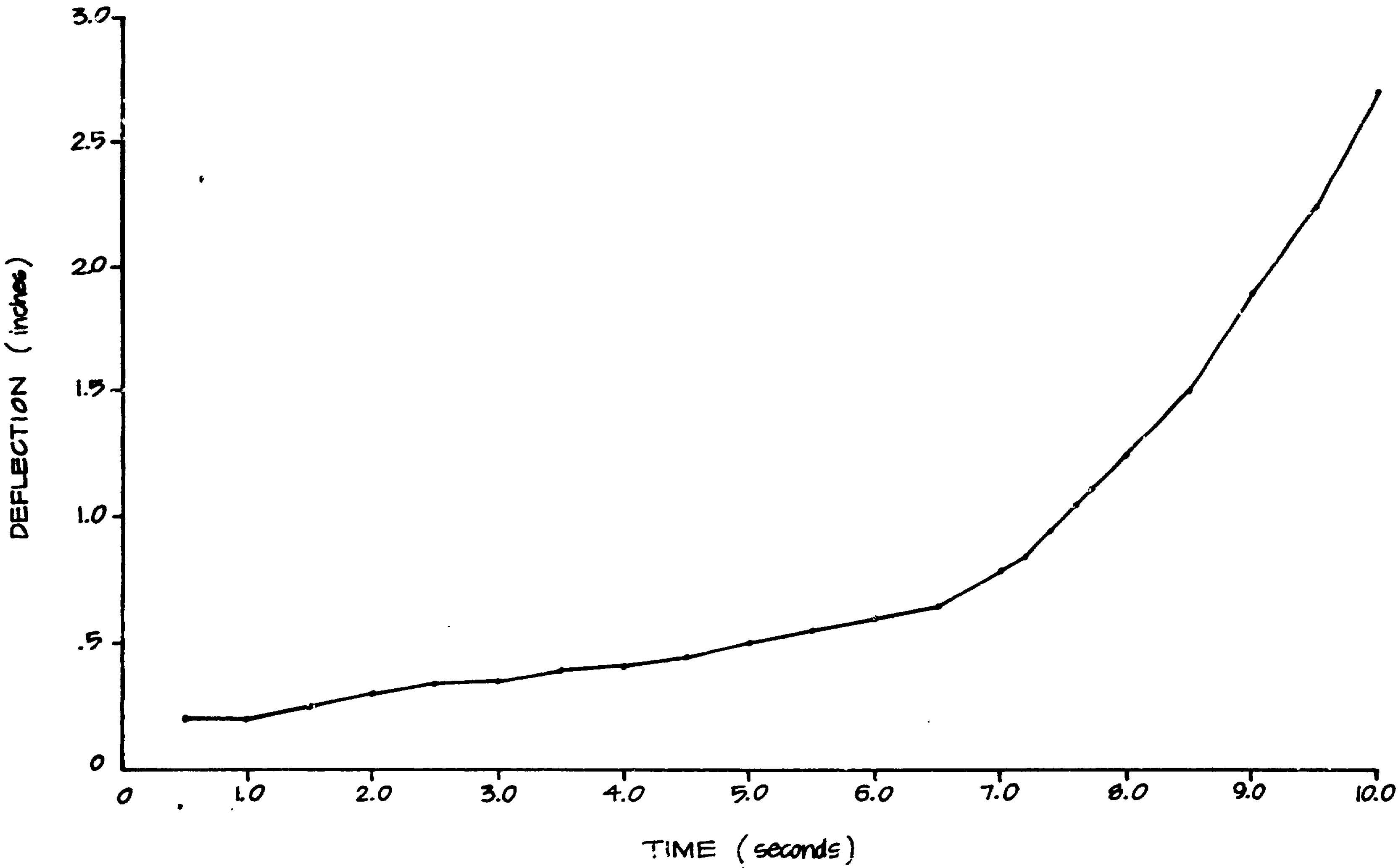

Fig. 3-5. Deflection vs Time, Specimen No. 1.

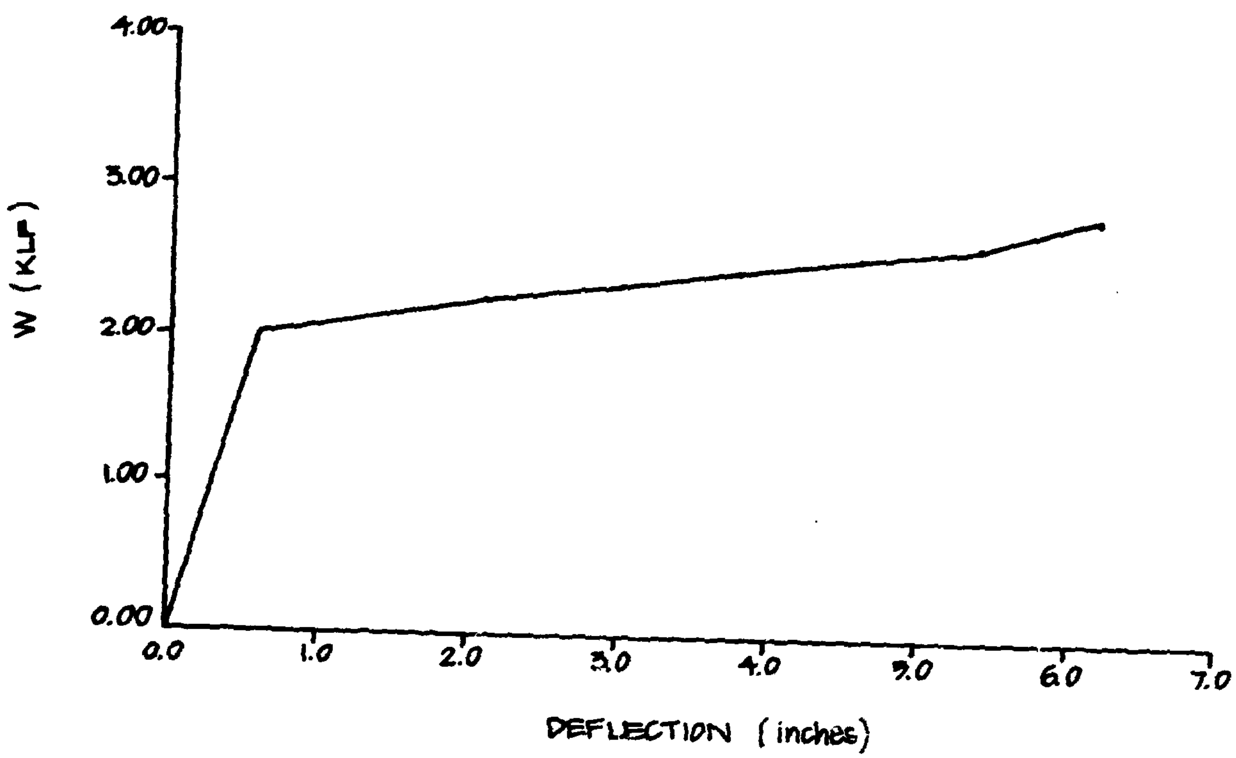

Fig. 3-6. Load vs Deflection, Specimen Nc. 1.

Specimen 2

The second test on the concrete floor systems was a test with a shore at the center. The shore used was a simple 8 x 8 post very similar to a railroad tie. The assumption was that if a slab of this nature had a shore every four feet along its centerline, it would form a yield line, or hinge, along this line of shores. The moment diagram in Fig. 3-7 shows the various hinge capacities or slab strengths at the various locations. Of course, the positive moment capacity of the slab in the middle zones is the same as a slab without a shore—36.72 kip/ft—and at the supports is still minus 65.26 kip/ft. The capacity, however, at the center of the slab to negative moment over the shore is nowhere near this capacity because the steel is in the bottom, that is, the slab is only 3/4 to 1 inch thick as far as the slab design is concerned. With the moment diagram and limit design philosophy, the ultimate capacity of the slab was predicted to be 9,914 lbs/linear ft, of 2,478 lbs/sq ft ultimate load capacity, while the actual ultimate load capacity was 2,580 psf or 10,300 lbs/linear ft, as shown in Fig. 3-8.

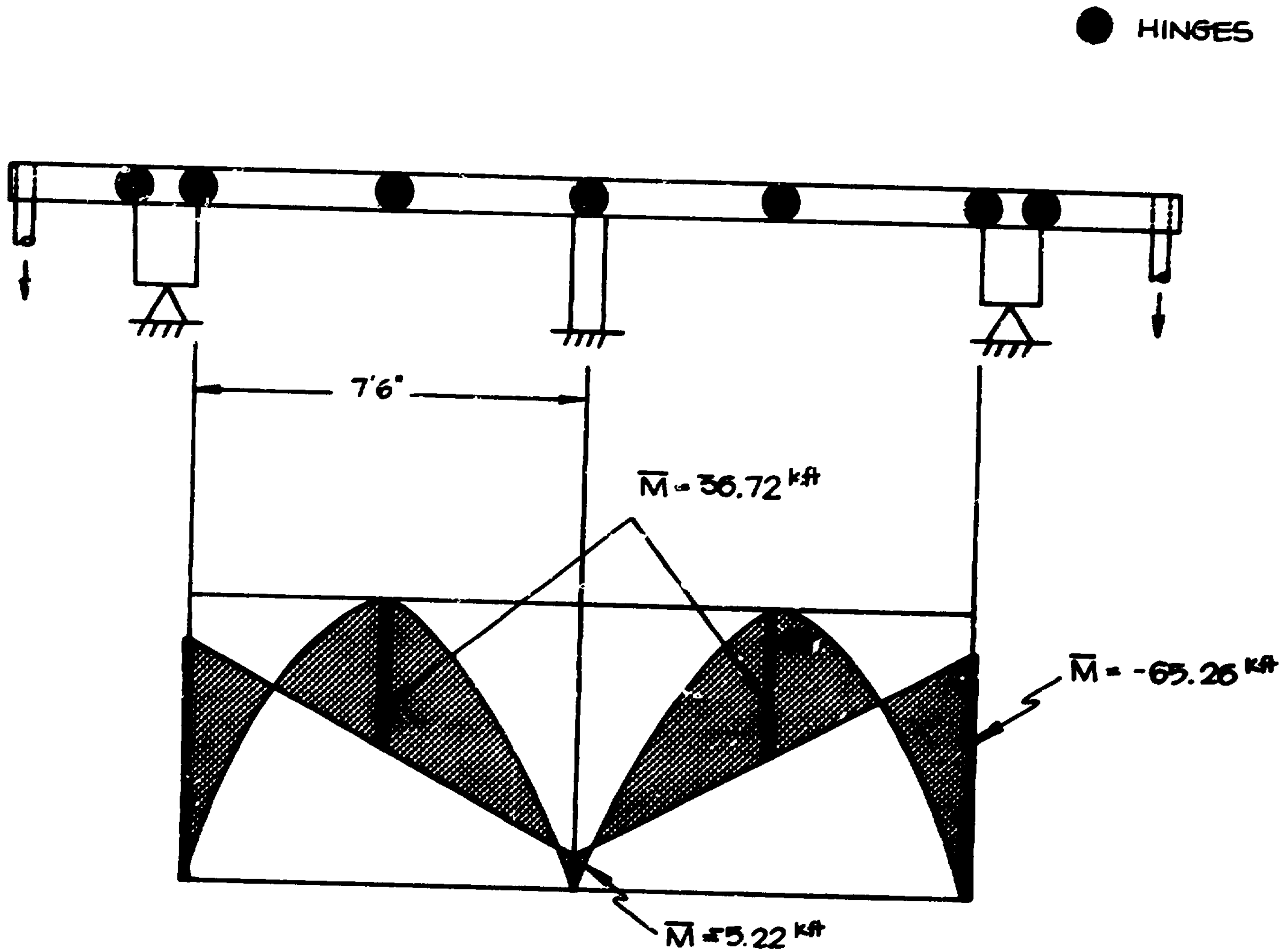

Fig. 3-7. Predicted Failure Moments for Shored Case.

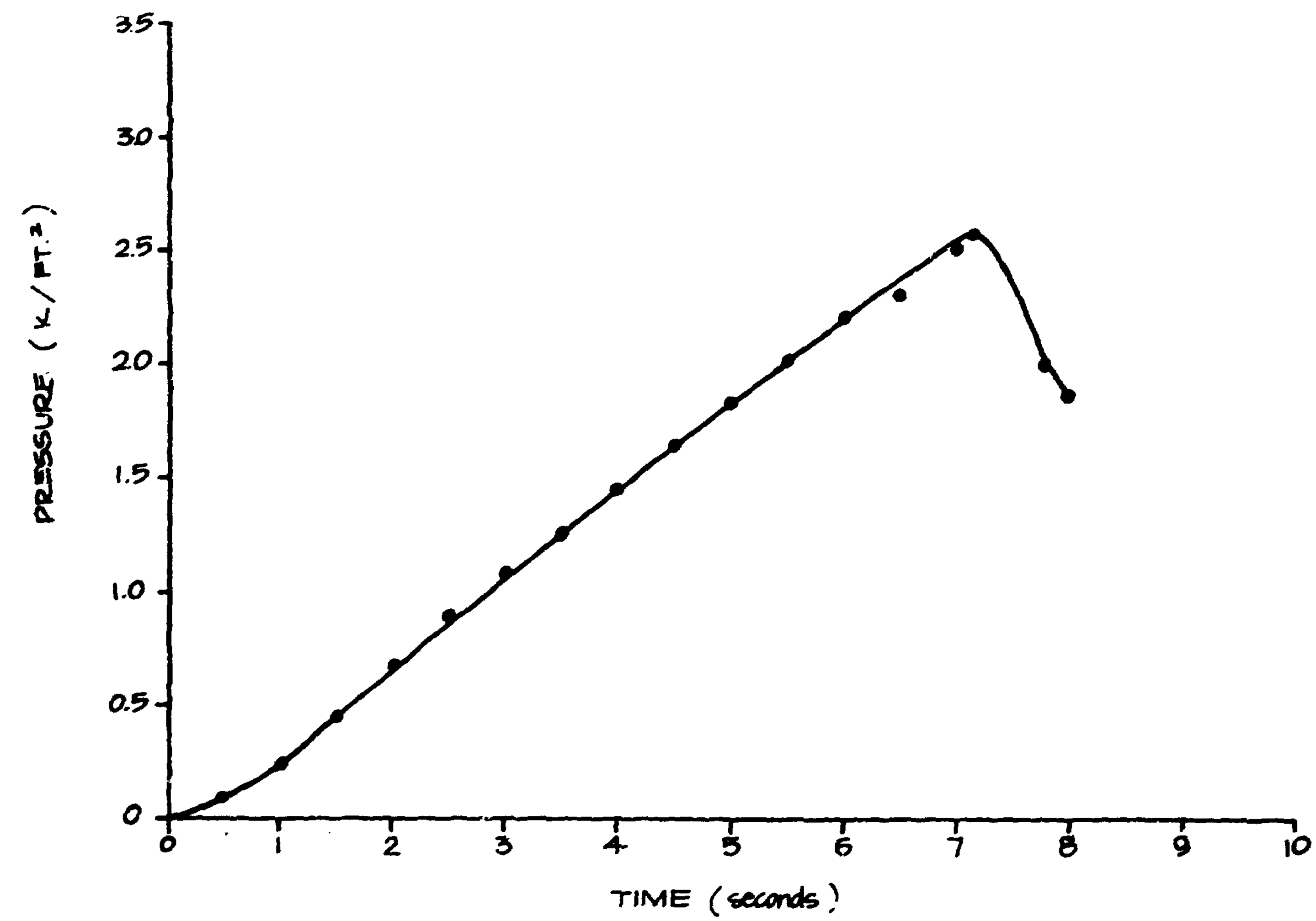

Fig. 3-8. Concrete Floor Specimen No. 2 Load History.

Specimen 3

Specimen 3 was not tested during this program but it is felt that the prediction is in order here as it demonstrates great potential for the risk area shelters. The planned shoring scheme is a simple 8 x 8 post placed approximately 5½ feet from each beam face (see Fig. 3-9). This arrangement provides a predicted failure strength of 20,000 lbs per foot 5,000 psf (about 35 psi).

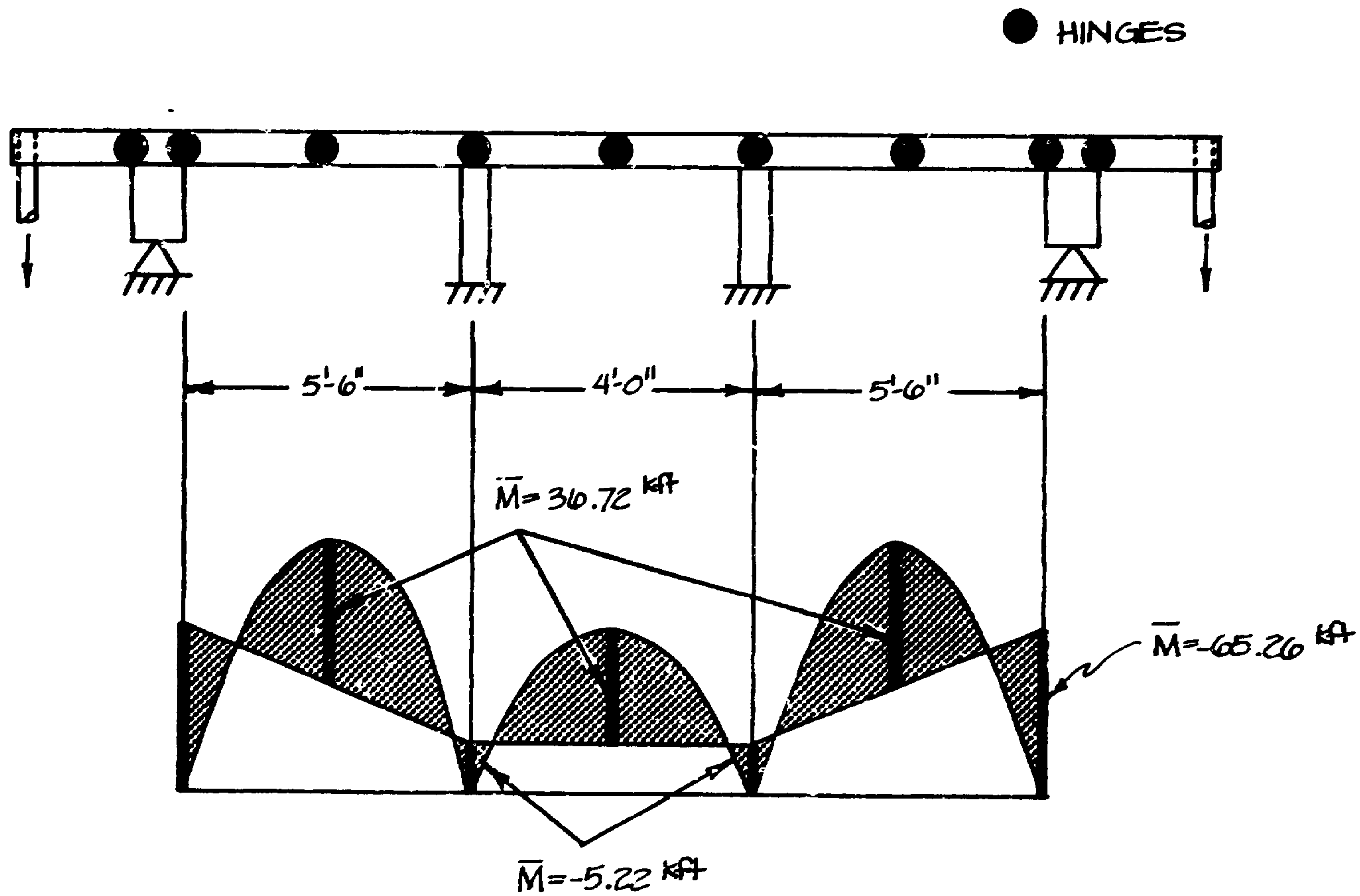

Fig. 3-9. Predicted Failure Moments for Double Shored Case.

Section 4
WOOD STRUCTURES

INTRODUCTION

Wood design and engineering is probably in its infancy with respect to ultimate strength concepts and limit design for structures. Some effort has been expended and published on the ultimate strength of simple members in bending, but generally this work has been associated with small, clear wood specimens. One of the more interesting characteristics of wood, which probably has delayed the development of the ultimate strength approach or limit design in wood structures, is the wide variability of the material. For example, in concrete a theoretical ultimate strength is calculated and then a 10% factor is applied to essentially account for the statistical unknowns in concrete beams. In wood, however, one finds far wider variabilities, not only of the statistics, but of the other characteristics of the material. For example, a clear wood may have a mean strength of 7,500 psi and a standard deviation of perhaps 1,500 psi, roughly a 20% coefficient of variation. When we move from a clear wood specimen — which is a rarety in the real world — to a graded material, this distribution will shift 50 to 60%. That is, the clear wood strength of a 7,500 psi mean value may move to as little as a 3,700 psi mean value. Then the properties may change another 25% or 35% because of moisture content. In addition, the loading rates can affect the strength of the material by as much as 200%. Throughout all these shifts in the mean values, the statistical variation or scatter of the data persists, making it rather complicated to predict the ultimate strength of a wood structural system.

In this section, the approach has been to take these items one at a time — statistics of material variability, grading, curing, aging, seasoning, loading rates, and the underlying probability aspects and combine them into a formulation that makes it possible to predict the behavior of wood or timber structures.

MATERIAL VARIABILITY*

Engineers assume considerable responsibility for the safety and performance of structures that they design. Discrepancies, however, between a given design and its performance can arise out of a poor understanding of the variability of the material being used. The responsibility of DCPA for the design and performance of structures is also great, but the potential discrepancies between performance and design are potentially far more significant since the luxury of a safety factor—as such—is removed. Hence, an understanding of material variability and properties becomes even more important than to the practicing engineer. While a comprehensive treatment of the statistical mathematics used in handling variability is beyond the scope of this text, its application to the development of allowable properties for design (and prediction of performance) will illustrate the utility of the methods.

Wood, like all other materials, displays a characteristic variability. In its simplest form, consider the frequency distribution of ultimate bending strength values of 1,000 clear straight-grained pieces of a species of wood such as Western Larch.

Fig. 4-1 is a histogram, with each vertical bar representing the number of pieces with an ultimate bending strength in the range which that bar spans on the horizontal axis. Thus, 40 pieces would break in the ranges 7,450 to 7,550 psi, five or six in the ranges 5,450 to 5,550 psi, with almost no chance of any failures in the ranges below 4,500. This is a

---

* This section of the report borrows heavily and freely from:
Ref.8) Hoyle, Robert J., "Wood Technology in the Design of Structures", Mountain Press Publishing Company, and
Ref. 9) Gurfinkel, German, "Wood Engineering", Southern Forest Products Association. We wish to ask their indulgence and thank them for a fine exposition of the fundamentals upon which this work is based.

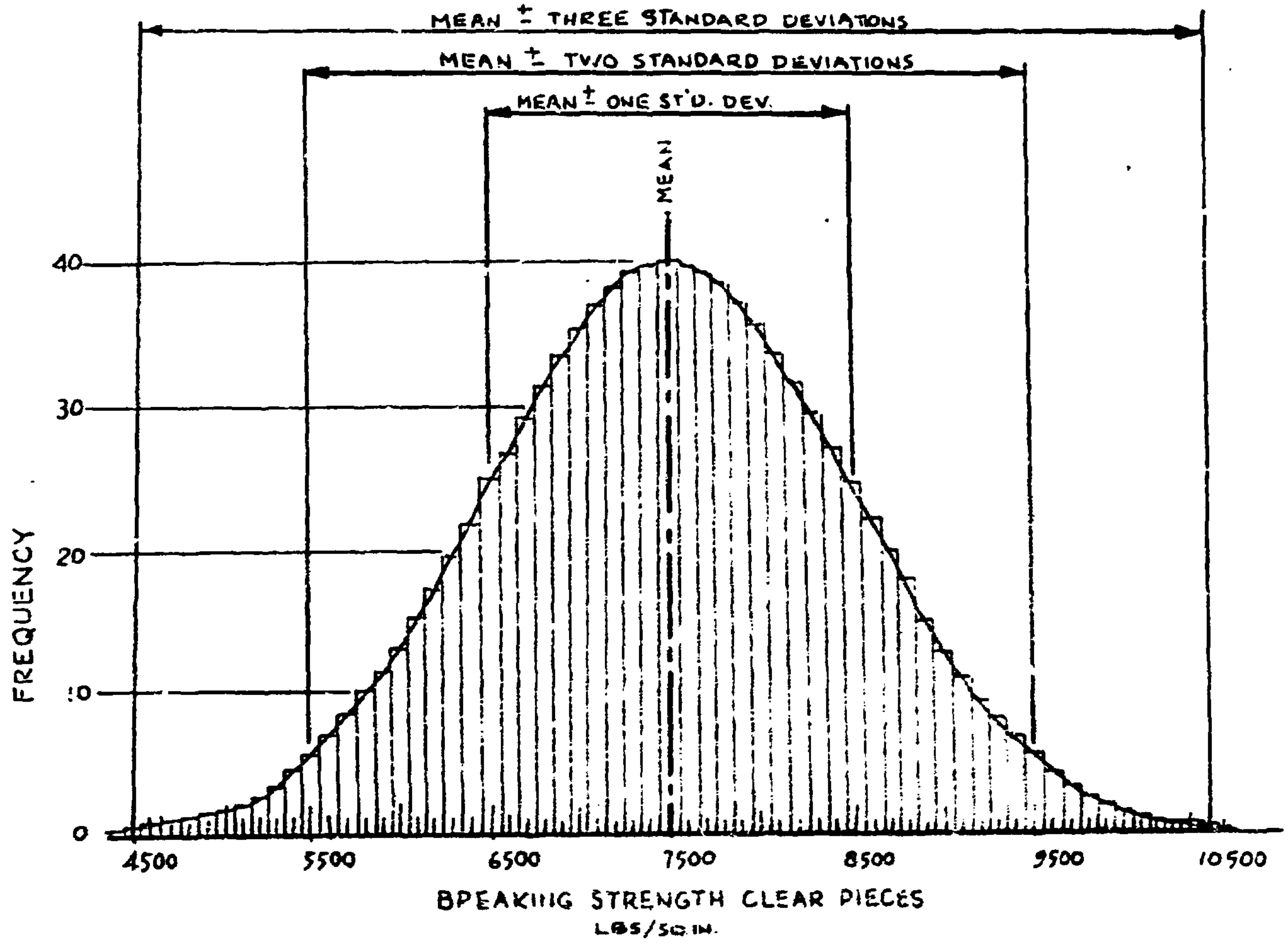

Fig. 4-1. A Normally Distributed Population of 1,000 Tests.

normal distribution obtained from a large random sampling of an infinitely large and unbiased population of material. The area under the curve (the sum of the bars) represents, in this case, the total sample of 1,000 pieces. This type of distribution is typical of wood, steel and concrete, although the values will differ from one material to another.

For a normal distribution, 67% of the pieces will lie within the mean plus or minus one standard deviation. Ninety-five percent will be in the range of the mean plus or minus two standard deviations; and 98% will be in the range of the mean plus or minus 2.33 standard deviations.

The means and standard deviations of each of the properties of the principal commercial woods in the United States and Canada, given in Ref. 10 (ASTM Standard D2555), serve as the basis for developing allowable design stresses. Table 4-1 lists a few of the species and their standard deviations, taken from Ref. 10. Using this kind of information, strength levels can be selected for any desired probability of occurrence. As an example, 98% of clear wood samples of unseasoned Western Larch may be expected to have bending strengths in the range 7,652 ± 2.33 x 1,001, or between 5,320 and 9,984 psi. Only 1% would fail below 5,320 psi. The bending strength value of the average minus 2.33 standard deviations (5,320 for Western Larch) is often called the 1% exclusion value, meaning that only one piece in 100 is likely to have a lower bending strength. Various exclusion levels for the bending strength property of Western Larch are illustrated in Table 4-2.

Table 4-1. Clear Wood Strength Values and Standard Deviations for Several Species of Wood (Unseasoned).

Species	Modulus of Rupture and Tension Parallel		Modulus of Elasticity		Compression Parallel to Grain		Shear Strength		Compression Per Perpendicular at Proportional Limit		Specific[1] Gravity	
	Avg. psi	Standard Deviation psi	Avg. 1000 psi	Standard Deviation 1000 psi	Avg. psi	Standard Deviation psi	Avg. psi	Standard Deviation psi	Avg. psi	Standard Deviation psi	Avg.	Standard Deviation
Douglas fir												
Coast	7665	1317	1560	315	3784	734	904	131	332	107	0.45	0.057
Interior West	7713	1322	1513	324	3872	799	936	137	418	117	0.46	0.058
Interior North	7438	1163	1409	274	3469	602	947	126	356	100	0.45	0.049
Interior South	5784	908	1162	200	3113	489	953	153	337	94	0.43	0.045
Southern pine												
Longleaf	8670	1387	1598	352	4300	774	1037	145	479	134	0.54	0.054
Slash	8570	1371	1588	349	4210	758	958	134	529	148	0.54	0.054
Loblolly	7340	1174	1406	309	3490	628	850	119	389	109	0.47	0.047
Shortleaf	7300	1168	1391	306	3430	619	851	119	353	99	0.46	0.046
Western hemlock	6637	1088	1307	258	3364	615	864	105	282	79	0.42	0.053
Western larch	7652	1001	1458	249	3756	564	869	85	399	112	0.48	0.048

[1]Based on volume when green and weight at 12 percent moisture content.

Table 4-2. Bending Strength Exclusion Level Values for Western Larch, An Example

Exclusion Level	Number of Standard Deviations	Exclusion Value
50.0%	0	7,652 psi
20.0%	0.68	6,971 psi
10.0%	1.28	6,371 psi
5.0%	1.65	6,000 psi
2.5%	1.96	5,690 psi
1.0%	2.33	5,320 psi
0.1%	3.00	4,650 psi

OTHER FACTORS AFFECTING DESIGN PROPERTIES

To establish design values for bending strength for wood, the 5% exclusion value on ultimate bending strength is customarily used.* The 5% exclusion level on Western Larch, for example, was about 6,000 psi (Table 4-2). This is considerably higher than the design allowable bending stress of Western Larch. Hence, there must be other considerations, these factors are set forth in Ref. 11 (ASTM D245, "Establishing Structural Grades for Visually Graded Lumber").

There are three conditions:

- o An increase in the property value due to the effect of seasoning;
- o The effect of the strength reducing defects permitted in the grade of lumber involved; and
- o A general adjustment factor (the composite result of other influences known to affect wood strength).

<u>Seasoning</u>

Seasoning effects, on the mechanical properties of wood, from Ref. 11 is reproduced in Table 4-3. To establish an allowable bending stress for lumber manufactured to 19% maximum moisture content, the increase for seasoning is 25%, etc.

<u>Strength Reducing Defects (Grading)</u>

Techniques for visually estimating the degree to which the growth features of wood reduce its performance from that to be expected from clear, straight-grained material have been developed and used for over 40 years. By measuring the effect of knot size, grain deviation and general slope, end splits, seasoning checks, and shakes (shakes are checks following the curve of growth rings, appearing as ring separations), and

* 5% exclusion value applies to all properties except compression perpendicular to grain and elastic modulus. The latter are not ultimate properties, averages are the basis for allowable values.

Table 4-3. Modification of Allowable Unit Stresses for Seasoning (Lumber Four Inches and Less in Nominal Thickness)

	Property	Percentage Increase in Allowable Stress Above That of Green Lumber When Maximum Moisture Content is:	
		19 Percent	15 Percent
F_b	Extreme Fiber in Bending (Modulus of Rupture)	25	35
F_t	Tension Parallel to Grain	25	35
F_v	Horizontal Shear	8	13
$F_{c\perp}$	Compression Perpendicular to Grain	50	50
F_c	Compression Parallel to Grain	50	75
E	Modulus of Elasticity	14	20

These adjustment factors apply to all the principal structural wood species. Exceptions are: Eastern Red and Incense Cedar, Eastern Hemlock, Subalpine Fir and Redwood, species not widely used for structural work. Adjustment factors for these exceptions are given in Ref. 11.

systematically codifying these characteristics, strength ratio estimating tables have been developed. These are published in Ref. 11 and are presented in Table 4-4. The concept of strength ratio has been created for visual grading and is defined as the ratio of that member's strength to that which it would have been if no weakening characteristics were present, i.e., 54% of the clear piece.

Bear in mind the strength ratio of a grade is the minimum strength ratio permitted in that grade. Within any single grade the strength ratio of pieces will vary from the minimum permitted up to the minimum permitted by the next higher grade. Furthermore, since minimum strength ratios for all of the properties of a piece do not occur simultaneously, some pieces that might be in one grade on the basis of the minimum strength ratio for compression, may be forced down into the next lower grade on the basis of the strength ratio in flexure. For such pieces, the compression strength ratio may actually be above the minimum value for the higher grade. Circumstances of this kind extend the range of strength ratios in any grade somewhat above the threshold value for the next higher grade.

Adjustment Factors

The third consideration in allowable design strength development is the general adjustment factor. It brings together in one number, several phenomena that are known to affect each of the mechanical properties of wood, as summarized in Table 4-5.

This general adjustment factor is in effect a safety factor applied to "Normal Duration Loading". That is, of the 1/2.1 factor about 1/1.6 is for the duration effects characteristic of timber. The other portion, about 1/1.3 is a safety factor that is used to cover other random variables not timber characteristics. Hence, the 1/1.3 will be dropped at this point in the development of the probabilistic timber properties.

Table 4-4. Strength Ratios of WWPA & WCLIB Grades (1970 Rules)

Grade Name[3]	Strength Ratio For					
	F_b[1]	F_t	F_v	$F_{c_\perp}$	F_c	E[2]
Light Framing & Studs						
Construction	32	19	50	100	56	80
Standard	18	10	50	100	46	80
Utility	9	5	50	100	30	80
Studs	24	14	50	100	30	80
Structural Light Framing And Appearance						
Select Structural	63	37	50	100	78	100
No. 1	54	31	50	100	62	100
Appearance	54	31	50	100	74	100
No. 2	44	26	50	100	49	90
No. 3	24	14	50	100	30	80
Structural Joists and Planks And Appearance						
Select Structural	54	36	50	100	69	100
No. 1	46	31	50	100	62	100
Appearance	46	31	50	100	74	100
No. 2	38	25	50	100	52	90
No. 3	22	14	50	100	33	80
Beams & Stringers						
Select Structural	61	41	50	100	75	100
No. 1	51	34	50	100	63	100
Posts and Timbers						
Select Structural	57	38	50	100	79	100
No. 1	46	31	50	100	69	100

[1] These values include a depth factor component for grades of lumber 4" and less in thickness. For 5" and thicker lumber, size effect adjustments are proper.

[2] Called a "Grade Quality Factor" since E is not a strength property.

[3] For "Dense" grades (not shown), a 17 percent increase is allowed for all properties except E. E may be increased 5 percent for "Dense" grades.

Table 4-5. Elements of the Adjustment Factor

Property		Normal Duration of Load Factor	Manufacture and Use Factor	Stress Concentration	End Position	ℓ/d	Adjustment Factor
F_b	Bending	10/16	10/13	--	--	--	1/2.1
F_c	Compression Parallel to Grain	2/3	4/5	--	--	--	1/1.9
F_v	Shear	10/16	8/9	4/9	--	--	1/4.1
F_t	Tension Parallel to Grain	10/16	10/13	--	--	--	1/2.1
$F_{c\perp}$	Compression Perpendicular to Grain	11/10	10/11	--	2/3	--	1/1.5
E	Elastic Modulus	1	--	--	--	1/0.94	1/0.94

Allowable Design Properties

The influences of seasoning, strength ratio, and general adjustment factor are applied as shown in Table 4-6 to produce the design properties. In the case of bending strength, a depth factor is also applied which, for nominal 12-inch dimension, is 0.36. Depth factor is a strength reducing phenomenon discussed later in the design of flexural members.

The values in the last column of a table such as Table 4-6 would be rounded off to the nearest 50 psi for all strength properties except shear, which would be rounded to the nearest 5 psi. Elastic modulus is rounded to the nearest 100,000 psi.

The foregoing has been an illustrative example using Western Larch. The allowable values will not agree exactly with those for No. 1 Structural Western Larch given in the National Design Spec because Western Larch is combined with Douglas Fir, a very similar species, growing on the same forest sites, as permitted by the procedures of ASTM D245 (Ref. 11).

Probabilistic Interpretation

A probabilistic interpretation of the preceding material could be based on the simple assumption of operating on a random variable by a constant multiplier. That is, if a property such as bending stress is a random variable (r.v.) and some constant (k).

Let X be a random variable with mean $\overline{X}$ and variance σ_X^2 then the expected value of X, written $E[X] = \overline{X}$, and the variance of X, written (from Ref. 12)

$Var[X] = \sigma_X^2$ may also be written

$$Var[X] = E[X^2] - E^2[X]$$

Define a new random variable $Y = kX$ then the

$$E[Y] = E[kX] \quad \text{or,}$$

$$E[Y] = kE[X]$$

Table 4-6. Allowable Properties for a Sample Stress Grade

Property	Clear Wood[1] Strength Value psi	Strength Ratio ÷ 100 (Minimum)	Seasoning Increase for 19% Max. M.C.	General Adjustment Factor	Depth Effect	Allowable[2] Property psi
F_b	6,000	0.54	1.25	1/2.1	0.86	1,660
F_c	2,826	0.62	1.50	1/1.9	--	1,380
F_v	729	0.50	1.08	1/4.1	--	96
F_t	6,000	0.31	1.25	1/2.1	--	1,100
$F_{c\perp}$[3]	399	1.00	1.50	1/1.5	--	399
$E \div 1000$	1,458	1.00	1.14	1/0.94	--	1,770

[1]Unseasoned, 5% Exclusion value, except E and $F_{c\perp}$ which are average values.

[2]For use at 19% maximum moisture content.

[3]It is noted that the mean value is used in establishing the allowable for $F_{c\perp}$. Further, this mean value is based on the yield stress not an ultimate stress.

Hence, the mean value of

$$\bar{Y} = kX \qquad \text{and}$$

$$Var\,[Y] = E\,[k^2X^2] - E^2[kx]$$

$$Var\,[Y] = \sigma_Y{}^2 = k^2\sigma_X{}^2$$

Hence, if a strength property such as the modulus of rupture (F_b) is a random variable with the

mean $E\,[F_b] = \bar{F}_b$

and $Var\,[F_b] = \sigma_{F_b}{}^2$

then kF_b would have a mean of $E[kF_b] = k\bar{F}_b$

and $Var\,[kF_b] = k^2\sigma_{F_b}{}^2$

or a standard deviation of

$$\sigma_{kF_b} = k\sigma_{F_b}$$

<u>Note</u> the coefficient of variation (the standard deviation divided by the mean) remains constant, i.e.

$$\frac{\sigma_{F_b}}{\bar{F}_b} = \frac{k\sigma_{F_b}}{k\bar{F}_b} = \sigma_{F_b}$$

Of these, the items that affect the strength of wood summarized in Table 4-6, only the strength ratio (visual grading) and the seasoning parameters are fundamental characteristics of the wood. Continuing with the examples of Western Larch No. 1, it follows from Table 4-1 that

$$E\ [F_b] = F_b = 7{,}652 \text{ psi}$$

and Std. dev. $= \sigma_{F_b} = 1{,}001$ psi

Further, the constant to be used in establishing the probability distribution for the material is (from Table 4-6):

$$k = \underset{\text{grading}}{(0.54)} \quad \underset{\text{seasoning}}{(1.25)}$$

or $\quad k = 0.675$ and

$$E\ [kF_b] = 0.675(7{,}652 \text{ psi}) = 5{,}165 \text{ psi},$$

and

$$\sigma_{kF_b} = 0.68\ (1{,}001 \text{ psi})$$

$$\sigma_{kF} = 676 \text{ psi}$$

This distribution implies a 5% exclusion value (from Table 4-2) of the design distribution, that is:

$$F_b(5\%) = 6{,}165 - 676\ (1.65)$$

$$F_b(5\%) = 4{,}050 \text{ psi}$$

A further implication is that the design allowable of $F_b = 1{,}660$ can now be appreciated in terms of the distribution and have a probability statement made about it, i.e.,

> The probability that $F_b \leq 1{,}600$ is equal to the area of the distribution function for $-\infty$ to 1,600.

Fig. 4-2 illustrates what the grading has done to the distribution. That is, by seasoning and grading the timber, the distribution has shifted toward the design stress and tightened, i.e., the standard deviation has been reduced. However, the coefficient of variation has remained the same, as illustrated in Fig. 4-2. The normal probability distribution, also

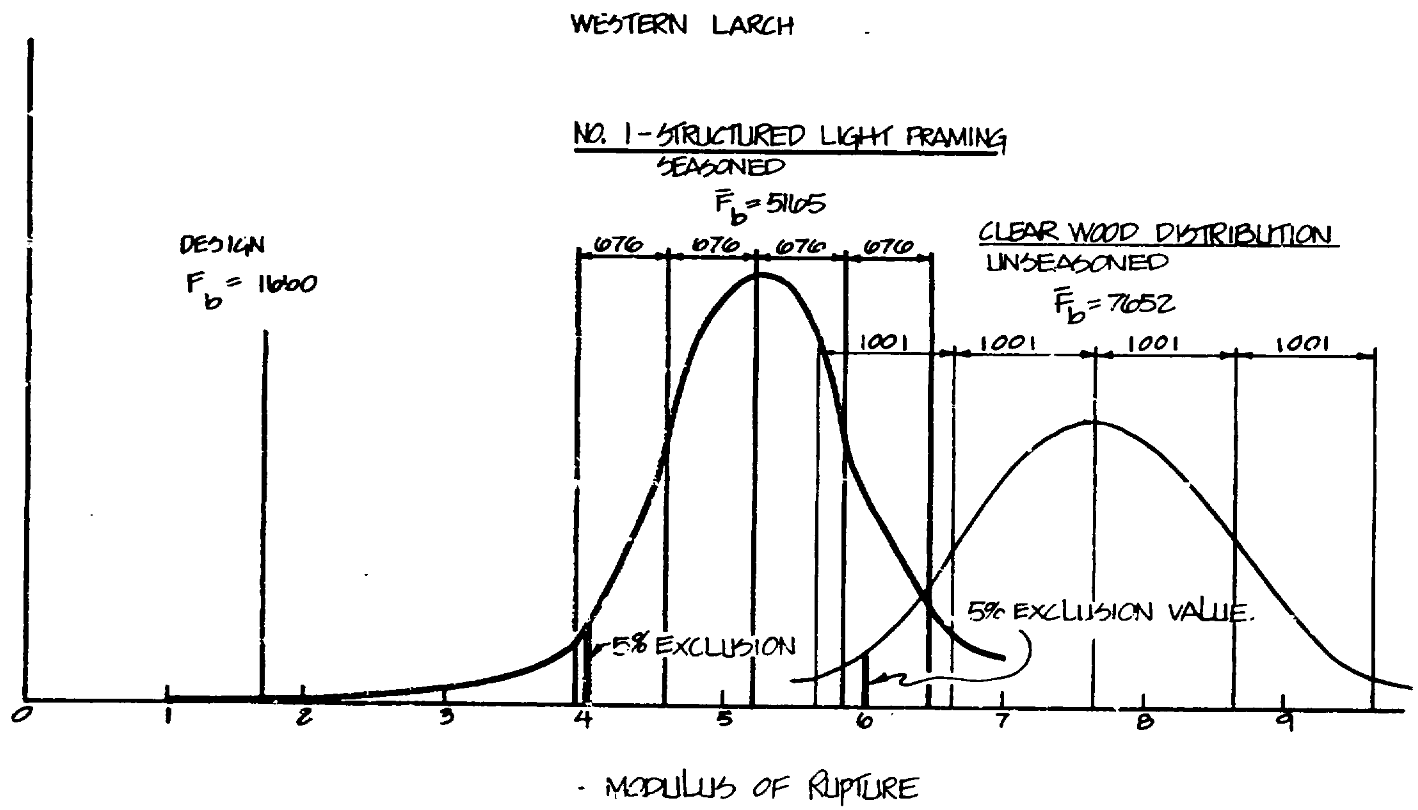

Fig. 4-2. Distribution Modification by Grading.

shown in this figure, is the distribution that would be obtained if sufficient No. 1 - Structural light framing Western Larch seasoned bending specimens were tested, that is, normal with mean = 5,165 psi and standard deviation = 676 psi, N(5165,676).

Load Duration Effects (from Ref. 9)

Consider the case of identical wood specimens loaded with large sustained loads of different values. Failure occurs at different times; the greater the load, the shorter time to failure. Below a certain load, however, the specimens do not fail independent of the duration of the load. If the results of these tests are plotted, using strength as ordinate and time-to-failure as abscissa, a curve such as shown in Fig. 4-3 is obtained. The asymptotic nature of the curve indicates that, although strength is reduced with duration of loading, a minimum strength, termed sustained strength, exists which is independent of time.

The difference in behavior between a specimen loaded to $F_0 < F_0$ sust, case I, and a specimen loaded to $F_0 > F_0$ sust, case II, is illustrated in Fig. 4-4. For case I, the deformation increases, but takes place at a reduced rate of change with time; in other words, in the course of time the deformation approaches a certain limit. For case II, deformation increases constantly with time. A deformation continuing to increase, but at a decreasing rate, even after a long period of time does not presage failure. On the other hand, deformation that continues to increase at a uniform rate may be a danger signal, and when the rate of change accelerates, failure may be imminent.

Loads acting on structures are not all sustained indefinitely. As a matter of fact, only the deadweight of the structure and other similar weights are permanent loads. All other loads such as produced by wind, live load, snow, earthquake and impact are applied for certain periods and are reduced in part, or altogether, at other periods. For design purposes, the total duration of the repeated loads is estimated as. 10 years for live load, 2 months for snow load, 7 days for temporary construction loads,

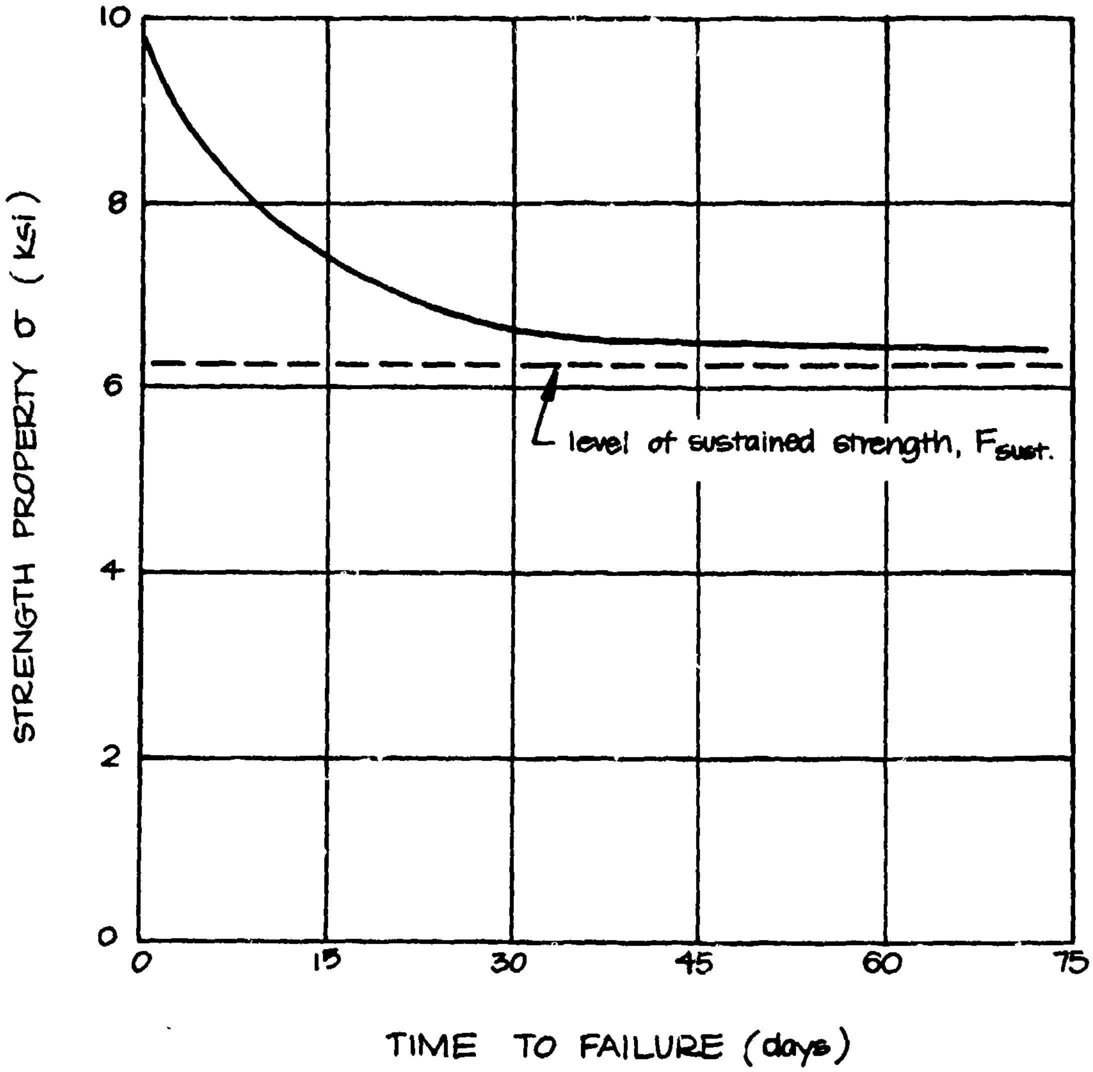

Fig. 4-3. Variation of Strength with Duration of Loading.

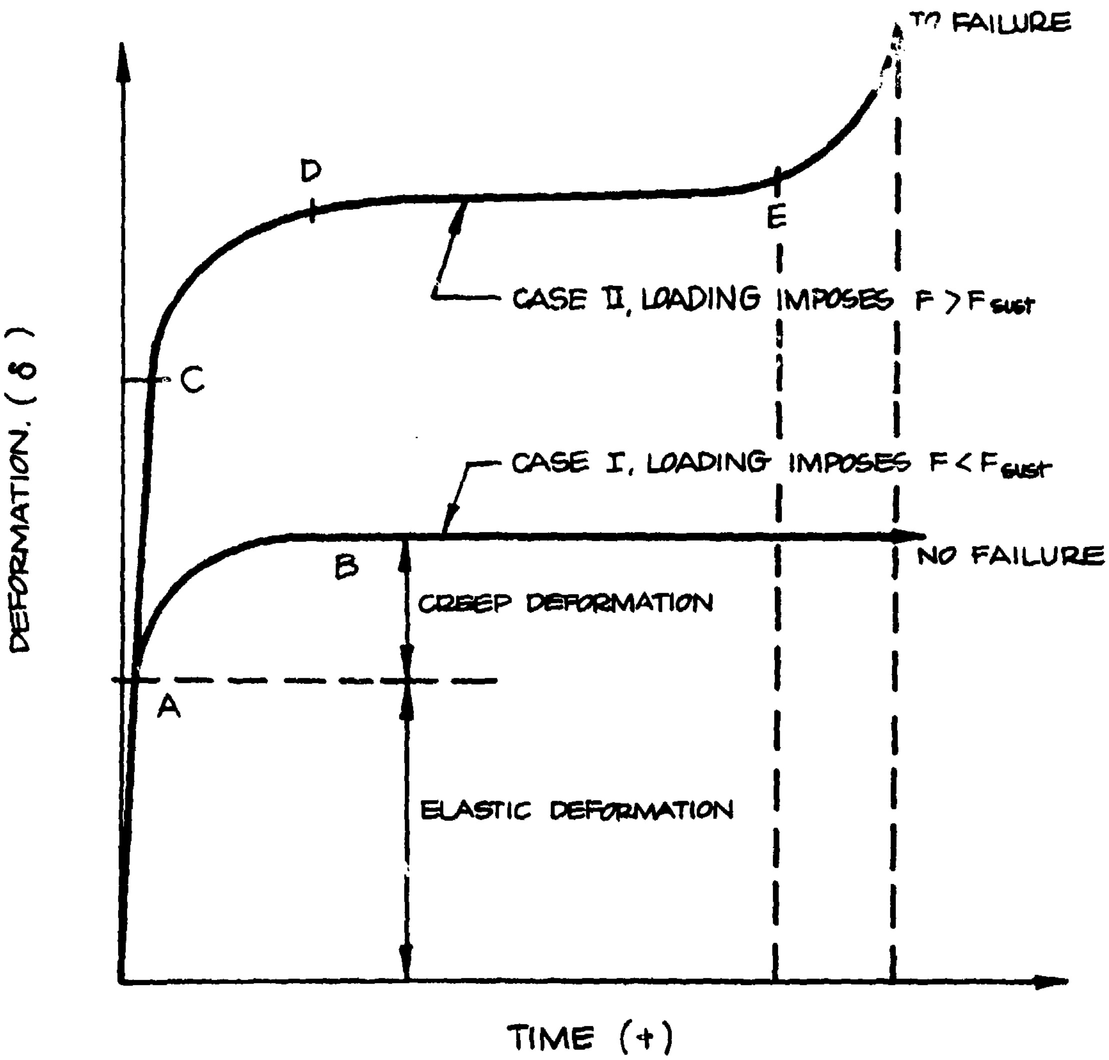

Fig. 4-4. Variation of Deformation with Time for Two Identical Wood Specimens Loaded to Different Stress Levels.

1 day for wind or earthquake load and 1 second for impact loads (see Fig. 4-5).

Based on the existing evidence of variation of strength with duration of loading, strength properties determined in tests that last usually from 6 to 8 minutes can be converted to other durations of loading. Strength properties for the so-called normal loading conditions* may be determined by multiplying standard strength properties by the factor 1/1.6; the same can be done for other loading conditions using corresponding factors. Present design of wood structures is based on service load conditions and the conversion of strength properties for different durations of loading has moderate practical value. However, the concept remains useful for the determination of allowable stresses for different loading conditions, as shown in Fig. 4-5. It will also be very useful in this work for DCPA where ultimate strength values are very important.

Based on the foregoing discussion of the load-duration effects on the behavior of wood structures, it becomes obvious that the general adjustment factor(s) shown in Table 4-5 are composed of the duration factor (1/1.6), which is a property of wood and the other factors are applied factors. Hence, only the duration effect shifts the distribution of strengths.

The manufacture and use factors in Table 4-5 came from a consideration of such things as the effect of fastenings, the possibility of broken edges or other damage, possible machine skip in dressing, small end splits that could occur after construction, and drilling of holes for wiring and plumbing, probability of error in grading, and shrinkage variability.

The stress concentration factor is listed separately because it is due to the shape and behavior of the standard test specimen rather than load duration, manufacturing or use practices.

---

* Normal loading is considered as continuous or cumulative for 10 years over the life of the structure.

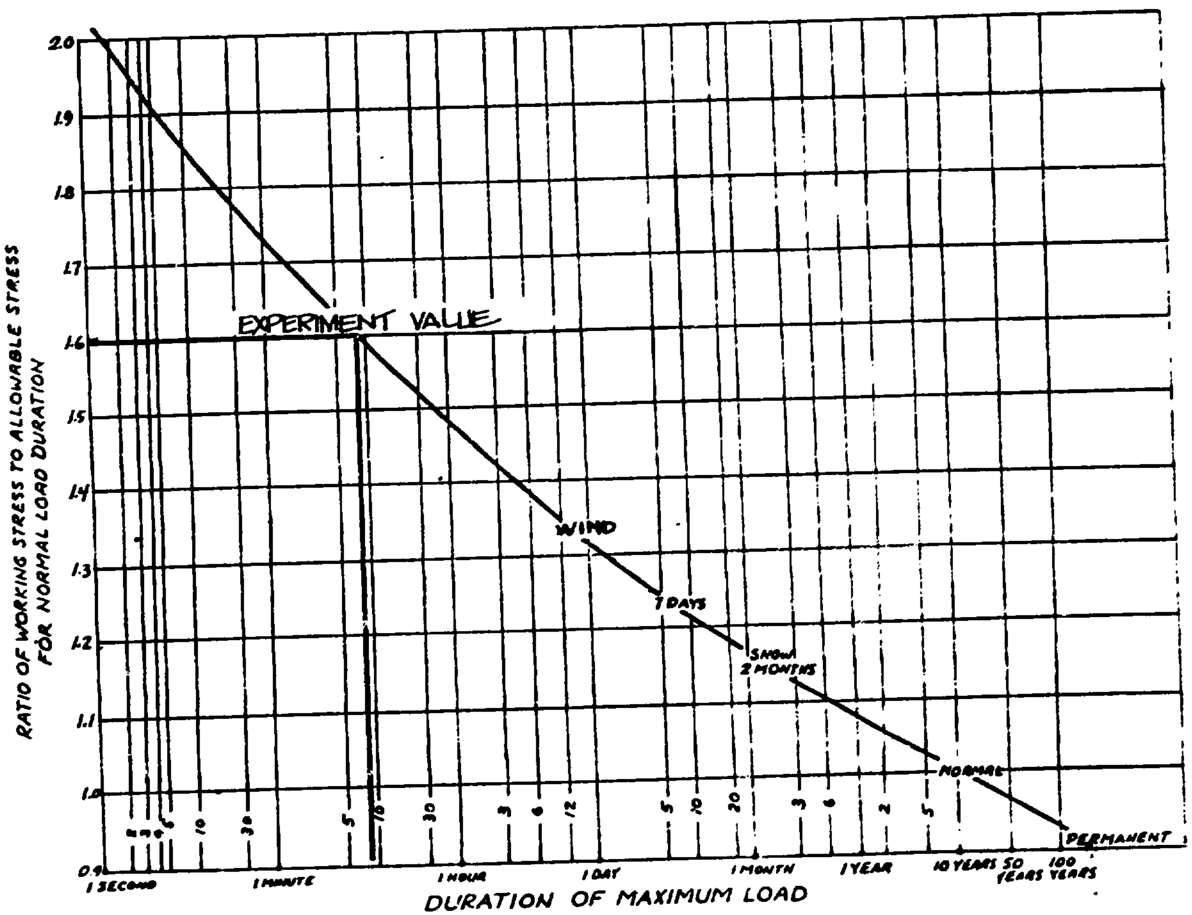

Fig. 4-5. Relation of Working Stress to Duration of Load.

The span-depth (ℓ/d) factor used to adjust elastic modulus arises from the influence of internal shear deformation in bending members. The apparent elastic modulus of pieces with uniform loads at typical ℓ/d ratios in the 18-24 range encountered in practice, is somewhat higher than the value obtained from the standard 2" x 2" x 30" test specimens loaded at mid-point on 28" spans. Under laboratory test conditions (Reference 13), the value of E is 94% of the value at $\ell/d = 21$ with uniformly distributed load as generally assumed for design of building structures.

In order to generate the probability distribution for wood subjected to "normal" loadings the distribution must be shifted for load duration effects. Continuing with the Western Larch example: The distribution shown on Fig. 4-2 with parameters

$$E\,[F_b] = 5{,}165 \text{ psi}$$

and

σ_{F_b} = 676 psi, is the distribution for <u>seasoned</u> and <u>graded</u> No. 1 – Structural light framing and a load duration of 5 to 8 minutes. Hence, for the "normal" loading

$$E\,[F_b] = E[\frac{1}{1.6}(5{,}165)] = 3{,}228 \text{ psi}$$

and

$$\sigma_{F_b} = \frac{1}{1.6}\,(676) = 422 \text{ psi}$$

This distribution is illustrated in Fig. 4-6, and then put into a more useful form on Fig. 4-7. The 5% exclusion values is F_b = 2,532 psi and the probability of failure at a load of 1,660 psi is less than 1 in 10,000.

Since there is a possibility of very rapid (blast) loadings in the DCPA environment, some study of loadings more rapid than testing (ASTM type) is in order. Fig. 4-7 implies that for impact types of loading the strength of wood is twice as high (at 50% exlusion) as in the normal loading case (i.e., $\overline{F}_b$ = 3,228 vs F_b = 1,660). Considerable attention has been given the resistance of structural materials exposed to high

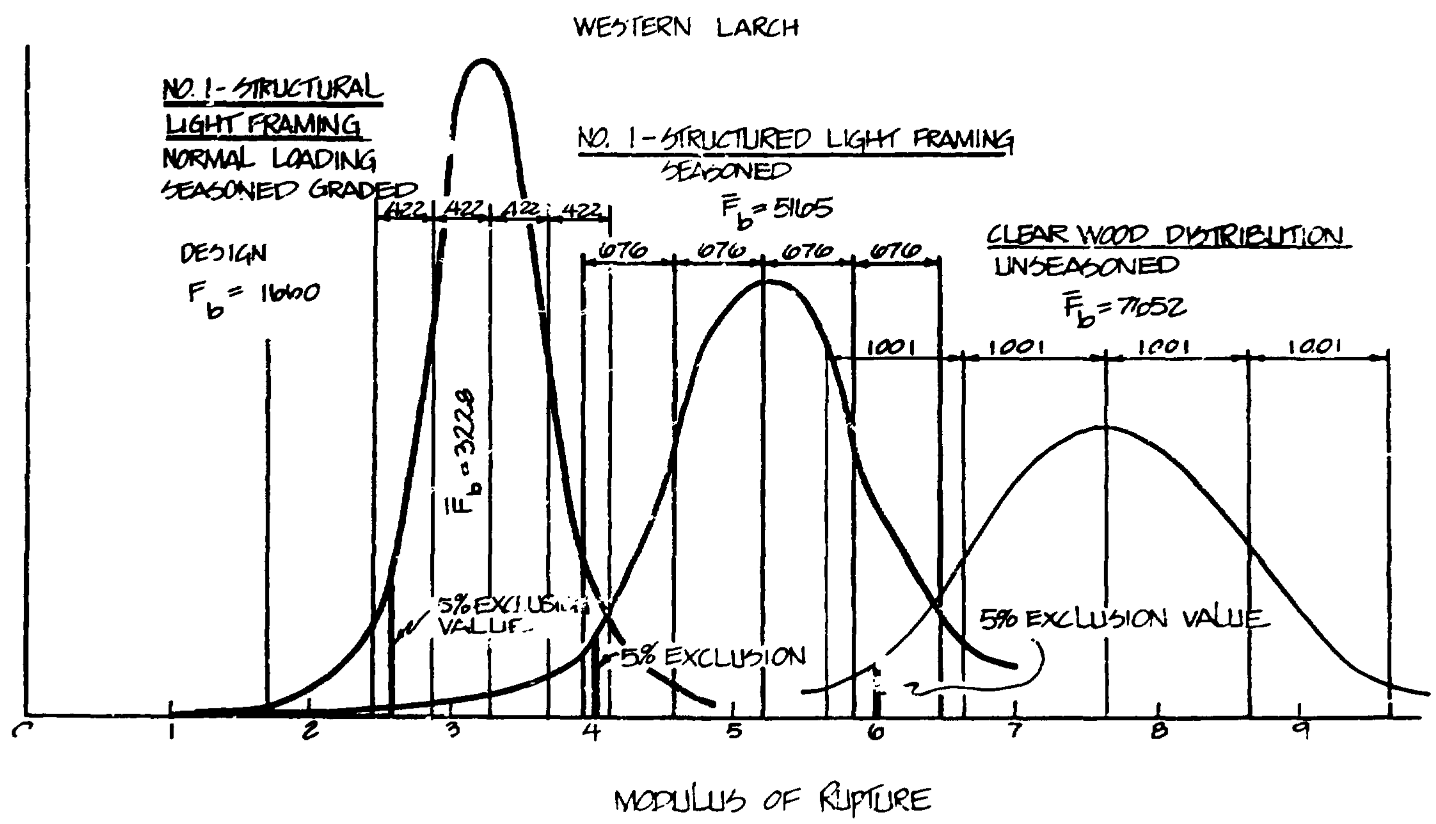

Fig. 4-6. Distribution Modification by Grading and Seasoning.

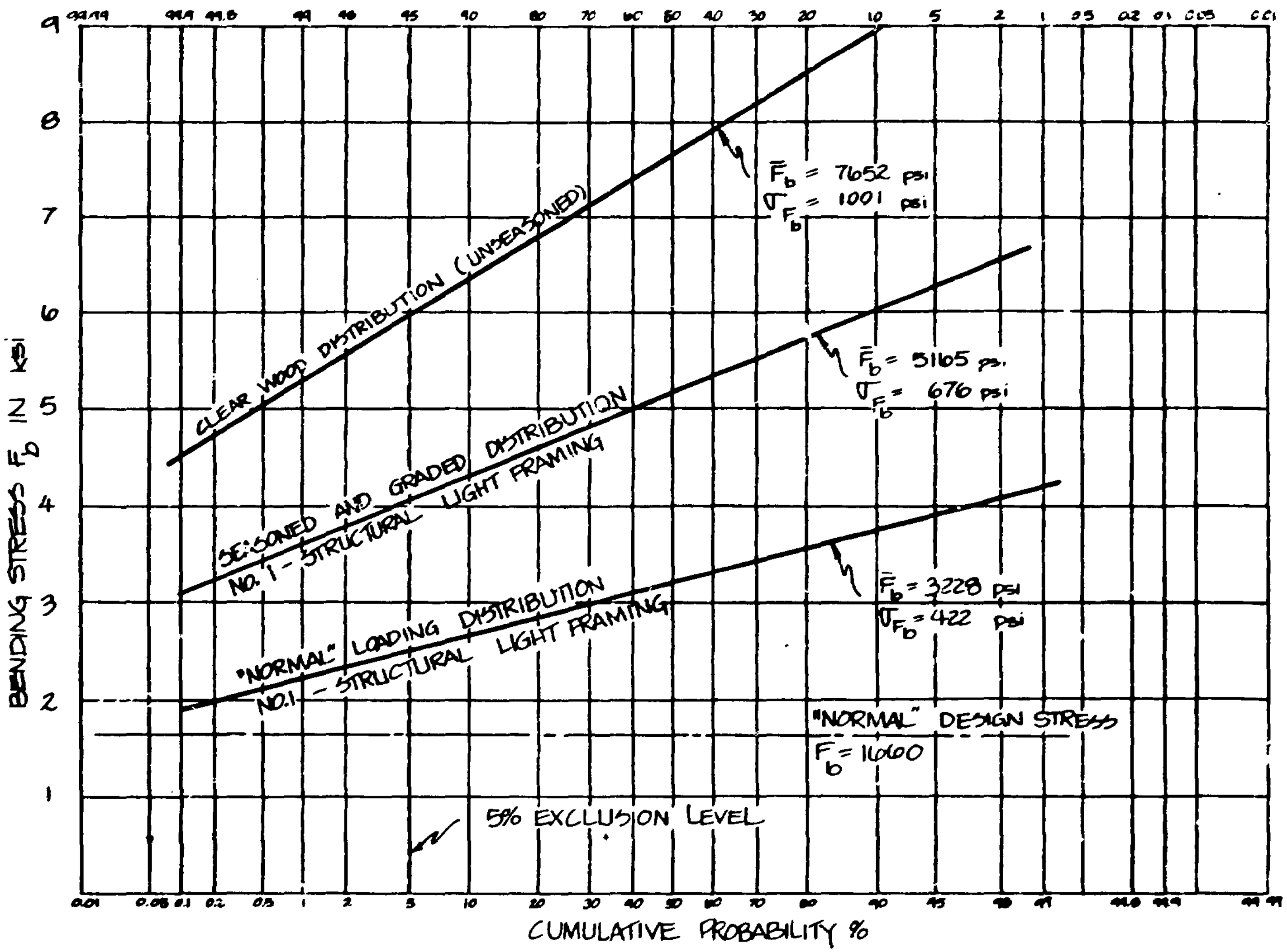

Fig. 4-7. Probability Distribution for Western Larch.

loading rates since the advent of atomic blasts. Ref. 6 provides a rather extensive program and considerable data on clear specimens in bending, shear compression, etc. of both green and dry, or seasoned (moisture content ≈ 11%), Coastal Douglas Fir. Before presenting some of this data for use it will be instructive to look at the strain rates implied by this study. The ultimate strains that can be expected in a timber are on the order of 0.005 to 0.006 in./in., Ref. 9.

Figs. 4-8 and 4-9 from Ref. 6 illustrate the increase in strength achieved by actual tests, (Tables 4-7 and 4-8 are the data for curves):

For the green timber

Static	Dynamic Speed 2
$\bar{F}_b = 7{,}066$	$\bar{F}_b = 9{,}000$ psi
$\sigma_{F_b} = 1{,}074$	$\sigma_{F_b} = 1{,}368$
n = 42 specimens	n = 42 specimens

Note that the ratio of static to dynamic is

$$\frac{\bar{F}_b(\text{dyn})}{\bar{F}_b(\text{static})} = \frac{2.04}{1.60} \quad \text{and} \quad \frac{\sigma_{F_b}(\text{dyn})}{\sigma_{F_b}(\text{static})} = \frac{2.04}{1.60}$$

which is virtually identical to the traditional increase shown in Fig. 4-5.

For the dry specimen (seasoned)

Static	Dynamic Speed 2
$\bar{F}_b = 12{,}941$	$\bar{F}_b = 14{,}658$ psi
$\sigma_{F_b} = 1{,}759$	$\sigma_{F_b} = 2{,}336$
n = 42 specimens	n = 42 specimens

and

$$\frac{\bar{F}_b(\text{dyn})}{\bar{F}_b(\text{static})} = \frac{1.81}{1.60} \quad \text{and} \quad \frac{\sigma_{F_b}(\text{dyn})}{\sigma_{F_b}(\text{static})} = \frac{2.12}{1.60}$$

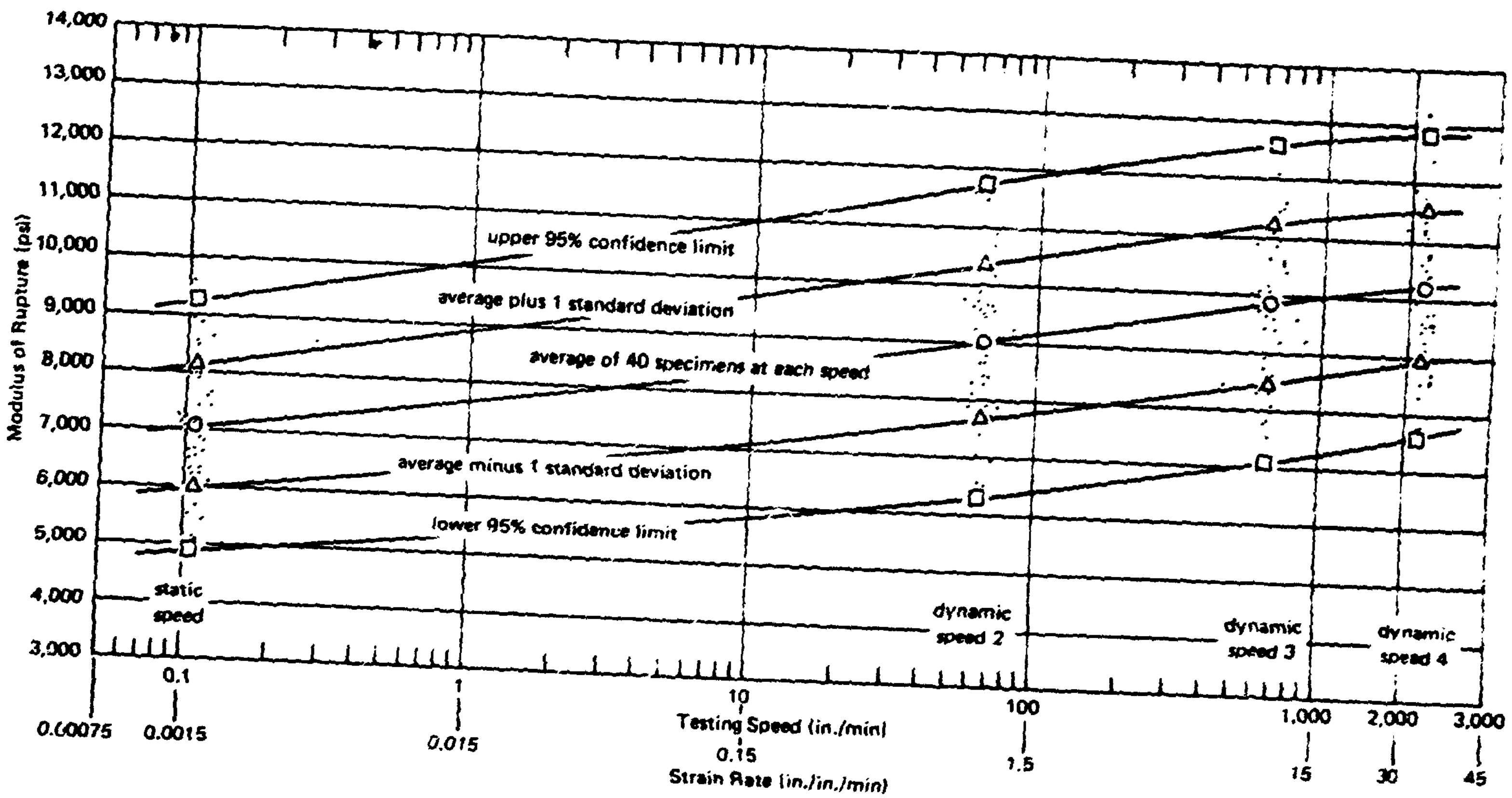

Fig. 4-8. Relation Between Modulus of Rupture and Testing Speed (Bending Tests on Green Specimens).

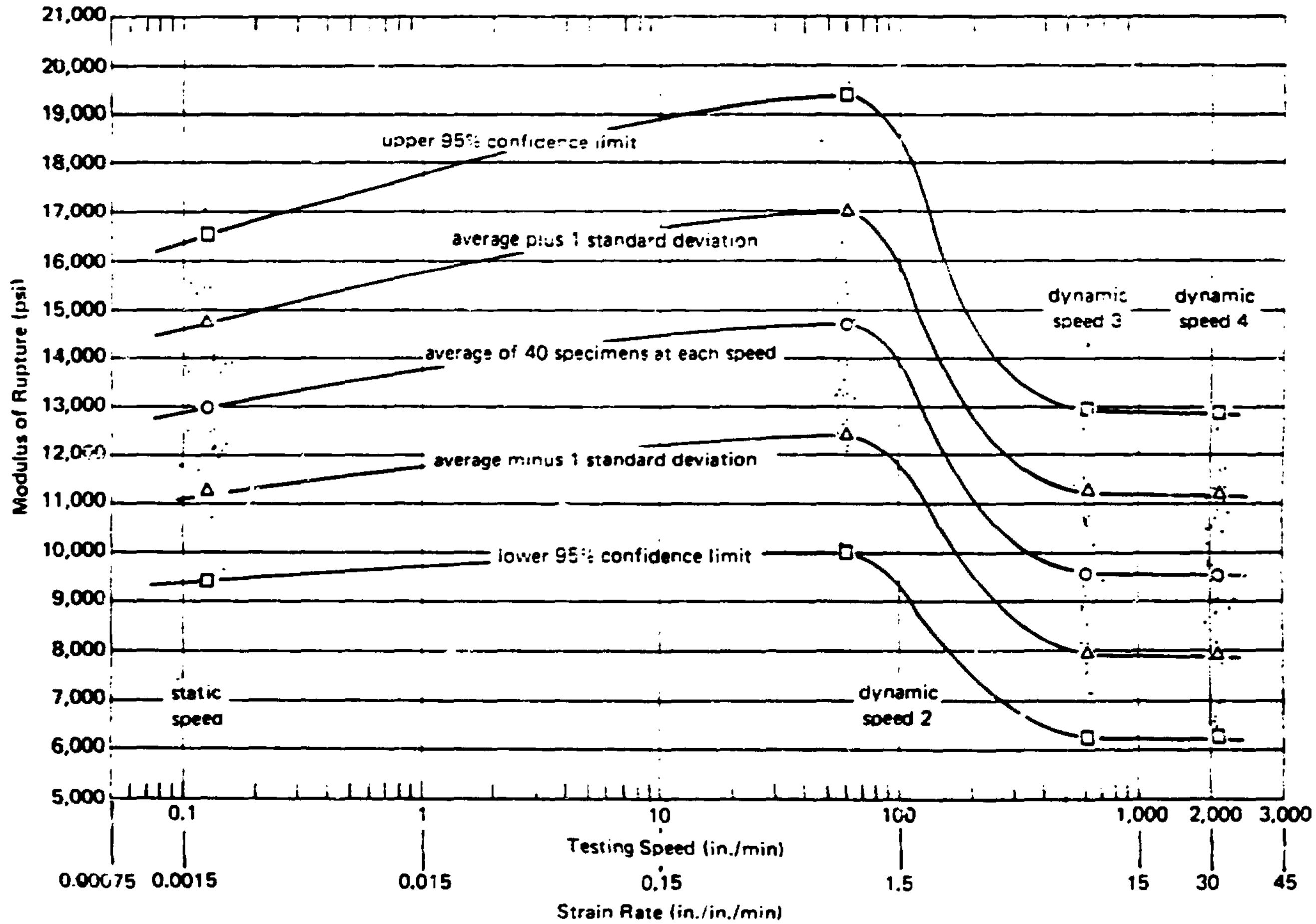

Fig. 4-9. Relation Between Modulus of Rupture and Testing Speed (Bending Tests On Dry Specimens).

Table 4-7. Results of Bending Tests — Green Timber

Timber No	Stress at Proportional Limit (psi)				Modulus of Elasticity, (psi x 10^6)				Modulus of Rupture (psi)				Testing Speed (in./min)			
	Static Speed	Dynamic Speed 2	Dynamic Speed 3	Dynamic Speed 4	Static Speed	Dynamic Speed 2	Dynamic Speed 3	Dynamic Speed 4	Static Speed	Dynamic Speed 2	Dynamic Speed 3	Dynamic Speed 4	Static Speed	Dynamic Speed 2	Dynamic Speed 3	Dynamic Speed 4
1	3,840	4,460	5,050	5,620	1.51	1.34	1.58	1.50	7,090	8,370	9,870	9,750	0.097	85	895	2,380
2	2,840	3,780	4,410	4,990	1.39	1.87	1.44	1.42	6,830	9,020	9,400	9,450	0.118	74	870	2,470
3	2,260	3,730	4,460	4,940	1.27	1.30	1.33	1.22	5,570	7,400	7,990	8,560	0.104	85	800	2,110
4	3,100	3,990	4,520	5,250	1.82	1.90	1.73	1.42	6,450	8,610	10,920	9,130	0.103	66	700	2,380
5	2,620	3,880	4,480	5,040	1.05	1.60	1.38	1.24	5,780	7,750	8,300	7,770	0.110	70	600	2,270
6	2,520	3,100	3,570	4,110	1.16	1.21	1.59	1.34	6,510	7,890	9,200	9,550	0.109	67	700	2,320
7	2,940	5,300	6,450	7,350	1.92	1.82	1.80	1.72	7,980	10,130	10,130	11,530	0.107	89	840	2,230
8	2,620	3,360	3,780	4,560	1.40	1.53	1.77	1.42	6,220	7,880	8,450	8,870	0.112	58	450	1,970
9	4,410	5,250	5,780	6,200	2.16	1.97	2.28	2.47	8,140	9,600	10,810	11,220	0.096	58	580	1,960
10	4,560	5,980	6,550	7,350	2.61	2.75	2.72	2.55	9,660	11,600	13,170	13,200	0.103	62	720	2,290
11	5,150	6,450	7,600	8,300	2.21	2.58	2.03	1.55	9,400	11,000	12,800	12,400	0.110	56	720	2,390
12	2,780	4,040	4,830	6,300	1.78	1.49	1.36	1.34	5,160	7,040	7,780	9,550	0.111	62	840	2,340
13	2,840	3,880	4,510	5,510	1.76	1.56	1.48	-	6,090	8,250	8,300	9,770	0.124	36	660	2,480
14	2,280	3,280	3,930	5,360	1.27	1.44	1.50	1.42	5,940	8,770	8,610	9,570	0.112	86	670	2,390
15	4,040	4,880	5,780	6,820	1.71	1.80	1.88	1.25	7,650	9,500	10,500	10,700	0.121	64	705	2,140
16	3,700	4,410	5,040	6,250	2.00	1.64	1.85	1.81	6,670	8,140	9,400	10,190	0.102	80	630	2,140
18	4,150	4,620	5,400	6,400	1.93	1.88	1.60	1.49	6,900	9,240	10,400	10,400	0.112	82	740	2,370
19	3,520	4,670	5,480	6,480	1.61	1.64	1.73	1.62	6,300	8,250	9,400	9,450	0.105	65	685	2,220
20	3,460	5,300	6,510	7,030	2.26	2.29	2.38	2.28	7,450	9,550	10,800	11,500	0.126	63	660	2,175
21	3,520	4,460	5,200	6,250	1.84	1.94	1.86	1.92	8,930	9,680	10,100	10,500	0.104	67	650	2,270
22	3,150	3,730	4,250	4,880	1.56	1.54	1.65	1.40	6,620	7,720	8,900	9,290	0.118	63	645	2,310
23	2,780	3,380	3,940	4,410	0.99	1.10	1.29	1.02	5,410	6,450	7,820	7,710	0.118	67	650	2,200
24	2,520	3,100	3,680	4,460	1.14	1.00	0.92	1.03	5,140	6,510	7,500	8,300	0.108	64	655	2,275
25	3,460	4,730	5,510	6,360	1.38	2.28	1.65	2.47	7,770	11,450	11,020	11,020	0.100	64	655	2,240
26	3,310	4,250	5,100	6,050	2.23	1.61	1.72	1.78	7,150	8,400	9,610	9,610	0.104	67	810	2,280
27	3,050	3,730	4,050	4,780	1.89	1.78	2.08	1.70	7,150	7,880	8,980	10,100	0.108	73	645	2,300
28	4,100	4,720	5,480	6,720	1.99	1.96	1.76	1.62	6,300	8,300	9,600	9,970	0.100	59	675	2,110
29	3,940	5,000	5,830	6,890	1.08	2.30	2.31	1.92	8,500	10,650	11,600	11,780	0.100	88	730	2,240
30	2,730	4,050	4,880	6,000	1.40	1.81	2.84	1.64	7,480	9,250	9,810	10,780	0.112	60	620	2,350
31	–	–	–	–	–	–	–	–	–	–	–	–	–	–		
32	2,200	4,100	5,050	5,780	1.92	1.78	1.77	1.72	7,200	9,850	10,040	11,070	0.094	59	590	2,310
33	3,100	4,150	4,940	6,300	1.80	1.93	1.93	1.43	6,200	9,400	9,780	10,200	0.105	67	580	2,040
34	2,380	4,250	5,360	8,520	1.84	1.70	2.10	1.88	7,900	9,670	10,600	11,350	0.104	61	720	2,250
35	3,310	4,360	5,610	8,250	2.04	2.17	1.88	1.52	8,450	11,550	12,120	12,800	0.108	58	670	2,320
36	2,000	3,260	4,040	4,990	1.52	1.49	1.47	1.33	6,390	6,940	8,040	8,700	0.112	88	670	2,440
37	2,840	4,100	4,940	6,200	1.80	1.87	2.29	1.47	7,150	9,560	9,020	10,850	0.104	70	645	2,360
38	4,620	5,890	6,350	7,000	1.91	2.07	2.32	2.51	8,880	10,880	11,500	11,910	0.116	69	700	2,075
39	4,040	4,560	5,250	5,990	1.62	0.81	1.32	1.29	6,830	8,610	8,710	8,550	0.099	64	620	2,400
40	3,420	4,730	5,570	6,720	1.84	1.42	1.52	1.31	7,660	9,820	10,600	10,600	0.108	62	645	2,200
41	3,940	4,830	5,720	7,150	2.38	1.93	2.10	1.58	7,940	9,980	11,440	11,130	0.102	57	670	2,270
42	3,360	4,410	5,250	7,040	1.44	1.52	1.40	0.84	6,880	9,750	9,660	[illegible]	0.115	54	635	[illegible]
Average	3,276	4,345	5,105	6,066	1.73	1.74	1.79	1.56	7,066	9,000	9,838	10,212	0.108	64	658	2,267
Standard deviation (interval)	737	773	885	1,023	0.37	0.40	0.40	0.48	1,074	1,337	1,368	[illegible]				
95% confidence interval	1,490	1,563	1,789	2,070	0.75	0.81	0.81	0.97	2,172	2,705	2,760	[illegible]				
Upper 95% confidence limit	4,766	5,908	6,894	8,136	2.48	2.55	2.60	2.53	9,238	11,705	12,598	[illegible]				
Lower 95% confidence limit	1,786	2,782	3,316	3,996	0.98	0.93	0.98	0.59	4,894	6,295	7,078	[illegible]				
Plus 1 standard deviation	4,013	5,118	5,990	7,089	2.10	2.14	2.19	2.04	8,140	10,337	11,206	[illegible]				
Minus 1 standard deviation	2,539	3,572	4,220	5,043	1.36	1.34	1.39	1.08	5,992	7,663	8,470	8,918				

Note: 95% confidence interval = standard deviation x 2.021

Table 4-8. Results of Bending Tests — Dry Timber

Timber No.	Modulus of Elasticity (psi × 10^6)				Modulus of Rupture (psi)				Testing Speed (in./min)			
	Static Speed	Dynamic Speed 2	Dynamic Speed 3	Dynamic Speed 4	Static Speed	Dynamic Speed 2	Dynamic Speed 3	Dynamic Speed 4	Static Speed	Dynamic Speed 2	Dynamic Speed 3	Dynamic Speed 4
1	1.90	1.84	1.11	1.14	11,780	13,100	[illegible]	8,830	0.097	58	610	2,430
2	1.44	1.59	1.17	0.99	11,090	12,330	7,490	6,540	0.125	61	610	2,100
3	1.64	1.46	0.90	1.01	11,930	12,440	6,540	7,830	0.139	55	600	2,140
4	2.17	2.42	1.63	1.44	13,050	15,950	11,500	10,700	0.104	51	590	2,350
5	1.63	1.79	1.12	1.02	9,640	12,130	8,140	6,930	0.145	62	610	2,190
6	1.43	1.34	0.87	0.94	11,700	12,880	8,140	6,010	0.114	57	590	2,170
7	2.36	2.39	1.43	1.69	14,090	15,650	10,800	10,560	0.132	62	610	2,130
8	1.91	2.04	1.28	[illegible]	11,910	13,230	9,400	9,610	0.104	55	710	2,220
9	2.24	2.35	1.51	[illegible]	14,500	[illegible]	11,400	11,340	0.098	54	550	2,130
10	2.63	2.80	1.56	1.05	15,500	17,870	11,000	11,340	0.108	62	660	2,080
11	2.48	2.81	1.66	1.92	13,500	19,300	12,550	12,550	0.103	58	590	2,150
12	1.75	1.88	1.06	1.09	12,180	13,960	7,720	7,980	0.134	57	710	2,290
13	1.96	1.92	1.22	1.84	12,760	13,230	8,820	8,380	0.178	56	590	2,080
14	1.47	1.73	1.09	1.21	15,790	17,790	7,510	8,130	0.130	61	590	2,170
15	2.21	2.21	1.14	1.40	13,750	16,400	10,560	10,400	0.105	57	620	2,280
16	1.74	2.03	1.07	1.06	11,920	13,960	8,870	9,400	0.123	61	590	2,230
18	–	–	–	–	–	–	–	–	–	–	–	–
19	2.04	2.60	1.78	1.27	13,910	14,000	9,200	9,360	0.134	65	590	1,990
20	2.74	2.28	1.51	1.56	14,000	15,440	10,500	10,500	0.102	61	620	2,006
21	2.22	2.11	1.47	1.61	14,500	14,700	9,140	10,190	0.129	64	590	1,520
22	1.99	1.84	1.22	1.35	12,230	13,120	8,720	8,560	0.149	65	630	1,940
23	1.29	1.32	0.79	0.83	10,000	10,100	7,150	6,410	0.177	60	630	2,180
24	1.38	1.48	0.98	0.96	10,400	12,450	7,940	8,730	0.100	64	620	2,140
25	1.71	1.87	1.33	1.49	13,910	13,330	10,200	11,020	0.158	57	650	2,150
26	1.97	2.16	1.26	1.42	12,500	14,800	11,190	9,450	0.132	65	600	2,040
27	2.08	2.21	1.34	1.20	13,880	15,650	9,880	7,730	0.150	65	650	2,220
28	1.98	2.02	1.09	1.29	12,910	13,550	9,660	9,030	0.101	55	630	2,140
29	2.68	2.73	1.63	1.66	17,000	20,200	11,020	11,680	0.122	59	640	2,210
30	1.56	1.85	1.26	1.36	12,980	15,180	10,130	10,500	0.132	56	650	1,970
31	1.64	1.49	1.04	1.53	8,650	12,400	7,570	9,570	0.136	80	600	2,720
32	2.02	2.26	1.26	1.35	12,430	15,530	10,710	9,550	0.130	61	600	2,390
33	2.12	2.26	1.32	1.03	12,700	14,910	10,600	10,660	0.144	75	610	2,100
34	2.05	2.07	1.24	1.25	13,970	15,490	9,450	11,020	0.122	63	600	2,280
35	2.30	2.38	1.59	1.70	15,330	19,640	14,280	11,710	0.112	62	620	2,300
36	1.90	2.08	1.11	1.18	12,070	13,240	6,100	5,780	0.146	61	610	2,220
37	2.05	1.88	1.23	1.28	12,130	10,090	9,750	9,710	0.134	57	600	2,020
38	2.47	2.42	1.55	1.76	15,440	15,870	11,020	11,350	0.122	62	600	2,290
39	1.85	2.08	1.18	1.44	11,800	13,880	8,500	9,000	0.112	61	610	2,520
40	2.26	2.41	1.29	1.79	14,800	15,330	9,450	9,710	0.153	61	600	1,990
41	2.23	2.82	1.35	1.52	15,430	15,440	10,710	11,130	0.139	47	630	1,980
42	1.73	1.65	1.15	1.18	13,020	15,020	9,870	10,220	0.104	57	600	2,120
Average	1.98	2.07	1.25	1.30	12,941	14,658	9,553	9,535	0.125	60	611	2,156
Standard deviation (interval)	0.36	0.40	0.21	0.27	1,759	2,336	1,658	1,645				
95% confidence interval	0.73	0.81	0.42	0.55	3,555	4,720	3,350	3,325				
Upper 95% confidence limit	2.71	2.88	1.67	1.91	16,496	19,378	12,908	12,860				
Lower 95% confidence limit	1.25	1.26	0.83	0.81	9,386	9,938	6,208	6,210				
Plus 1 standard deviation	2.34	2.47	1.46	1.63	14,700	16,994	11,216	11,180				
Minus 1 standard deviation	1.62	1.67	1.04	1.09	11,182	12,324	7,900	7,890				

*Note: 95% confidence interval = standard deviation interval x 2.021

which is close to the ratio of Fig. 4-6 . Note that the average of all ratios is exactly 2.00/1.60.

This type of analysis not only correlates well to the traditional approach — design strength ratios — but takes a step toward verifying the probabilitistic correlations performed within this report, i.e., the mathematical manipulations of the proper constants.

Moisture Content and Timber Strengths

Formulation of the effect of moisture content on the strength of wood is presented below. It seems appropriate, however, to first give the reader an indication of what are typical moisture content values and what is the relationship between environment and moisture content. Table 4-9 is a table of Equilibrium Moisture Content and Relative Humidity. From this the following correspondence is observed:

19% M.C. vs. Relative Humidity 90%,
15% M.C. vs. R.H. of 80%,
12% M.C. vs. R.H. of 70%

Hence, design values at M.C. of 15% to 19% are on the conservative side most of the time as noted on Figure 4-10, a map of the U.S., which provides a gross overview of expected M.C.

The shift in timber strengths as a function of moisture content can also be checked with this data:

Static	Dynamic
$\dfrac{\overline{F}_b(\text{dry})}{\overline{F}_b(\text{green})} = 1.83$	$\dfrac{F_b(\text{dry})}{F_b(\text{green})} = 1.63$
$\dfrac{\sigma_{F_b}(\text{dry})}{\sigma_{F_b}(\text{green})} = 1.64$	$\dfrac{\sigma_{F_b}(\text{dry})}{\sigma_{F_b}(\text{green})} = 1.71$

Table 4-9. Relative Humidity and Equilibrium Moisture Content Table for Use with Dry-Bulb Temperatures and Wet-Bulb Depressions (Ref. 14)

Wet bulb depression (°F.)

Temperature dry bulb (°F.)	1	2	3	4	5	6	7	8	9	10	11	12	13	14	15	16	17	18	19	20	21	22	23	24	25	26	27	28	29	30	32	34	36	38	40	45	50
30	89	78	67	57	46	36	27	17	6																												
		15.9	12.9	10.8	9.0	7.4	5.7	3.9	1.6																												
35	91	81	72	63	54	45	37	28	19	11	3																										
		16.8	13.9	11.9	10.3	8.5	7.4	6.0	4.6	2.9	0.8																										
40	92	83	75	68	60	52	45	37	29	22	15	8																									
		17.6	14.8	12.9	11.2	9.9	8.6	7.4	6.2	5.0	3.5	1.9																									
45	93	85	79	72	64	58	51	44	37	31	25	19	12	6																							
		18.3	15.6	13.7	12.0	10.7	9.5	8.5	7.5	6.5	5.3	4.2	2.8	1.5																							
50	93	86	80	74	68	62	56	50	44	38	32	27	21	16	10	5																					
		19.0	16.3	14.4	12.7	11.5	10.3	9.4	8.5	7.6	6.7	5.7	4.8	3.9	2.8	1.5																					
55	94	88	82	76	70	65	60	54	49	44	39	34	28	24	19	14	9	5																			
		19.5	16.9	15.1	13.4	12.2	11.0	10.1	9.3	8.4	7.6	6.5	6.0	5.3	4.5	3.6	2.5	1.3																			
60	94	89	83	78	73	68	63	58	53	48	43	39	34	30	26	21	17	13	9	5	1																
		19.9	17.4	15.6	13.9	12.7	11.6	10.7	9.9	9.1	8.5	7.6	6.9	6.3	5.6	4.9	4.1	3.2	2.3	1.3	0.2																
65	95	90	84	80	75	70	66	61	56	52	48	44	39	36	32	27	24	20	16	13	8	6	2														
		20.3	17.8	16.1	14.4	13.3	12.1	11.2	10.4	9.7	8.9	8.3	7.7	7.1	6.5	5.8	5.2	4.5	3.9	3.0	2.3	1.4	0.4														
70	95	90	86	81	77	72	68	64	59	55	51	48	44	40	36	33	29	25	22	19	15	12	9	6	3												
		20.6	18.2	16.5	14.9	13.7	12.5	11.6	10.9	10.1	9.4	8.8	8.3	7.7	7.2	6.6	6.0	5.5	4.5	4.5	3.7	2.9	2.3	1.5	0.7												
75	95	91	86	82	78	74	70	66	62	58	54	51	47	44	41	37	34	31	28	24	21	18	15	12	9	7	4	1									
		20.9	18.5	16.8	15.2	14.0	12.9	12.0	11.2	10.5	9.8	9.3	8.7	8.2	7.7	7.2	6.7	6.2	5.6	5.1	4.7	4.1	3.5	2.9	2.3	1.7	0.9	0.2									
80	96	91	87	83	79	75	72	68	64	61	57	54	50	47	44	41	38	35	32	29	26	23	20	18	15	12	10	7	5	3							
		21.0	18.7	17.0	15.5	14.3	13.2	12.3	11.5	10.9	10.1	9.7	9.1	8.6	8.1	7.7	7.2	6.8	6.3	5.8	5.4	5.0	4.5	4.0	3.6	3.0	2.4	1.8	1.1	0.3							
85	96	92	88	84	80	76	73	70	66	63	59	56	53	50	47	44	41	38	36	33	30	28	25	23	20	18	15	13	11	9	4						
		21.2	18.8	17.2	15.7	14.5	13.5	12.5	11.8	11.2	10.5	10.0	9.5	9.0	8.5	8.1	7.6	7.2	6.7	6.3	6.0	5.6	5.2	4.8	4.3	3.9	3.4	3.0	2.4	1.7	0.9						
90	96	92	89	85	81	78	74	71	68	65	61	59	55	52	49	47	44	41	39	36	34	31	29	26	24	22	19	17	15	13	9	5	1				
		21.3	18.9	17.3	15.9	14.7	13.7	12.8	12.0	11.4	10.7	10.2	9.7	9.3	8.8	8.4	8.0	7.6	7.2	6.8	6.5	6.1	5.7	5.3	4.9	4.6	4.2	3.8	3.3	2.8	2.1	1.3	0.4				
95	97	93	89	85	82	79	75	72	69	66	63	60	57	55	52	49	46	44	42	39	37	34	32	30	28	26	23	22	20	17	14	10	6	2			
		[illegible]	19.0	17.4	16.1	14.9	13.9	12.9	12.2	11.6	11.0	10.5	10.0	9.5	9.1	8.7	8.2	7.9	7.5	7.1	6.8	6.4	6.1	5.7	5.3	5.1	4.8	4.4	4.0	3.6	3.0	2.3	1.6	0.6			
100	[illegible]	93	89	86	83	80	77	73	70	68	65	62	59	56	54	51	49	46	44	41	39	37	35	33	30	28	26	24	22	21	17	13	10	7	4		
		21.5	19.0	17.5	16.1	15.0	13.9	13.1	12.4	11.8	11.2	10.6	10.1	9.6	9.2	8.9	8.5	8.1	7.8	7.4	7.0	6.7	6.4	6.1	5.7	5.4	5.2	4.9	4.6	4.2	3.6	3.1	2.4	1.6	0.7		
105	96	93	90	87	83	80	77	74	71	69	66	63	60	58	55	53	50	48	46	44	42	40	37	35	34	31	29	28	26	24	20	17	14	11	8		
		21.4	19.0	17.5	16.2	15.1	14.0	13.2	12.6	11.9	11.3	10.8	10.3	9.8	9.4	9.0	8.7	8.3	7.9	7.6	7.3	6.9	6.7	6.4	6.1	5.7	5.4	5.2	4.8	4.6	4.2	3.6	3.1	2.4	1.8		
110	97	93	90	87	84	81	78	75	73	70	67	65	62	60	57	55	52	50	48	46	44	42	40	38	36	34	32	30	28	26	23	20	17	14	11	4	
		21.4	19.0	17.6	16.2	15.1	14.1	13.3	12.6	12.0	11.4	10.9	10.4	9.9	9.5	9.2	8.8	8.4	8.1	7.7	7.5	7.2	6.8	6.6	6.3	6.0	5.7	5.4	5.2	4.8	4.5	4.0	3.6	3.0	[illegible]	1.1	
115	97	93	90	88	85	82	79	76	74	71	68	66	63	61	58	56	54	52	50	48	45	43	41	40	38	36	34	32	31	29	26	23	20	17	14	8	2
		21.4	19.0	17.5	16.2	15.1	14.1	13.4	12.7	12.1	11.5	10.9	10.4	10.0	9.6	9.3	8.9	8.6	8.2	7.8	7.6	7.3	7.0	6.7	6.6	6.2	5.9	5.6	5.4	5.2	4.7	4.3	3.5	3.4	2.9	1.3	0.4
120	97	94	91	88	85	82	80	77	74	72	69	67	65	62	60	58	55	53	51	49	47	45	43	41	40	38	36	34	33	31	28	25	22	19	17	19	3
		21.3	19.0	17.4	16.2	15.1	14.1	13.4	12.7	12.1	11.6	11.0	10.5	10.0	9.7	9.4	9.0	8.7	8.3	7.9	7.7	7.4	7.2	6.8	6.6	6.5	6.1	5.8	5.6	5.4	5.0	4.6	4.2	3.7	3.3	2.3	1.1
125	97	94	91	88	86	83	80	77	75	73	70	68	65	63	61	59	57	55	53	51	48	47	45	43	41	39	38	36	[illegible]	33	30	27	24	22	19	13	8
		21.2	18.9	17.3	16.1	15.0	14.0	13.4	12.7	12.1	11.5	11.0	10.5	10.0	9.7	9.4	9.0	8.7	8.3	8.0	7.7	7.6	7.2	7.0	6.7	6.6	6.2	6.0	5.8	5.5	5.2	4.8	4.4	4.0	3.6	2.7	1.6
130	97	94	91	89	86	83	81	78	76	73	71	69	67	64	62	60	58	56	54	52	50	48	47	45	43	41	40	38	37	35	32	29	26	24	21	15	10
		21.0	18.5	17.2	16.0	14.9	14.0	13.4	12.7	12.1	11.5	11.0	10.5	10.0	9.7	9.4	9.0	8.7	8.5	8.0	7.8	7.6	7.3	7.0	6.8	6.6	6.4	6.1	5.9	5.6	5.3	4.9	4.6	4.2	3.8	3.0	2.0
140	97	95	92	89	87	84	82	79	77	75	73	70	68	66	64	62	60	58	56	54	53	51	49	47	46	44	43	41	40	38	35	32	30	27	25	19	14
		20.7	18.6	16.9	15.8	14.8	13.8	13.2	12.5	11.9	11.4	10.9	10.4	10.0	9.6	9.4	9.0	8.7	8.4	8.0	7.8	7.6	7.3	7.1	6.9	6.6	6.4	6.2	6.0	5.8	5.4	5.1	4.8	4.4	4.1	3.4	2.6
150	98	95	92	90	87	85	82	80	78	76	74	72	70	68	66	64	62	60	58	57	55	53	51	49	48	46	45	43	42	41	38	36	33	30	28	23	18
		20.2	18.4	16.6	15.4	14.5	13.7	13.0	12.4	11.8	11.2	10.7	10.3	9.9	9.5	9.2	8.9	8.6	8.3	8.0	7.8	7.5	7.3	7.1	6.9	6.7	6.4	6.2	6.0	5.8	5.4	5.2	4.9	4.5	4.2	3.6	2.9
160	98	95	93	90	88	86	83	81	79	77	75	73	71	69	67	65	64	62	60	58	57	55	53	52	50	49	47	46	44	43	41	38	35	33	31	25	21
		19.8	18.1	16.2	15.2	14.2	13.4	12.7	12.1	11.5	11.0	10.6	10.1	9.7	9.4	9.1	8.8	8.5	8.2	7.9	7.7	7.4	7.2	7.0	6.8	6.7	6.4	6.2	6.0	5.8	5.5	5.2	4.9	4.6	4.3	3.7	3.2
170	98	95	93	91	89	86	84	82	80	78	76	74	72	70	69	67	65	63	62	60	59	57	55	53	52	51	49	48	47	45	43	40	38	35	33	28	24
		19.4	17.7	15.8	14.5	13.9	13.2	12.4	11.8	11.3	10.8	10.4	9.9	9.6	9.2	9.0	8.6	8.4	8.0	7.8	7.6	7.3	7.2	6.9	6.7	6.6	[illegible]	6.2	6.0	5.7	5.5	5.2	4.9	4.6	4.4	3.7	3.2
180	98	96	94	91	89	87	85	83	81	79	77	75	73	72	70	68	67	65	63	62	60	58	57	55	54	52	51	50	48	47	45	42	40	39	35	30	25
		18.9	17.2	15.5	14.5	13.7	12.9	12.2	11.6	11.1	10.6	10.1	9.7	9.4	9.0	8.8	8.4	8.1	7.8	7.6	7.4	7.2	7.0	6.8	6.5	6.4	6.2	6.0	5.8	5.7	5.4	5.2	4.8	4.6	4.4	3.8	3.5
190	98	96	94	92	90	88	85	84	82	80	78	76	75	73	71	69	68	66	65	63	62	60	58	57	56	54	53	51	50	49	46	44	42	39	37	32	28
		18.5	16.9	15.8	14.2	13.4	12.7	12.0	11.4	10.9	10.5	10.0	9.6	9.2	8.9	8.6	8.2	7.9	7.7	7.4	7.2	7.0	6.8	6.6	6.4	6.2	6.0	5.9	5.7	5.5	5.3	5.0	4.8	4.5	[illegible]	3.8	3.3
200	98	96	94	92	90	88	86	84	82	80	79	77	75	74	72	70	69	67	66	64	63	61	60	58	57	55	54	53	52	51	48	46	43	41	39	34	30
		18.1	16.4	14.9	14.0	13.2	12.4	11.8	11.2	10.6	10.3	9.8	9.4	9.1	8.8	8.4	8.1	7.7	7.5	7.2	7.0	6.9	6.6	6.4	6.2	6.0	5.9	5.7	5.6	5.4	5.2	4.9	4.7	4.5	4.3	3.8	3.5
210	98	96	94	92	90	88	86	85	83	81	79	78	76	75	73	71	70	68	67	65	64	63	61	60	59	57	56	54	53	52	50	47	45	43	41	36	32
		17.7	16.0	14.6	13.5	13.0	12.2	11.7	11.1	10.6	10.0	9.7	9.2	9.0	8.7	8.5	8.0	7.6	7.4	7.1	6.9	6.8	6.5	6.3	6.1	5.9	5.8	5.5	5.4	5.3	5.1	4.8	4.6	4.4	4.2	[illegible]	3.2

[1] Relative-humidity values in roman type.
[2] Equilibrium-moisture-content values in italic type.

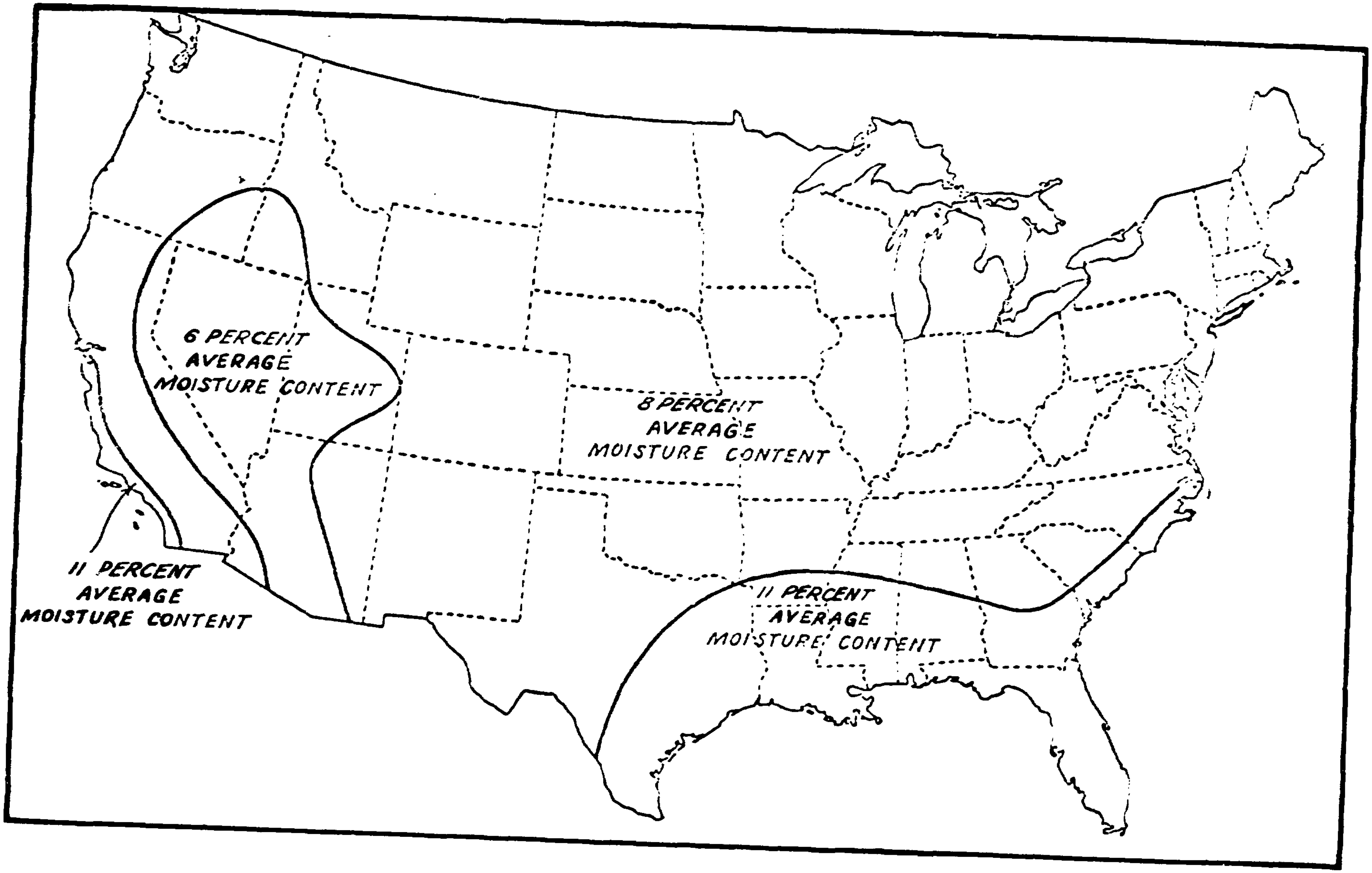

Fig. 4-10. Recommended Moisture Content Averages for Interior-Finishing Woodwork for use in Various Parts of the United States.

or an average increase of 1.70, from green to an 11% moisture content. The values of strength increase for moisture content shown in Table 4-3 are common values used in establishing allowables. Fig. 4-11 below gives a more general formula. Letting M_1 = 11% and $M_2 = M_p$

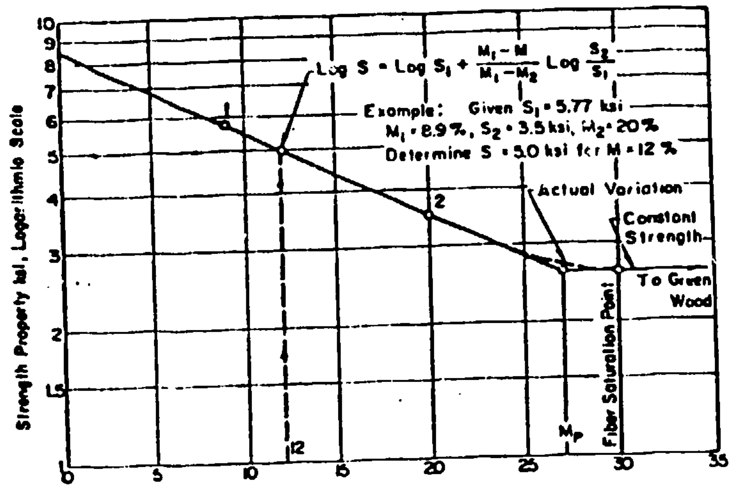

Fig. 4-11. Variation of Strength with Moisture Content. (Ref. 14)

or the moisture content at which properties begin to change, i.e., M_p, and M is the moisture content at which the stress is desired, see Table 4-10 for this value.

Static Properties

M_1 = 11%

M_p = 24% = M_2

F_{b_2} = 7,066 psi

$\sigma_{E_{b_2}}$ = 1,074 psi

Table 4-10. Moisture Content at Which Properties Change Due to Drying for Selected Species

Species	M.
	Pct.
Ash, White	24
Birch, Yellow	27
Chestnut, American	24
Douglas-Fir	24
Hemlock, Western	28
Larch, Western	28
Pine, Loblolly	21
Pine, Longleaf	21
Pine, Red	24
Redwood	21
Spruce, Red	27
Spruce, Sitka	27
Tamarack	24

$F_{b_1} = 12,941$

$\sigma_{F_{b_1}} = 1,759,$

at 15% M.C.

$F_b = 10,743$

$\sigma_{F_b} = 1,511$

at 19% M.C.

$F_b = 8,918$

$\sigma_{F_b} = 1,298$

$$\frac{F_{b_1}}{F_b} = 1.52, \quad \frac{\sigma_{F_{b_1}}}{\sigma_{F_b}} = 1.41, \quad \frac{F_{b_1}}{F_b} = 1.26, \quad \frac{\sigma_{F_{b_1}}}{\sigma_{F_b}} = 1.21$$

<u>Dynamic Properties</u>

$M_1 = 11\%$

$M_p = 24\% = M_2$

$F_{b_2} = 9,000$ psi

$\sigma_{F_{b_2}} = 1,368$ psi

$F_{b_2} = 14,658$ psi

$\sigma_{F_{b_2}} = 2,336$ psi

at 15% M.C.

$F_b = 12,615$

$\sigma_{F_b} = 1,981$

$$\frac{F_{b_1}}{F_b} = 1.40$$

at 19% M.C.

$F_b = 10,857$

$\sigma_{F_b} = 1,680$

$$\frac{F_{b_1}}{F_b} = 1.21$$

$$\frac{{}^{\sigma}F_{b_1}}{{}^{\sigma}F_b} = 1.45 \qquad \frac{{}^{\sigma}F_{b_1}}{{}^{\sigma}F_b} = 1.23$$

The average ratio at 19% M.C. is 1.23 and 1.45 at 15% M.C., which compares very well with the recommendations in Table 4-3, which are averages for all common timbers and based on M_p = 25%.

Fig. 4-12 is a plot of these data points showing the data in the manner of Fig. 4-11. The plot illustrates the consistent behavior of the data, both stress and the standard deviation of stress. Hence, one must conclude that the theory is reasonable and can be used to adjust the distributions of strength as well as the 5% exclusion value as done in general practice. Further, it is reasonable to use the values in Table 4-3 for these distribution adjustments.

Size Effects

Beam depth and corrections for depth, have been part of timber design for many years. Up to this point in the study all the work and manipulations presented are based on the standard specimen, i.e., a 2" x 2" x 30" clear wood beam. Gurfinkel (Ref. 9) and Hoyle (Ref. 8) discuss this problem rather extensively and it appears that it is reasonable to use the traditional depth correction = 0.86, to correct the bending stress distribution and the most recent formulation

$$C_d = \left(\frac{12}{d}\right)^{1/a}$$

for depths greater than 12 inches. The bending allowables presented here will be for a 12-inch deep beam: further corrections will be required for other depths and those will be discussed later in this report.

Table 4-11 illustrates the building of a basic set of strength parameters for timber and is the completion of the parameters for Western Larch timber carried through the chapter.

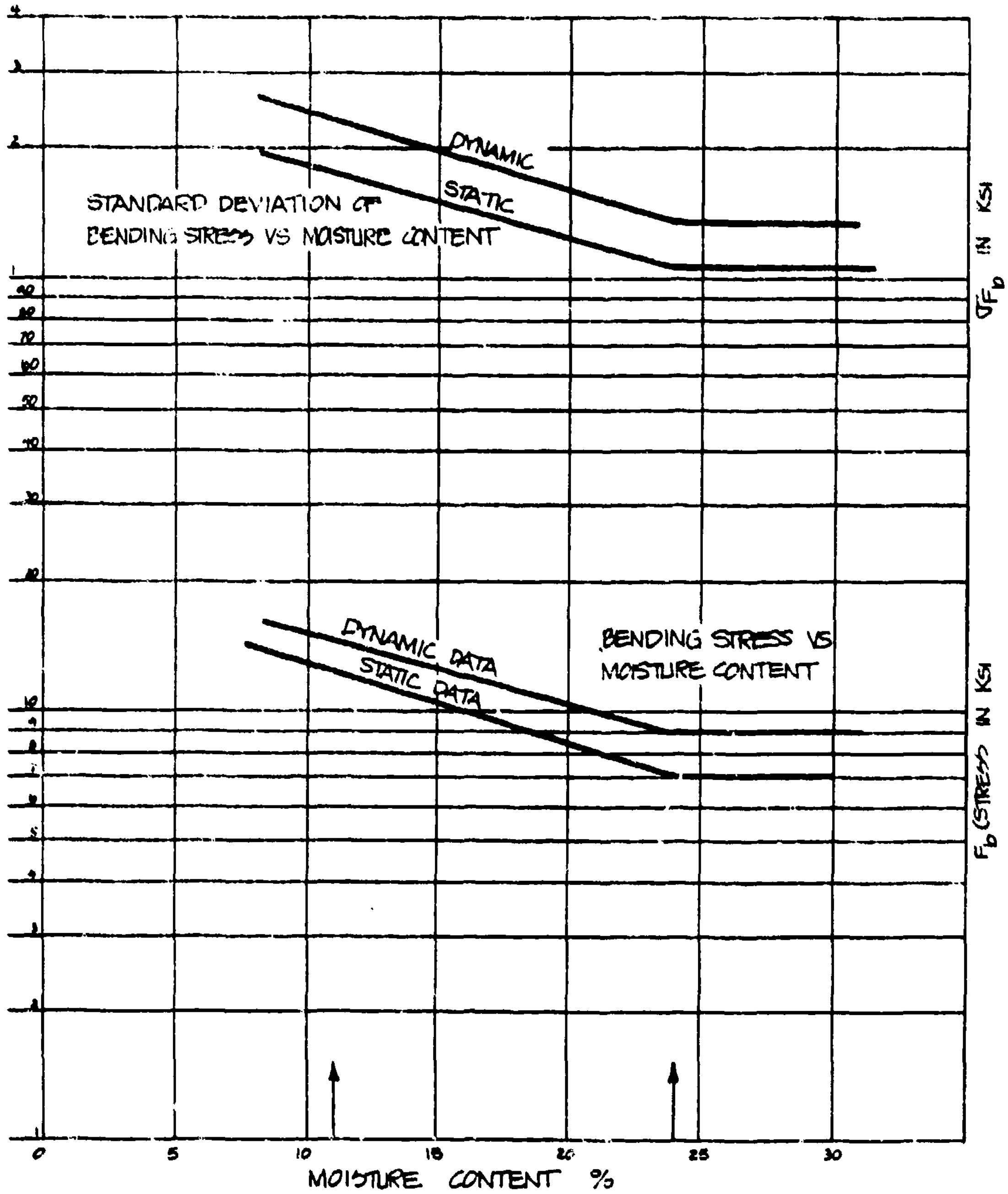

Fig. 4-12. Plot of Bending Stress Versus Moisture Content.

Table 4-11. Structural Property Evaluation of Western Larch

Property	Mean psi	Std. Dev. psi	Strength Ratio	Seasoning 19%	Duration	Depth	Combined	Mean	Std. Dev.	5% Excl.	Example Prediction	NDS Allow.
F_b	7652	1001	0.54	1.25	1/1.6	0.86	0.363	2776	363	2177	1660	1750
F_c	3756	564	0.62	1.50	1/1.6	--	0.581	2183	327	1642	1380	1250
F_v	869	85	0.50	1.08	1/1.6	--	0.338	293	29	246	192*	190*
F_t	7652	1001	0.31	1.25	1/1.6	--	0.242	1853	337	1296	1100	1050
$F_{c\perp}$	399	112	1.00	1.50	1.0	--	1.500	599**	168	--*	399	385
E/1000	1458	249	1.00	1.14	1.0	--	1.140	1662	289	--*	1770	1800
	Clear Wood Strength, Ref. Tables 4-1 & 4-6 Western Larch		Ref. Table 4-4 Struc. Lt. Framing No. 1	Ref. Tables 4-3 & 4-6	Fig. 4-5 & Table 4-5			Normal Load Distribution			Ref. Col. 7 Table 4-6	Douglas-Fir-Larch NDS does not specify Larch

*Mean values are used.
**Reduce by 2/3 for end effects, i.e., $F_{c\perp} = 399$.

AN EXAMPLE (Using Data from Ref. 4)

To further verify the approach presented within this report, it is desirable to look at as many examples as possible. DCPA funded a program at Waterways Experiment Station that is very useful for this purpose. This program which tested several schemes to upgrade residential floor systems also tested 5 unmodified floor system specimens. The basic design is shown in Fig. 4-13. The 2 x 10 joists used were specified as Southern Pine No. 2 medium grain or better. They arrived from the lumber yard as No. 1 dense and No. 2 medium grain joists. The design properties for these materials is as follows:

	No. 1 Dense 15% M.C.	No. 2 Med. 15% M.C.
F_b	1,900 psi	1,350 psi
F_t	1,300 psi	900 psi
F_v	95(190*) psi	95(190*) psi
$F_{c\perp}$	475 psi	405 psi
$F_{c_{11}}$	1,700 psi	1,250 psi
E	2.0×10^6	1.7×10^6

*Without splits or checks.

The five non-reinforced floors tested by W.E.S. were I, V, VII, XIV and XV. The test arrangement in shown in Fig. 4-14 and the flexural data is shown below, adjusted to normal duration.

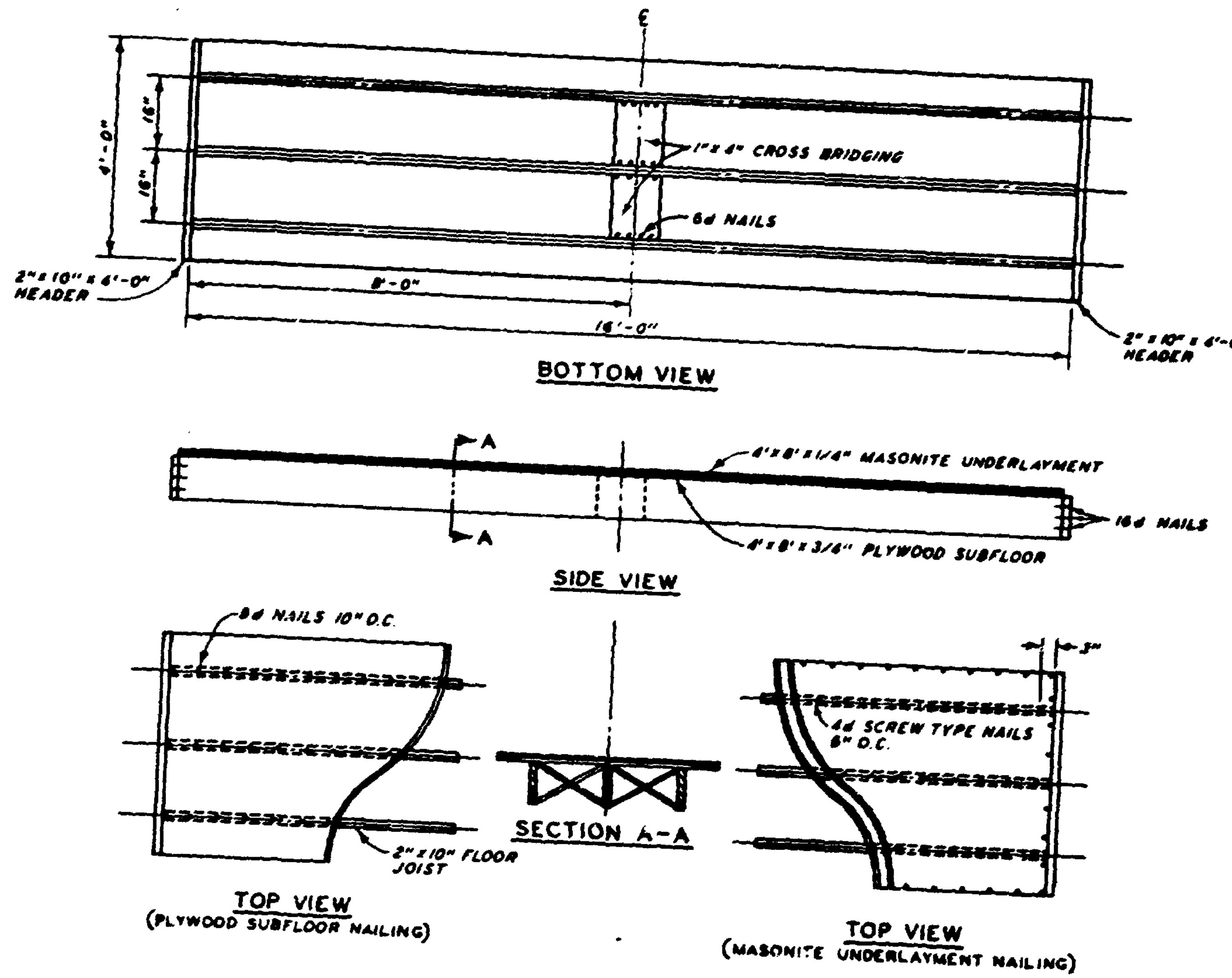

Fig. 4-13. Construction Drawing for the Unreinforced Test Specimens (I, V, VII, XIV, and XV).

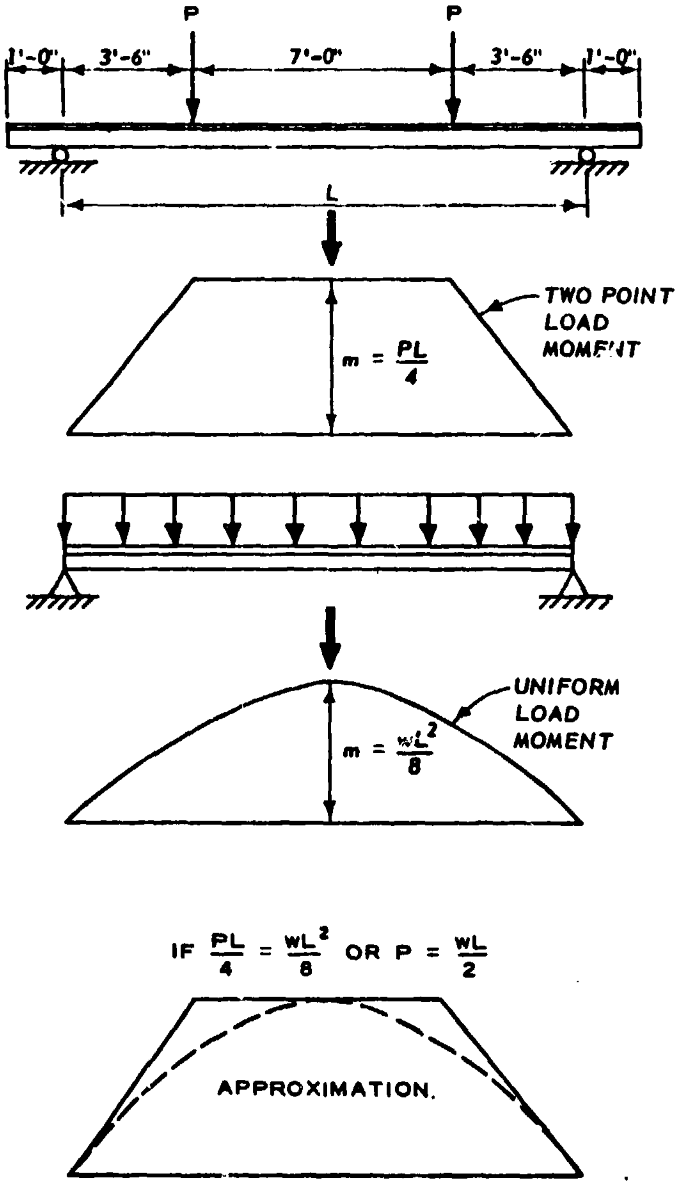

TEST SPECIMEN MOMENT

c. Load configuration.

Fig. 4-14. Test Arrangement for Five Nonreinforced Floors Tested by W.E.S.

Rank	Test No.	Modulus of Rupture at Test	Adjusted by 1/1/6 for Test	Cumulative Percentage $\frac{n}{N+1}$ 100
1	XIV	2,533 psi	1,583	17%
2	VII	4,539	2,837	33%
3	I	4,750	2,969	50%
4	XV	4,882	3,051	67%
5	V	5,436	3,398	83%
Mean Value		4,428	2,767	

The next task is to establish the probability distributions for the material used for the joists.

Material - Use Southern Pine/Clear Wood - Green

(see Table 4-1)

		Mean	std. dev.
$\overline{F}_b$	=	8,570 psi	1,387 psi
$\overline{F}_{c_{11}}$	=	4,210 psi	758 psi
$\overline{F}_v$	=	958 psi	134 psi
$F_{c\perp}$	=	529 psi	148 psi
E	=	1.588×10^6	0.344×10^6

Grading - Strength Ratios

(see Table 4-4, footnote 3)

For No. 1 Dense

F_b	=	0.46	(1.17)	=	0.54
F_t	=	0.31	(1.17)	=	0.36
F_v	=	0.50	(1.17)	=	0.59
$F_{c\perp}$	=	1.00	(1.17)	=	1.17
$F_{c_{11}}$	=	0.62	(1.17)	=	0.73
E	=	1.00	(1.05)	=	1.05

For No. 2 Medium

F_b	=	0.38
F_t	=	0.25
F_v	=	0.50
$F_{c\perp}$	=	1.00
$F_{c_{11}}$	=	0.52
E	=	0.90

Duration Effects

Since these were static tests and no times were reported it will be assumed that 1/1.6 is the adjustment, i.e., test took 5-8 minutes.

Duration Factor = 1/1.6

except for E & $F_{c\perp}$ for which duration factor = 1/1

Moisture Content

The adjustment for moisture content is from green to 15% M.C. (see Table 4-3).

Property		Adjustment Factor
F_b	=	1.35
F_t	=	1.35
F_v	=	1.13
$F_{c\perp}$	=	1.50
$F_{c_{11}}$	=	1.75
E	=	1.20

The computations are all shown on Table 4-12 and Table 4-13 for these distribution calculations.

Fig. 4-15 is a plot of the derived distributions for the Modulus of Rupture F_b (bending stress). Also shown on the same plot are the test values from the W.E.S. tests shown in Table 4-13. Basically the tests fall exactly between (except in one point) the two derived distributions. Also, shown is a dashed curve, which is the average distribution of No. 1 Dense and No. 2 Medium. This distribution fits the test data very well and could be used as a performance predictor if more of these particular floor systems were to be used.

Table 4-12. Structural Property Evaluation of Southern Pine, No.1 Dense

Property	Mean psi	Std. Dev. psi	Strength Ratio	Seasoning 15%	Duration	Depth	Combined	Mean	Std. Dev.	5% Excl.	NDS Allow.
F_b	8570	1387	0.54	1.35	1/1.6	0.86	0.392	3358	543	2461	1900
F_c	4210	758	0.73	1.75	1/1.6	--	0.798	3361	605	2363	1700
F_v	958	134	0.59	1.13	1/1.6	--	0.417	399	56	307	190*
F_t	8570	1387	0.25	1.35	1/1.6	--	0.211	1808	293	1325	1300
$F_{c\perp}$	529	148	1.17	1.50	1.0	--	1.755	928	260	--**	475
E/1000	1588	349	1.05	1.20	1.0	--	1.260	2000	440	--	2000
	Clear Wood							Normal Load Dist.			

* No checks.
** Mean used adjust by 2/3 for end bearing.

Table 4-13. Structural Property Evaluation of Southern Pine, No. 2 Medium

Property	Me psi	Std. Dev. psi	Strength Ratio	Seasoning 15%	Duration	Depth	Combined	Mean	Std. Dev.	5% Excl.	NDS Allow.
F_b	8570	1387	0.38	1.35	1/1.6	0.86	0.276	2363	383	1731	1350
F_c	4210	758	0.52	1.75	1/1.6	--	0.569	2394	431	1683	1250
F_v	958	134	0.50	1.13	1/1.6	--	0.353	338	47	260	95
F_t	8570	1387	0.25	1.35	1/1.6	--	0.211	1807	293	1325	900
$F_{c\perp}$	529	148	1.00	1.50	1.0	--	1.500	794	222	--	405
E/1000	1588	349	0.90	1.20	1.0	--	1.080	1715	377	--	1700
	Clear Wood										

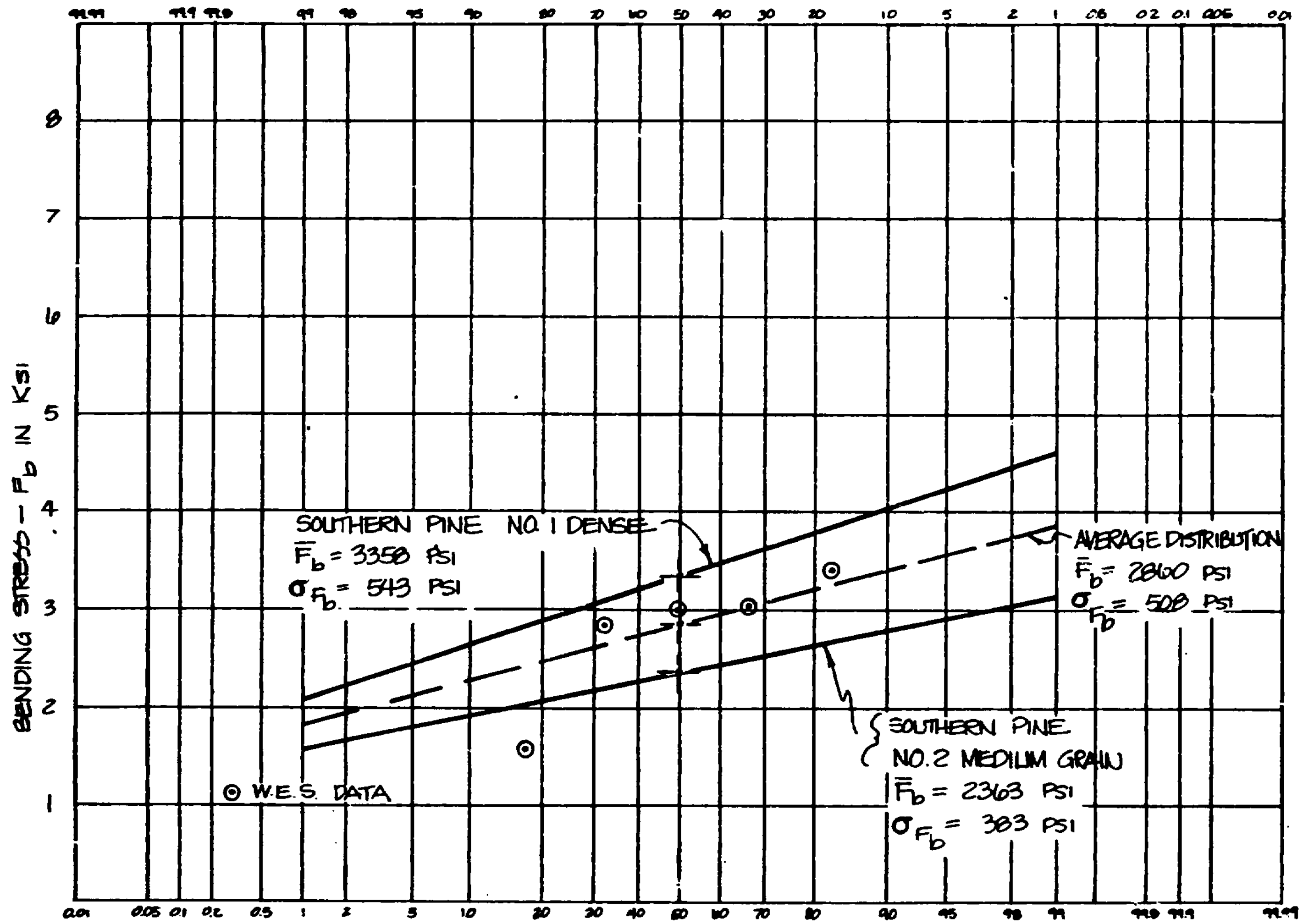

Fig. 4-15. Theoretical Modulus of Rupture Curve vs Plots of W.E.S. Data.

Fig. 4-16 is a plot of this average distribution, with other distributions shown for various loading cases. Curve 1 is for the "normal" loading, curve 2 is for a two week loading (such as an emergency fallout protection of soil), 3 is the curve upon which static tests (5-8 minute duration) and curve 4 is an impulsive loading like blast loading.

To illustrate the use of these curves a brief example will be presented below.

Given: The W.E.S. Floor

For Design

Live Load = 40 psf

Dead Load = 1 psf

Span ℓ = 16 ft

Joist 2 x 10 @ 16 in. ℄ to ℄

Material properties use average values since No. 1 Dense or No. 2 Medium are mixed.

F_b = 1,625 psi

F_v = 95 psi

$F_{c\perp}$ = 440 psi

E = 1.85×10^6 psi

for 2 x 10 joist. $I = 98.93$ in.^{4}

$S = 21.39$ in.^{3}

$A = 13.88$ in.^{2}

$d = 9.25$

$b = 1.5$

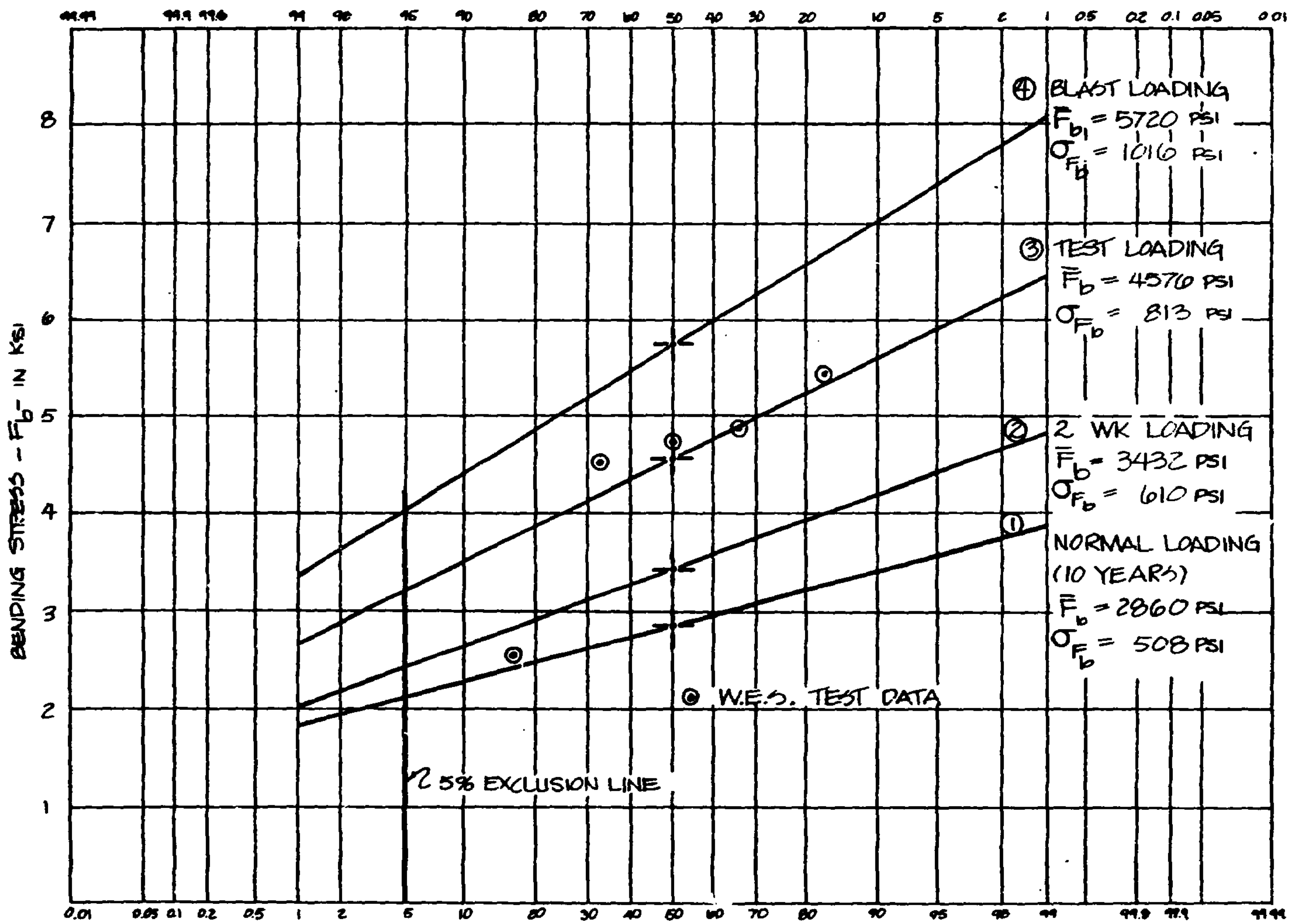

Fig. 4-16. Probability Distribution for W.E.S. Floor Strengths for Various Loadings.

Check Bending

$$M = \frac{w\ell^2}{8} = \frac{(10 + 40)\ 16^2}{8} \text{ ft lbs}$$

$$M = 19{,}200 \text{ in.lbs/ft of width}$$

$$M = 25{,}600 \text{ in.lbs/joist}$$

$$f_b = \frac{M}{S} = \frac{25{,}600}{21.29} = \frac{1197 \text{ psi} < 1625}{\text{safe}}$$

Shear

$$V = (10 + 40)8 \times \frac{16}{12} \text{ lbs/joist}$$

$$V = 533 \text{ lbs}$$

$$f_v = \frac{3}{2}\frac{(V - wd)}{A} = \frac{3}{2(13.88)} [533 - 50\ (16/12)(10/12)]$$

$$f_v = 51.6 \text{ psi} < 95 \text{ safe}$$

Deflection (live load)

$$\delta = \frac{5\ wl^4}{384\ EI}$$

$$\delta = \frac{5\ (40)\ 16\ (192)^3}{384 \times 1.85 \times 10^6} \times 98.93$$

$$\delta = 0.32\ \frac{\ell}{360} = 0.53 \text{ O.K.}$$

Bearing at Support

$$\ell_b = 3.5 - 1.5 = 2 \text{ in.}$$

$$fc_\perp = \frac{V}{b\ell_b} = \frac{533}{1.5(2)}$$

$$fc_\perp = \frac{178 \text{ psi} < 440 \text{ psi}}{\text{O.K.}}$$

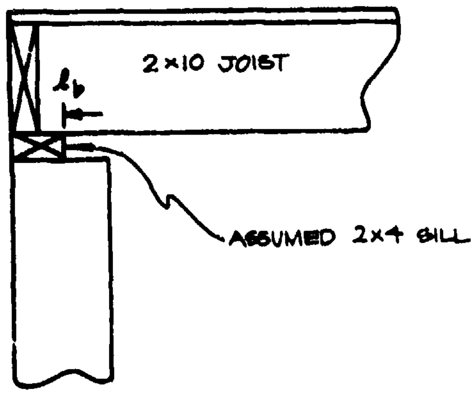

The above is a set of conventional design calculations for a simple floor system. However, the problem faced by DCPA is far different. They have a limit design problem and must push their shelter spaces to some optimum.

Assume it is desired to place soil on this floor (as is) for fallout protection. Further, assume a 5% risk of some collapse is reasonable. Since curve 2 on Fig. 4-16 is for a two-week loading, these data will be used (flexure controlled the design).

$$F_b = 3{,}432$$

$$\sigma_{F_b} = 610$$

$$F_b(5\%) = \underline{\underline{2{,}426 \text{ psi}}}$$

or a load of $50(\frac{2{,}426}{1{,}197})$ or 101 psf could be sustained for 2 weeks which is 10 psf dead load (91 psf live load).

$$\text{Shear } f_v = 2.03(51.6) = 105 \text{ psi, and}$$

$$\text{bearing } f_{c\perp} = 2.03\ (178) \text{ are} = 361 \text{ psi}$$

well within conventional safe limits, therefore safe.

The question could be pushed further into the second area of DCPA interest; that is, blast. Assume the 5% value is acceptable and flexure still controls (curve 4, Figure 4-16).

$$F_b = 5{,}720 \text{ psi}$$

$$\sigma_{F_b} \doteq 1{,}016 \text{ psi}$$

$$F_b(5\%) = 4{,}044 \text{ psi}$$

or $$W = 50(\frac{4{,}044}{1{,}197})$$

$$W = 169 \text{ psf}$$

which is 10 psf dead and 159 psf blast

or W = 10 psf dead

+ 100 psf soil (1 foot)

+ 49 psf blast.

EXAMPLE (USING TEST DATA FROM THIS PROGRAM)

As presented in Section 2, a series of 4' x 16' floor specimens were tested to failure. These floors which were similar in design to the W.E.S. tests consisted of two base-case studies and several modifications for upgrading as described in Section 2. The basic floor system was constructed of three 2" x 10" x 16' joists, two sheets of 3/4 inch CDX plywood and 3/8 inch particle board subflooring (see Figs. 2-1 through 2-3). The floor joists were Douglas-Fir Select Structural, with the following properties.

Douglas-Fir Larch

M.C. 19%-Select Structural

F_b = 1,800 psi

F_t = 1,200 psi

F_v = 95(190) psi

$F_{c\perp}$ = 385 psi

$F_{c_{11}}$ = 1,400 psi

E = 1.8×10^6

To establish the probability distributions for this material the following data are required.

o Basic Material - Ref. Table 4-1

Douglas Fir Coast - Clear Green

Property	Mean	Std. Dev.
F_b	7,665	1,317
F_v	904	131
$F_{c\perp}$	382	107
$F_{c_{11}}$	3,784	734
E/1,000	1,560	315

o Grading - Ref. Table 4-4

"Strength Ratios"

F_b = 0.54

F_t = 0.31

F_v = 0.50

$F_{c\perp}$ = 1.00

$F_{c_{11}}$ = 0.62

E = 1.00

o Seasoning - Moisture Content

F_b = 1.25 @ M.C. = 19%

F_t = 1.25

F_v = 1.08

$F_{c\perp}$ = 1.50

$F_{c_{11}}$ = 1.50

E = 1.14

Using 19% is probably reasonable as the timbers arrived quite green and were not stored very long (a few days to a few weeks).

o Duration effects are to be treated next. The tests were an attempt at approximating a blast load and most failures (maximum loads) took place in the 2 to 10 second range. Hence, the duration factor will be set at 1/1.9 except $F_{c\perp}$ and E which will be 1/1 for test data. The factors 1/1.6 and 1/1, respectively, are used for conversion of clear green wood to normal design allowables.

The basic properties are derived in Table 4-14 and Table 4-15 then plotted on Fig. 4-17 and Fig. 4-18.

<u>Analysis of the Floor System</u>

Since the system is basically the same design as the W.E.S. system the analysis results only are presented.

o Dead load = 10 psf

o Live load = 40 psf (normal)

F_b = 1,197 psi < 1,993 psi

F_v = 51.6 psi < 232 psi

$F_{c\perp}$ = 178 psi < 573 psi

Therefore safe as designed.

o Test Loading Prediction/Analysis: Here one must expect actual failure near the mean or expected value(s).

$\overline{F_b}$ = 5,284 psi

or $\overline{W} = \frac{5,284}{1,197}(50 \text{ psf})$

$\overline{W}$ = 221 psf

or an applied loading of

W = 211 psf expected.

Table 4-14. Structural Property Evaluation of Douglas-Fir, Select Structural

Property	Mean psi	Std. Dev. psi	Strength Ratio	Seasoning 19%	Duration	Depth	Combined	Mean	Std. Dev.	5% Excl.	NDS Allow.
F_b	7665	1317	0.54	1.25	1/1.6	0.86	0.363	2781	478	1993	1800
F_c	3784	734	0.62	1.50	1/1.6	--	0.581	2199	427	1495	1400
F_v	904	131	0.50	1.08	1/1.6	--	0.338	305	44	232	190*
F_t	7665	1317	0.31	1.25	1/1.6	--	0.242	1856	319	1330	1200
$F_{c\perp}$	382	107	1.00	1.50	1.00	--	1.500	573	161	--	385
$F_{c\perp}$(ult.)	855	194	1.00	1.50	1.00	--	1.500	1282	291	802**	--
E/1000	1560	315	1.00	1.14	1.00	--	1.140	1778	356	--	1800
	Clear Wood Green							Normal Load Properties			

* No checks.

** These data are from Ref. #1 (also see Tables 4-7, 4-8 and Figure 4-10). Further the Ref. had $F_{c\perp}$ = 1341 and $\sigma_{F_{c\perp}}$ = 430 for dry specimens (11% M.C.) and corrected to 19% M.C. $F_{c\perp}$ = 1016 and $\sigma_{F_{c\perp}}$ = 263.

Table 4-15. Structural Property Evaluation of Douglas-Fir, Select Structural

Property	Mean	Std. Dev.	5% Excl.	Mean	Std. Dev.	5% Excl.	Mean	Std. Dev.	5% Excl.
F_b	2781	478	1993	3337	574	2390	5284	908	3785
F_c	2199	427	1495	2639	512	1793	4178	811	2839
F_v	305	44	232	366	53	279	580	84	442
F_t	1856	319	1330	2227	383	1596	3526	606	2526
$F_{c\perp}$	573	161	Constant values →						
$F_{c\perp}$(ult.)*	1016	263	Constant values →						
E/1000	1778	356	Constant values →						
	Normal Load Parameter Load Factor - 1.0			2 week load Parameter Load Factor - 1.2			Dynamic Parameter Load Factor - 1.9		

** Estimated at 19% M.C. Based on Ref. 1 no increase in $F_{c\perp}$, seems consistent for Dry Material.

NOTE: No increase for E & $F_{c\perp}$ and Means conventionally used.

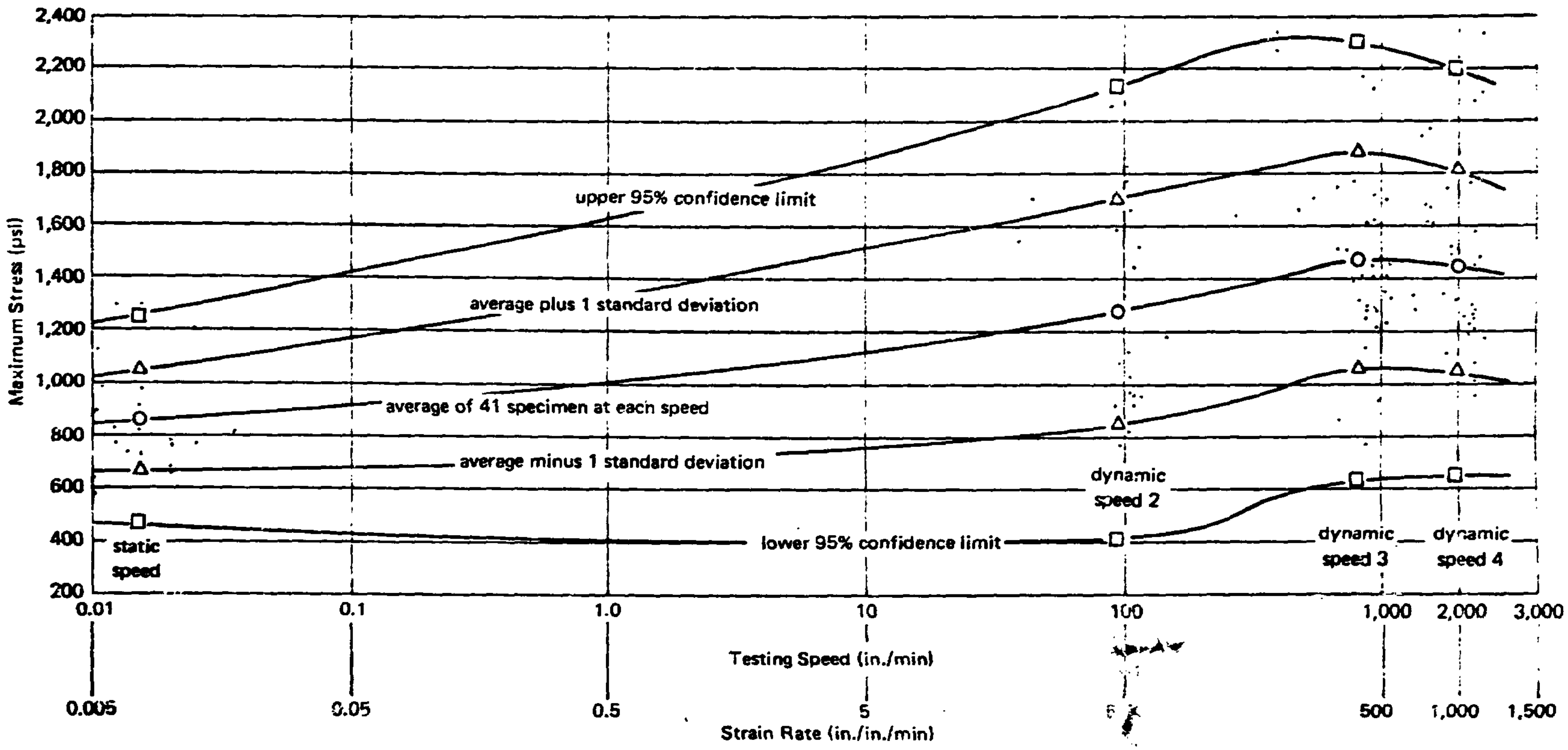

Fig. 4-17. Relation Between Maximum Stress and Testing Speed (Green Specimens, Compression Perpendicular to Grain).

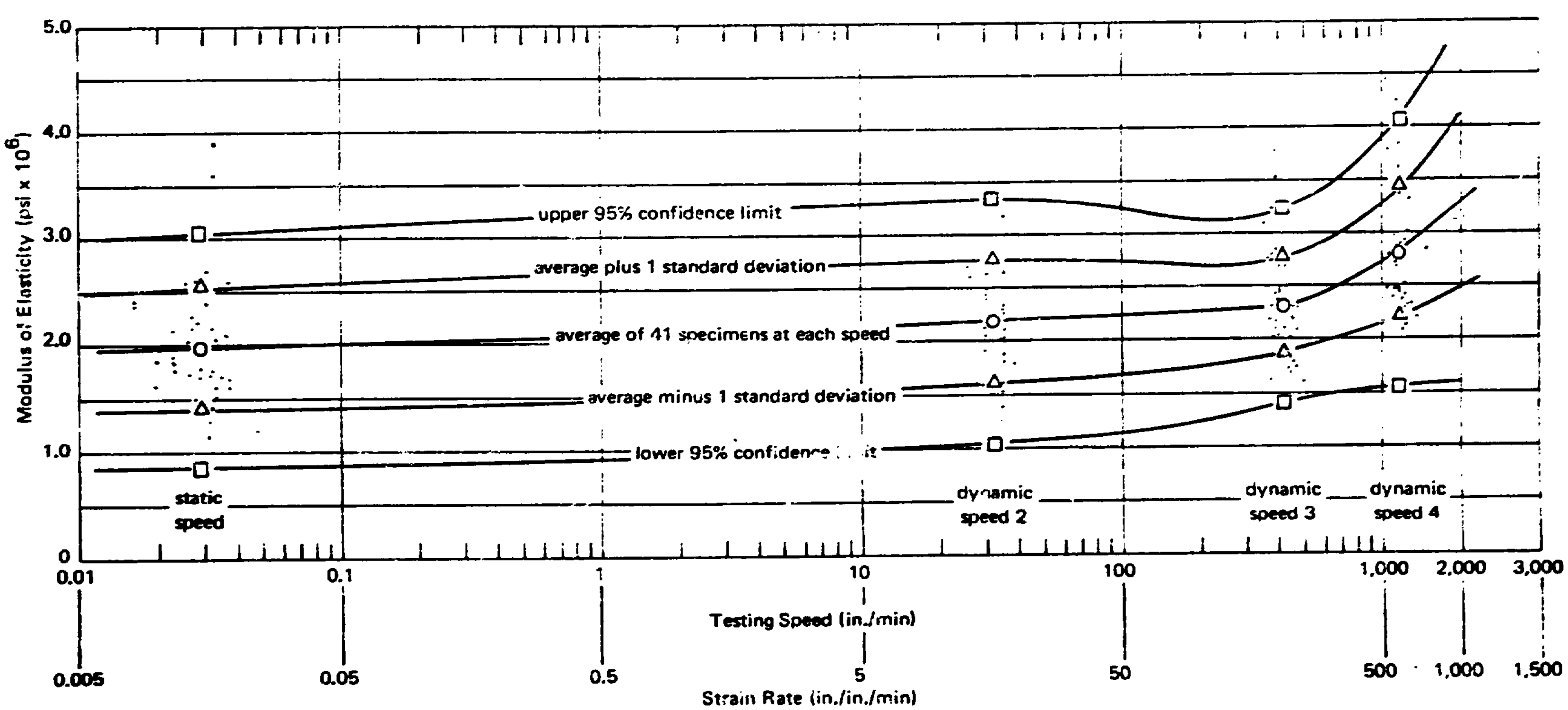

Fig. 4-18. Relation Between Modulus of Elasticity and Testing Speed (Dry Specimens, Compression Parallel to Grain).

Actual test value for floor No. 1: $w = 166$, and

floor No. 4: $w = 224$, which are plotted on Fig. 4-19.

Note that the bearing stress at the support ends also increases or

$$F_{c\perp} = \left(\frac{5,284}{1,197}\right) 178 \text{ psi}$$

$F_{c\perp} = 786$ psi which,is greater than $\overline{F}_{c\perp} = 573$ psi.

Some minor bearing deformations did occur, but not as much as the above number might indicate. However, $F_{c\perp} = 786$ is indeed lower than the $F_{c\perp}$(ult.) shown in Table 4-15 ($\overline{F}_{c\perp}$(ult.) = 1,016 psi). Hence, it appears that the ultimate bearing stress is on the order of 2 times the proportional limit.

Specimens 3 and 6 were tested on mode 3, that is with a 2 x 6 glued to the bottom flange. No. 3 had a maximum load of 288 psf and No. 6, 472 psf. The corresponding flexural stresses are plotted on Fig. 4-20.

Rank	Specimen	F_b	%
1	No. 3	3,973	20
2	No. 1	4,210	40
3	No. 4	5,362	60
4	No. 6	6,410	80
		4,989	

It is observed that the experimental mean bending stress (4,989 psi) is 5.6% below the predicted mean of 5,284, which is exceptionally close for theory vs. experimental work of any kind. Also, a small variation in M.C. alone could account for more than the 5.6% difference.

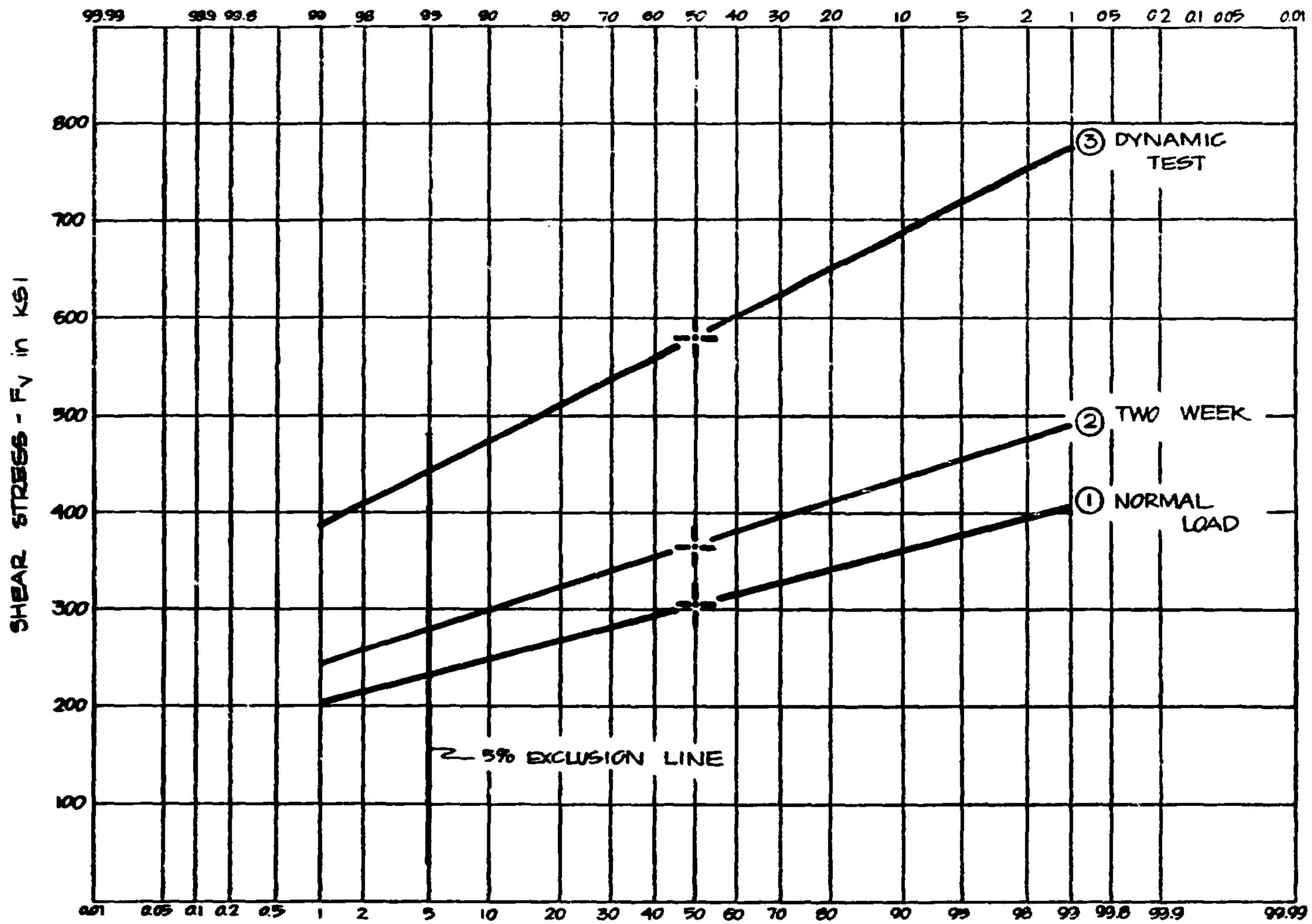

Fig. 4-19. Shear Strength Distributions.

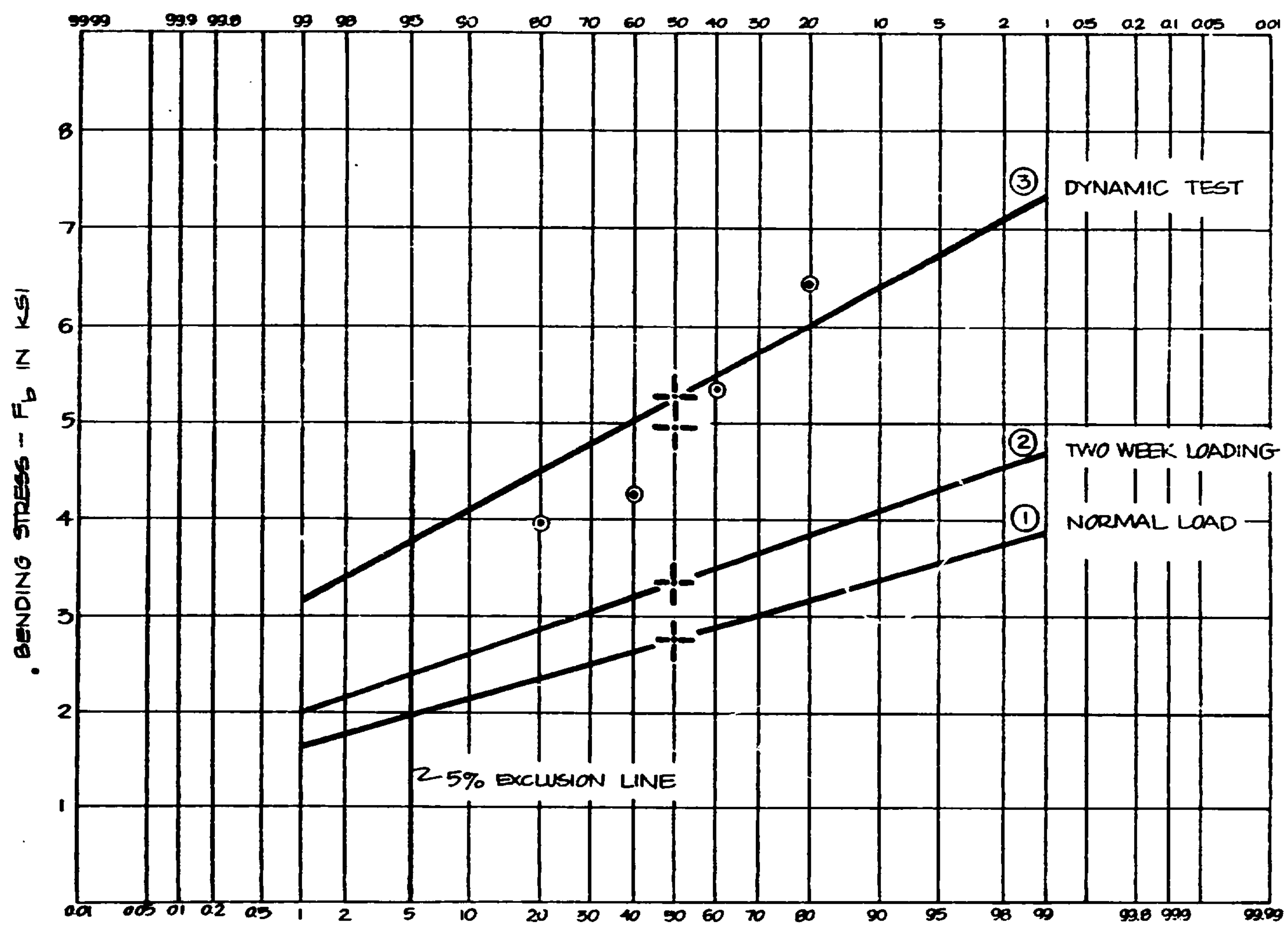

Fig. 4-20. Modulus of Rupture Distributions.

Section 5
OPEN-WEB STEEL JOISTS

INTRODUCTION

The behavior of steel structures is relatively well defined and understood on into the plastic or ultimate range and the body of knowledge concerning steel design is broad and even included in the building codes. Thus, the emphasis in this program was concentrated on predicting the behavior of upgrading techniques. The approach used is known as stress control, that is, if stresses can be controlled in the various portions of the structure such that each portion of the structure can achieve its maximum capability or near so, the system's overall efficiency in load carrying is increased. In the text of the report it is shown that by using flexible supports or shores the stresses in the members can indeed be controlled. For example, by allowing the proper flexibility of the shore one can keep the bottom chord from going into compression. This is very desirable in a structure like a roof or floor system truss supported as the lower chords are usually very minimally braced. Hence, they are designed for tension and if rigidly shored would result in a stress reversal in the bottom chord causing failure at a lower load than design load because of the mode of failure change. It is felt that this stress control approach to structural upgrading of systems will be a significant factor in the development of viable upgrading techniques.

Two open-web steel joists were analyzed for this report. The first was a 28-foot long 18J6 and the second was a 20-foot long 18H8. The 18J6 open-web steel joist was selected for anlaysis so that it could be compared with the test results obtained by Waterways Experiment Station (Ref. 4). The 18H8 was selected for analysis because it is more commonly used in the construction of commercial buildings.

Open-web steel joists will typically fail in one of two primary modes of failure. Long spans will generally fail due to the buckling of a top chord member (moment failure), and in short spans, a web member will generally buckle (shear failure). The joists selected for analysis for 18J6 and 18H8 exhibit both primary modes of failure, moment and shear failures, respectively.

O.W.J. ANALYSIS MODEL SELECTIONS

The W.E.S. report gave no specific details of the O.W.J. member sizes or dimensions (see Fig. 5-1). Therefore, an equivalent Bethlehem Steel 18J6 open-web steel joist was selected for computer analysis. The basic Bethlehem Steel joist specifications are shown in Table 5-1. It has been found that O.W.J. vary from manufacturer to manufacturer — the W.E.S. open-web joist had back-to-back angles for both top and bottom chord members, whereas the Bethlehem Steel O.W.J upper chord is made up of two back-to-back angles, but two bars 23/32 in. in diameter make up the lower chord.

In an attempt to model as closely as possible the W.E.S joist, the bottom chord of the basic Bethlehem Steel O.W.J was assumed (for the sake of analysis) to be identical to the top chord. A sketch of the modified 18J6 O.W.J. can be seen in Fig. 5-2. In making this assumption, the bottom chord cross-sectional area was increased by 30% over the Bethlehem design. One would expect the analyzed joist to deflect about 20% to 30% less than the joist found in the standard load tables. Since the bottom chord did not fail in the original Bethlehem design, this change should not affect the failure mechanism.

Although the W.E.S. joist and the modified Bethlehem Steel joist are probably not exactly the same, they should be sufficiently similar to allow approximate comparisons to be made.

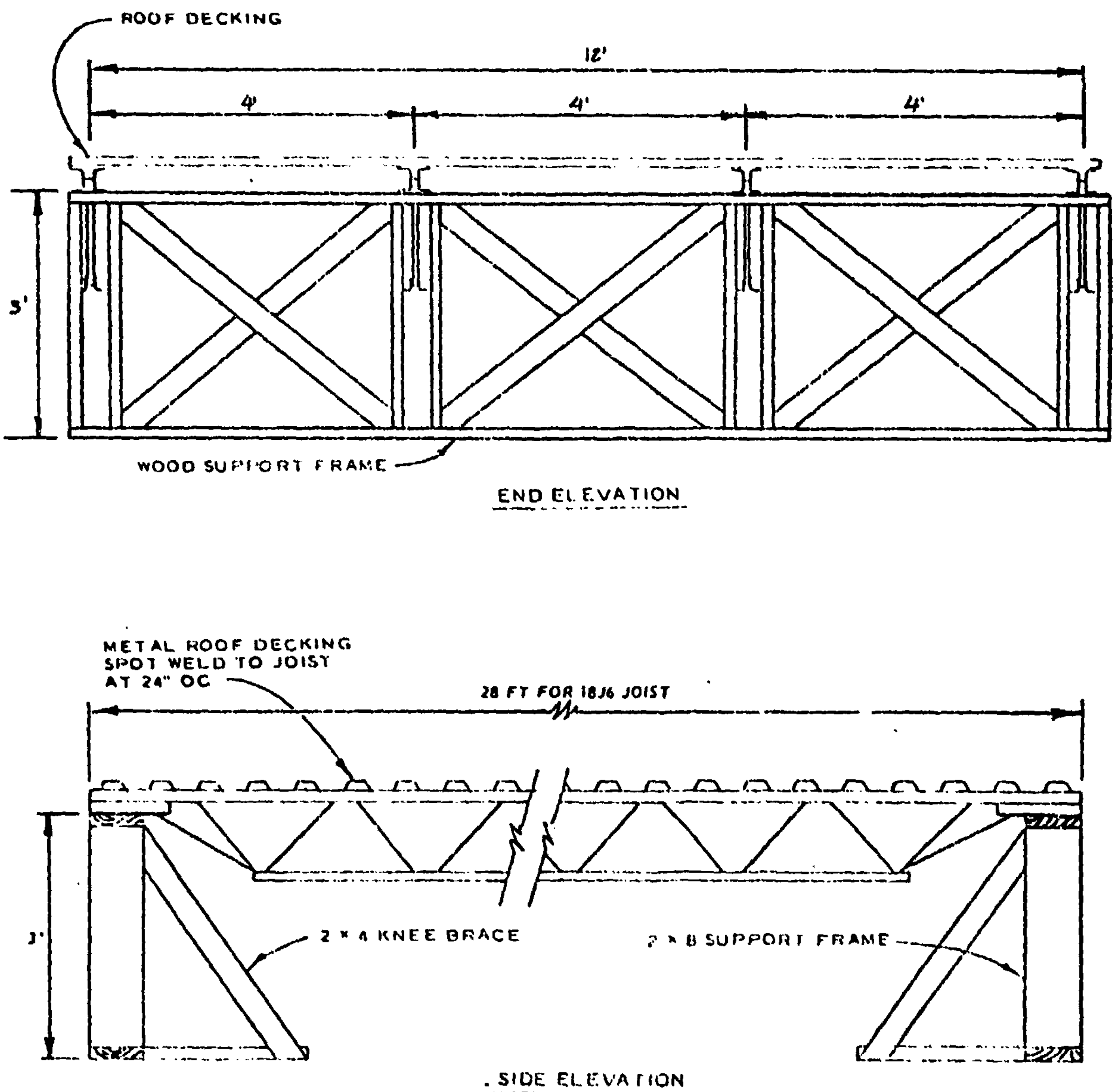

Fig. 5-1. Test Setup for O.W.J. Roof Systems (from Ref. 4).

Table 5-1. Properties of J Series Open-Web Joists (from Ref. 15)

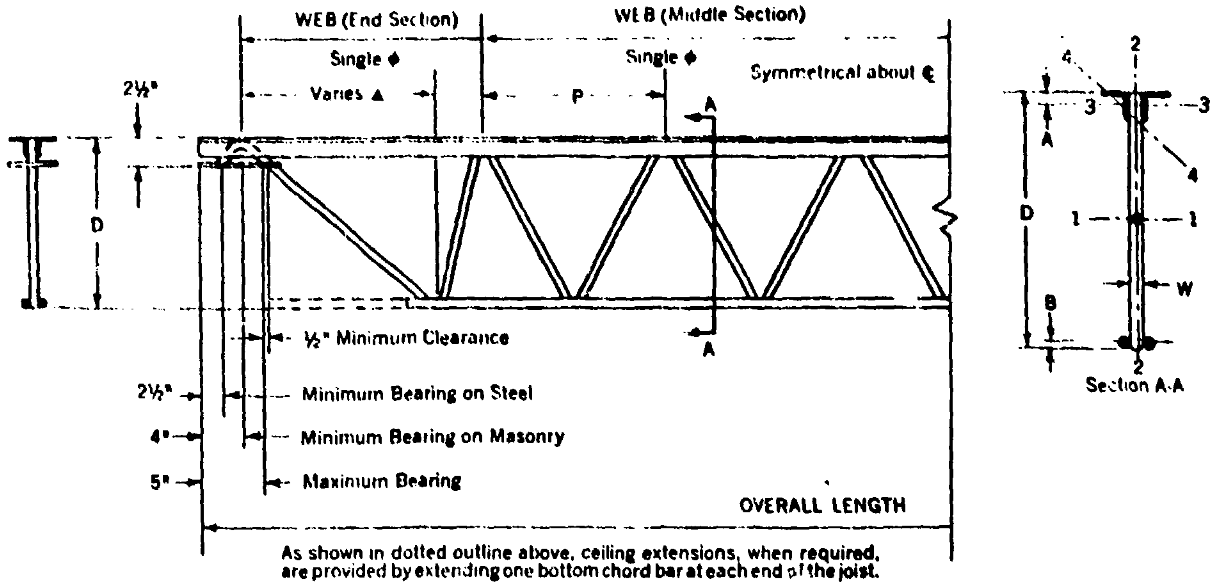

As shown in dotted outline above, ceiling extensions, when required, are provided by extending one bottom chord bar at each end of the joist.

▲ 1¼ D for 8" thru 12" joists
D for 14" thru 24" joists

J-SERIES HOT-ROLLED

Joist Designation	Actual Depth D	Top Chord (2 L's) Angles	Top Chord Area	Top Chord r axis 4-4	Top Chord s axis 3-3	A	Bottom Chord (2 bars) Diam	Bottom Chord Area	B	P	Web End Section Diam W	Web End Section Area	Web End Section r axis 2-2	Web Middle Section Diam W	Web Middle Section Area	Web Middle Section r axis 2-2	Moment of Inertia axis 1-1
	in.	in.	in.²	in.	in.³	in.	in.	in.²	in.	in.	in.	in.²	in.	in.	in.²	in.	in.⁴
8J2	8	1 x 1 x ⅛	0.46	.20	.062	.30	15/32	.345	.234	14	17/32	.222	.133	13/32	.130	.102	11.4
10J2	10	1 x 1 x ⅛	0.46	.20	.062	.30	15/32	.345	.234	14	19/32	.277	.148	15/32	.172	.117	17.7
10J3	10	1¼ x 1¼ x ⅛	0.60	.25	.098	.36	17/32	.443	.266	18	19/32	.277	.148	15/32	.172	.117	22.5
10J4	10	1½ x 1½ x ⅛	0.72	.30	.148	.42	19/32	.554	.297	18	19/32	.277	.148	17/32	.222	.133	27.1
12J2	12	1 x 1 x ⅛	0.46	.20	.062	.30	15/32	.345	.234	14	19/32	.277	.148	15/32	.172	.117	26.0
12J3	12	1¼ x 1¼ x ⅛	0.60	.25	.098	.36	17/32	.443	.266	18	19/32	.277	.148	17/32	.222	.133	33.0
12J4	12	1½ x 1½ x ⅛	0.72	.30	.148	.42	19/32	.554	.297	18	21/32	.338	.164	17/32	.222	.133	40.0
12J5	12	1½ x 1½ x 5/32	0.89	.29	.175	.43	21/32	.676	.328	18	21/32	.338	.164	17/32	.222	.133	48.4
12J6	12	1½ x 1½ x 3/16	1.06	.29	.204	.44	23/32	.811	.359	18	21/32	.338	.164	17/32	.222	.133	57.9
14J3	14	1¼ x 1¼ x ⅛	0.60	.25	.098	.36	17/32	.443	.266	18	21/32	.338	.164	17/32	.222	.133	45.6
14J4	14	1½ x 1½ x ⅛	0.72	.30	.148	.42	19/32	.554	.297	18	21/32	.338	.164	17/32	.222	.133	55.4
14J5	14	1½ x 1½ x 5/32	0.89	.29	.175	.43	21/32	.676	.328	18	23/32	.406	.180	19/32	.277	.148	67.0
14J6	14	1½ x 1½ x 3/16	1.06	.29	.204	.44	23/32	.811	.359	18	23/32	.406	.180	19/32	.277	.148	80.3
14J7	14	1¾ x 1¾ x 3/16	1.24	.34	.290	.51	25/32	.959	.391	18	23/32	.406	.180	19/32	.277	.148	93.2
16J4	16	1½ x 1½ x ⅛	0.72	.30	.148	.42	19/32	.554	.297	18	23/32	.406	.180	19/32	.277	.148	73.3
16J5	16	1½ x 1½ x 5/32	0.89	.29	.175	.43	21/32	.676	.328	18	23/32	.406	.180	19/32	.277	.148	88.6
16J6	16	1½ x 1½ x 3/16	1.06	.29	.204	.44	23/32	.811	.359	18	23/32	.405	.180	19/32	.277	.148	106
16J7	16	1¾ x 1¾ x 3/16	1.24	.34	.290	.51	25/32	.959	.391	18	23/32	.406	.180	21/32	.338	.164	124
16J8	16	2 x 2 x 3/16	1.42	.39	.380	.57	27/32	1.118	.422	18	23/32	.406	.180	21/32	.338	.164	142
→ 18J5	18	1½ x 1½ x 5/32	0.89	.29	.175	.43	21/32	.676	.328	20	25/32	.479	.195	21/32	.338	.164	113
→ 18J6	18	1½ x 1½ x 3/16	1.06	.29	.204	.44	23/32	.811	.359	20	25/32	.479	.195	21/32	.338	.164	136 ←
18J7	18	1¾ x 1¾ x 3/16	1.24	.34	.290	.51	25/32	.959	.391	20	25/32	.479	.195	21/32	.338	.164	159
18J8	18	2 x 2 x 3/16	1.42	.39	.380	.57	27/32	1.118	.422	20	25/32	.479	.195	23/32	.406	.180	182
20J5	20	1½ x 1½ x 5/32	0.89	.29	.175	.43	21/32	.676	.328	22	25/32	.479	.195	23/32	.406	.180	141
20J6	20	1½ x 1½ x 3/16	1.06	.29	.204	.44	23/32	.811	.359	22	25/32	.479	.195	23/32	.406	.180	170
20J7	20	1¾ x 1¾ x 3/16	1.24	.34	.290	.51	25/32	.959	.391	22	25/32	.479	.195	23/32	.406	.180	198
20J8	20	2 x 2 x 3/16	1.42	.39	.380	.57	27/32	1.118	.422	22	25/32	.479	.195	23/32	.406	.180	227
22J6	22	1½ x 1½ x 3/16	1.06	.29	.204	.44	23/32	.811	.359	24	27/32	.559	.211	23/32	.406	.180	207
22J7	22	1¾ x 1¾ x 3/16	1.24	.34	.290	.51	25/32	.959	.391	24	27/32	.559	.211	25/32	.479	.195	241
22J8	22	2 x 2 x 3/16	1.42	.39	.380	.57	27/32	1.118	.422	24	27/32	.559	.211	25/32	.479	.195	277
24J6	24	1½ x 1½ x 3/16	1.06	.29	.204	.44	23/32	.811	.359	24	29/32	.645	.227	25/32	.479	.195	248
24J7	24	1¾ x 1¾ x 3/16	1.24	.34	.290	.51	25/32	.959	.391	24	29/32	.645	.227	25/32	.479	.195	289
24J8	24	2 x 2 x 3/16	1.42	.39	.380	.57	27/32	1.118	.422	24	29/32	.645	.227	25/32	.479	.195	332

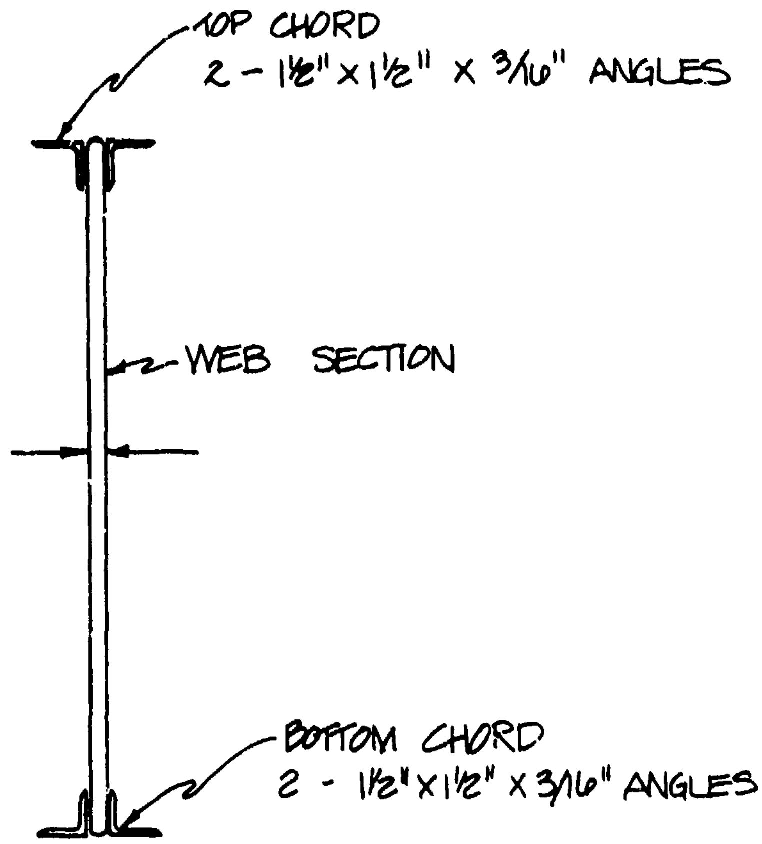

Fig. 5-2. Sketch of Analyzed 18J6 O.W.J.

DISCUSSION OF TESTS CONDUCTED BY W.E.S. ON 18J6 OPEN-WEB STEEL JOISTS

The Waterways Experiment Station (W.E.S.) conducted a series of tests on open-web steel joists for the Defense Civil Preparedness Agency under Contract No. DCPA01-75-C-0286. With the help of an architect they selected two open-web steel joists to be tested based upon "Modern School Construction in Most Parts of the Country". After reviewing their reported test arrangement and scrutinizing the report photographs, one apparent omission of the recommended open-web joist construction procedure stands out; there is no evidence that any lateral bridging of the bottom chord was present during testing. Reference 16 (The Manual of Steel Construction, page 5-284, Section 5.4) recommends that no less than three rows of bridging for 18J6 joists spanning 28 feet be installed. Each row of bridging should resist 700 pounds of horizontal force, with the ends of the bridging anchored into walls or beams. Without adequate bottom chord bridging, a simply supported 18J6 joist with a 28-ft span is very likely to be unstable and certainly will be unstable should the bottom chord go into compression, which occurs when shoring is installed.

Another problem observed with the test arrangement was that all of the O.W.J., in the roof systems tested, did not receive identical loads. A typical cross-section of the roof section is shown below:

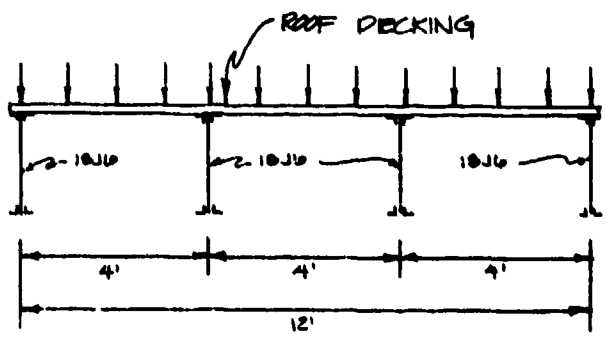

Typical Cross-Section of 18J6 Open-Web Steel Joist Testing Arrangement Conducted by the Waterways Experiment Station.

In this test the two outside joists received only one-half the load compared to the interior joists. An alternate test arrangement would be to continue the deck 2 ft beyond the 18J6 as shown below. Provisions would of course have to be made to prevent the 2-ft overhanging sections from failing. However, with this type of testing arrangement, the roof system would insure failure as a unit rather than having a situation where the interior joists may begin to buckle, and as they fail the two outer joists pick up additional load until they in turn fail and the roof finally collapses. There is some evidence of this problem shown in photographs in the W.E.S. report; that is, the two inside trusses appear to be more severly damaged.

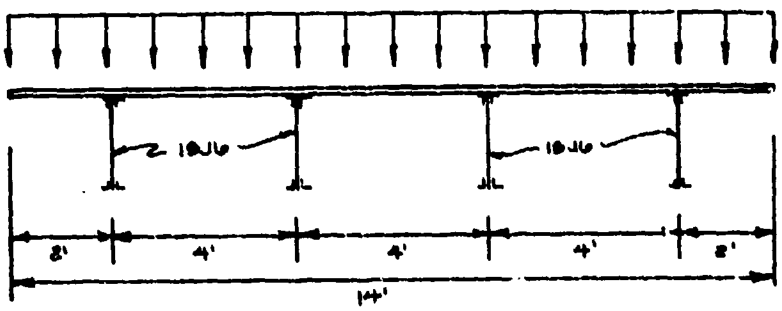

O.W.J. 18J6 Case No. 1

The results for the 18J6 open-web steel joist analysis are presented in Table 5-2. Case No. 1 represents a simply supported O.W.J. without any interior shoring. The analysis found that at a load of 269 PLF, the top chord at mid-span reached the maximum compression stress allowed for that particular member. If the load is increased to approximately 1.8 times the allowable load (484 PLF) the top chord would buckle and cause collapse at mid-span. The Manual of Steel Construction (see Ref. 16) gives an allowable total safe load for this O.W.J. of 249 PLF, about 8% below that determined by analysis (269 PLF). The standard load table also indicates that for the O.W.J. under consideration, the mode of failure would be due to chord buckling (i.e., moment failure). The analysis results and published values (from Ref. 16) for Case No. 1 are presented in Fig. 5-3. In this load versus deflection plot, the modified Bethlehem Steel joist is about 35%

PLF = pounds per linear foot of span

Table 5-2. Open-Web Joist, J-Series, 18J6, 28-ft Span, Simply Supported at Its Ends

Case No.	Type of Shoring	Allowable Load	Ultimate Load	Type of Failure	Percent of Case No. 1
1	None - Base Case	269 PLF*	487 PLF	Top chord buckling	100%
2	Rigid shore at center span	397 PLF	715 PLF	Web buckling	148%
3	Rigid shores at the third points	684 PLF	1,121 PLF	Web buckling	254%
3a	Flexible shores at the third points with 1/8 in. deflection at the allowable working load	707 PLF	1,273 PLF	Web buckling	262%
3b	Flexible shores at the third points with 1/4 in. deflection at the allowable load	707 PLF	1,273 PLF	Web buckling	262%

* The values given in the AISC Manual for this case are:

- 249 PLF; Total safe uniformly distributed load carrying capacity.
- 204 PLF; Live load which produces an approximate deflection of 1/360 of the span.

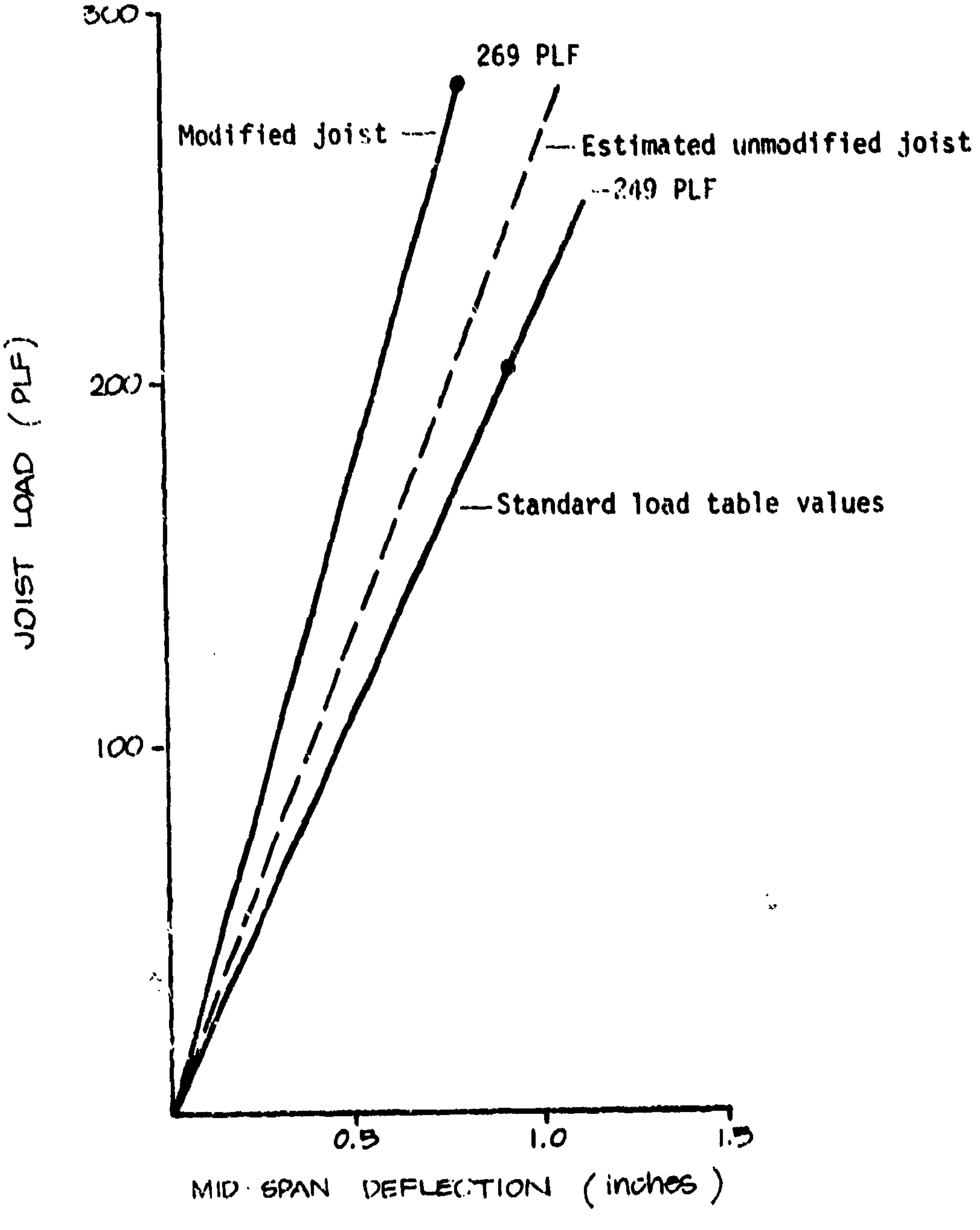

Fig.5-3. Load vs Deflection Comparison of Modified, Unmodified, and Standard Values — Bethlehem Steel Open-Web Joist.

stiffer than the standard load table (see Ref. 15) values. The modified lower chord is 30% larger in area than the unmodified lower chord. This would account for a corresponding decrease in deflection. The dashed line in Fig. 5-3 represents the Bethlehem Steel O.W.J. with the unmodified bottom chord. The standard Bethlehem O.W.J. is about 16% stiffer than that from the standard load tables.

The allowable load and failure mechanisms were found to be about the same for the analyzed and standard load table joists, although the analyzed joist was found to be a bit stiffer. These close correlations between the analyzed results and published values seem to indicate that comparisons between joists of different manufacturers, and of identical joist designations and spans, can indeed be made.

Simple-Span Analysis Results Versus W.E.S. Test. The analysis results and the test results (see Ref. 4) for a simply supported 18J6, 28-ft long, are presented in Fig. 5-4. There exists a very close correlation between our model analysis and the actual test results. Based on the model analysis results and using a factor of safety on the allowable load of 1.8, the open-web steel joist roof system should collapse at 484 PLF. W.E.S. reported a failure load of 650 PLF (20 in. of sand) or a factor of safety of 2.4. The probable explanation for this discrepancy lies in their assumption that each of the floor joists received an effective load equivalent to 4 ft of width. For example, from Ref. 4:

$$W \text{ equivalent} = 20'' \times 100 \text{ lb/ft}^2 \times 4 \text{ ft} = 667 \text{ lb/ft} \cong 650 \text{ PLF}$$

The W.E.S. report states that: "Previous tests on O.W.J. roofs . . . indicate that the failure load was approximately 1.8 times the allowable load from standard joist load tables . . . ." (see Ref. 4), but offers no explanation as to why a factor of safety of 2.4 was used and not 1.8 as expected.

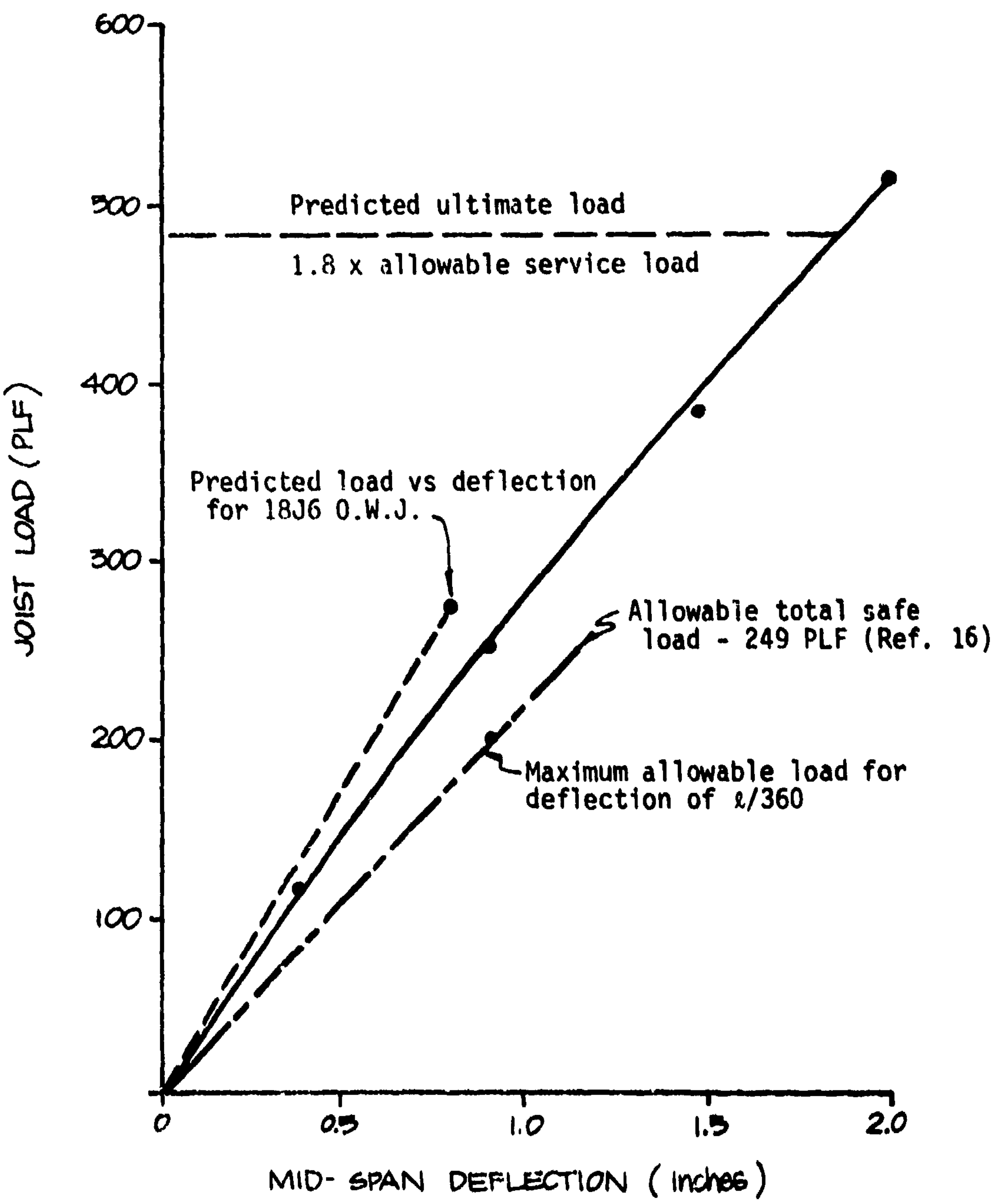

Fig. 5-4. Analysis and Test Results for 28-ft Long 18J6. Note: Actual Failure Occurred at W = 559 PLF (Ref. 4).

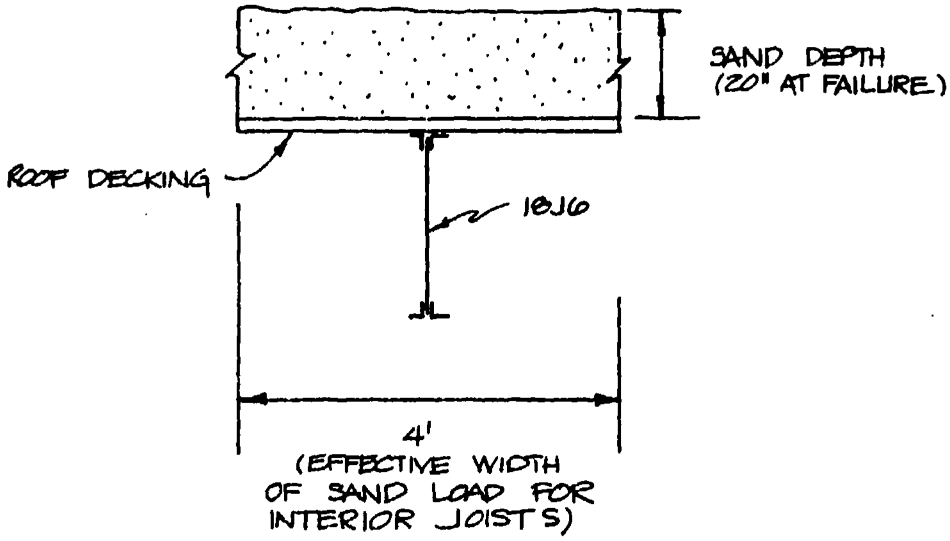

The fact is that the roof decking will be able to transfer a portion of the load to the outside, less stressed, joists. As the load was increased to 484 PLF (14½ in. of sand), the middle joists probably began to fail (buckle). They continued to support the 484 PLF but as more load was added, the middle two joists, already at or near critical load, could not take any additional load. Hence, the decking transferred the additional load to the two outside joists. The roof system finally collapsed when the outer two joists reached their critical load. If the load transfer through the deck is assumed effective, the actual values should have been 75% of the reported W.E.S. joists loads, or

$$W = 0.75\ (650) = 488\ \text{PLF}$$

which is within 1% of the value predicted by the model analyzed for this report and about 8% higher than shown in the standard load tables (Ref. 16).

<u>O.W.J. 18J6 Case No. 2</u>

Prior to failing the roof joist system, W.E.S. also tested it with mid-span shores and two-third point shores. Load versus deflection plots were made for both tests.

Fig. 5-5 shows the shore arrangement for the center shore. The shore was placed left from the center of the span in order to place the shore under a web member; i.e., at a joint. Sand was piled on top of the roof system until a weld under one of the shores failed. The load versus deflection data for the center shoring are presented in Fig. 5-6, along with the analyzed joist assuming a rigid center support.

It should be noted that the model prediction is much softer than the actual test data. In reality, the shore will deflect slightly downward and should produce more deflection than the prediction indicated (assuming a perfectly rigid shore). Three possibilities exist which might explain this discrepancy. The first is that it appears that deflections were measured on the outside joists. The outside joists having less load, due to the test arrangement, would, as expected, have less deflection than the two interior joists. The second possible explanation could be that the load plotted on the ordinates might be as much as 33% too large. This is due to the load sharing between the interior and outside joists. Some load is most likely to be transferred through the decking to the outside joists. Finally the weld failure, at the center shore, would produce unrealistically large deflections near failure.

The weld failure problem at the shore was corrected in the next test (third-point shores) by placing the shore supports under the web members rather than under the chord members (see Fig. 5-7). If this type of shore arrangement had been used for the center shore test, then the safe allowable load (from the S.S.I. joist model analysis) would have been 397 PLF, and the predicted ultimate failure would be about 1.8 times this value, or 715 PLF. The allowable load represents a 48% increase in load over the simply supported O.W.J. The failure mode has also changed from mid-span chord buckling to web buckling (see Figs. 5-8 and 5-9). One important difference between the simply supported case and the center shore case is that in the latter case significant compressive stresses develop in the lower chord. With three rows of horizontal bracing as required by AISC Manual (in the W.E.S. test none), lateral buckling of the lower chord becomes a very real possibility. The joist analyzed had two back-to-back

A. Support System

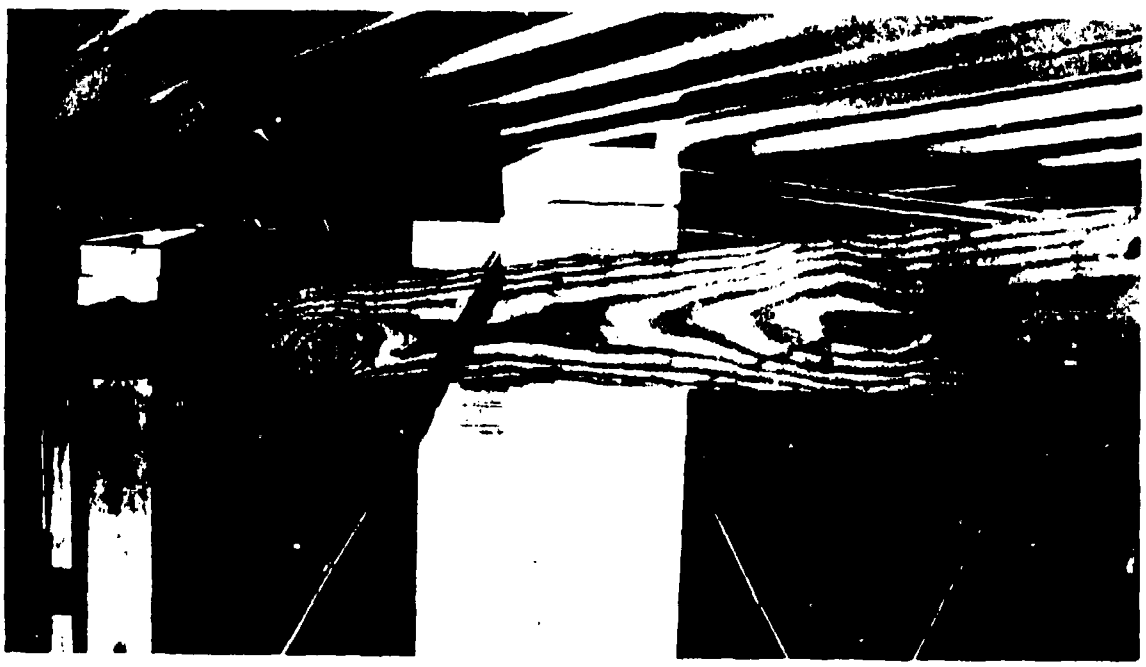

B. Closeup of Connection Between O.W.J and Support

Fig. 5-5. Twenty-eight-foot O.W.J Roof with Supports (shores) at Mid-Span (from Ref. 5).

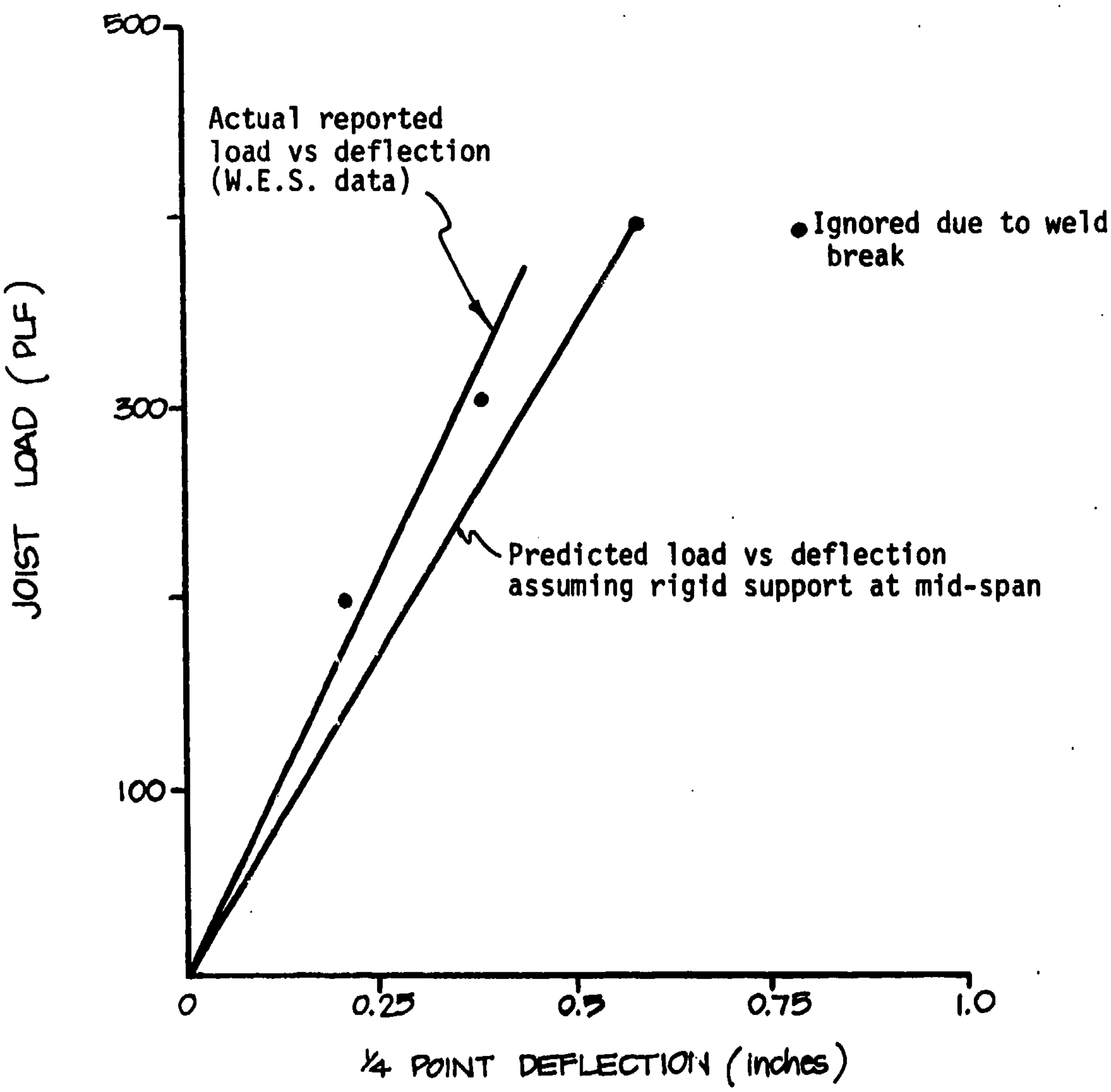

Fig. 5-6. Actual and Predicted Load vs Deflection Data for Center Shore Case.

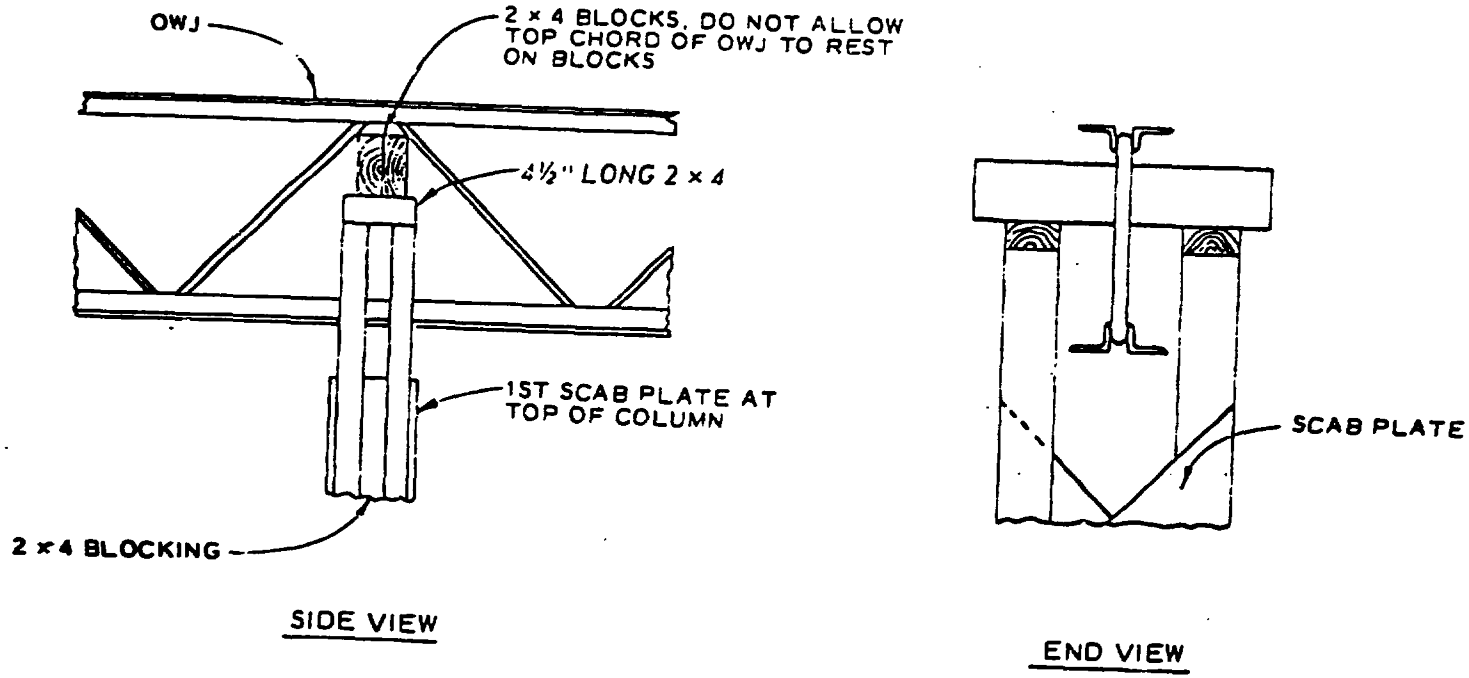

Fig. 5-7. Connection Detail O.W.J. to Column (from Ref. 5).

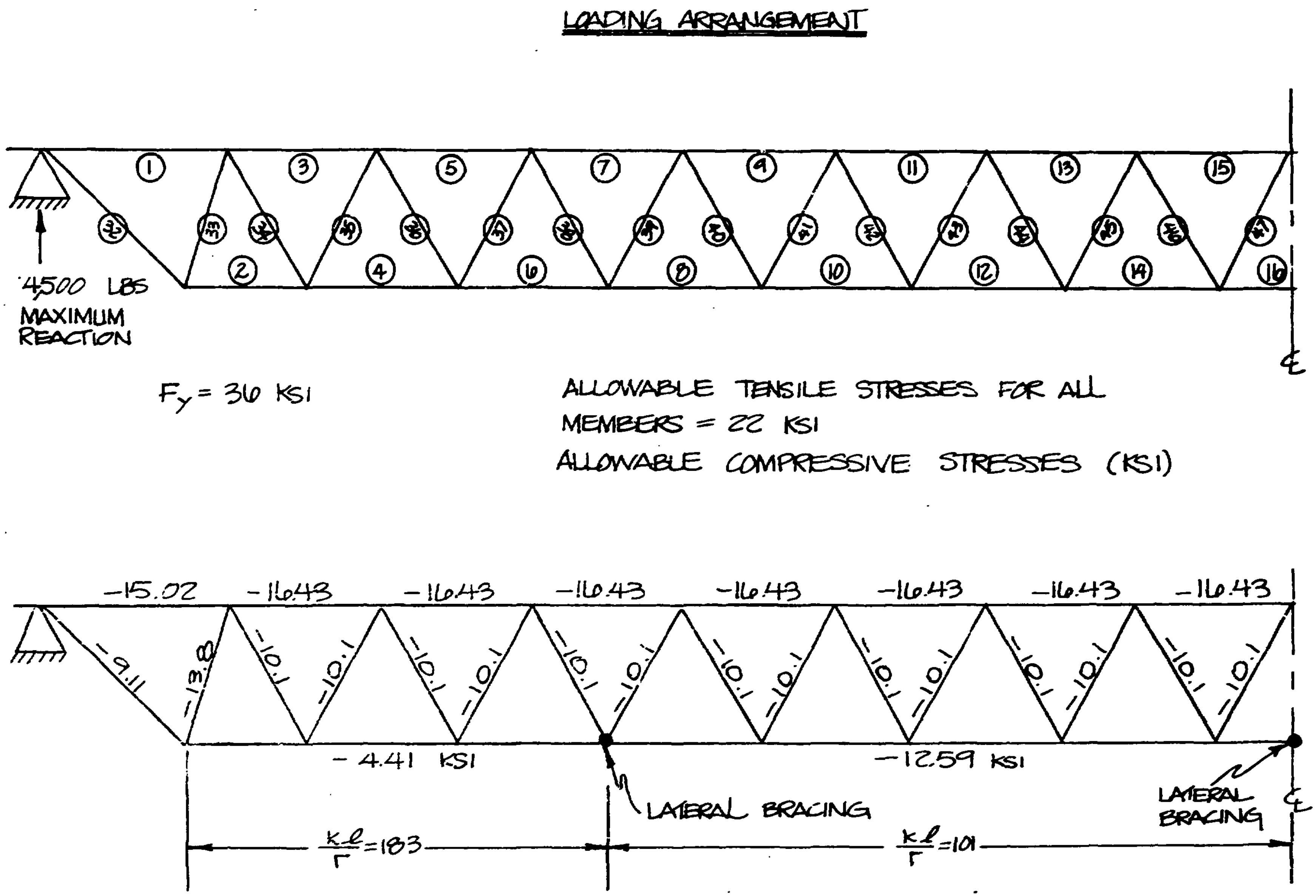

Fig. 5-8. Analysis of 18J6 Open-Web Joist — 28-ft Span.

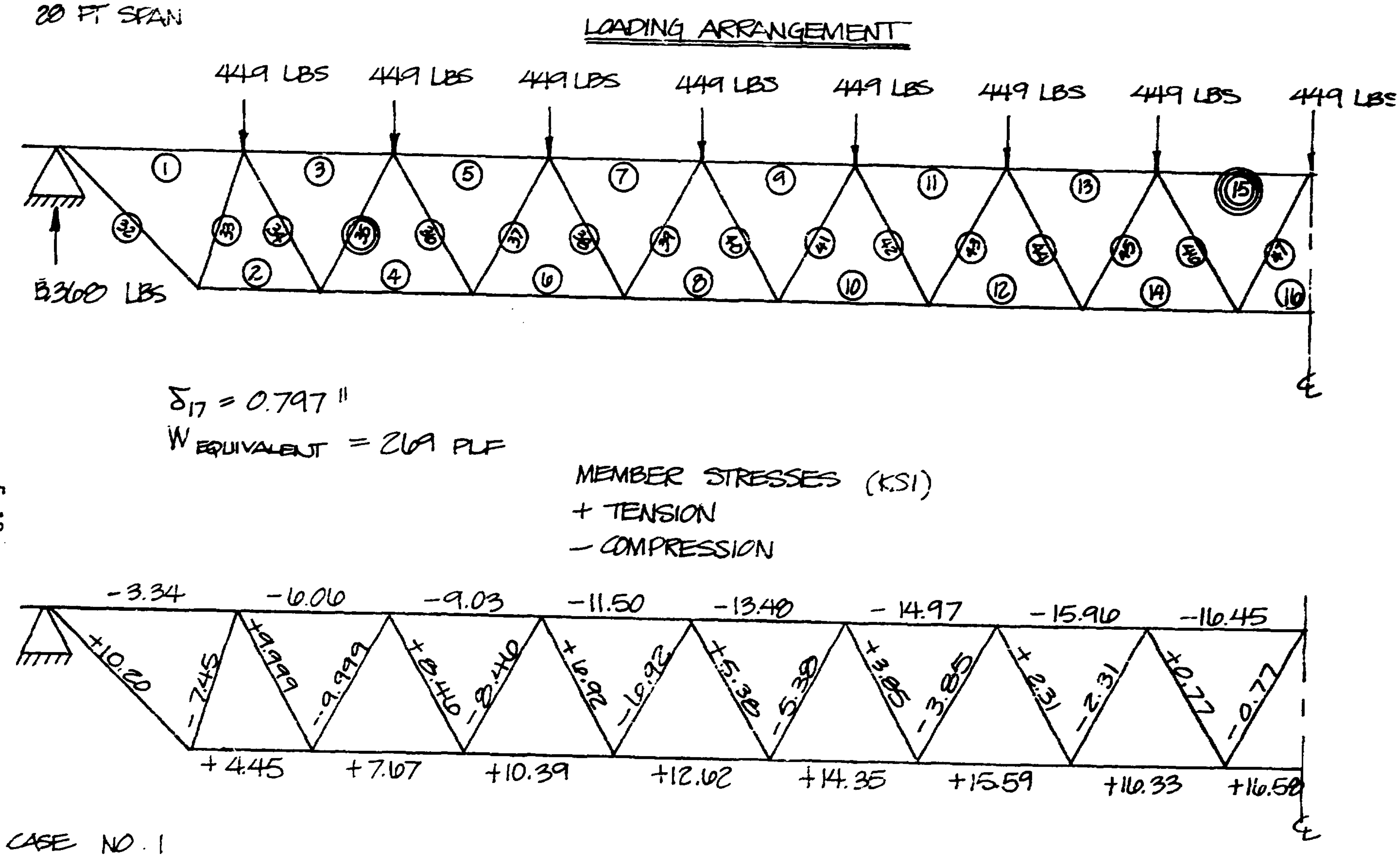

Fig. 5-9. Analysis of 18J6 Open-Web Joist — 28-ft Span — Case No. 1 (W = 269 PLF).

angles making up the lower chord. If the specified bracing is present, the lower chord is well understressed (refer to Figs. 5-8, 5-9, and 5-10). With inadequate bracing or if the lower chord is made up of two round No. 6 steel bars, as in the Bethlehem design, the allowable compression stresses would become larger and could result in the lower chord becoming critically stressed and collapsing first.

Analysis of Third-Point Shoring. Three third-point shoring arrangements were analyzed. The first (Case No. 3) assumed the shore to be rigid; the second and third (Cases No. 3a and 3b) assumed flexible shores with 1/8 in. and 1/4 in. deflections, respectively, at the maximum allowed safe load. The results are presented in Table 5-2. The member stress levels for Cases 3, 3a, and 3b are presented in Figs. 5-11, 5-12, and 5-13, respectively. The critical member is also circled for each shoring case.

Web buckling (i.e., shear failure) is the mode of failure for each of these shoring cases, but the rigid shore once again produces large compressive stresses in the bottom chord at the shore location and has a slightly lower maximum allowed load, 684 PLF for Case 3 versus 707 PLF for Cases 3a and 3b. When a flexible shore is used, virtually all of the bottom chord compressive stresses are eliminated (see Figs. 5-12 and 5-13). The critical web member shifts from the left side of the shore to the right side, and by doubling the shore deflection (1/4 in. deflection instead of 1/8 in. deflection), the critical member and allowable load remain the same. Flexible shores produce two very desirable conditions. The first is the reduction and/or elimination of bottom chord compressive stresses (stress control), and the second is that flexible third-point shores are not very sensitive to the amount of downward deflections, which is indeed a desirable situation from the standpoint of expedient shelter construction, since it would be hard from the construction standpoint to build in a specified amount of deflection at the allowable load for all O.W.J. Further analysis and tests will be necessary to enable a set of shoring tables and construction guidelines to be developed.

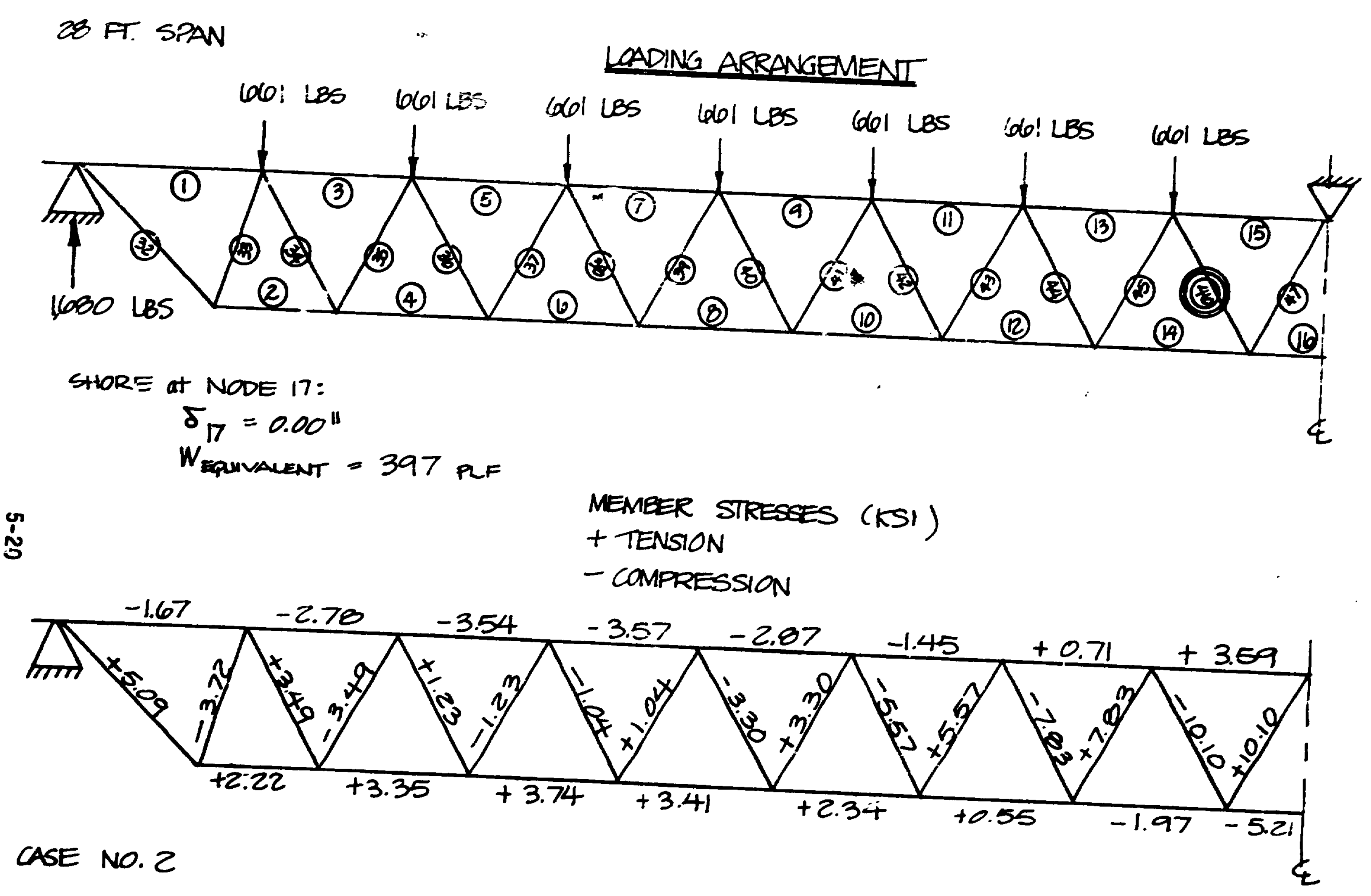

Fig. 5-10. Analysis of 18J6 Open-Web Joist—28-ft Span—Case No. 2 (W = 397 PLF).

28 FT SPAN

LOADING ARRANGEMENT

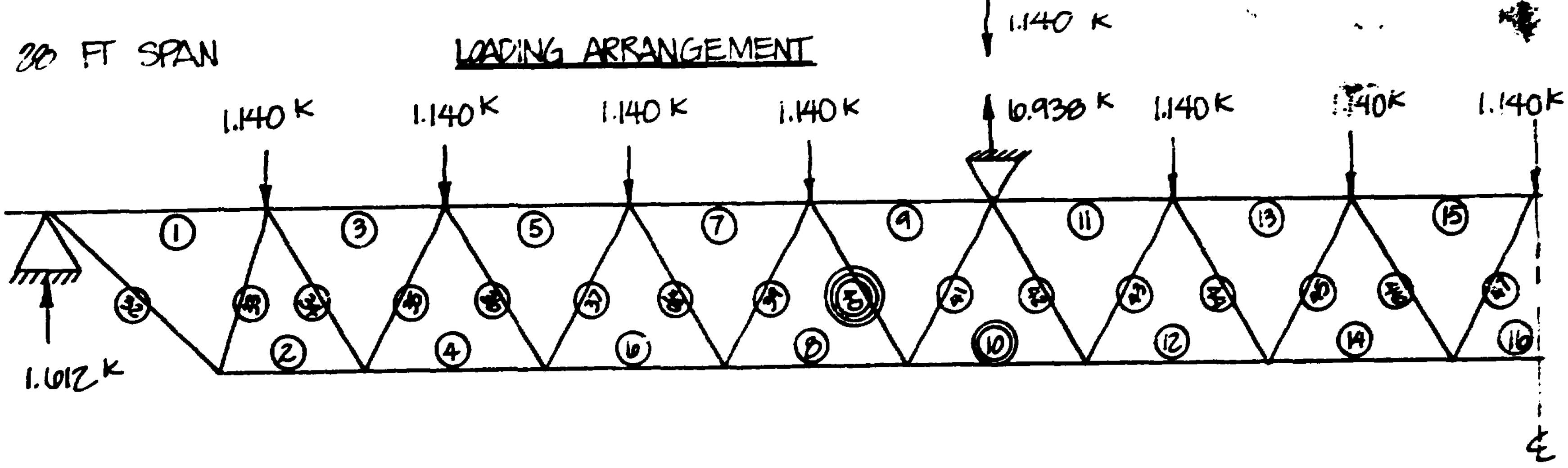

AT NODE 11; $\Delta_y = 0$; ROLLER SUPPORT

$w_{EQUIVALENT}$ = 684 PLF

MEMBER STRESSES (KSI)
+ TENSION
− COMPRESSION

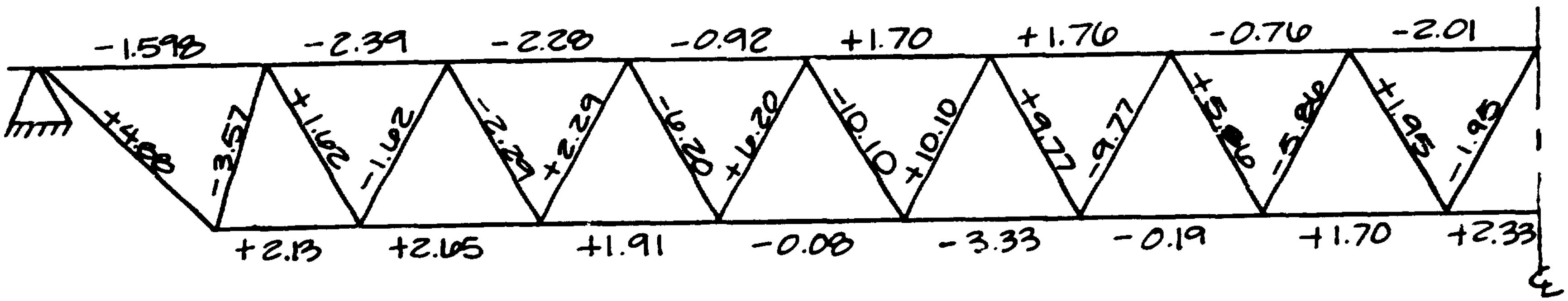

CASE NO. 3

Fig. 5-11. Analysis of 18J6 Open-Web Joist —28-ft Span Assuming Rigid Third-Point Shoring.

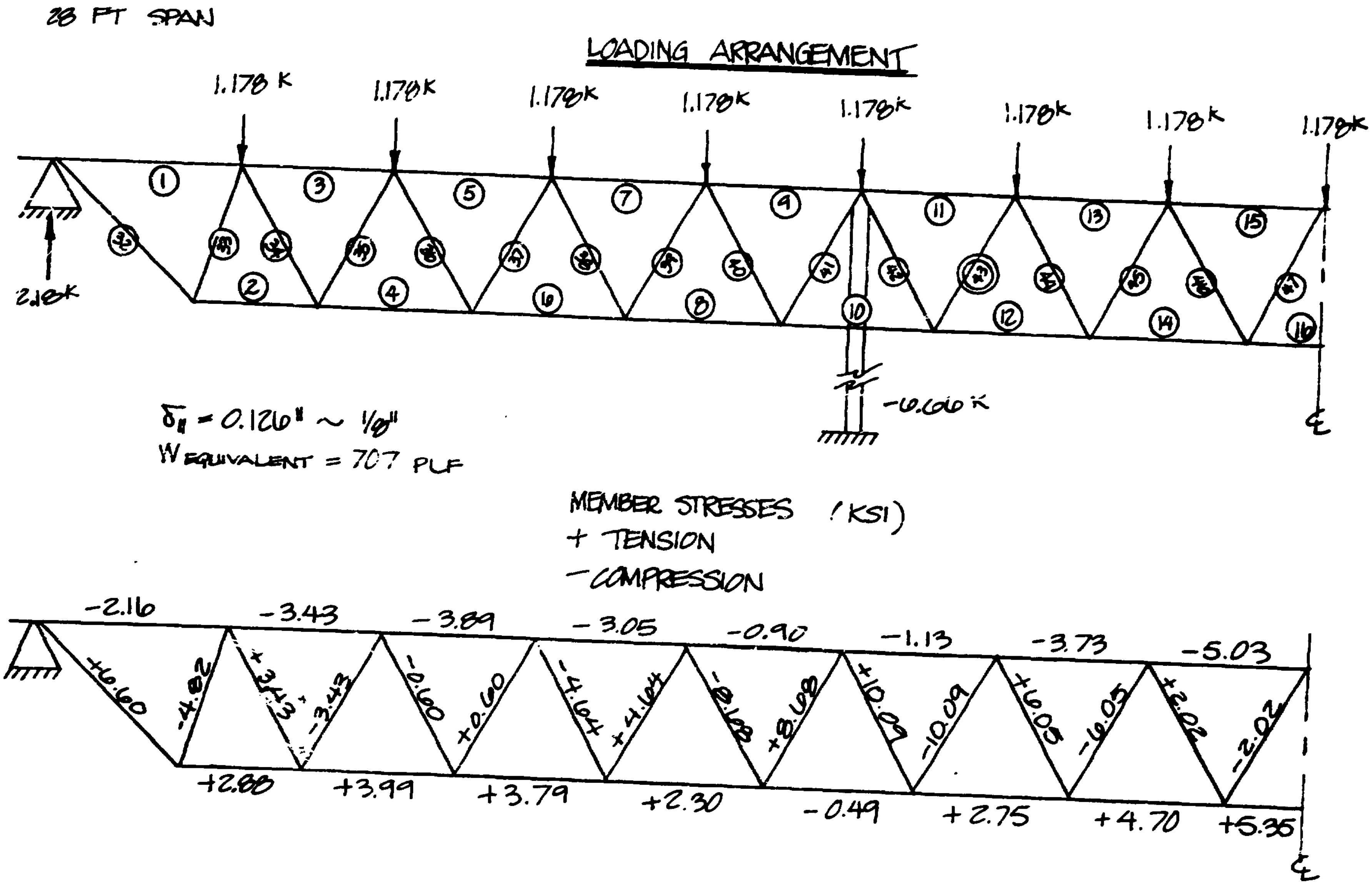

Fig. 5-12. Analysis of 18J6 Open-Web Joist—28 ft Span -Assuming Flexible Support—1/8 in. Gap.

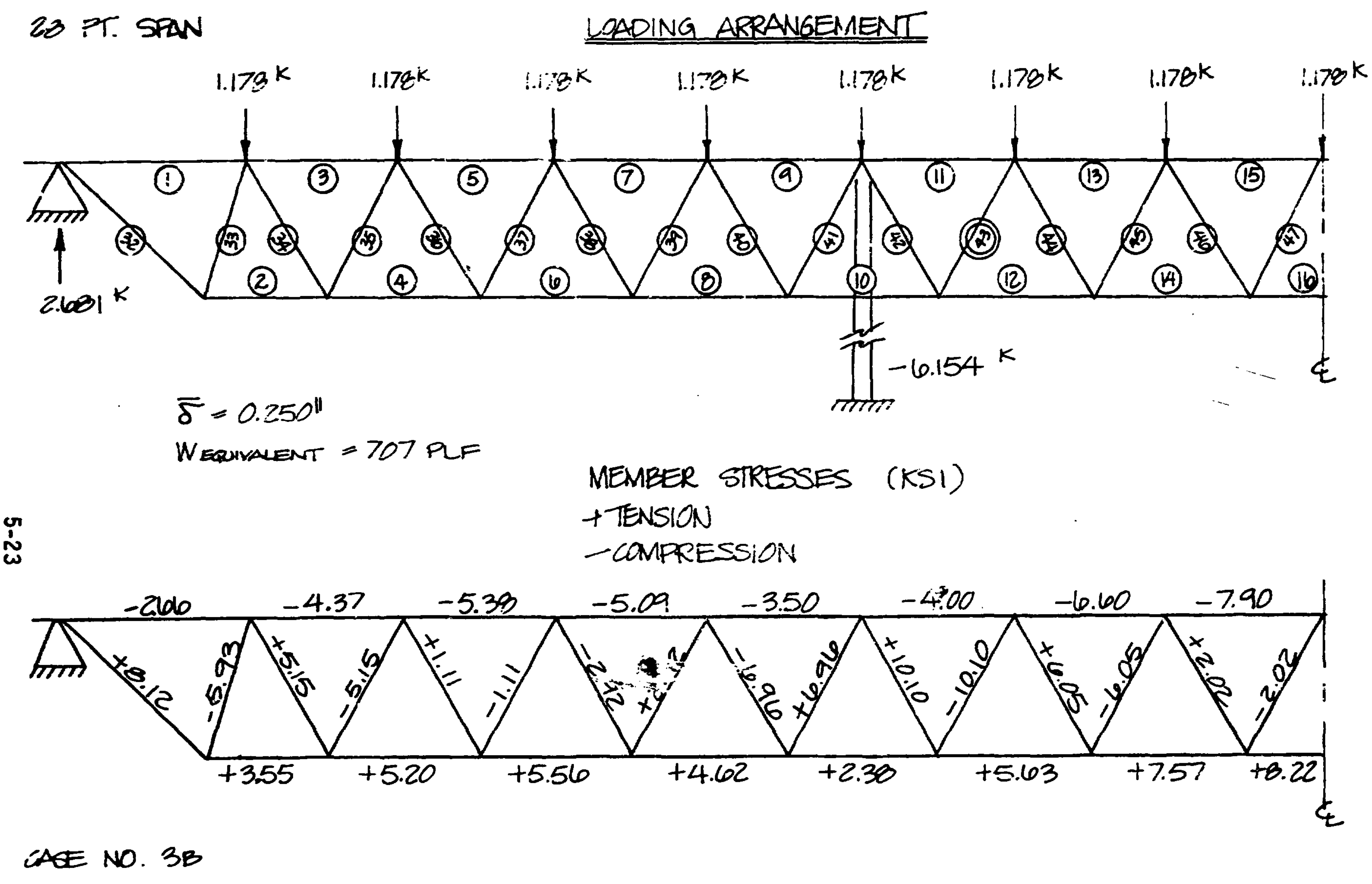

Fig. 5-13. Analysis of 18J6 Open-Web Joist — 28-ft Span — Assuming Flexible Support — 1/4 in. Gap.

Comparisons of W.E.S. Test Data Versus SSI Analysis Results

W.E.S. loaded the roof system with third point shoring (see Figs. 5-7 and 5-14 for shoring details) to about 450 PLF. Load versus mid-span deflection was also recorded and is shown in Fig. 5-15. The W.E.S. roof system, with their improved shoring arrangement, was in reality a flexible shored system. Under load (see Fig. 5-16), the web members actually seated themselves by crushing the corners of the two 2 x 4 in. shore seats. This had the effect of producing significant downward deflections (see the sketch in Fig. 5-16) — in other words, a flexible shore. The actual analyzed data presented by W.E.S. are in considerable doubt for the reasons expressed on pages 5-10 and 5-12. The predicted joist load versus deflection for our modified Bethlehem Steel joist is shown in Fig. 5-15. The W.E.S. rigid shore assumption results in a very stiff roof system and is quite unrealistic in this case. An O.W.J. roof system based on the flexible shore assumption produces a much softer and more realistic roof structure. From Fig. 5-16, the probable deflection under 449 PLF at the shores was about 0.6 in. If this had been used in the analyzed model, the resulting deflection at mid-span would have been quite close to the actual deflections recorded by W.E.S.

A. O.W.J. Roof with Supports at Third Points.

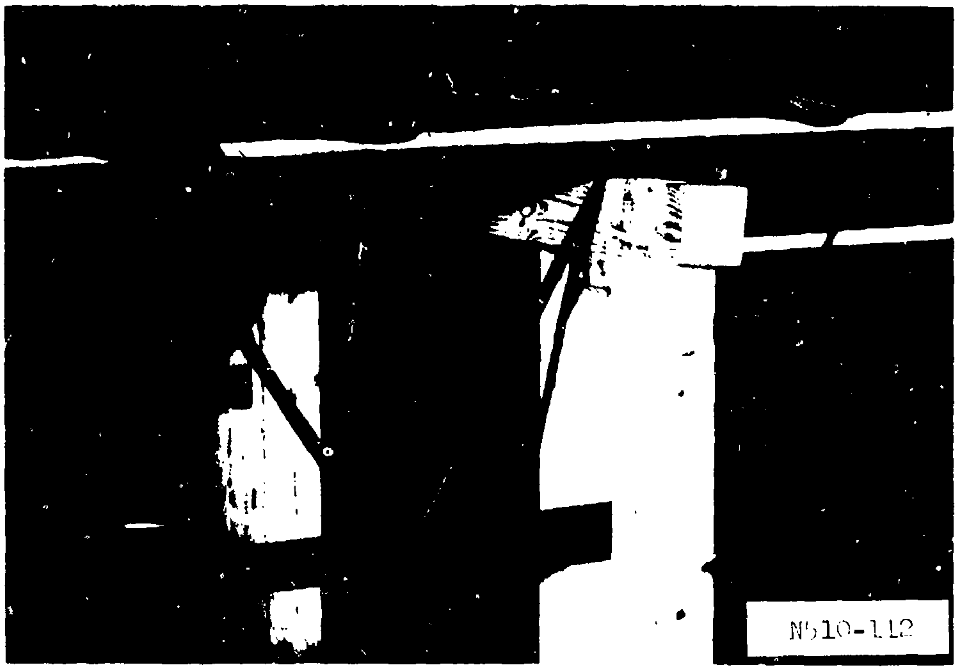

B. Closeup of Connection Between O.W.J. and Supports.

Fig. 5-14. Twenty-eight-foot O.W.J. Roof with Supports at Third Points and a Simulated 24-in. Sand Loading.

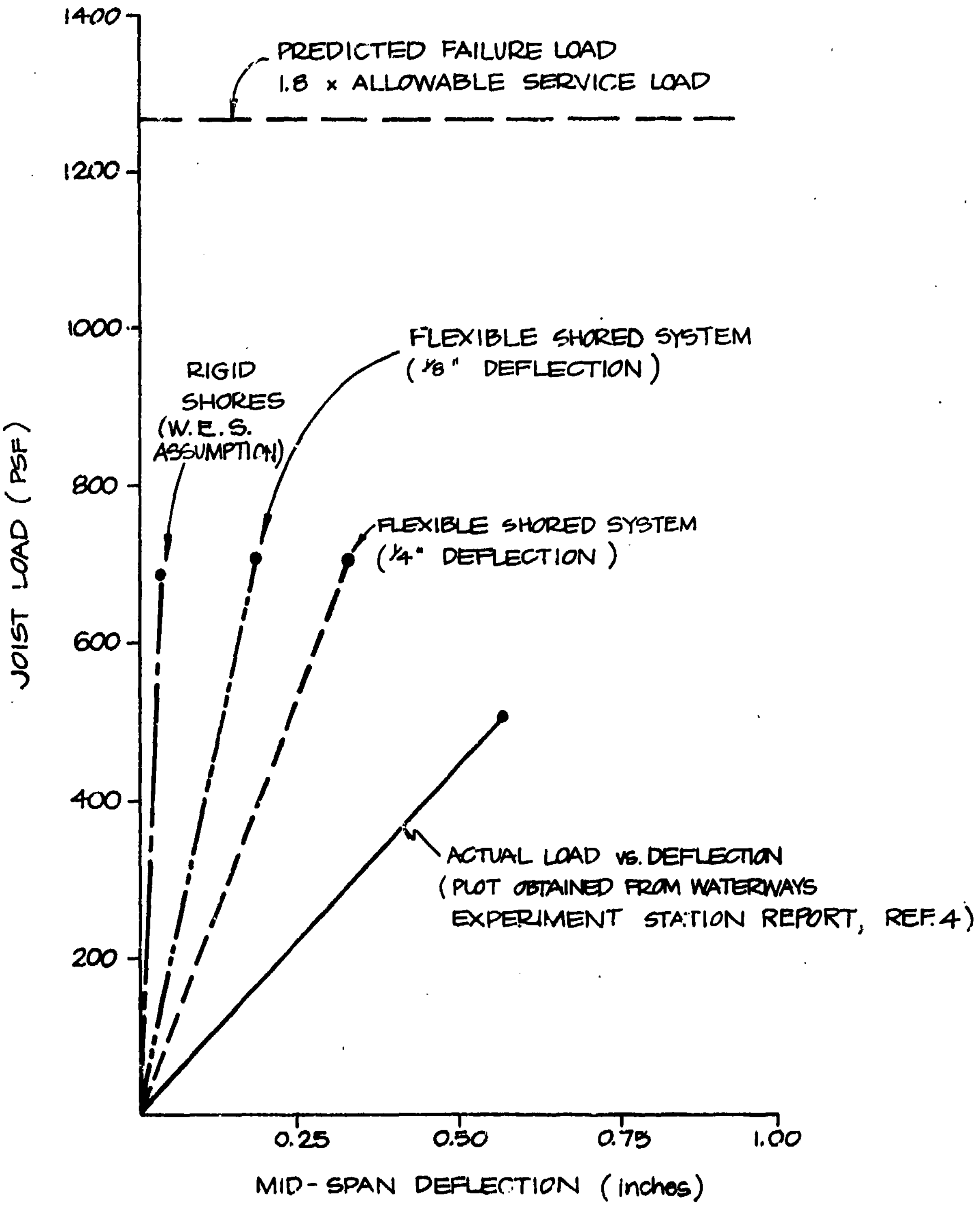

Fig. 5-15. Comparison of Analysis with W.E.S. Load vs Deflection Data.

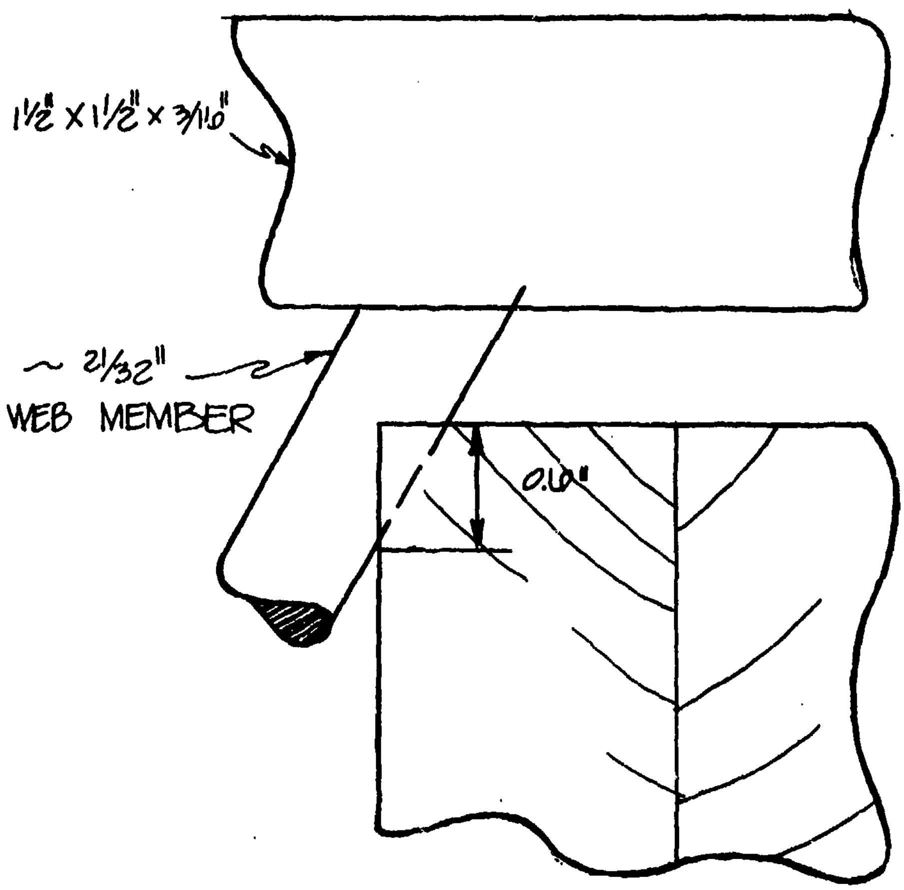

Fig. 5-16. Sketch of Support for W.E.S. Tests Showing Probable Deflection Due to Crushing of 2 x 4 in. Blocks by Web Member.

COMPUTER ANALYSIS RESULTS FOR A SIMPLY SUPPORTED OPEN-WEB JOIST (18H8) ROOF SYSTEM

As previously mentioned, an 18H8 open web steel joist with a 20-ft span was selected on the basis of a shear, or web buckling controlling the design. Another reason was that for this particular joist, one row of bridging is recommended (Ref. 12) for spans from 0 to 20 ft; therefore, this particular joist-span combination produces near the maximum effective length for the lower joist chord. In other words, the lower chord will have a minimum allowable compressive stress under this particular combination of span and bridging.

A Bethlehem Steel joist was selected for analysis. The member sizes and dimensions are found in Table 5-3. Analyzing the joist as a truss resulted in a maximum allowable load of 576 lbs/linear ft. The loading arrangement and member stresses are shown for the left half of the joist in Fig. 5-17. If the factor of safety is assumed to be 1.8, then at 1,037 PLF a web member near the support will buckle first. The standard load tables give an allowable load of 540 PLF* and this load is governed by shear (i.e., web member buckling; see Table 5-4). The analysis resulted in a loading only 6% higher than the value given in the standard load table. It should be noted that both cases were governed by the same mode of failure — web buckling.

Twelve 18H8, 20-ft long open-web joists were obtained for future testing, but when they arrived so many discrepancies existed that it was deemed necessary to run a new analysis on them. The results of the analysis on the delivered joists found that the maximum allowable load was 441 PLF and that at about 750 PLF** a web member near the support would buckle. The maximum allowable load is 18% below the recommended maximum

* Original design was live load = 100 psf; dead load = 80 psf; and 18H8 joists at 3-ft centers for the floor system.

** The ultimate load is assumed to be 1.8 times the allowable load.

Table 5-3. Properties of H Series Open-Web Joists (from Ref. 15)

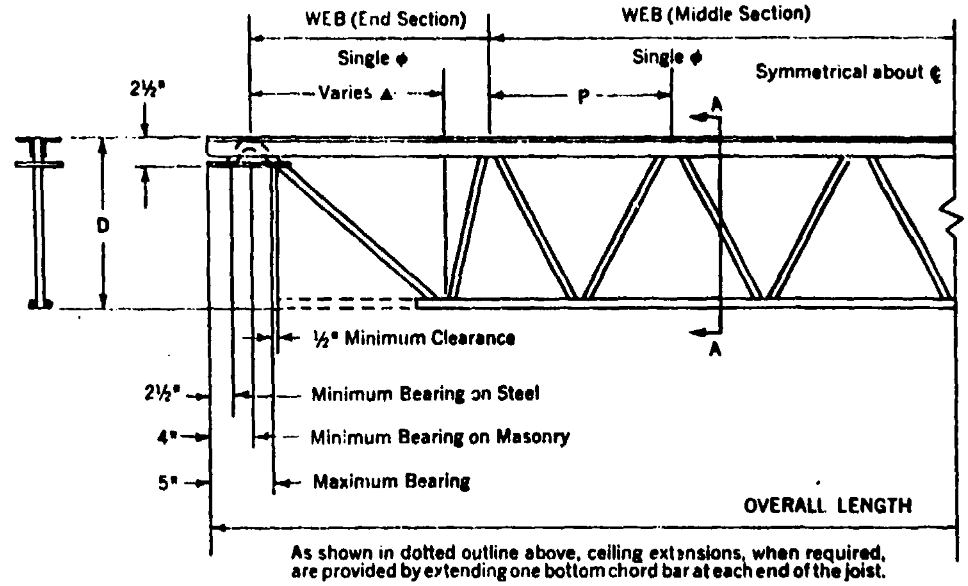

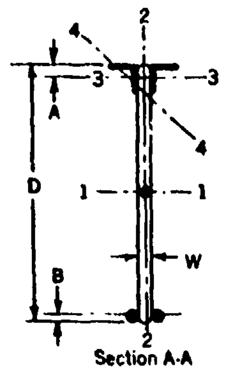

As shown in dotted outline above, ceiling extensions, when required, are provided by extending one bottom chord bar at each end of the joist.

▲ 1¼ D for 8" thru 12" joists
D for 14" thru 24" joists

H-SERIES HOT-ROLLED

Joist Designation	Actual Depth D	Top Chord (2 L's) Angles	Top Chord Area	Top Chord r axis 4-4	Top Chord s axis 3-3	Bottom Chord (2 bars) A	Bottom Chord Diam	Bottom Chord Area	Bottom Chord B	P	Web End Section Diam W	Web End Section Area	Web End Section r axis 2-2	Web Middle Section Diam W	Web Middle Section Area	Web Middle Section r axis 2-2	Moment of Inertia axis 1-1
	in.	in.	in.²	in.	in.³	in.	in.	in.²	in.	in.	in.	in.²	in.	in.	in.²	in.	in.⁴
8H2	8	1 x 1 x ⅛	0.46	.20	.062	.30	15/32	.345	.234	14	17/32	.222	.133	15/32	.172	.117	11.4
10H2	10	1 x 1 x ⅛	0.46	.20	.062	.30	15/32	.345	.234	14	19/32	.277	.148	15/32	.172	.117	17.7
10H3	10	1¼ x 1¼ x ⅛	0.60	.25	.098	.36	17/32	.443	.266	18	19/32	.277	.148	17/32	.222	.133	22.5
10H4	10	1½ x 1½ x ⅛	0.72	.30	.148	.42	19/32	.554	.297	18	21/32	.338	.164	17/32	.222	.133	27.1
12H2	12	1 x 1 x ⅛	0.46	.20	.062	.30	15/32	.345	.234	14	19/32	.277	.148	15/32	.172	.117	26.0
12H3	12	1¼ x 1¼ x ⅛	0.60	.25	.098	.36	17/32	.443	.266	18	21/32	.338	.164	17/32	.222	.133	33.0
12H4	12	1½ x 1½ x ⅛	0.72	.30	.148	.42	19/32	.554	.297	18	21/32	.338	.164	19/32	.277	.148	40.0
12H5	12	1½ x 1½ x 5/32	0.89	.295	.175	.43	21/32	.676	.328	18	23/32	.406	.180	19/32	.277	.148	48.4
12H6	12	1½ x 1½ x 3/16	1.06	.29	.204	.44	23/32	.811	.359	18	23/32	.406	.180	19/32	.277	.148	57.9
14H3	14	1¼ x 1¼ x ⅛	0.60	.25	.098	.36	17/32	.443	.266	18	23/32	.406	.180	19/32	.277	.148	45.6
14H4	14	1½ x 1½ x ⅛	0.72	.30	.148	.42	19/32	.554	.297	18	23/32	.406	.180	19/32	.277	.148	55.4
14H5	14	1½ x 1½ x 5/32	0.89	.295	.175	.43	21/32	.676	.328	18	23/32	.406	.180	19/32	.277	.148	67.0
14H6	14	1½ x 1½ x 3/16	1.06	.29	.204	.44	23/32	.811	.359	18	25/32	.479	.195	21/32	.338	.164	80.3
14H7	14	1¾ x 1¾ x 3/16	1.24	.34	.290	.51	25/32	.959	.391	18	25/32	.479	.195	21/32	.338	.164	93.2
16H4	16	1½ x 1½ x ⅛	0.72	.30	.148	.42	19/32	.554	.297	18	25/32	.479	.195	21/32	.338	.164	73.3
16H5	16	1½ x 1½ x 5/32	0.89	.295	.175	.43	21/32	.676	.328	18	25/32	.479	.195	21/32	.338	.164	88.6
16H6	16	1½ x 1½ x 3/16	1.06	.29	.204	.44	23/32	.811	.359	18	25/32	.479	.195	21/32	.338	.164	106
16H7	16	1¾ x 1¾ x 3/16	1.24	.34	.290	.51	25/32	.959	.391	18	25/32	.479	.195	23/32	.406	.180	124
16H8	16	2 x 2 x 3/16	1.42	.39	.380	.57	27/32	1.118	.422	18	25/32	.479	.195	23/32	.406	.180	142
18H5	18	1½ x 1½ x 5/32	0.89	.295	.175	.43	21/32	.676	.328	20	27/32	.559	.211	23/32	.406	.180	113
18H6	18	1½ x 1½ x 3/16	1.06	.29	.204	.44	23/32	.811	.359	20	27/32	.559	.211	23/32	.406	.180	136
18H7	18	1¾ x 1¾ x 3/16	1.24	.34	.290	.51	25/32	.959	.391	20	27/32	.559	.211	23/32	.406	.180	159
18H8	18	2 x 2 x 3/16	1.42	.39	.380	.57	27/32	1.118	.422	20	27/32	.559	.211	23/32	.406	.180	182
20H5	20	1½ x 1½ x 5/32	0.89	.295	.175	.43	21/32	.676	.328	22	27/32	.559	.211	23/32	.406	.180	141
20H6	20	1½ x 1½ x 3/16	1.06	.29	.204	.44	23/32	.811	.359	22	27/32	.559	.211	23/32	.406	.180	170
20H7	20	1¾ x 1¾ x 3/16	1.24	.34	.290	.51	25/32	.959	.391	22	27/32	.559	.211	25/32	.479	.195	198
20H8	20	2 x 2 x 3/16	1.42	.39	.380	.57	27/32	1.118	.422	22	27/32	.559	.211	25/32	.479	.195	227
22H6	22	1½ x 1½ x 3/16	1.06	.29	.204	.44	23/32	.811	.359	24	29/32	.645	.227	25/32	.479	.195	207
22H7	22	1¾ x 1¾ x 3/16	1.24	.34	.290	.51	25/32	.959	.391	24	29/32	.645	.227	25/32	.479	.195	241
22H8	22	2 x 2 x 3/16	1.42	.39	.380	.57	27/32	1.118	.422	24	29/32	.645	.227	25/32	.479	.195	277
24H6	24	1½ x 1½ x 3/16	1.06	.29	.204	.44	23/32	.811	.359	24	29/32	.645	.227	27/32	.559	.211	248
24H7	24	1¾ x 1¾ x 3/16	1.24	.34	.290	.51	25/32	.959	.391	24	29/32	.645	.227	27/32	.559	.211	289
24H8	24	2 x 2 x 3/16	1.42	.39	.380	.57	27/32	1.118	.422	24	29/32	.645	.227	27/32	.559	.211	332

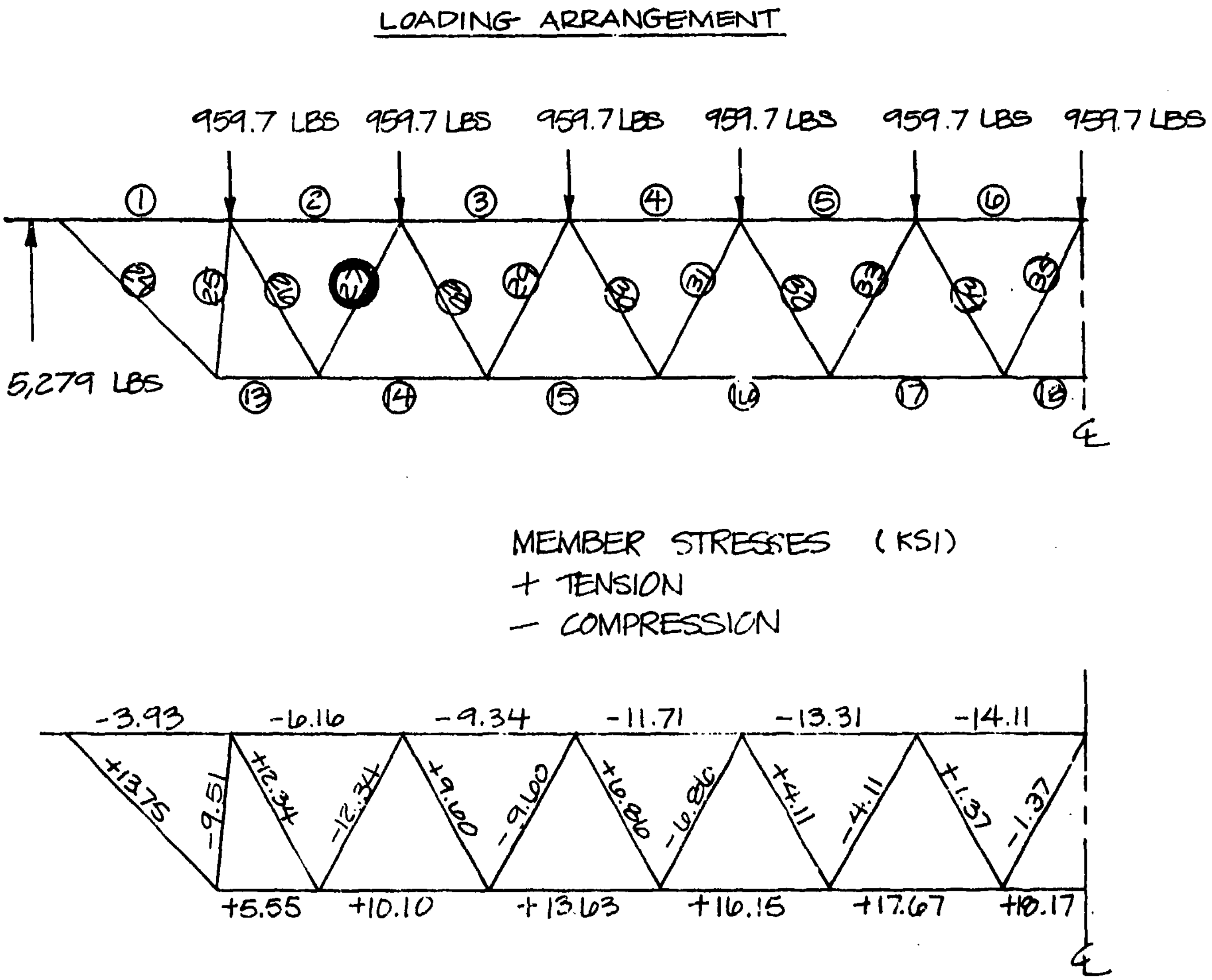

Fig. 5-17. Analysis of Bethlehem Steel Open-Web Joist — 20-ft Span (W = 576 PLF).

Table 5-4. Allowable Total Safe Loads in Pounds per Linear Foot of H Series Joists — for Joist Depths of 16 in. to 24 in. Inclusive (from Ref. 15)

Joist Designation	16H4	16H5	16H6	16H7	16H8	18H5	18H6	18H7	18H8	20H5	20H6	20H7	20H8	22H6	22H7	22H8	24H6	24H7	24H8
*Depth in Inches	16	16	16	16	16	18	18	18	18	20	20	20	20	22	22	22	24	24	24
Resisting Moment in Inch-Pounds	221,000	289,000	344,000	413,000	478,000	325,000	383,000	466,000	540,000	365,000	406,000	499,000	602,000	422,000	526,000	653,000	462,000	576,000	716,000
Maximum End Reaction in Pounds	3800	4300	4600	4900	5200	4500	4800	5200	5400	4800	5100	5400	5600	5400	5600	5800	5600	5800	6000
†Approximate Weight in Pounds per Foot	6.6	7.8	8.6	10.3	11.4	8.0	9.2	10.4	11.6	8.4	9.6	10.7	12.2	9.7	10.7	12.0	10.3	11.5	12.7
Span in Feet																			
16	475	538	575	613	650														
17	447	506	541	576	612														
18	422	476	511	544	578	500	533	578	600										
19	400	453	484	516	547	474	505	547	568										
20	368	430	460	490	520	450	480	520	540	480	510	540	560						
21	334	410	438	467	495	429	457	495	514	457	486	514	533						
22	304	391	418	445	473	409	436	473	491	436	464	491	509	491	509	527			
23	279	364	400	426	452	391	417	452	470	417	443	470	487	470	487	504			
24	256	334	383	408	433	375	400	433	450	400	425	450	467	450	467	483	467	483	500
25	238	308	367	392	416	347	384	416	432	384	408	432	448	432	448	464	448	464	480
26	218	285	339	377	400	321	369	400	415	360	392	415	431	415	431	446	431	446	462
27	202	264	315	363	385	297	350	385	400	334	371	400	415	386	415	430	415	430	444
28	188	246	293	350	371	276	326	371	386	310	345	386	400	359	400	414	393	414	429
29	175	229	273	327	359	258	304	359	372	289	322	372	386	335	386	400	366	400	414
30	164	214	255	306	347	241	284	345	360	270	301	360	373	313	373	387	342	387	400
31	153	200	239	287	332	225	266	323	348	253	282	346	361	293	361	374	320	374	387
32	144	188	224	269	311	212	249	303	338	238	264	325	350	275	342	363	301	363	375
33						199	234	285	327	223	249	305	339	258	322	352	283	352	364
34						187	221	269	311	210	234	288	329	243	303	341	266	332	353
35						177	208	254	294	199	221	272	320	230	286	331	251	313	343
36						167	197	240	278	188	209	257	310	[illegible]	271	322	238	296	333
37										178	198	243	293	206	256	314	225	280	324
38										169	187	230	278	195	243	301	213	266	316
39										160	178	219	264	185	231	286	202	252	308
40										152	169	208	251	176	219	272	193	240	298
41														167	209	259	183	228	284
42														159	199	247	175	218	271
43														152	190	235	167	208	258
44														145	181	225	159	196	247
45																	152	190	236
46																	146	181	226
47																	139	174	216
48																	134	167	207

GOVERNED BY SHEAR

GOVERNED BY MOMENT

*Indicates Nominal Depth of Steel Joists only.

†Approximate Weights per Linear Foot of Steel Joists only. Accessories and nailer strip not included.

*†See manufacturers' catalogs for detailed information on specific joist types.

LOADS BELOW BLACK DOTTED LINES ARE TO BE USED FOR ROOF CONSTRUCTION ONLY.

Tests on steel joists designed in accordance with the Standard Specifications have demonstrated that the Standard Load Tables are applicable for concentrated top chord loadings (such as are developed in bulb-tee roof construction) when the sum of the equal concentrated top chord loadings does not exceed the allowable uniform loading for the joist type and span and the loads are placed at spacings not exceeding 33" along the top chord.

Adopted by Steel Joist Institute May 31, 1961 and American Institute of Steel Construction, Inc., June 19, 1963.

safe allowable load given in the standard load tables. The reason for this is that the web members were undersized.

The analysis on the following pages will refer to the joists delivered and not the Bethlehem O.W.J.'s. Three basic cases were analyzed for the 18H8 joists. The first was the simply supported case mentioned above; the second case was for a single shore placed at mid-span; and the final case was that of two shores placed at the third points. The analysis results for all three cases are presented in Table 5-5.

<u>18H8 - Simply Supported at Ends</u>

The maximum allowable stresses for all load cases is presented in Fig. 5-18. It should be noted that the allowable compressive stresses given for the bottom chord members is based on a $k\ell/r$ ratio of 234 where k is the effective length factor* ($k = 2.10$ in this case), ℓ is the unbraced length ($\ell = 98$ in.), and r is the radius of gyration of the lower chord about the vertical axis ($r = 0.883$ in.). This assumes that the lower chord member is braced at mid-span**. Fig. 5-19 shows the member stresses in the joist under its maximum allowable safe load of 441 PLF. As in the case of the Bethlehem steel joist, and that quoted in the standard load tables, web buckling (or shear) controls the design.

<u>Case No. 2 - Simply Supported at the Ends and Shored at Mid-Span</u>

Three shoring arrangements were considered: Case No. 2) rigid shore; Case No. 2a) flexible shore with 1/8 in. deflection at the maximum allowable safe load; and Case No. 2b) flexible shore with 1/4 in. deflection at the maximum allowable safe load. The failure loading for each is given in Table 5-5 along with the percent improvement on the simply supported case.

For the rigid shore case, member stresses are shown in Fig. 5-20. Although a web member buckles first near mid-span, the lower chord member

* See AISC pg. 5-138; Table C 1.81, Fig. (E). (Ref. 16)

** See AISC pg. 5-240; Section 5.4(c). (Ref. 16)

Table 5-5. Open-Web Joist, H-Series, 18H8, 20-ft Span, Simply Supported at Its Ends

Case No.	Type of Shoring	Allowable Load	Ultimate Load	Type of Failure	Percent of Case No. 1
1	None - Base Case	441 PLF* (540 PLF - AISC Allow.)	750 PLF	Web buckling	100%
2	Rigid shore at center of span	425 PLF	723 PLF	Web buckling	96%
2a	Flexible shore at center with 1/8 in. deflection at failure load	615 PLF	1,046 PLF	Web buckling	139%
2b	Flexible shore at center with 1/4 in. deflection at failure load	805 PLF	1,369 PLF	Web buckling	182%
3	Rigid shores at the third points	991 PLF	1,685 PLF	Bottom chord buckles	225%
3a	Flexible shores at the third points with 1/8 in. deflection at failure	1,028 PLF	1,748 PLF	Web buckling	233%
3b	Flexible shores at the third points with 1/4 in. deflection at failure	1,028 PLF	1,748 PLF	Web buckling	233%

*18% below the total recommended maximum applied load or allowable load is the load at which the stress in one of the members is equal to the allowable stresses given in Table 1-36 of Ref. 16.

20 FT. SPAN

ALLOWABLE COMPRESSIVE STRESS

ALLOWABLE TENSILE STRESS = 30 KSI

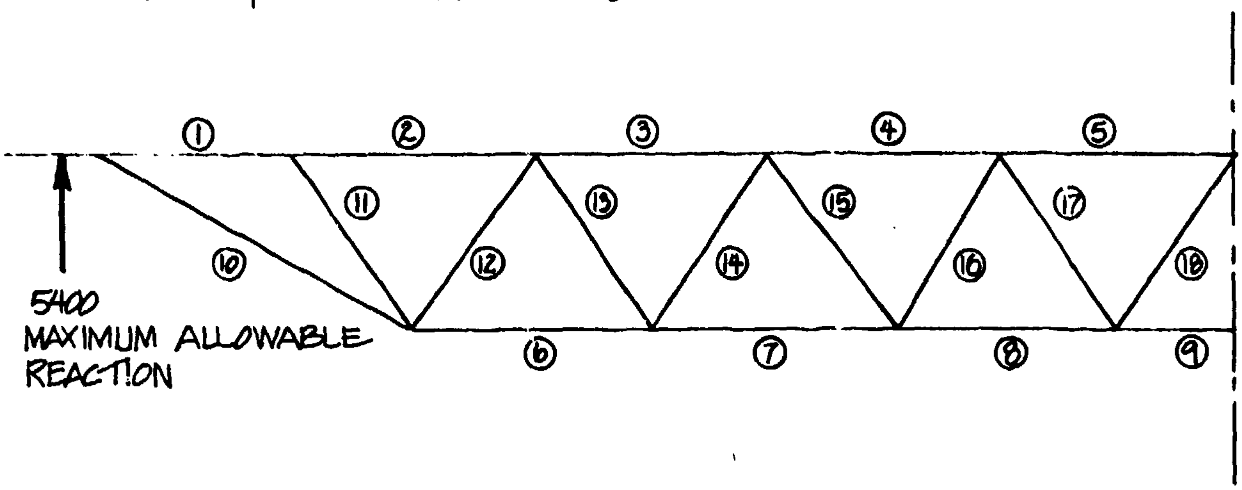

(−) ALLOWABLE COMPRESSIVE STRESS (KSI)

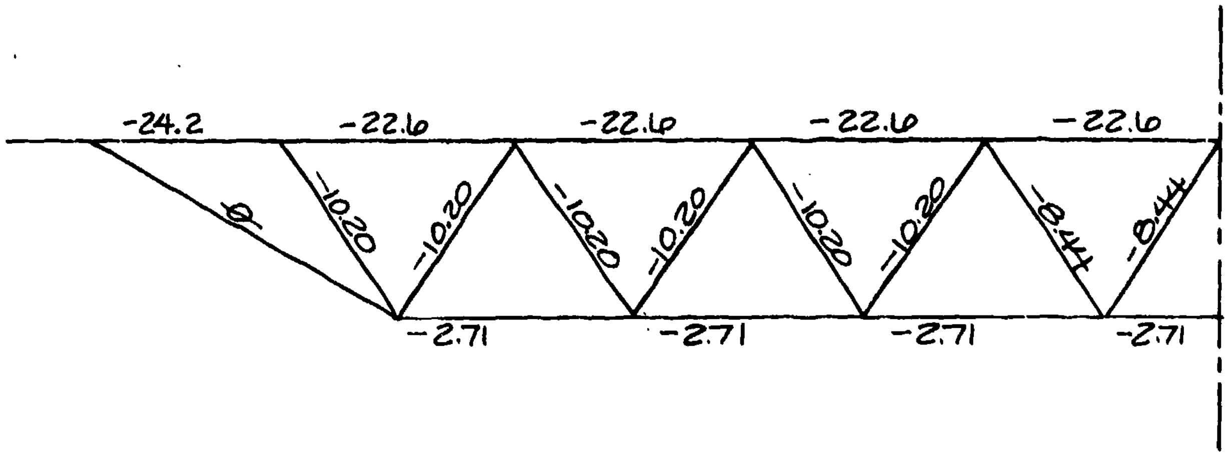

NOTE: BOTTOM CHORD COMPRESSIVE STRESSES ARE GOVERNED BY LATERAL BUCKLING

Fig. 5-18. Analysis of 18H8 Open-Web Joist.

20 FT SPAN

W EQUIVALENT = 441 PLF

LOADING ARRANGEMENT

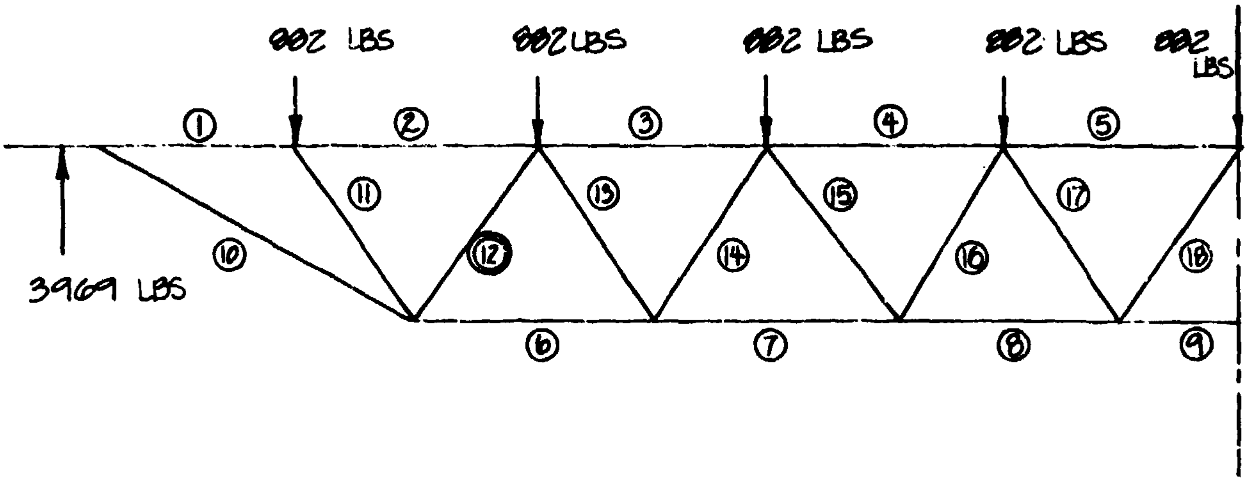

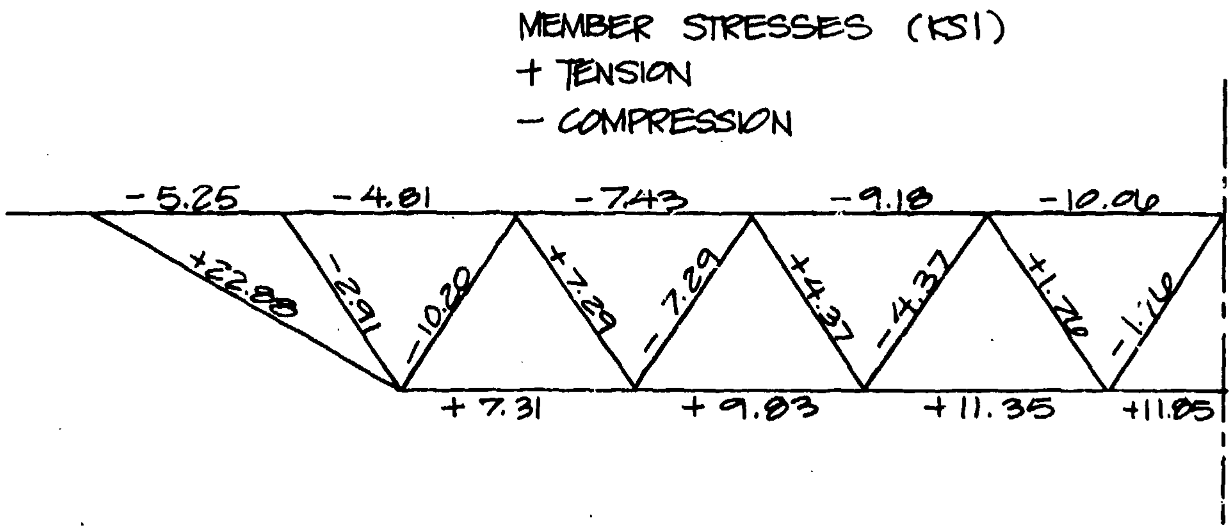

CASE NO. 1

Fig. 5-19. Analysis of 18H8, Open-Web Joist at Maximum Allowable Safe Load (W = 441 PLF).

20 FT. SPAN

RIGID MID-SPAN SHORE

$\delta_{1.0} = 0.0''$

$W_{EQUIVALENT}$ = 425 PLF

LOADING ARRANGEMENT

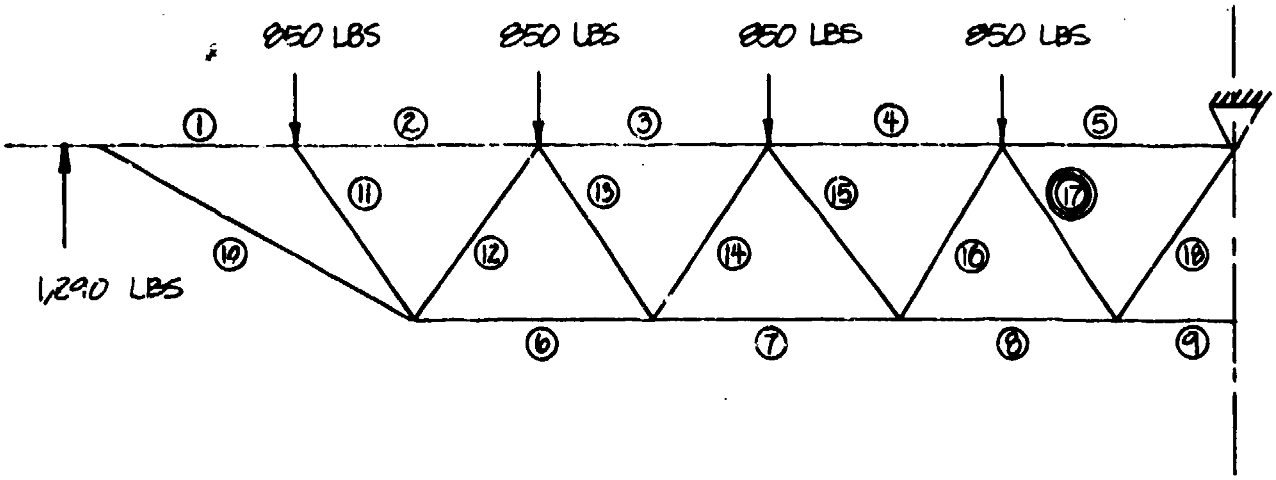

MEMBER STRESSES (KSI)
+ TENSION
− COMPRESSION

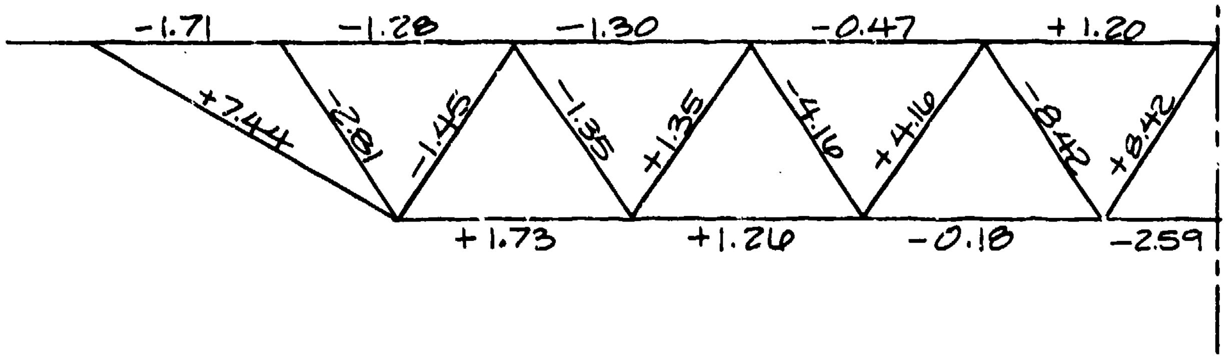

CASE NO. 2

Fig. 5-20. Analysis of 18H8, Open-Web Joist with Rigid Mid-Point Shore (W = 425 PLF).

at mid-span is very close to failing. Allowing 1/8 in. deflection at the shore in addition to allowing an increase in applied load also allows the lower chord to remain in tension throughout its length (see Fig. 5-21). A bit more load can be applied if the shore is allowed to deflect 1/4 in. but once again the entire lower chord remains in tension throughout its length (Fig. 5-22).

Case No. 3 - Simply Supported at the Ends with Two Shores at the Third Points

Three shoring cases were considered: Case 3) rigid shores; Case 3a) flexible shores with 1/8 in. deflection at the shores; and Case 3b) flexible shores with 1/4 in. deflection at the shores.

Rigid shoring at the third points was governed by lateral buckling of the lower chord, as shown in Fig. 5-23. Allowing either 1/8 in. or 1/4 in. deflection at the shores brought the lower chord into tension throughout (see Figs. 5-24 and 5-25). But in this case, increasing the deflection at the shore from 1/8 in. to 1/4 in. produced no improvement in the load-carrying capacity of the joist.

This work demonstrates the potential of stress control and emphasizes that upgrading can be effective if carefully executed. It is envisioned that the eventual Upgrading Manual will have a series of tables like Table 5-5 such that an engineer and/or shelter manager would be able to predict performance of his structure before and after upgrading.

20 FT. SPAN

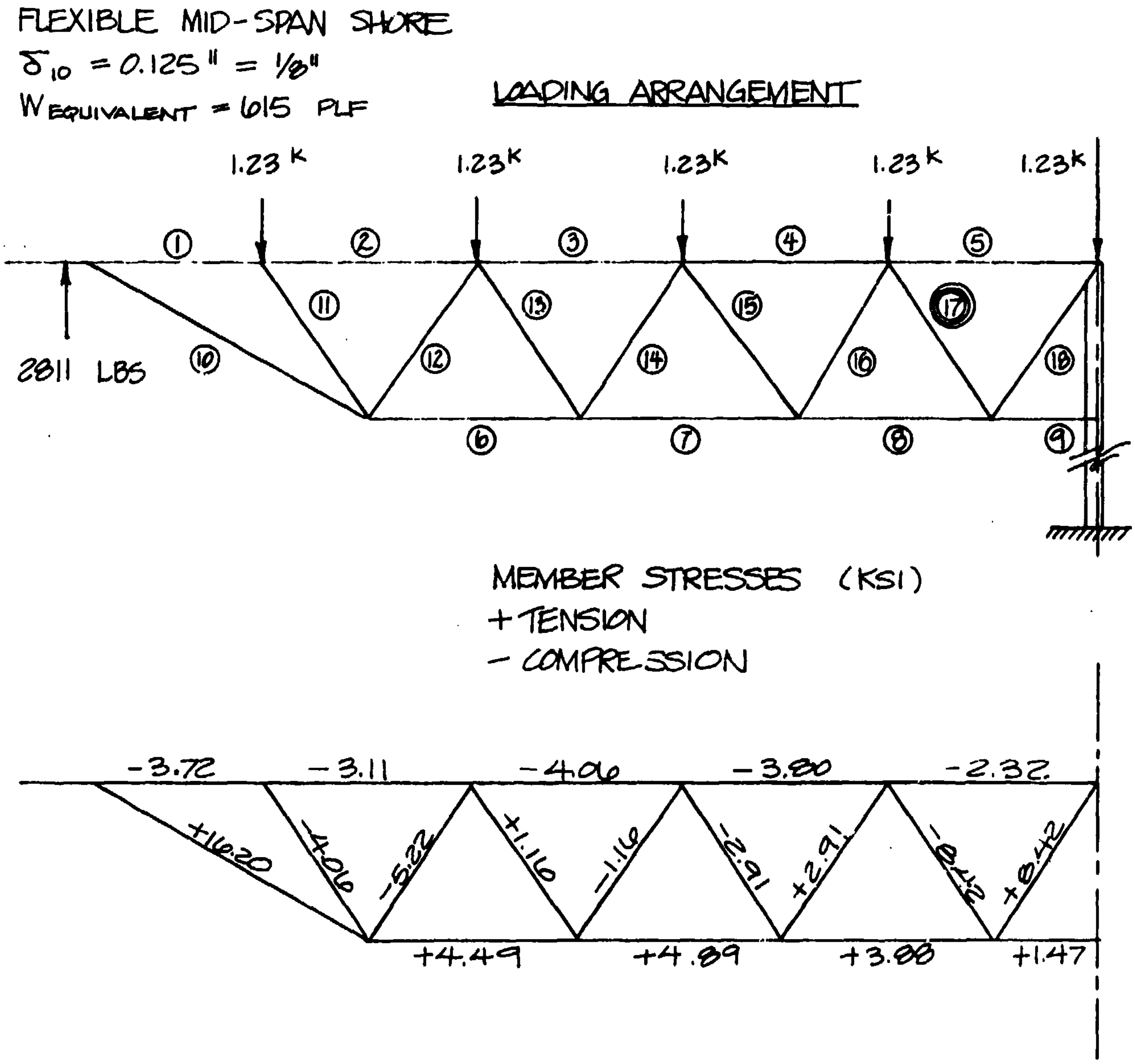

CASE NO. 2A

Fig. 5-21. Analysis of 18H8, Open-Web Joist with Flexible Mid-Point Shore — 1/8 in. Gap (W = 615 PLF).

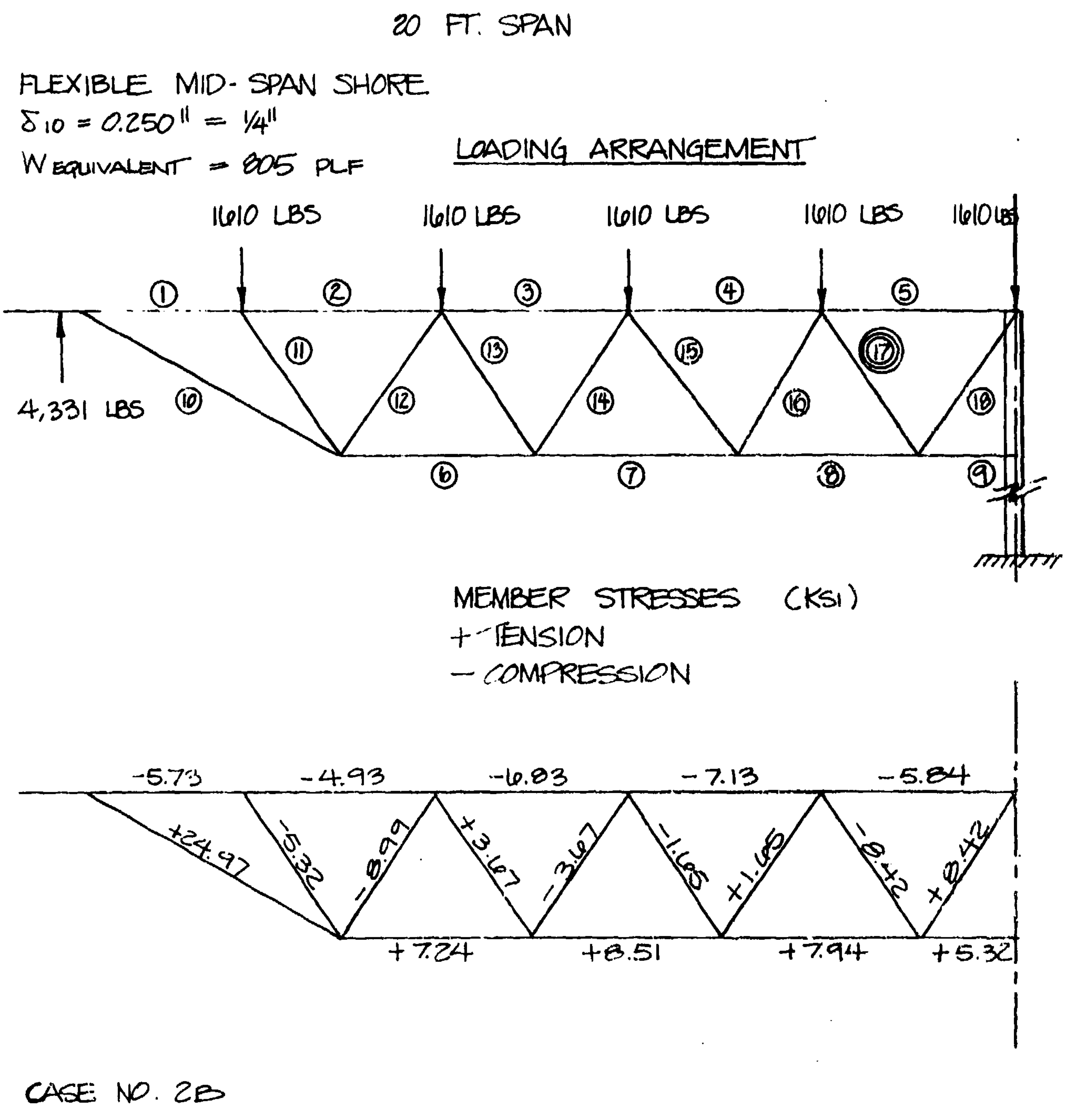

Fig. 5-22. Analysis of 18H8, Open-Web Joist with Flexible Mid-Point Shore — 1/4 in. Gap (W = 805 PLF).

20 FT. SPAN

RIGID THIRD POINT SHORE

$\delta_6 = \delta_{14} = 0.00''$

$W_{EQUIVALENT} = 991$ PLF

LOADING ARRANGEMENT

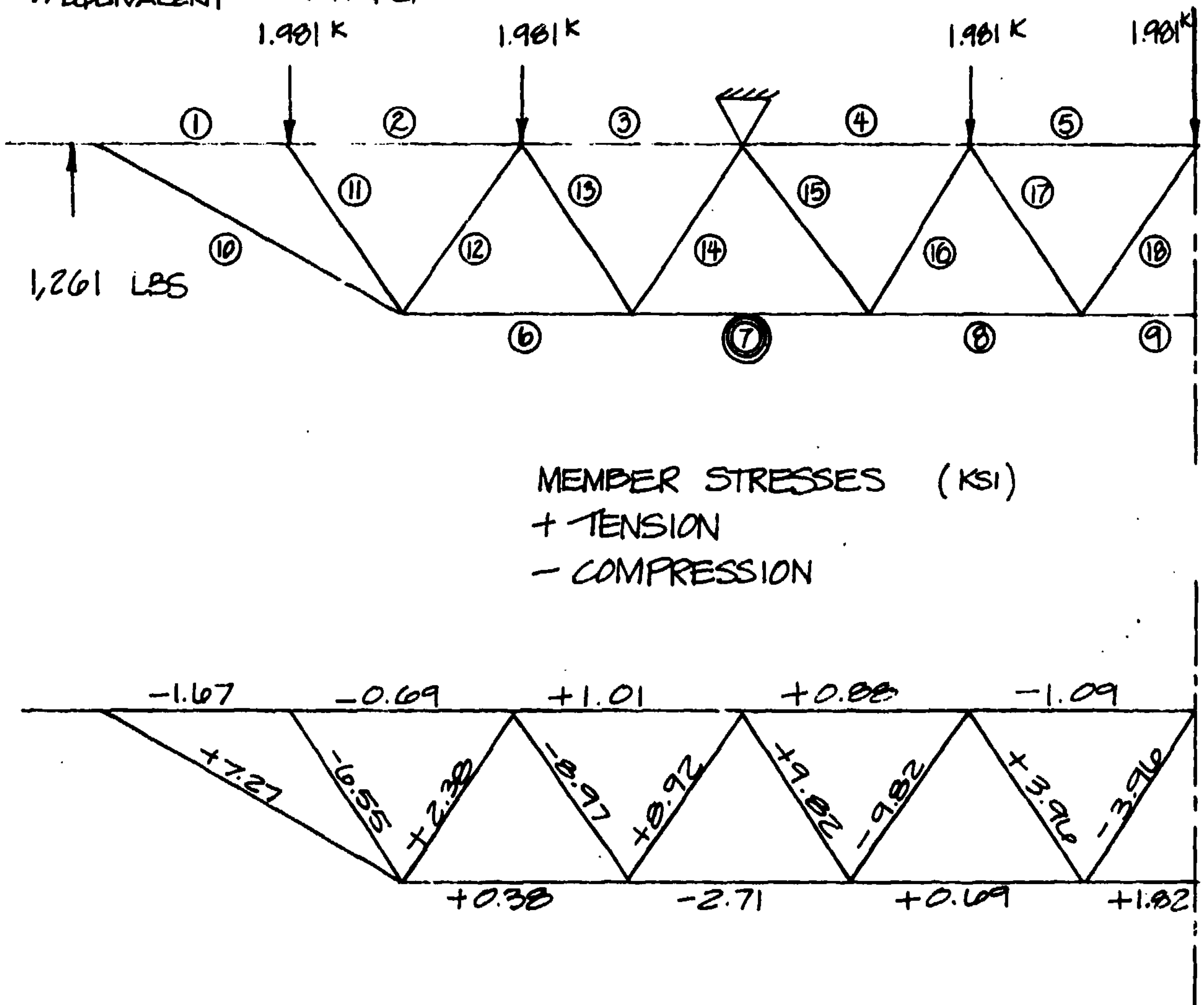

CASE NO. 3

Fig. 5-23. Analysis of 18H8, Open-Web Joist with Rigid Third-Point Shore (W = 805 PLF).

20 FT. SPAN

FLEXIBLE THIRD POINT SHORE

$\delta_6 = 0.125'' = \delta_{14} = 1/8''$ LOADING ARRANGEMENT

$W_{EQUIVALENT} = 1028$ PLF

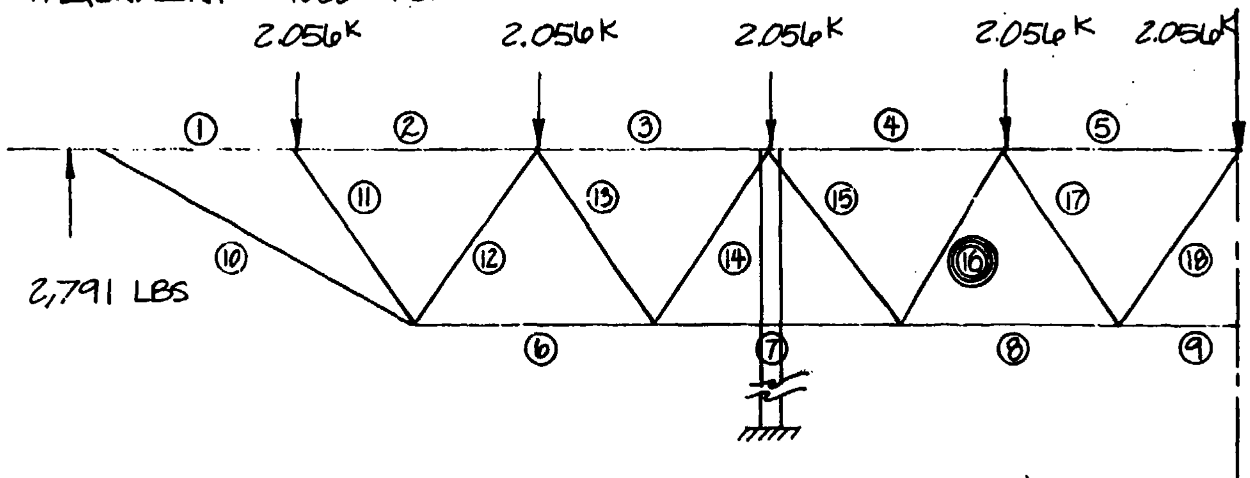

MEMBER STRESSES (KSI)

\+ TENSION

\- COMPRESSION

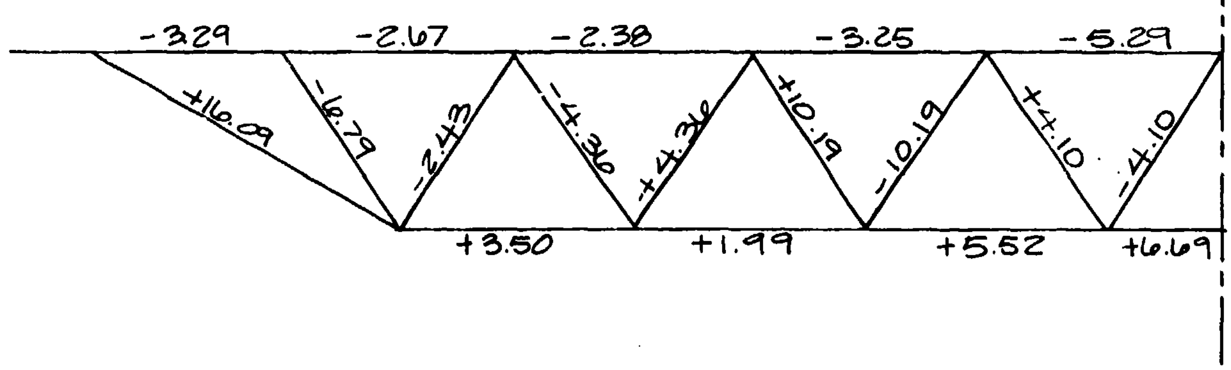

CASE NO. 3A

Fig. 5-24. Analysis of 18H8, Open-Web Joist with Flexible Third-Point Shore — 1/8 in. Gap (W = 1,028 PLF).

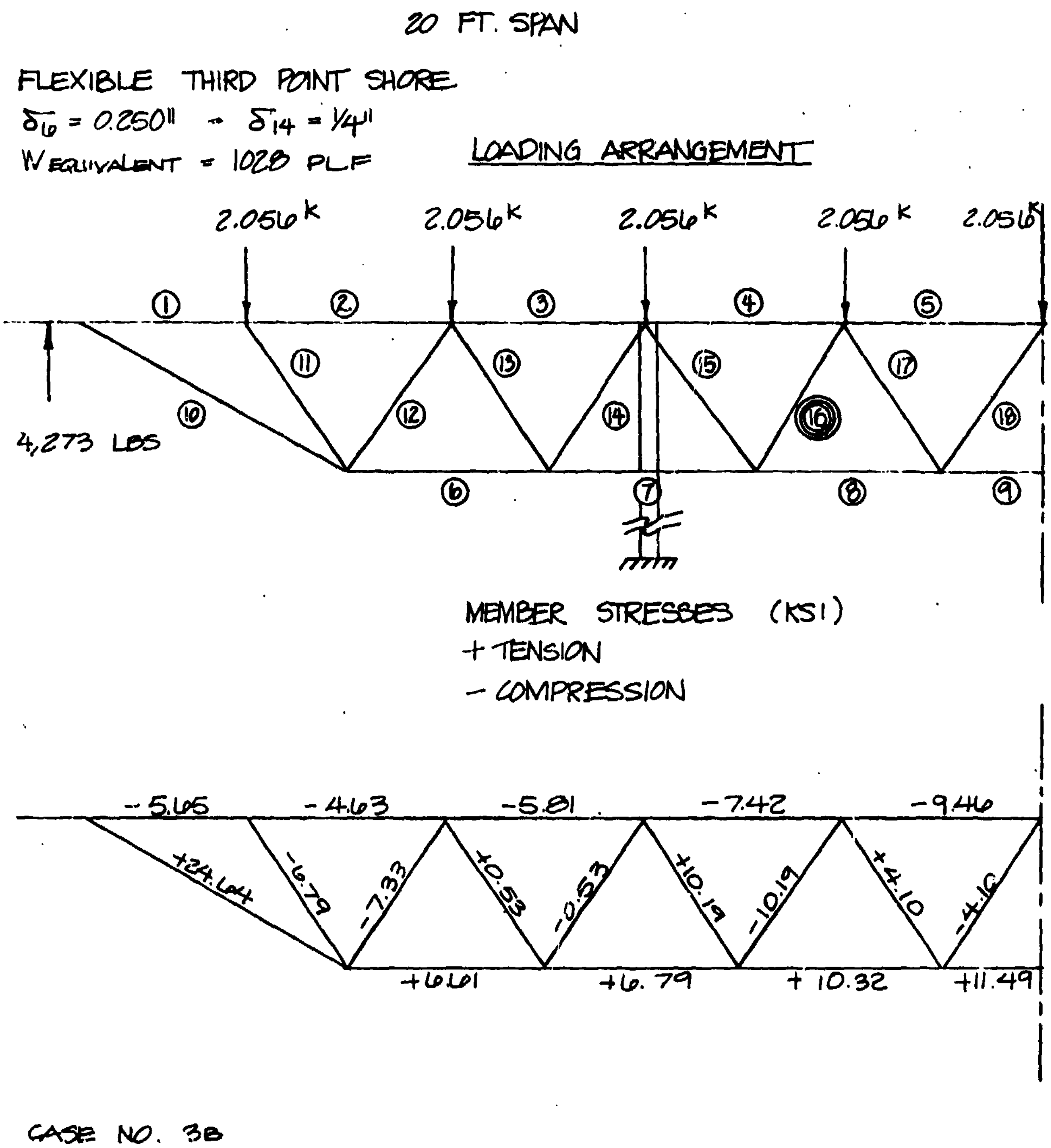

Fig. 5-25. Analysis of 18H8, Open-Web Joist with Flexible Third-Point Shore — 1/4 in. Gap (W = 1,028 PLF).

Section 6
SUMMARY AND CONCLUSIONS

The technical portion of this report is broken down into three fundamental areas: wood floor and roof systems, concrete slabs, and open-web joist floor and roof systems. These are in decreasing order of unpredictability; that is, timber floor systems are probably more difficult to predict failure loads accurately than are concrete floors or open-web steel joists. Steel structures in general are relatively predictable in that the property variability is far less than most other building materials and the codes allow the ultimate or limit design approach for predicting the behavior of steel structures. Concrete, on the other hand, is not quite as far along. The current codes and literature present a thorough and accurate development of methods of predicting ultimate strengths of components, and it is possible to make a good estimate of the ultimate strength of a simple concrete beam. Currently, however, it is not possible to predict the response of entire concrete building systems.

WOODEN FLOOR SYSTEMS

Several methods of upgrading wood floor systems were tested. All showed promise for structural upgrading and anywhere from two- to ten-fold increases were demonstrated, with shoring showing the greatest promise. Significant progress was made toward a probabilistic method of evaluating timber structures which will allow DCPA to establish "safe" design levels for these expedient techniques, make casualty predictions, etc. The work, however, needs to be continued to other facets of timber design, such as glue-laminated beams, bolted and nailed joints, and structural systems.

CONCRETE FLOOR SYSTEMS

Exploratory tests were conducted on full-scale, one-way slab systems at San Jose State University by Scientific Service, Inc. The emphasis of the program was to establish the credibility of a shoring technique. Tests conducted included:

1) A base case where prediction was within 6% of measured value,

2) A single shore case where prediction was within 4 % of tests and resulted in a 400% increase in load-carrying capacity.

STEEL OPEN-WEB JOISTS

The work to date was strictly analytical and testing must be performed. The breakthrough, or most significant part of this effort, is the introduction of "Stress Control" into expedient techniques for upgrading. Not only will this method improve the potential of O.W.J., but we are confident that "Stress Control" can be adapted to other systems (particularly the difficult problem of prestressed concrete floors), as well.

Section 7

REFERENCES

1. Wilton, C. et al., "The Shock Tunnel: History and Results," Vols. 1 through 5, 7618-1 thru 5, Scientific Service, Inc., Redwood City, CA, March 1978.

2. Murphy, H. L., C.K. Wiehle, and E.E. Pickering, "Upgrading Basements for Combined Nuclear Weapons Effects: Expedient Options." Stanford Research Institute, Menlo Park, CA, May 1976.

3. Murphy, H. L., et al., "Upgrading Basements for Combined Nuclear Weapons Effects by Designed Expedient Options." Stanford Research Institute, Menlo Park, CA, October 1977.

4. Black, Michael S., "Evaluation of Expedient Techniques for Strengthening Floor Joist Systems in Residential Dwellings." Weapons Effects Laboratory, U.S. Army Engineer Waterways Experiment Station, Vicksburg, MS, July 1975.

5. Huff, William L., "Expedient Upgrading of Existing Structures for Fallout Protection." Weapons Effects Laboratory, U.S. Army Engineer Waterways Experiment Station, Vicksburg, MS, April 1978.

6. Naval Civil Engineering Laboratory, "Dynamic Properties of Small, Clear Specimens of Structural-Grade Timber." Port Hueneme, CA, April 1968.

7. International Conference of Building Officials, Uniform Building Code, 1976 Edition.

8. Hoyle, Robert J., Jr., Wood Technology in the Design of Structures. Mountain Press Publishing Company, Missoula, MT, 1972.

9. Gurfinkel, German, Wood Engineering. Southern Forest Products Association, New Orleans, LA, 1973.

10. ASTM Designation D 2555-70 "Standard Methods for Establishing Clear Wood Strength Values." American Society for Testing and Materials, 1971 ASTM Book of Standards, July 1971.

11. ASTM Designation D 245-70 "Standard Methods for Establishing Structural Grades and Related Allowable Properties for Visually Graded Lumber." American Society for Testing and Materials, 1971 Book of ASTM Standards, July 1971.

12. Cornell, Benjamin, Probability Statistics and Decision for Civil Engineers, McGraw Hill, 1970.

13. ASTM Designation D 143-52 (Reapproved 1965) "Standard Methods for Testing Small Clear Specimens of Timber." American Society for Testing and Materials, 1971 Book of ASTM Standards, July 1971.

14. U.S. Department of Agriculture, Forest Products Laboratory, Wood Handbook: Wood as an Engineering Material, Forest Service Agricultural Handbook No. 72, 1974.

15. Bethlehem Steel Corporation, Open-Web Steel Joists, Longspan Steel, Joists, Deep Longspan Steel Joists.

16. American Institute of Steel Construction, Inc. Manual of Steel Construction, Seventh Edition, 1970.

Appendix A

WOOD FLOOR TEST DATA

Appendix A
WOOD FLOOR TEST DATA

Presented in this appendix are the construction details, test geometry and results of eleven tests on wood floors. The wood floor systems used in this series were typical of floor systems found in residential and commercial structures throughout the U.S. and were 16 ft long, 4 ft wide, and were constructed of three 2-in. x 10-in. joists covered with 3/4-in. plywood and 3/8-in. particle board flooring. A listing of the tests in order of their appearance in this appendix is presented below.

Floor Panel Numbers	Upgrading Modification	Page Numbers
1 & 4	None - Base case	3
3 & 6	2 x 6's glued on bottom of joists	18
5 & 9	½ in. plywood (2-¼ in.) glued and nailed on bottom joists	31
2	Shored at 1/3 points	44
10	Shored at center	51
7, 8, & 11	King post truss	55

Each panel was subjected to four types of tests as follows:

1) Natural Frequency Test - An accelerometer was fastened to the top center of the panel. The panel was then deflected by an impact and the resulting decaying sinusoidal motion was recorded. From this record the natural frequency and the damping factor of the panel was determined.

2) Oscillating Vertical Load Test - A vertical load on the panel was

oscillated sinusoidally between two values (from approximately one half the designed service load to slightly over the designed service load) for approximately 100 cycles and at various frequencies. The vertical motion at each joist was measured and recorded. The purpose of this test was first to check the operation of the loading and measuring system dynamically and second, to age the panel. Since the results of the program will be used to upgrade existing and used buildings, it seemed prudent to impose an aging process on each panel prior to testing.

3) Load-Deflection Test - With dial gauges placed underneath the center of each joist, the load on the panel was statically increased in increments of 500 lbs per ram. At each increment, the reading at each dial gauge was recorded. From a plot of load versus deflection the static spring rate of the panel was determined.

4) Load to Failure Test - A ramp function increasing linearly with time and at a controlled loading rate was programmed to the hydraulic rams. A three-point loading was used on the first base case test. This was increased to a six-point loading on subsequent tests.

For each of the floor panels tested the equivalent uniform load has been plotted against deflection. The loads were below the yield point for the floor panels so deflection may be expected to vary linearly with load.

Predicted upper and lower bounds to the load-deflection test data are also presented in each figure. The lower bound represents the floor panel reaction if the plywood subflooring is ignored in the calculations, and the upper bound represents the reaction if the subflooring is considered fully effective. Because the subflooring is nailed to the floor joists, the degree of load that can be transferred through these nails will, in reality, determine the effectiveness of the subflooring. As a result, in most cases actual data will be closer to the lower bound.

BASE CASE FLOOR PANELS 1 AND 4

Construction Details

Panels 1 and 4 were base case specimens and were 16 feet long, 4 feet wide, and constructed of three 2-inch x 10-inch joists covered with 3/4-inch plywood and 3/8-inch particle board flooring. Photographs of those panels under construction are presented in Figs. A-1 and A-2. Construction details are shown in Figs. A-3, A-4, and A-5.

Test Results - Floor Panel 1

The load-deflection test on this floor system was a slowly applied loading to slightly above the designed service load (service load includes 10 psf dead load and 40 psf live load). The test arrangement for this test is shown in Fig. A-6 and the load deflection data are plotted in Fig. A-7. On this plot, the test data are compared with a predicted deflection versus load if the plywood floor and joist system act as a "T" beam and the prediction without "T" beam response. It will be noted that the data tend to follow this latter curve very closely indicating very little composite action between the flooring and joists.

The last test on this panel was an ultimate load test. The panel failed at 166 psf, which is about 4.2 times the design live load of 40 psf. The mode of failure was flexural failure at the mid-point of the front and middle joists as shown in Figs. A-8 and A-9. The near joist showed no signs of failure.

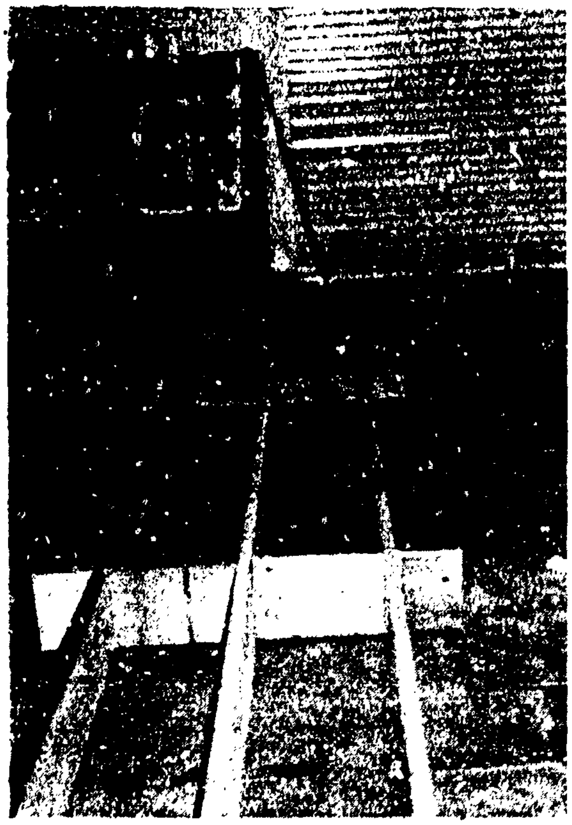

A. View of 2 x 10 Joists With End and Mid Span Blocking.

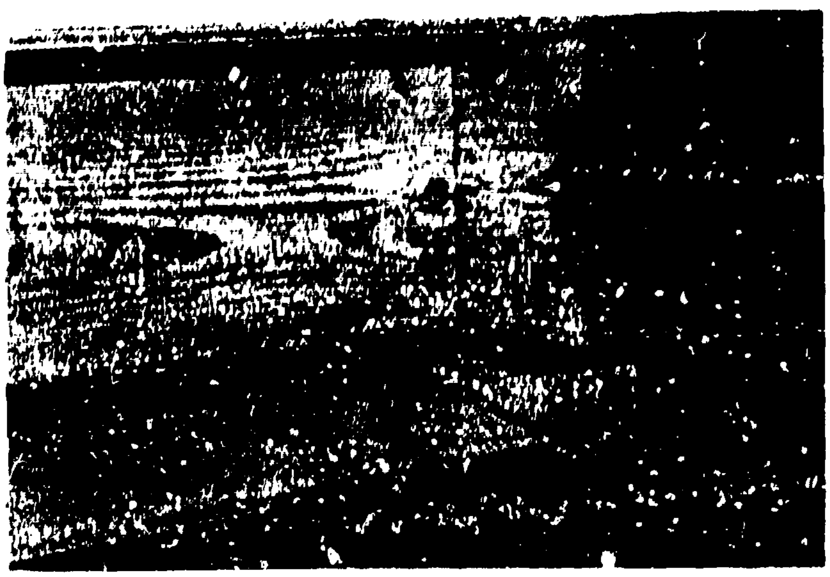

B. Detail of Joist/Sill/End Blocking.

Fig. A-1. Construction Photographs, Floor Panels 1 and 4.

A. Plywood Subfloor Being Moved into Place.

B. Plywood Subfloor Being Attached.

Fig. A-2. Construction Photographs, Floor Panels 1 and 4.

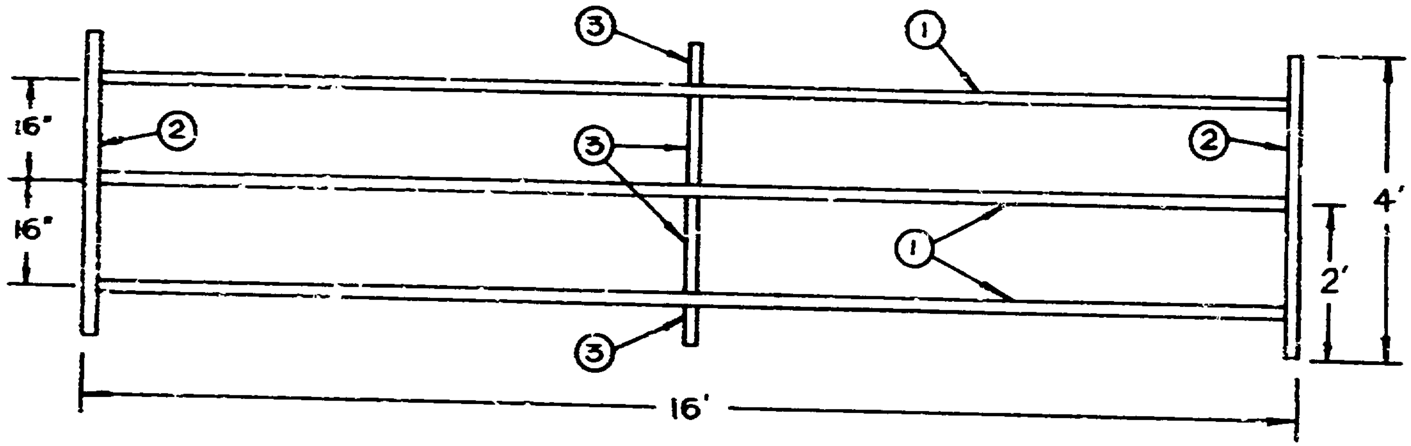

① 2" × 10" × 15'9" JOIST ON 16" CENTERS

② 2" × 10" × 4' HEADER

③ 2" × 10" BLOCKING

ALL FRAMING MATERIAL IS:
- DOUGLAS FIR
- SELECT STRUCTURAL

HEADERS NAILED TO JOISTS WITH 3 16-d COMMON NAILS / JOIST

BLOCKING NAILED TO JOISTS WITH EITHER:
ⓐ 2-16-d COMMON NAILS (if nailed)
ⓑ 3-16-d COMMON NAILS (if toenailed)

Fig. A-3. Framing Detail for All Floor Panels.

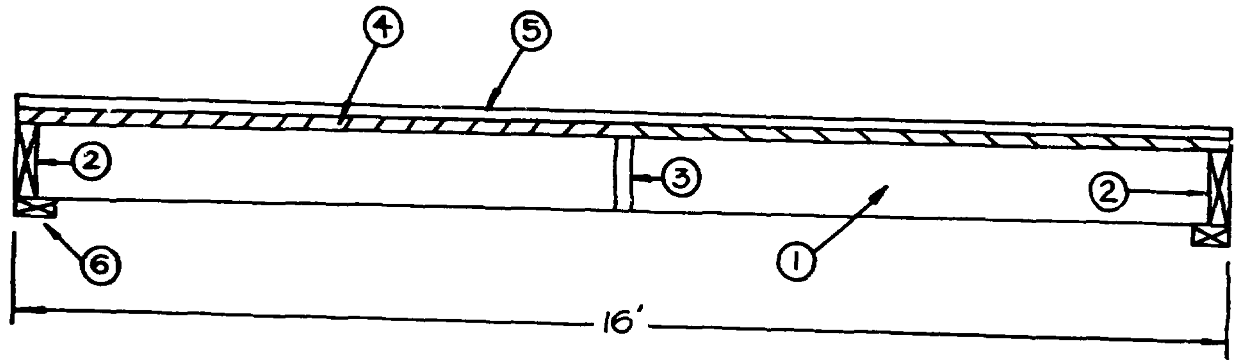

1. 2" x 10" x 15'9" JOIST
2. 2" x 10" x 4' END BLOCK
3. 2" x 10" BLOCKING
4. 3/4" 4'x8' PLYWOOD SUBFLOOR (C-D EXTERIOR)
5. 3/8" PARTICLE BOARD
6. 2" x 4" x 4' SILL

Fig. A-4. Construction Details for Floor Panels 1 and 4.

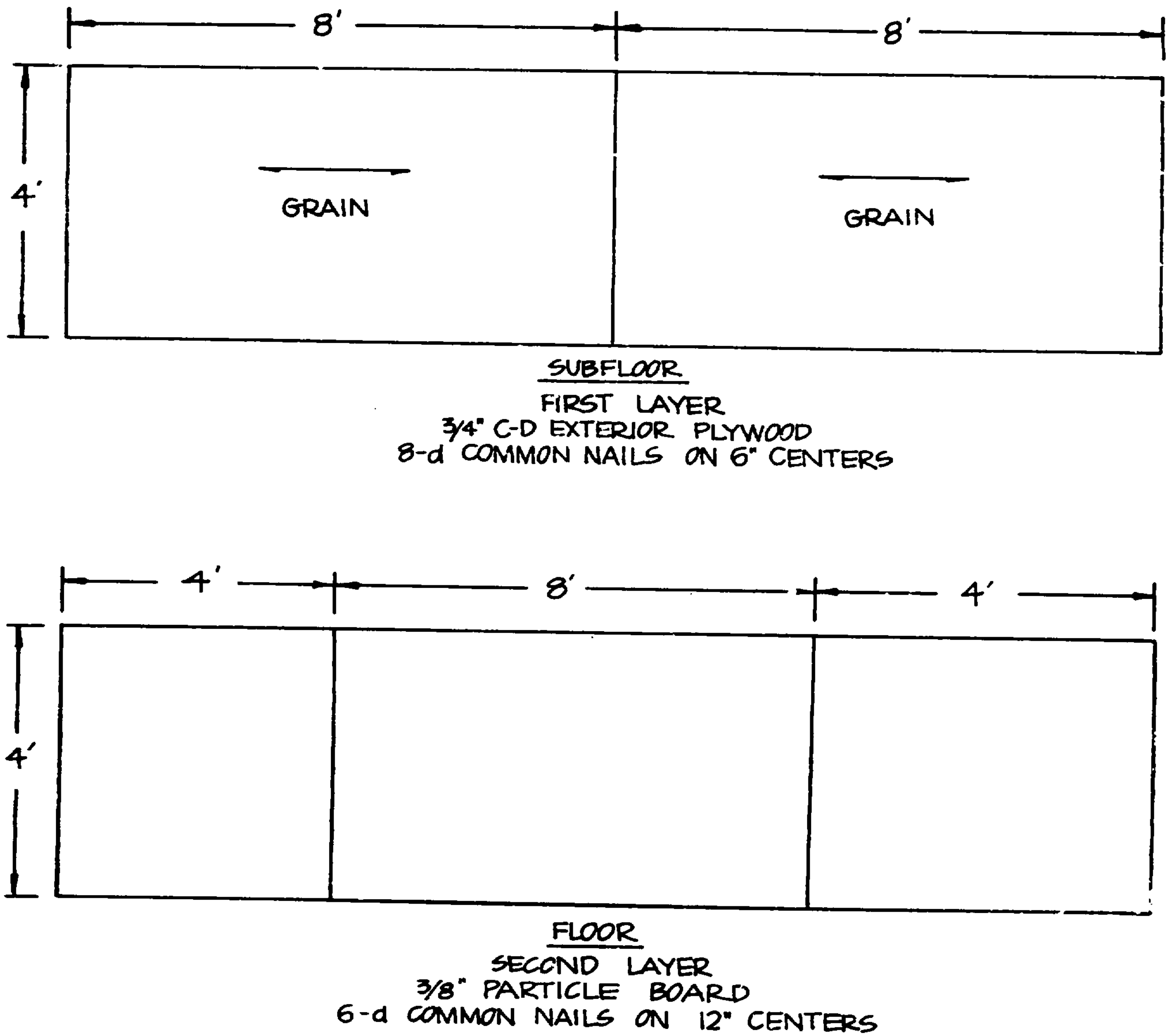

Fig. A-5. Flooring Details for all Floor Panels.

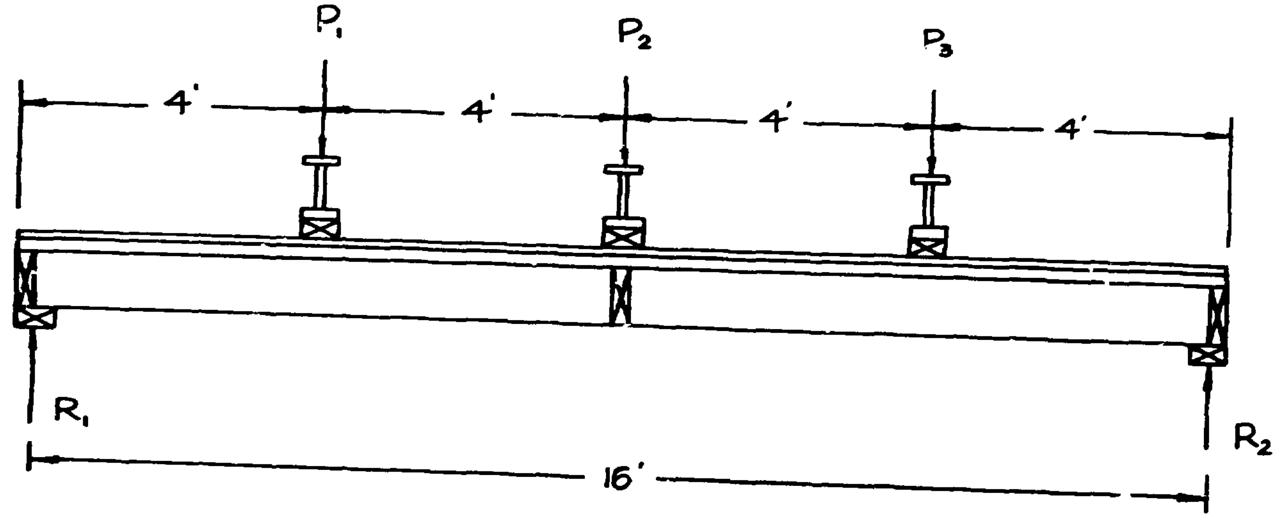

Fig. A-6. Test Arrangement for Floor Panel 1.

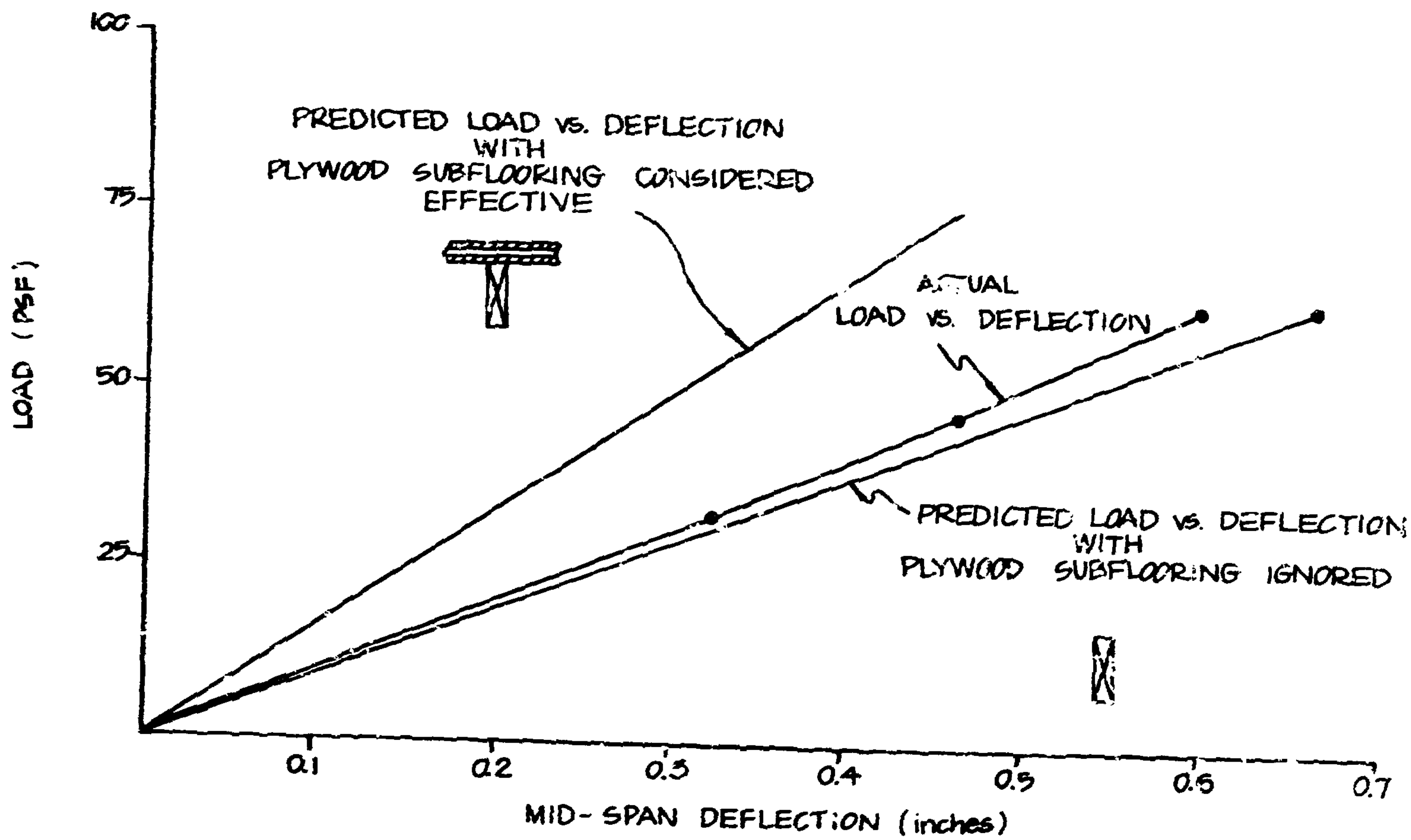

Fig. A-7. Load vs Deflection Data for Floor Panel 1.

A

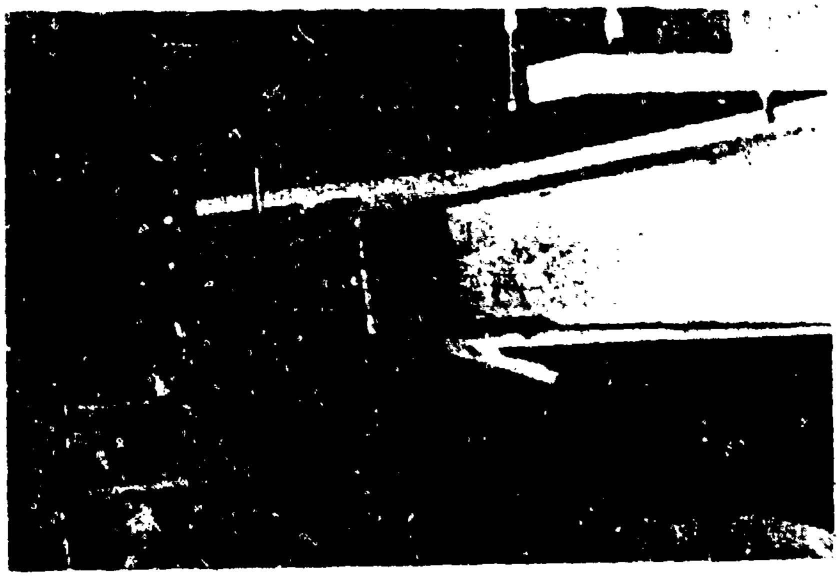

B

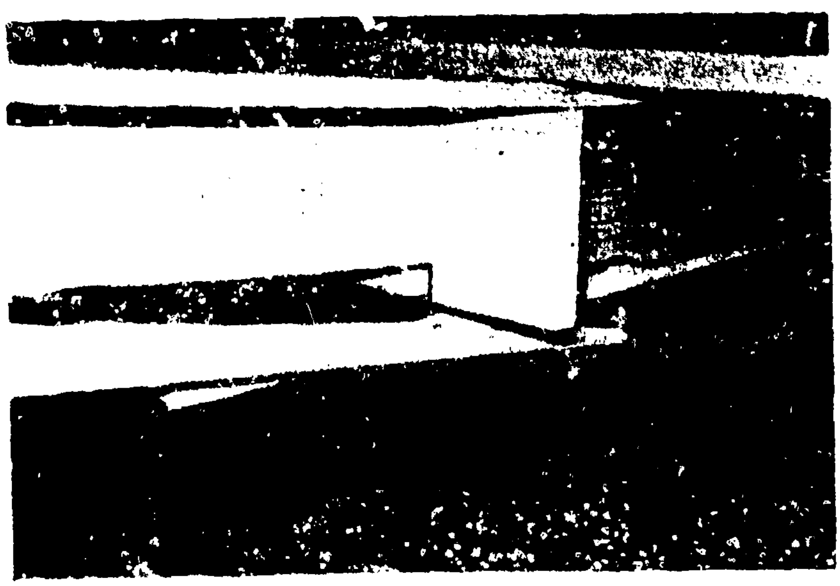

Fig. A-8. Post-Test Photographs, Floor Panel 1.

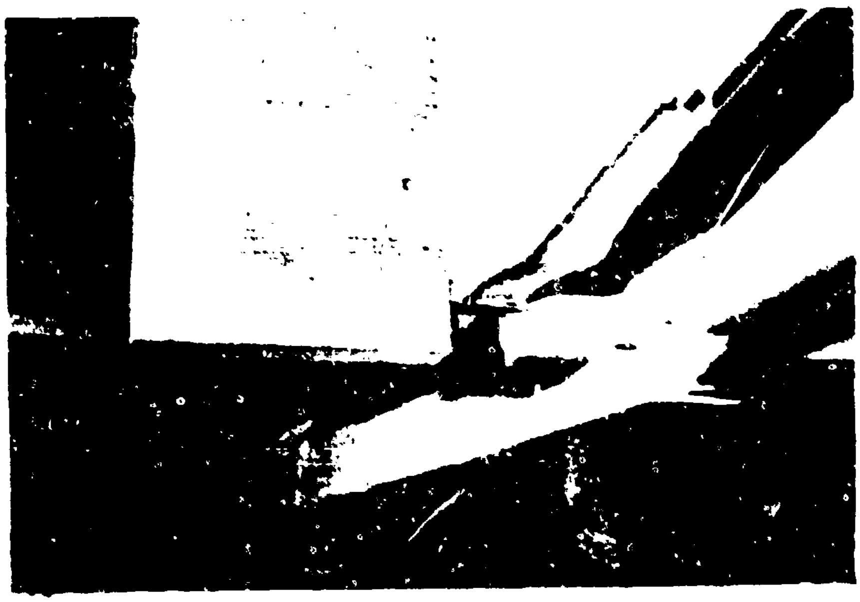

Fig. A.9. Post-Test Photograph, Floor Panel 1.

Test Results - Floor Panel 4

For this and all subsequent wood floor tests, a six-point loading arrangement was used rather than the three-point system used for Panel 1. This test arrangement is shown in Fig. A-10.

Under static design loads, this panel was also well-behaved and fell within the upper and lower predicted deflection limit. The floor panel did exhibit some composite action with the plywood subfloor, as shown in the load-deflection plot in Fig. A-11.

Panel 4 failed due to flexure in the front and middle joists under the point of maximum moment, as shown in the sketches in Fig. A-12. The ultimate load was 224 psf, or about 5.6 times the design live load. Post-test photographs are presented in Fig. A-13. It should be noted that the tensile fiber failure occurred at a knot-weakened section, as shown in Fig. A-13A.

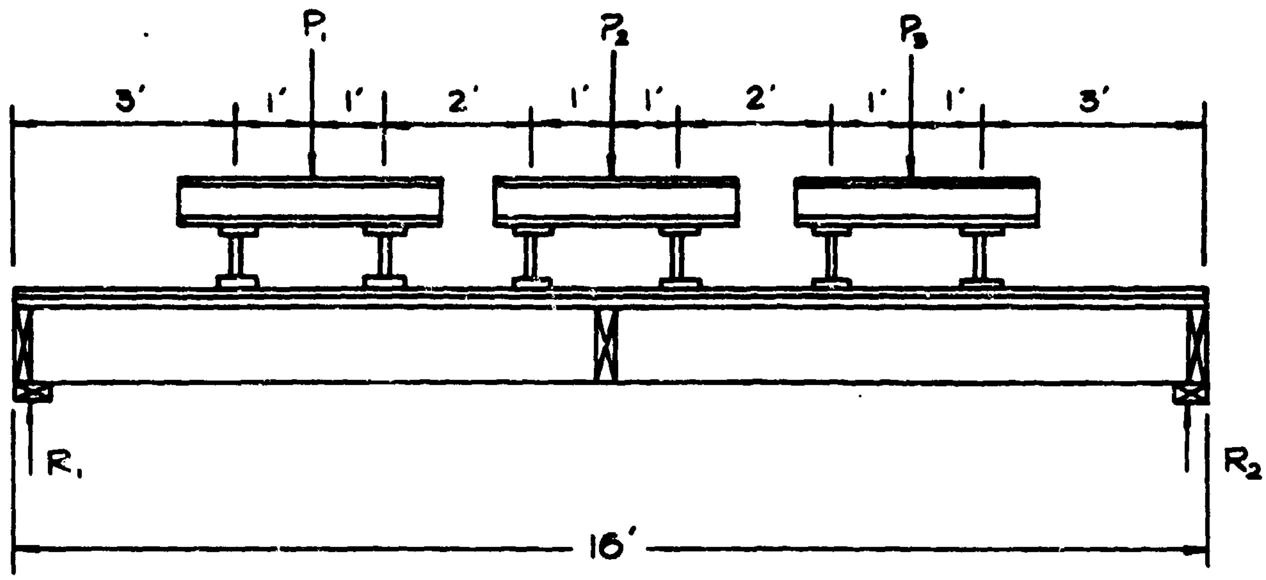

Fig. A-10. Sketch and Photograph of Six-Point Loading Arrangement.

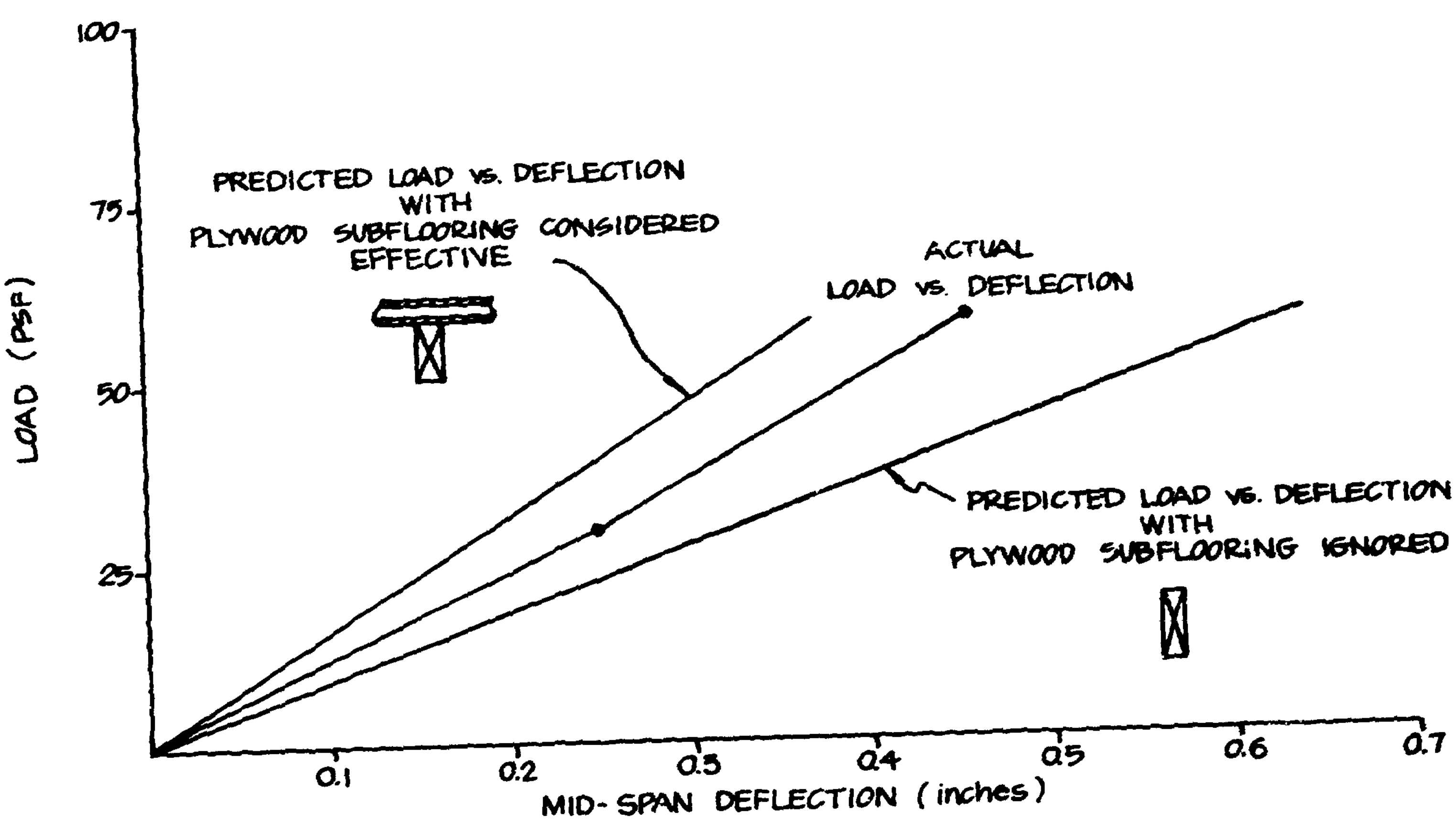

Fig. A-11. Load vs Deflection Data for Floor Panel 4.

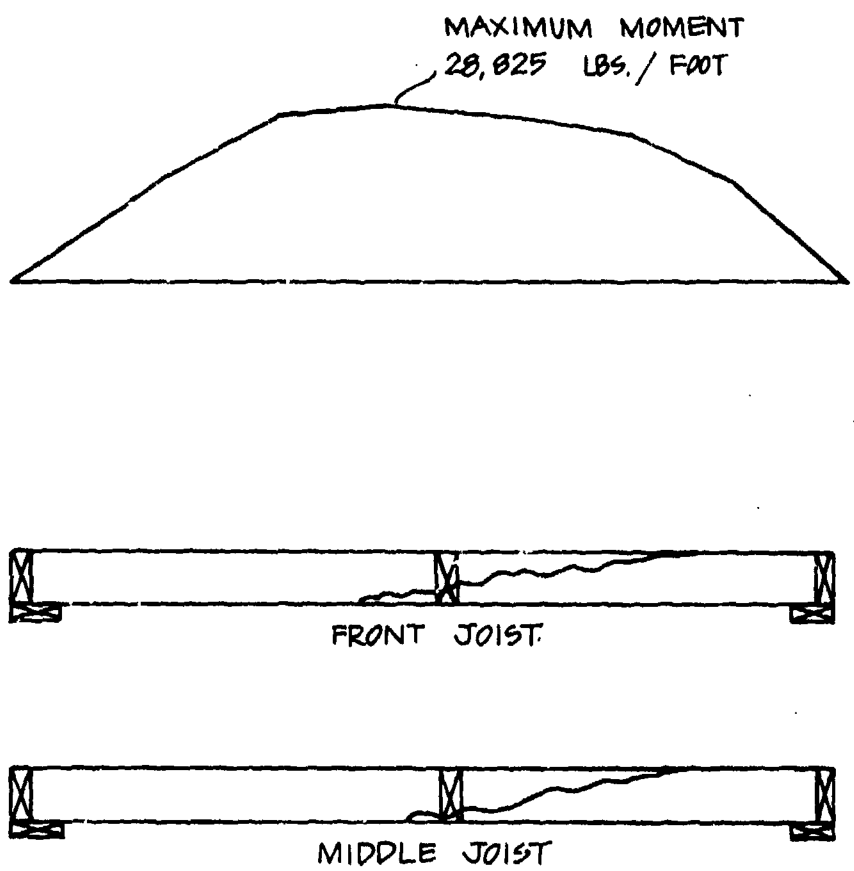

Fig. A-12. Sketch of Failure Cracks and Moment Diagram, Floor Panel 4.

A

B

Fig. A-13. Post-Test Photographs, Floor Panel 4.

FLANGED JOIST FLOOR PANELS 3 AND 6

Construction Details

For these tests the base case floor panel system was upgraded by the addition of 2-inch x 6-inch flanges glued to the bottom of the floor joists. Construction details are shown in Figs. A-14 and A-15 and construction photographs in Figs. A-16 and A-17. Nails were used to hold the 2 x 6's in place until the glue cured.

Test Results - Floor Panel 3

Using the six-point loading system as shown in Fig. A-18, Panel 3 was tested to the design service load (10 psf dead load plus 40 psf live load). The resulting load-deflection curve was somewhat non-linear as shown in Fig. A-19. Also shown in this figure are predicted curves for "T" beam effects.

This floor panel failed at an ultimate load of 310 psf with a shear failure that began at the right hand support (see Fig. A-20). The failure progressed in a cross-grain splitting action across the joist. Under close examination of the shearing stress at the right hand support the mechanism of failure is easily seen (see sketch in Fig. A-21). At section 1-1 the shear stress is found to vary from zero at the bottom edge to a maximum at the ℄ of the joist. Section 2-2 just to the left of section 1-1 the shear stress at the bottom of the 2 x 10 goes from zero to 69% of the maximum shearing stress of section 1-1. This abrupt change in the cross section causes a stress concentration at the glue line, which along with the high shearing stress makes this point the weak link in the floor system.

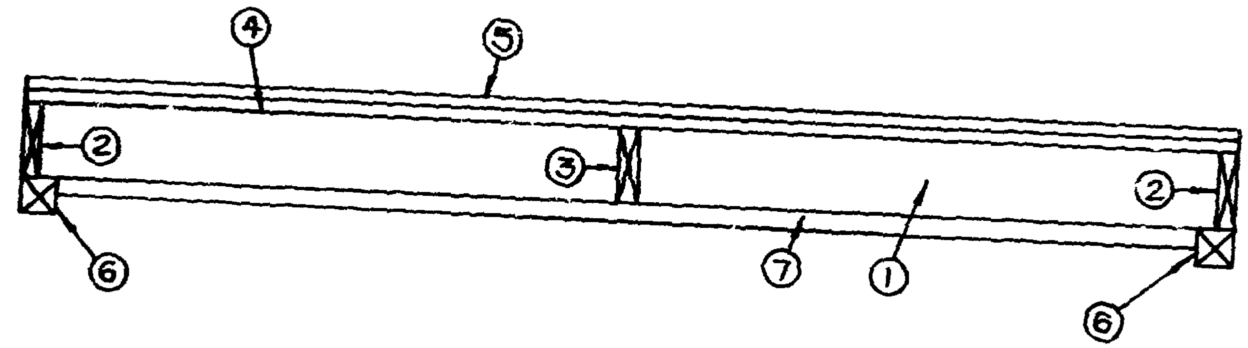

1. 2" × 10" × 15'9" JOIST ON 16" CENTERS
2. 2" × 10" × 4' HEADER
3. 2" × 10" BLOCKING
4. 3/4" PLYWOOD SUBFLOOR (C-D EXT)
5. 3/8" PARTICLE BOARD
6. 4" × 4" × 4' SILL
7. 2" × 6" × 15'5" FLANGE; GLUED AND NAILED 16-d COMMON NAILS ON 12" CENTER

ALL 2 × 10'S ARE STRUCTURAL GRADE DOUGLAS FIR
4" × 4" SILL: CONSTRUCTION GRADE DOUGLAS FIR
2" × 6 FLANGE: CONSTRUCTION GRADE DOUGLAS FIR

Fig. A-14. Construction Details for Floor Panels 3 and 6.

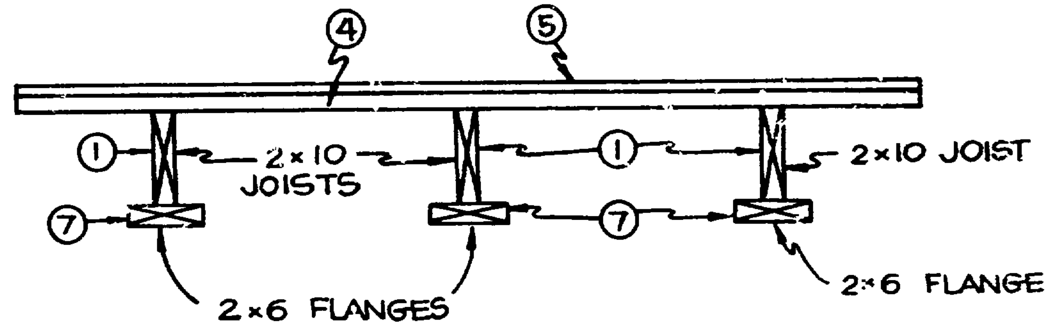

Fig. A-15. Construction Details for Floor Panels 3 and 6.

A. Placing Glue on Bottom of Joists.

B. Installing 2 x 6 Flange.

Fig. A-16. Construction Photographs, Floor Panels 3 and 6.

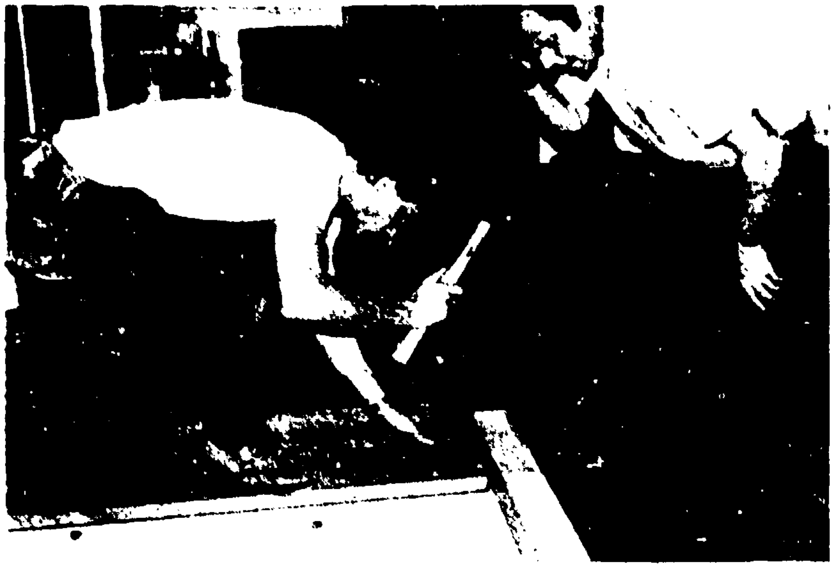

A. Nailing 2 x 6 Flanges.

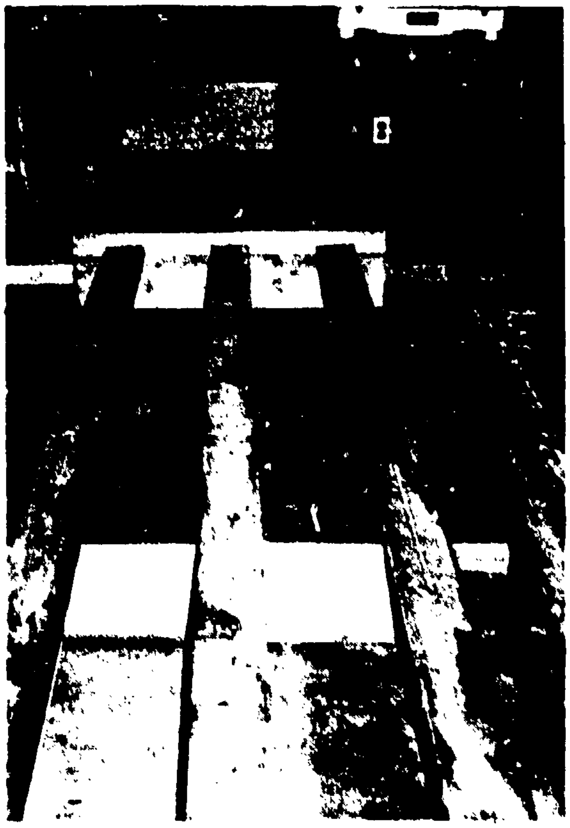

B. Completed Floor System.

Fig. A-17. Construction Photographs, Floor Panels 3 and 6.

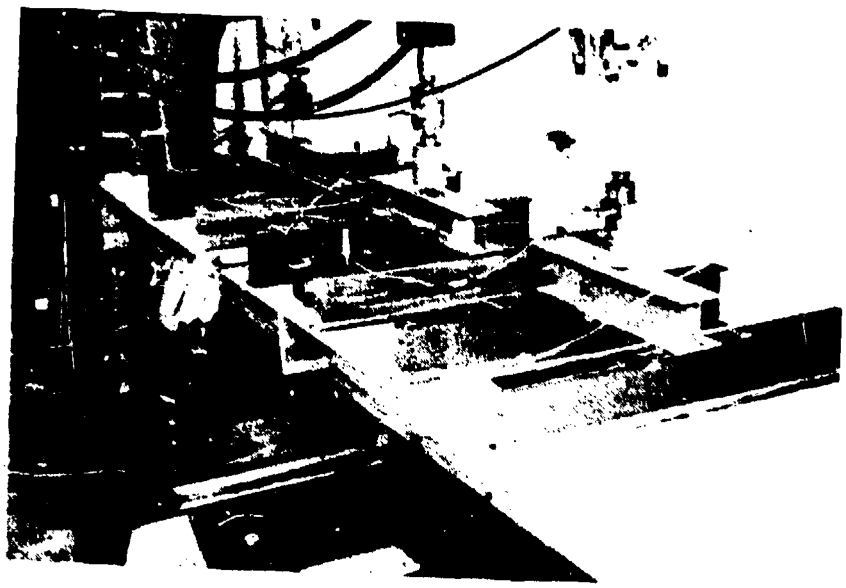

Fig. A-18. Test Geometry, Floor Panel 3.

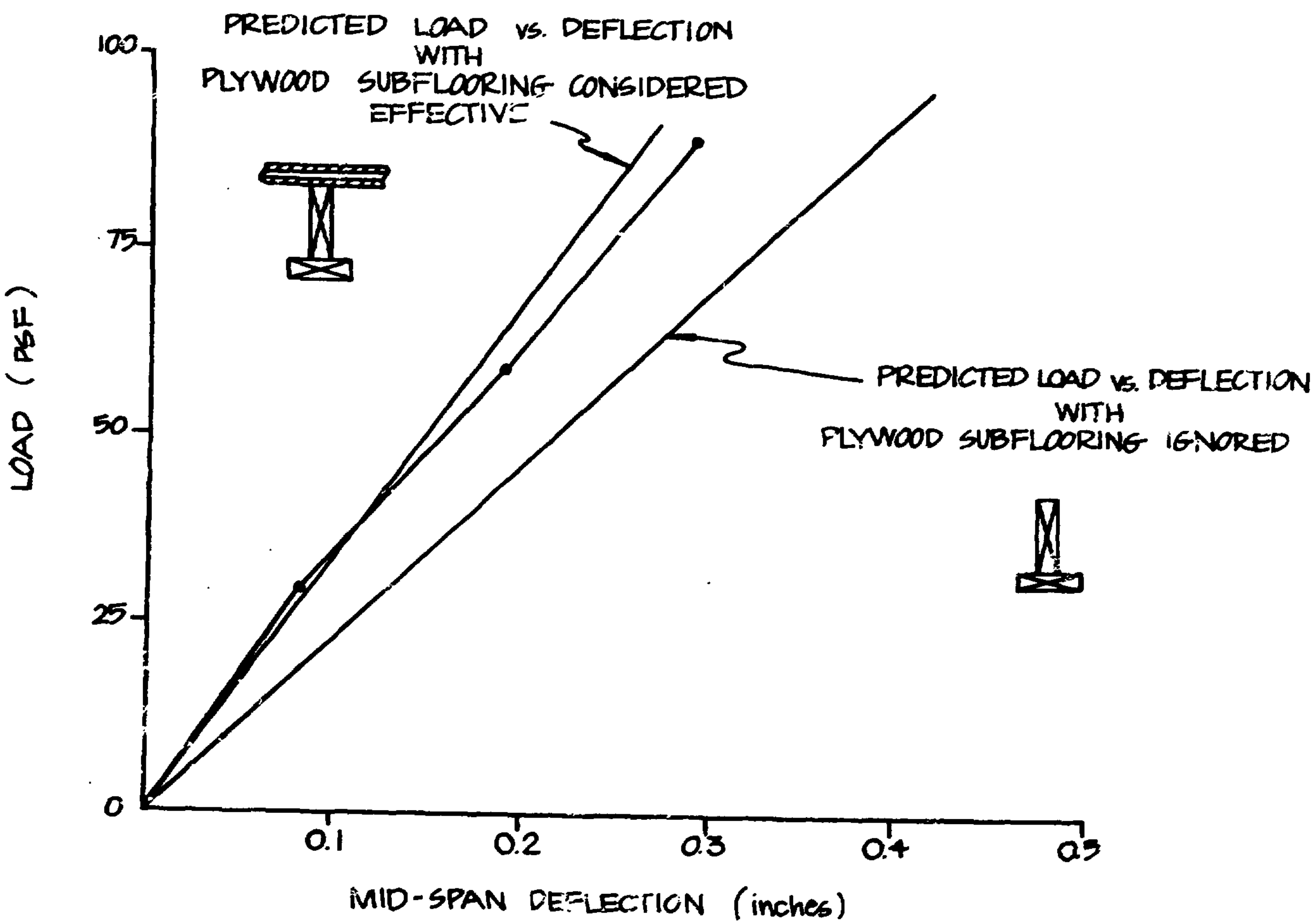

Fig. A-19. Load vs Deflection Data for Floor Panel 3.

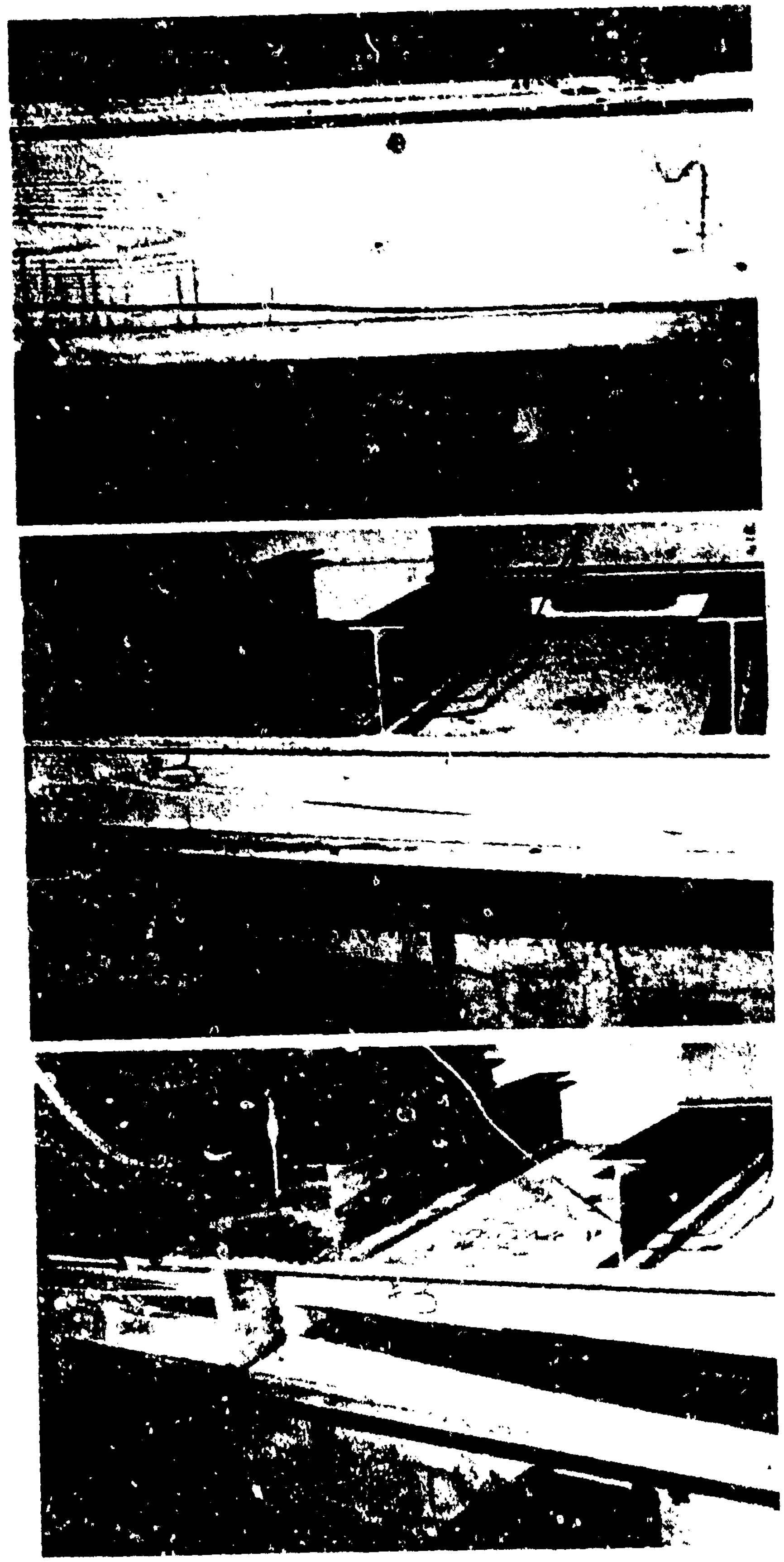

Fig. A-20. Post-Test Photographs, Floor Panel 3.

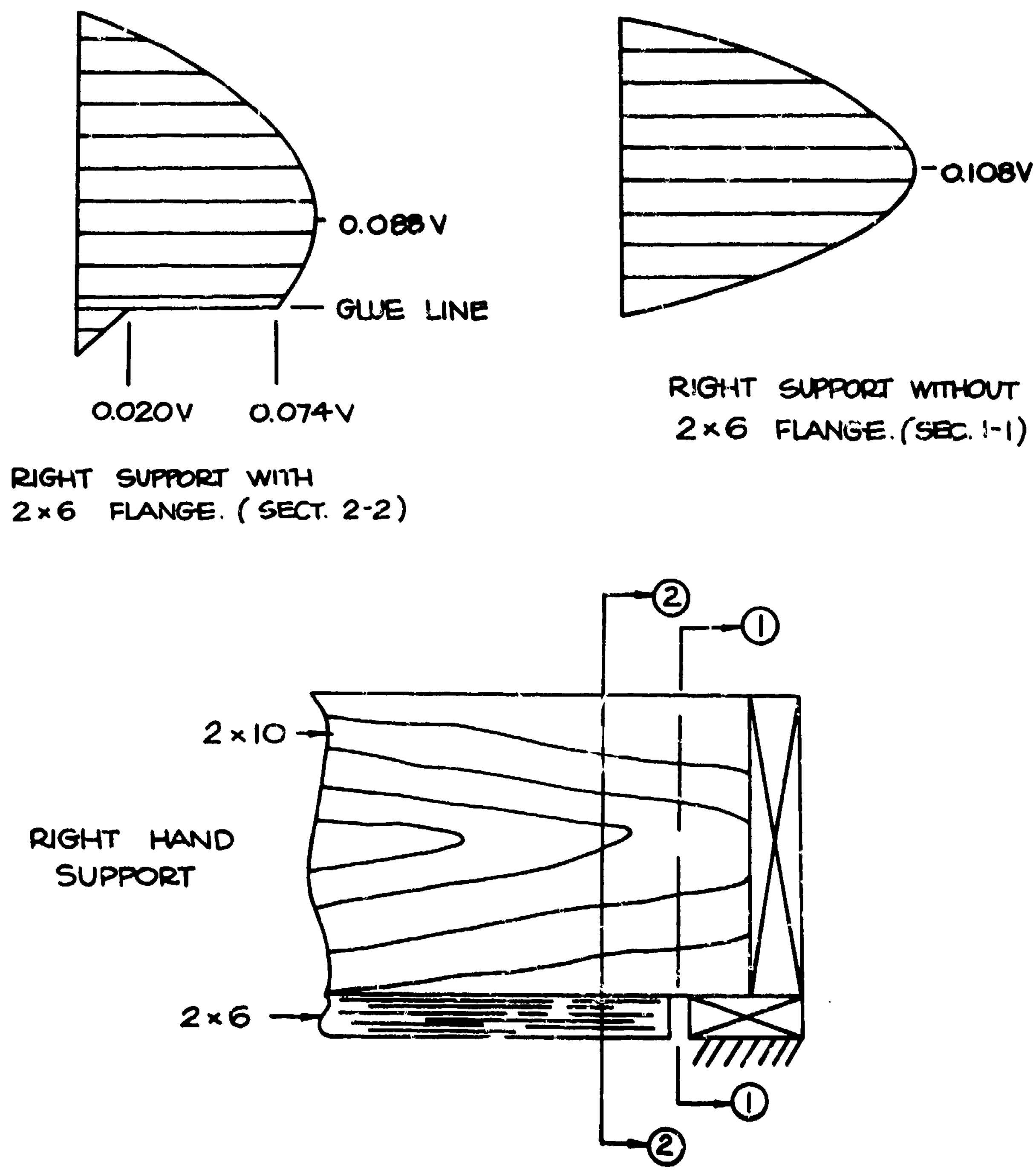

Fig. A-21. Shear Stress Distribution Analysis for Floor Panel 3.

Test Results - Floor Panel 6

The test arrangement of this panel was identical to panel 3, i.e., six-point loading. Under static service loading conditions this panel was well behaved and fell well within the anticipated upper and lower limits of deflection, as shown in Fig. A-22.

The load deflection data for this test was quite linear. Ultimate failure occurred at 472 psf, which is 11.8 times the design load. The front joist was first to fail, see Fig. A-23. The joist failed in flexure at midspan. The upper fibers failed in compression and the failure progressed downward until a tensile failure finally occurred in the flange. A shear failure also occurred at the left support and was identical to the failure that occurred with Panel 3. The middle joist failed at the right support in shear, as seen in Fig. A-24A. The rear joist failed at midspan due to a flexural failure in the tensile fibers. In Fig. A-24B the knot-weakened section at which this failure occurred can be seen. The rear joist also had a shear failure which ran along the neutral axis until it was intercepted by the flexural failure at midspan.

It appears that the failure mechanisms for Panels 3 and 6 are the same. The stress concentration at the support due to the abrupt change in cross section initiates the failure and a cross-grain or parallel-grain split moves across the floor joists to midspan. To reduce the stress concentration it is suggested that the 2 x 6 flange be tapered, as shown in in the sketch below.

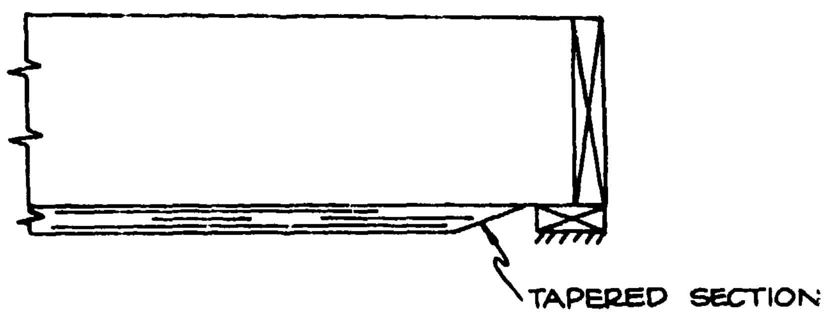

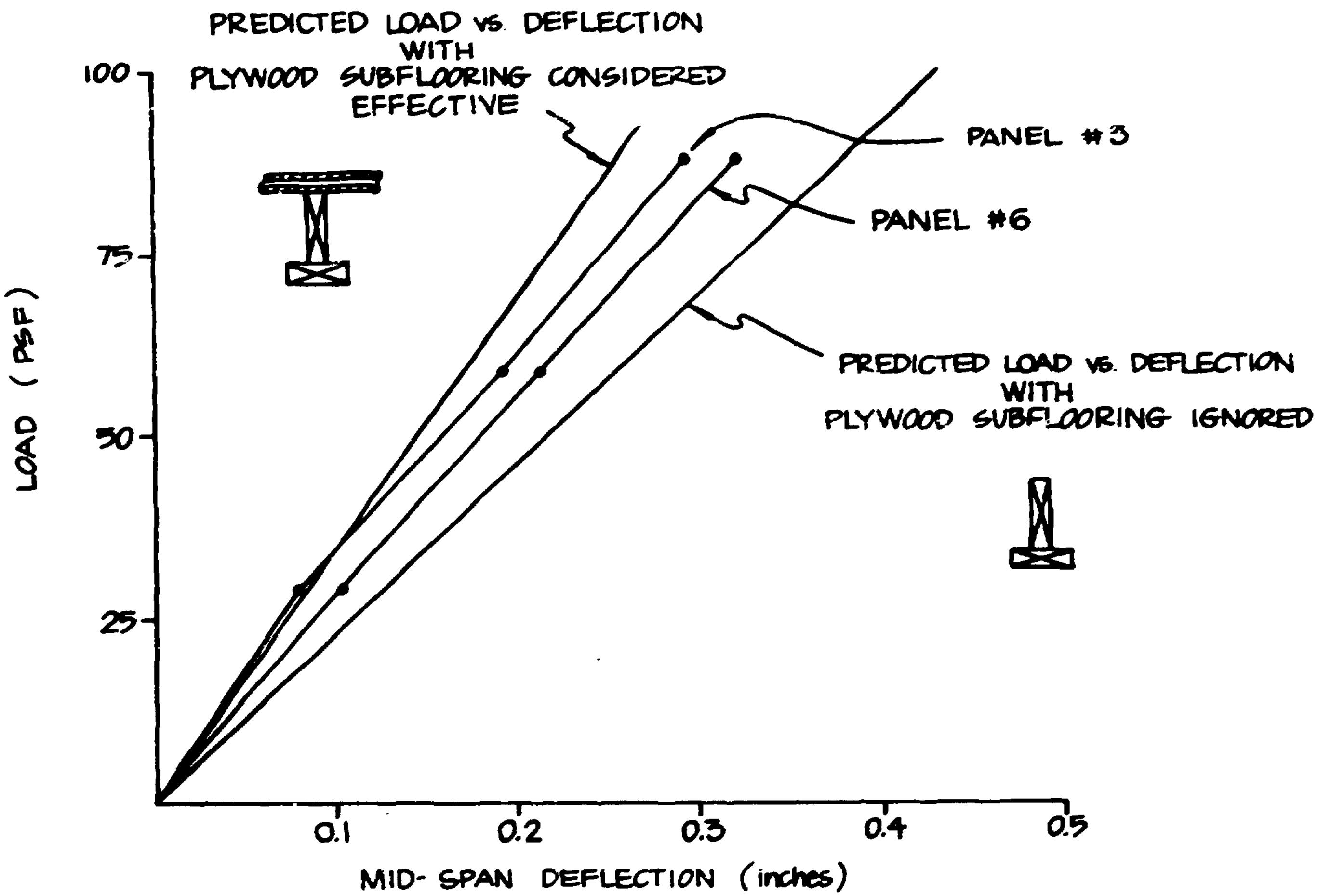

Fig. A-22. Load vs Deflection Data for Floor Panels 3 and 6.

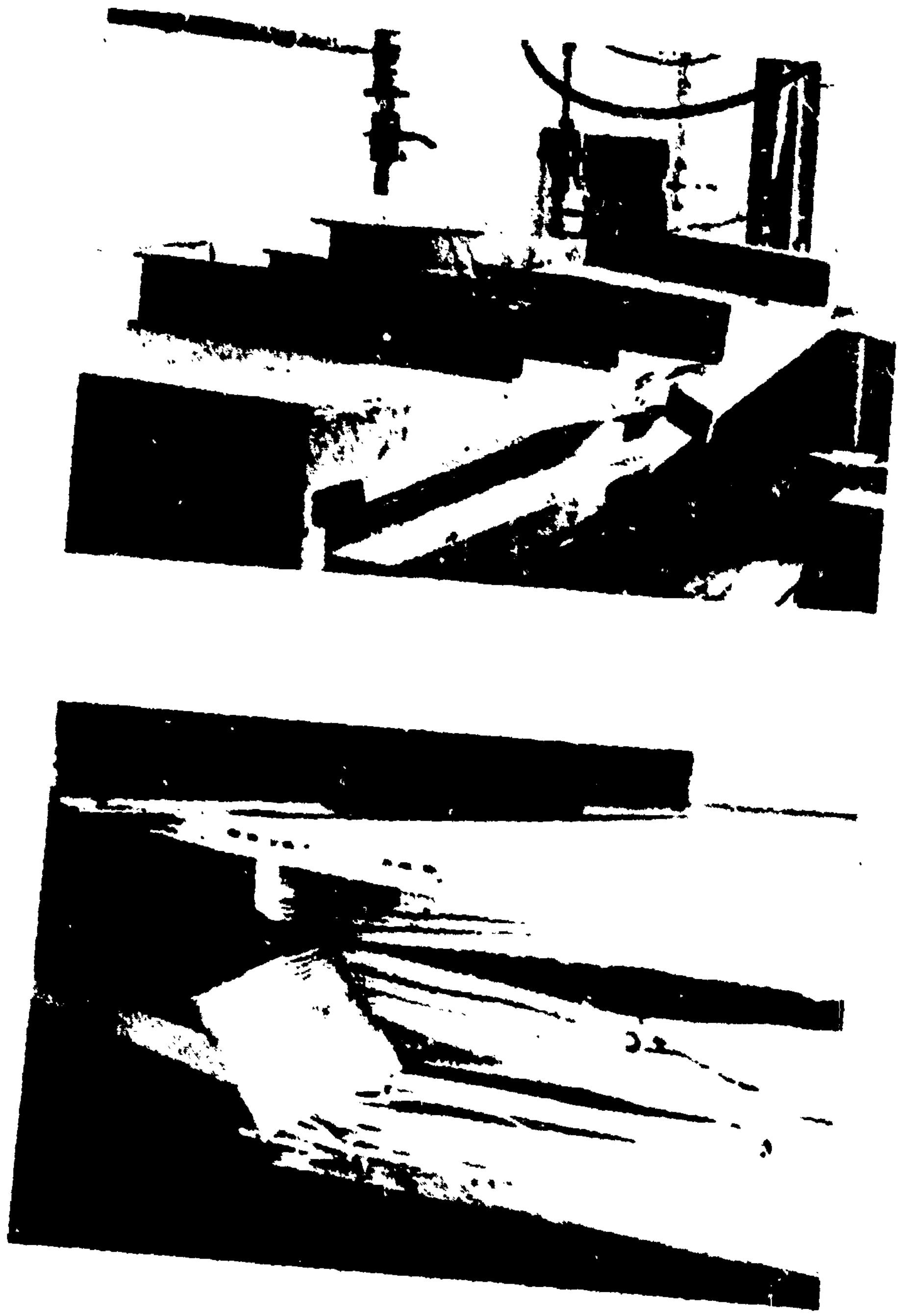

Fig. A-23. Post-Test Photographs, Floor Panel 6.

A

B

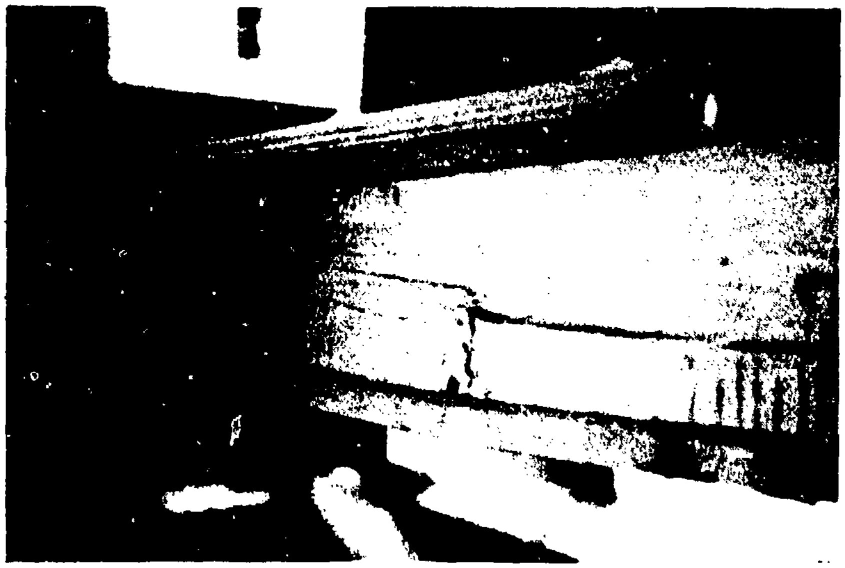

Fig. A-24. Post-Test Photographs, Floor Panel 6.

BOXED BEAM FLOOR PANELS 5 AND 9

Construction Details

For these tests the base case floor panel was upgraded by gluing two layers of 1/4-in. plywood to the bottom of the floor joists. The contruction sequence can be seen in Figs. A-25 and A-26 and detail in Figs. A-27 and A-28. Panel 9 differed from Panel 5 in that a 1-ft splice was added to the bottom ofthe second layer at the end quarter points.

Tests Results - Floor Panel 5

Under static loading Panel 5 deflected well within the predicted limits of deflection as shown in the load vs deflection plot in Fig. A-29. Note that the lower bound predicted curve considered the plywood to be only 75% effective. The 1/4-in. plywood was nailed and glued to the bottom of the 2 x 10 joists and joined at the quarter and mid points. This left only 25% of the plywood effective at the quarter points and 75% of the plywood effective at the mid point of the floor panels. Thus, it was felt that the lower predicted bound could best be represented using the 2 x 10 joists and 75% of the plywood as being effective.

Ultimate failure occurred at 479 psf, which is more than 12 times the design live load. The floor system failed in flexure at the quarter point as shown in the post-test photographs in Figs. A-30 and A-31. Fig. A-30B shows a closeup of the three joists at the left quarter point looking toward midspan. The weakened section originally failed in flexure where the plywood glued to the tensile fibers ripped apart at the quarter point. Then, the middle joist failed in flexure with the tensile fibers failing until the neutral axis was reached, at which point the middle joist then failed in shear with a continuous split from the left quarter point to about midspan. A glue-line failure occurred at the front joist, as shown in Fig. A-31A. The rear joist failed in a very similar manner and can be seen in Fig. A-31B.

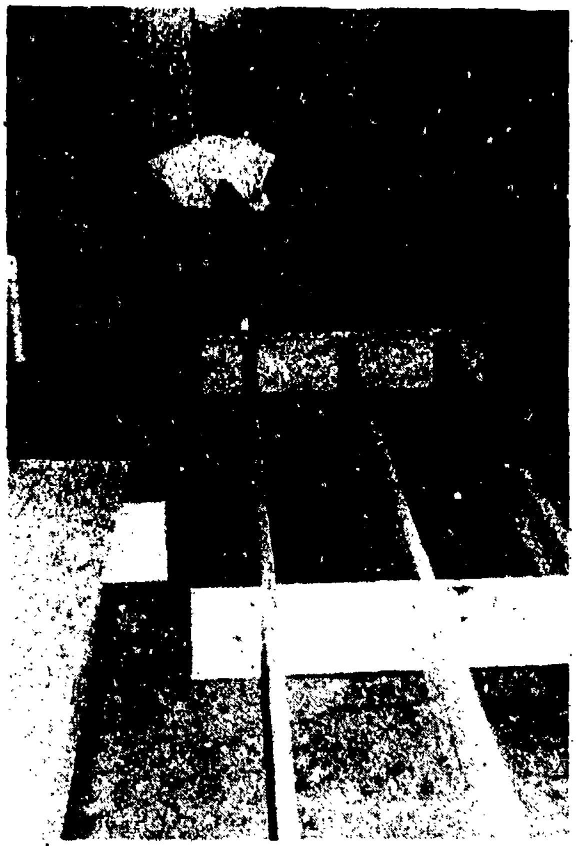

A. Applying Glue to Bottom of Floor Joist.

B. Nailing First Layer of Plywood.

Fig. A-25. Construction Photographs, Floor Panels 5 and 9.

A. Adhesive Being Applied to the First Layer.

B. Aligning the Second Layer of Plywood.

Fig. A-26. Construction Photographs, Floor Panels 5 and 9.

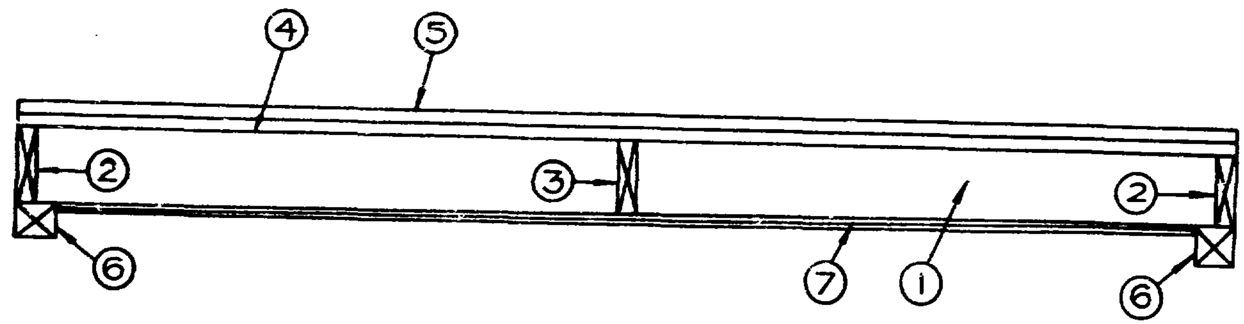

① 2" × 10" × 15'9" JOIST

② 2" × 10" × 4' HEADER

③ 2" × 10" BLOCKING

④ 3/4" PLYWOOD SUBFLOOR (C-D EXTERIOR)

⑤ 3/8" PARTICLE BOARD

⑥ 2" × 4" × 4' SILL

⑦ 2 LAYERS OF 1/4" A-C EXTERIOR PLYWOOD NAILED AND GLUED.
(6-d common nails on 6" centers)

Fig. A-27. Construction Details for Floor Panels 5 and 9.

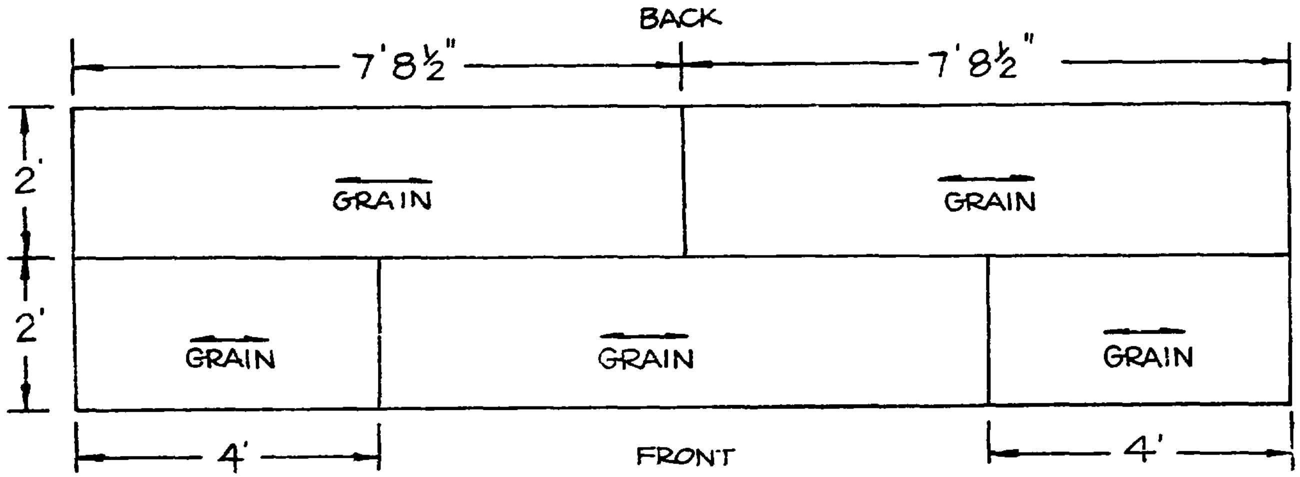

FIRST LAYER ¼" AC EXTERIOR PLYWOOD (NAILED AND GLUED TO 2×10 JOISTS)
(6-d COMMON NAILS ON 6" CENTERS)

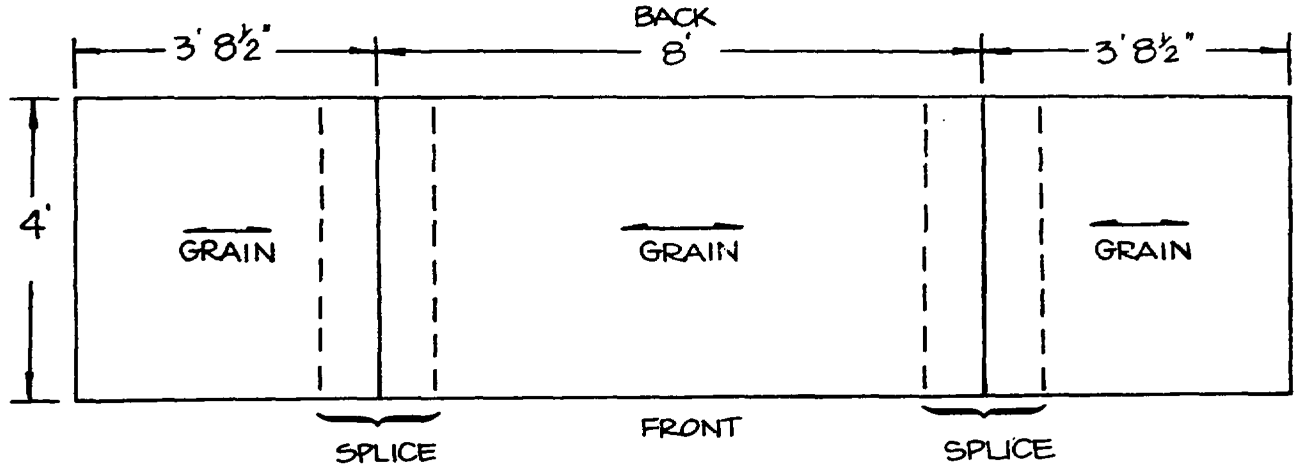

SECOND LAYER ¼" EXTERIOR PLYWOOD (NAILED AND GLUED TO FIRST LAYER)
(6-d COMMON NAILS ON 6" CENTERS)

Fig. A-28. Construction Details for Floor Panels 5 and 9.

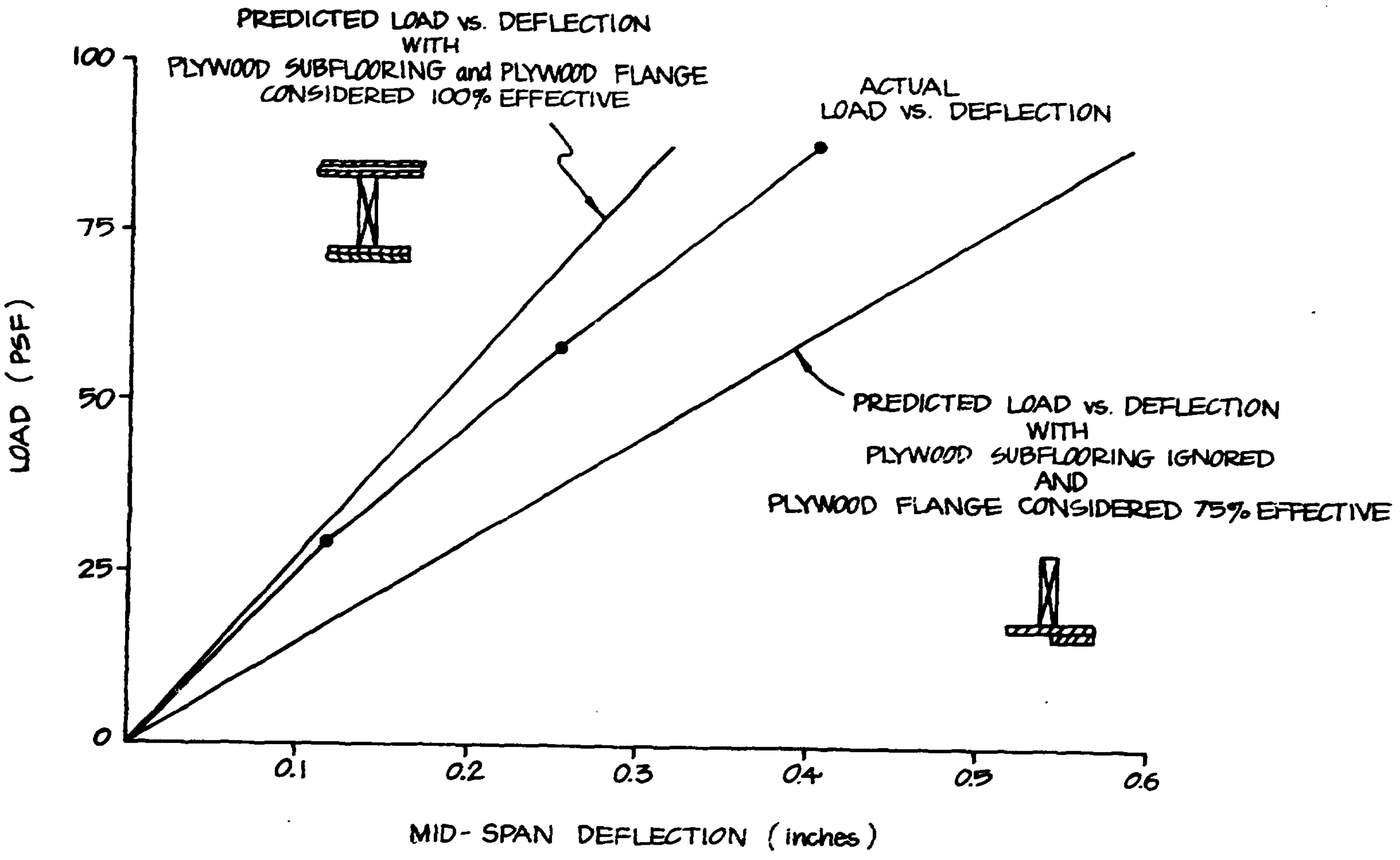

Fig. A-29. Load vs Deflection Data for Floor Panel 5.

A

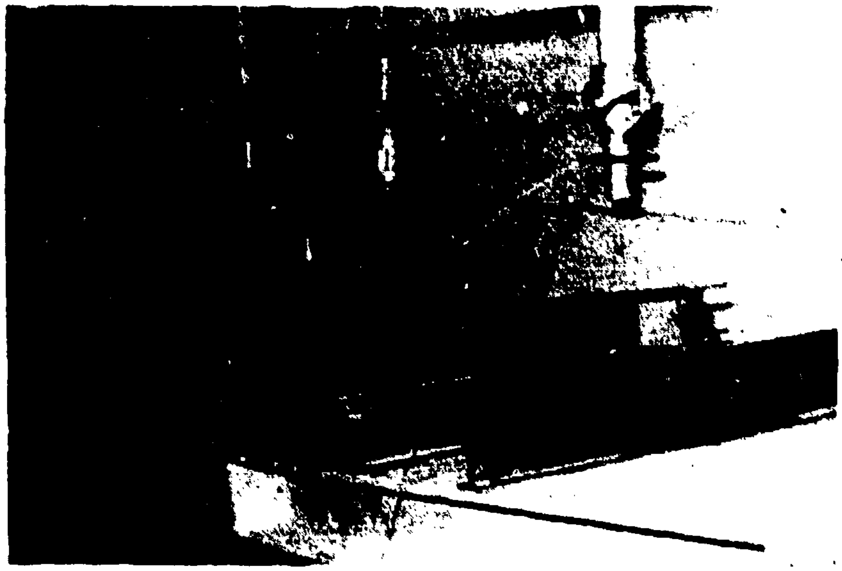

B

Fig. A-30. Post-Test Photographs, Floor Panel 5.

A

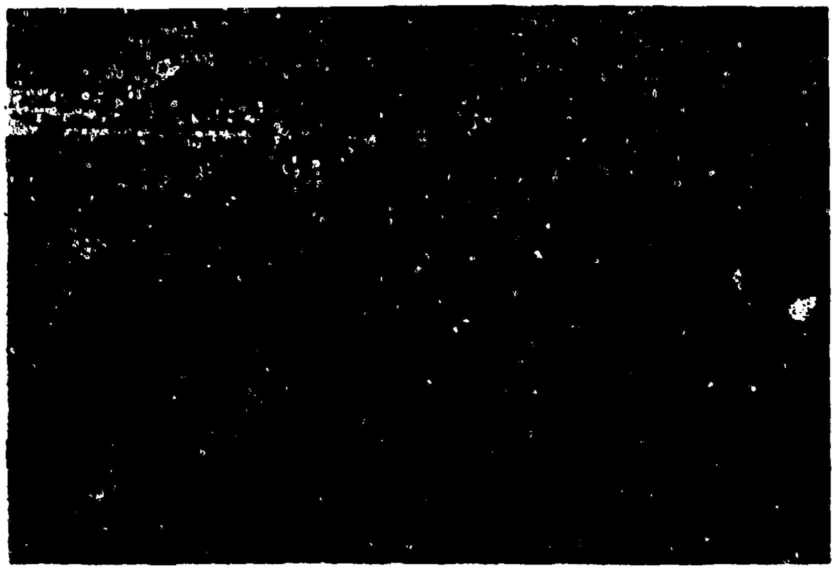

B

Fig. A-31. Post-Test Photographs, Floor Panel 5.

Test Results - Floor Panel 9

Under static loading Panel 9 deflected linearly with load and the results were within the upper and lower limits of the predicted deflection as shown in Fig. A-32. The ultimate failure load occurred at 456 psf, an increase of 11.4 times the design live load.

The construction details of this panel were slightly different from Panel 5 in that two 1 ft x 4 ft x ¼ in. plywood splices were added at the quarter points in hopes of alleviating the flexural failure encountered in Panel 5. The splices can be seen in the post-test photograph in Fig. A-33A. The front joist appears to have first failed in shear and then in flexure at the left quarter point This failure can be clearly seen in Figs. A-33B and A-34A. The shear failure began at the neutral axis at the support and progressed in a cross-grain splitting action to the compressive fibers at about the left one third point. Once weakened by the reduced section, the compressive fibers failed due to flexure (see Fig. A-34B). The rear joist failed in an almost identical manner, first a shear failure at the support (see Fig. A-35A), and then a flexural failure as shown in Fig. A-35B. Note that the flexural failure did not occur at the splice but tended to be closer to midpsan.

Comparing the failures of Panels 5 and 9 it appears that the splices added at the quarter points were sufficient to prevent flexural failure from first occurring at those points.

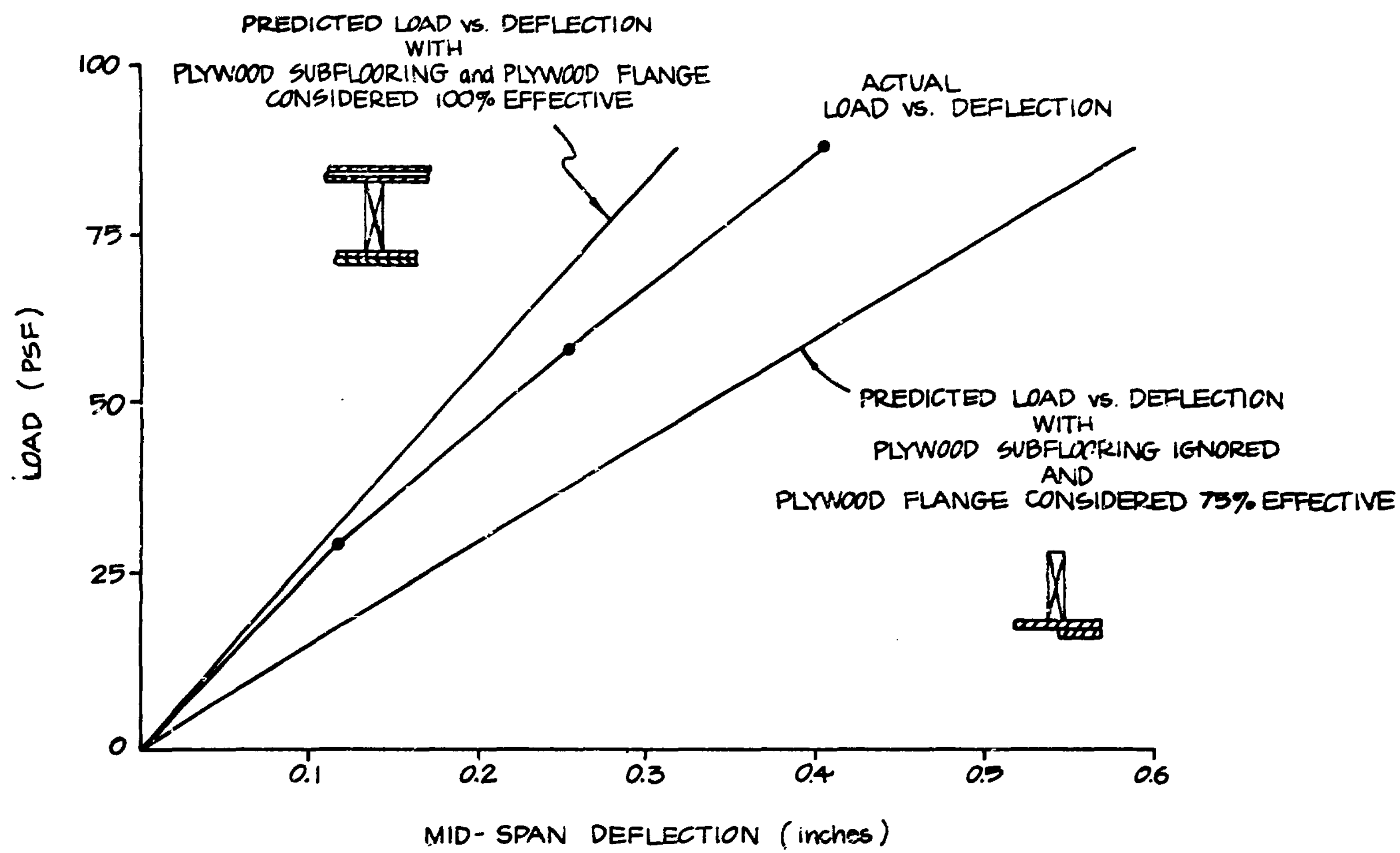

Fig. A-32. Load vs Deflection Data for Floor Panel 9.

A

B

Fig. A-33. Post-Test Photographs, Floor Panel 9.

A

B

Fig. A-34. Post-Test Photographs, Floor Panel 9.

A

B

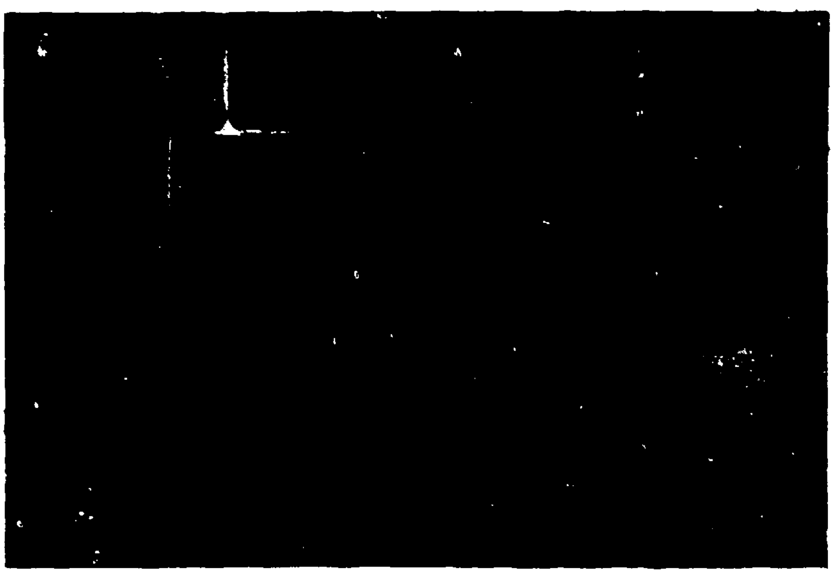

Fig. A-35. Post-Test Photographs, Floor Panel 9.

SHORED FLOOR PANELS 2 AND 10

Construction Details

For these tests the base case floor panel was upgraded by the use of shores. Panel 2 had two supports at the one third points as shown in Fig. A-36 and Panel 10 had a single support at the center as shown in Fig. A-37. Photographs of the construction detail of the shoring are presented in Fig. A-38.

Test Results - Floor Panel 2

Panel 2 with two shores was loaded to design live load twice to seat the joist shoring system. Load deflection data for the second test are presented in A-39. It will be noted that the deflection is still somewhat greater than would be predicted from a purely rigid support. This is probably due to the fact that all surfaces between the post-support beam and floor are not perfectly smooth and a small amount of re-alignment and local crushing occurred.

This panel failed at an ultimate load of 1,470 psf — approximately 37 times the design live load. Both front and center joists failed. The failure was initiated as a bearing failure followed by cross-grain splitting. Post-test photographs of the front joist failure are shown in Fig. A-40. The middle joist bearing failure is shown in Fig. A-41A and the end support crushing in Fig. A-41B.

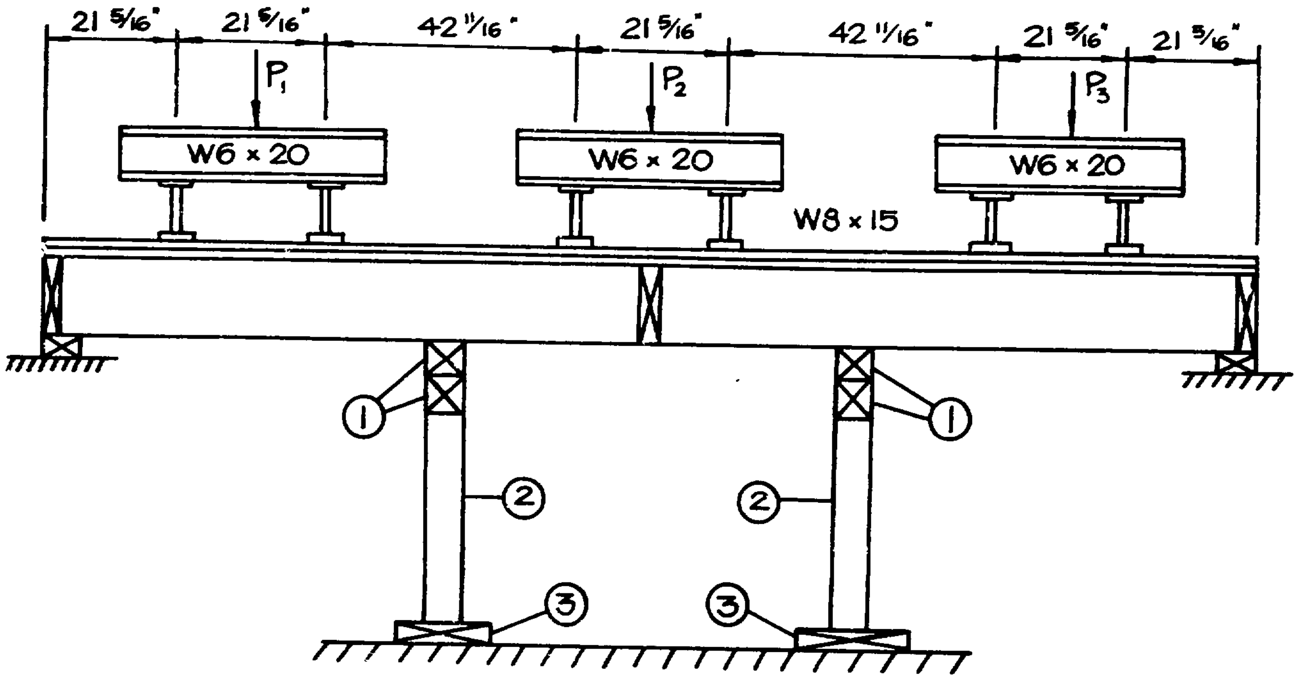

1. 4" x 4" x 4' SHORING SUPPORT
2. 2 - 4" x 4" x 4' SHORE
3. 2" x 10" BLOCK

Fig. A-36. Test Arrangement for Floor Panel 2.

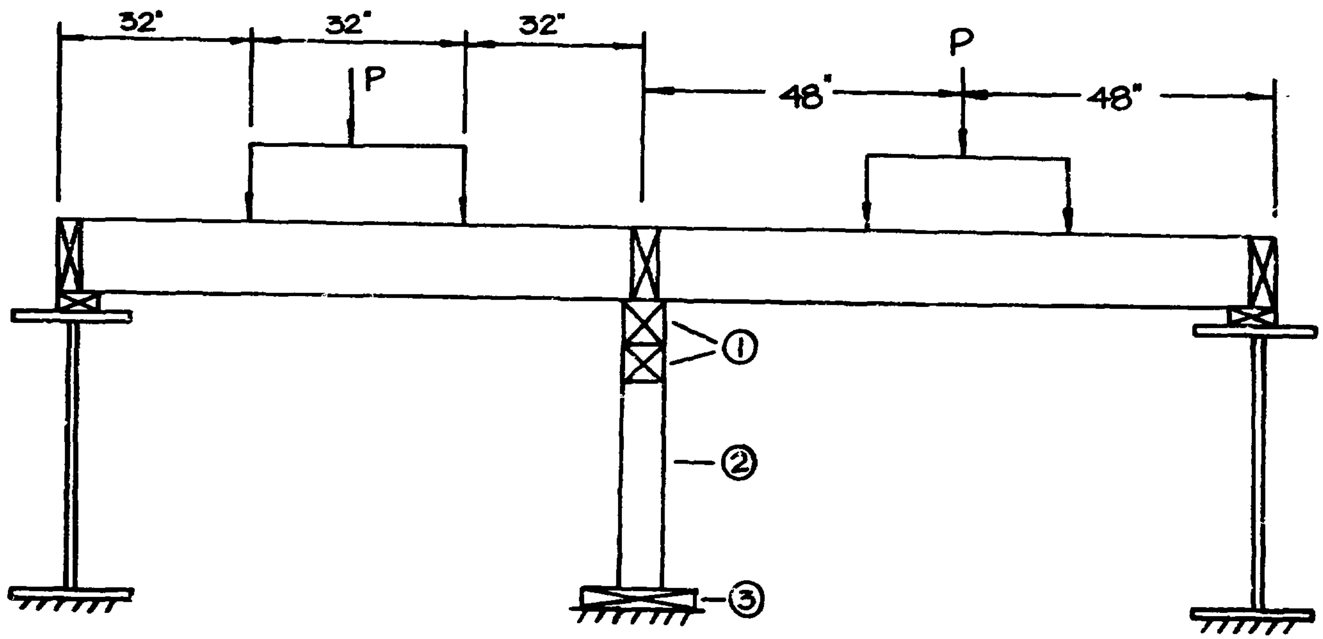

① 4" x 4" x 4' SHORING SUPPORT
② 2 - 4" x 4" x 4' SHORE
③ 2" x 10" BLOCK

Fig. A-37. Test Arrangement for Floor Panel 2.

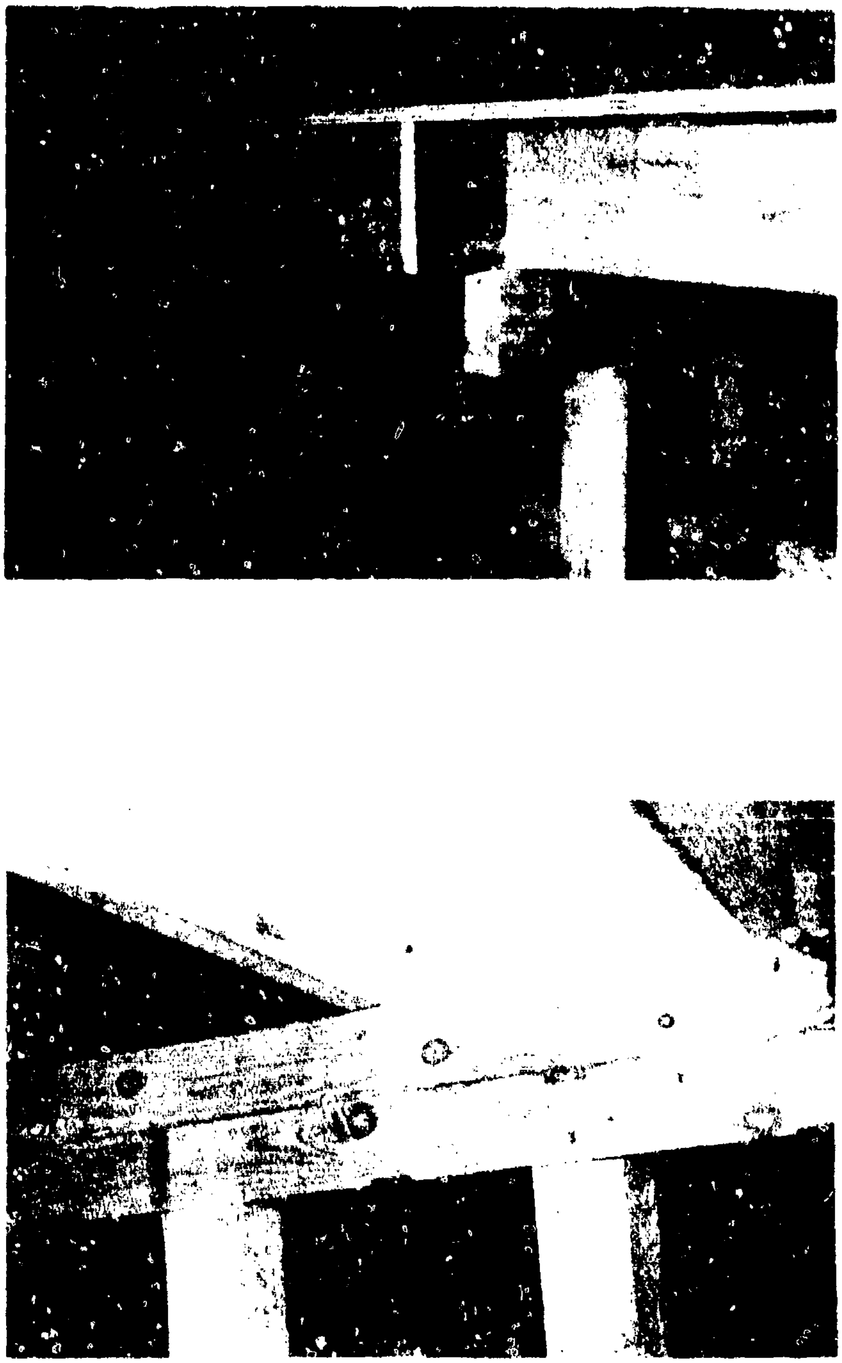

Fig. A-38. Shoring Detail Photographs.

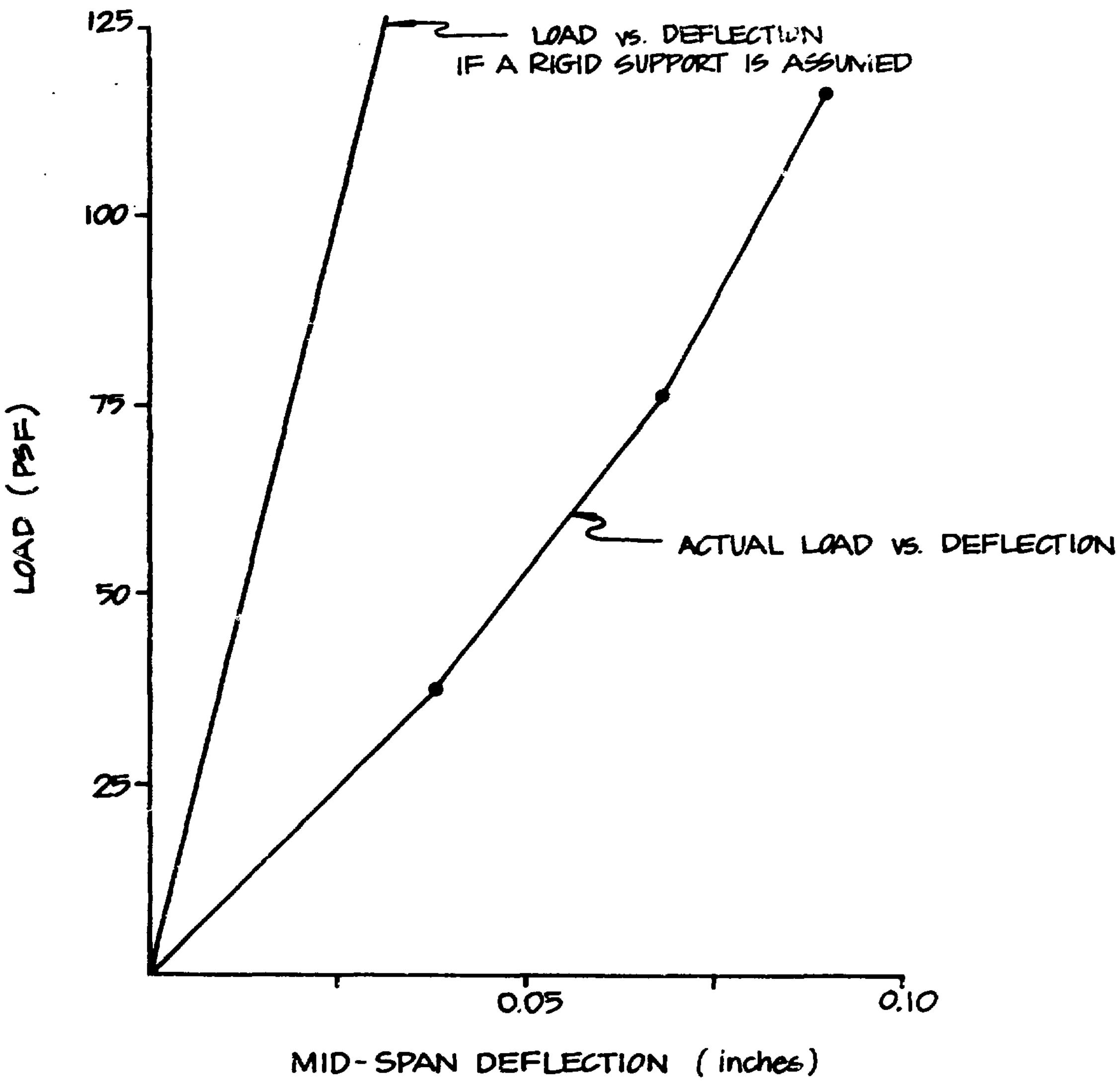

Fig. A-39. Load vs Deflection for Floor Panel 2.

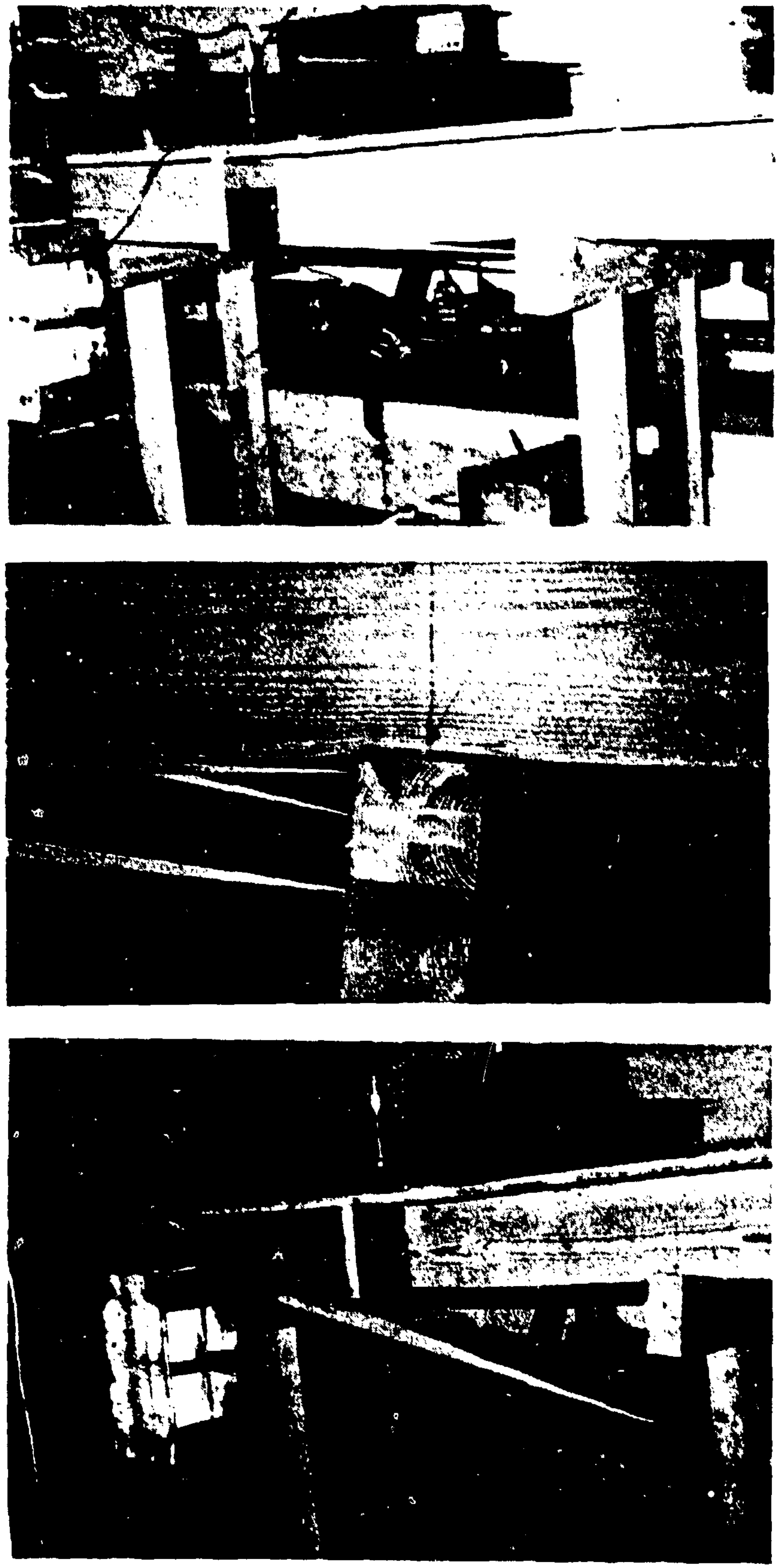

Fig. A-40. Post-Test Photographs, Floor Panel 2.

A
B
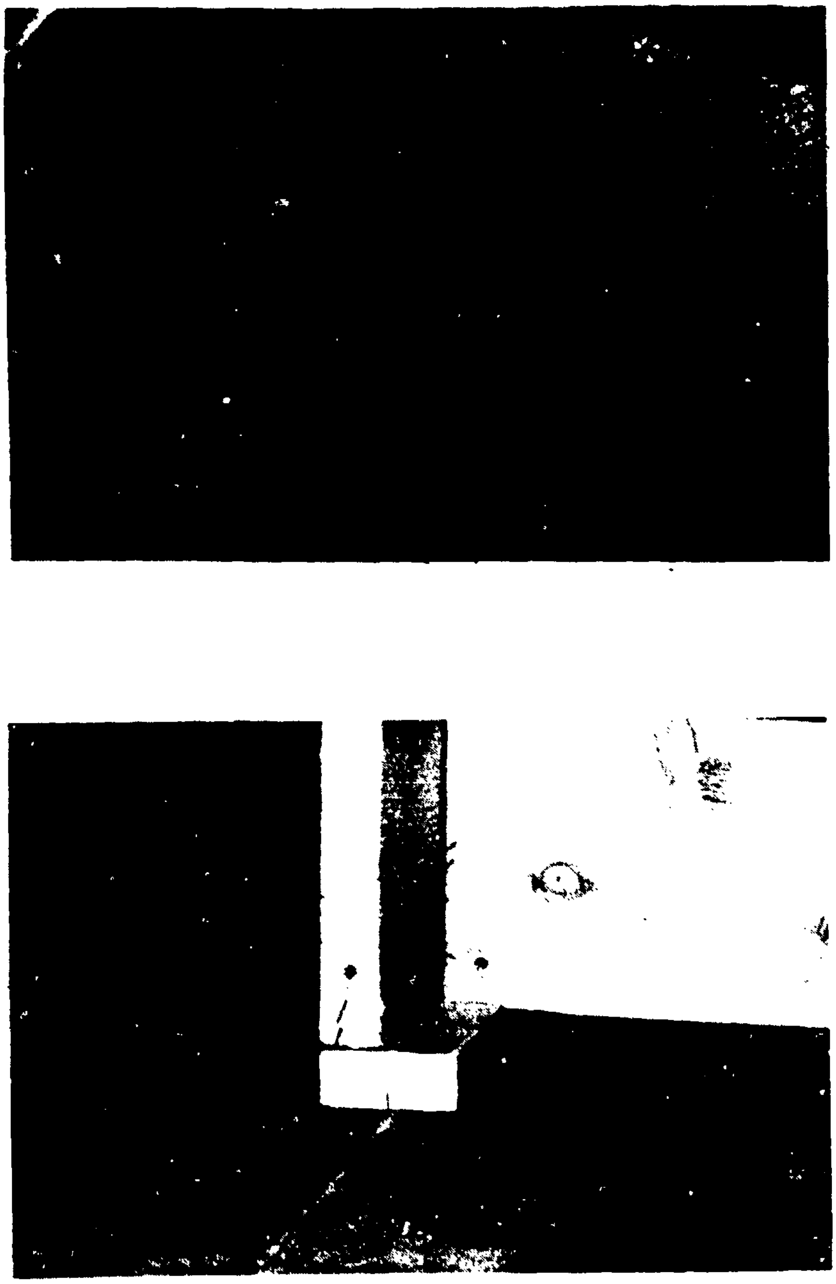

Fig. A-41. Post-Test Photographs, Floor Panel 2.

Test Results - Floor Panel 10

The load deflection data for Panel 10, with one shore, is presented in Fig. A-42. This panel failed at an ultimate load of 1,240 psf, which is 31 times larger than the design live load. A flexural crack occurred at a knot, approximately at the quarter point, on the front joist (see Fig. A-43). This allowed the shoring to rotate and ultimately kick out. Once the shoring kicked out the front joist failed at midspan. Local bearing failures also occurred at the end and center supports as shown in Fig. A-44.

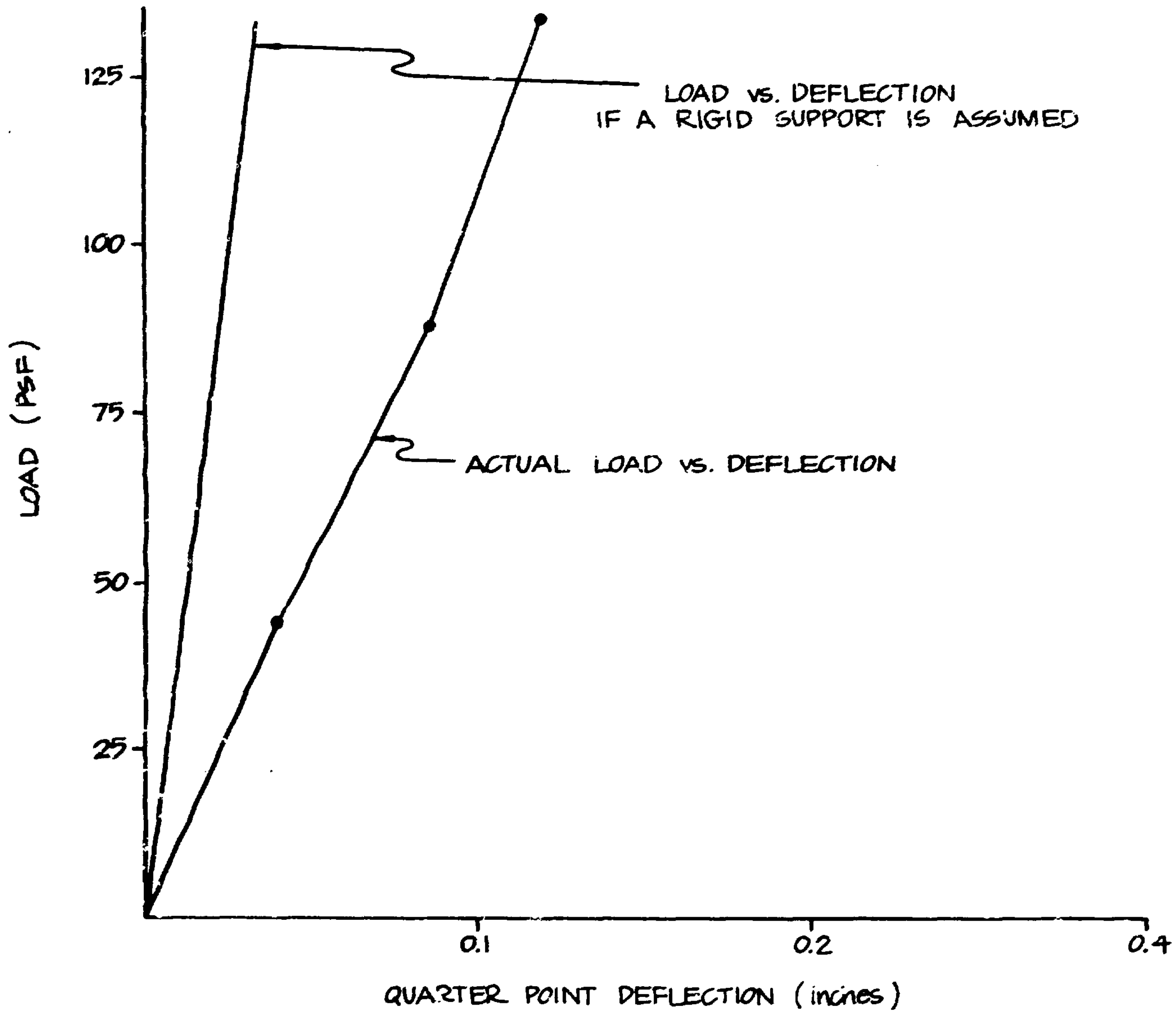

Fig. A-42. Load vs Deflection Data for Floor Panel 10.

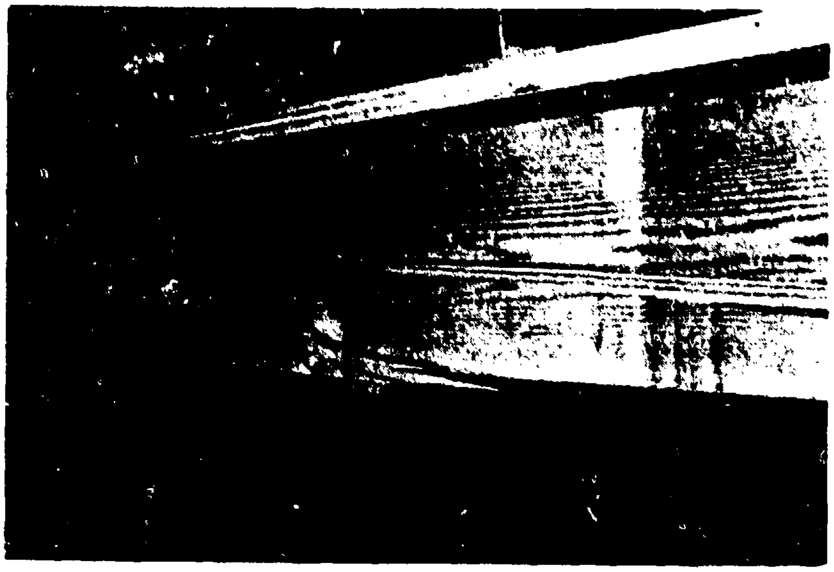

Fig. A-43. Post-Test Photographs, Floor Panel 10.

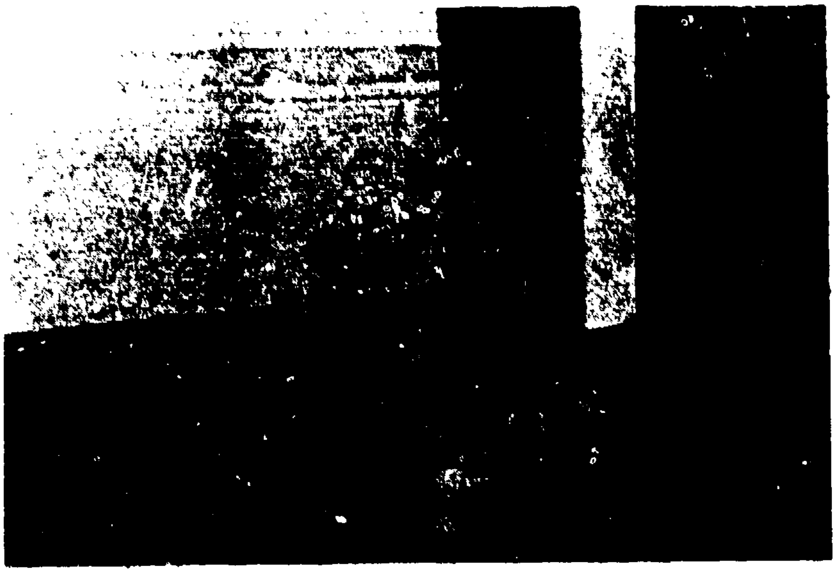

Fig. A-44. Post-Test Photographs, Floor Panel 10.

KING POST TRUSS FLOOR PANELS 7, 8 AND 11

Construction Details Floor Panels 7 and 8

For floor Panels 7 and 8 a king post truss system utilizing three reinforcing rods was used. Construction details and photographs of this system are presented in Figs. A-45 through A-48.

To enable load deflection predictions to be made on the floor system a separate test was conducted on the shear plate, holddown and rebar system. The arrangement can be seen in Fig. A-49. Two tests were conducted and the resulting load vs deflection plots are presented in Fig. A-50. The post-failure photographs of the holddowns, rebar, and shear plate can be seen in Fig. A-51.

Test Results - Floor Panel 7

Floor Panel 7 was tested with 780 lb pre-tension on each of the rebars. Under the static loading the deflection, as shown in Fig. A-52, was about 16% larger than would be predicted from the pull tests described earlier. This occurred because the pull test did not account for the bending of the rebar at the support post shown in the sketch below.

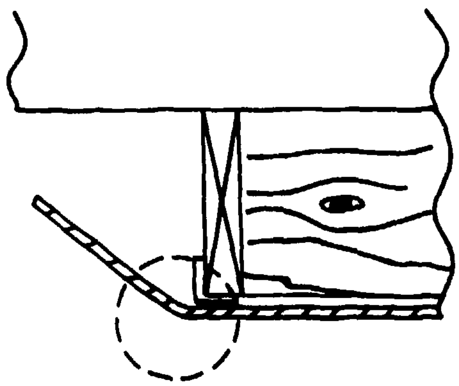

Apparently a much larger pre-stress load will be required to correctly form the bend at this point.

The ultimate load to failure for this panel was 411 psf, or about 10 times the design live load. The back joist failed first, as shown in the sketches in Fig. A-53. Also shown in this figure are the failures that occurred in the middle and front joists. Post-test photographs are shown in Fig. A-54, A-55, and A-56.

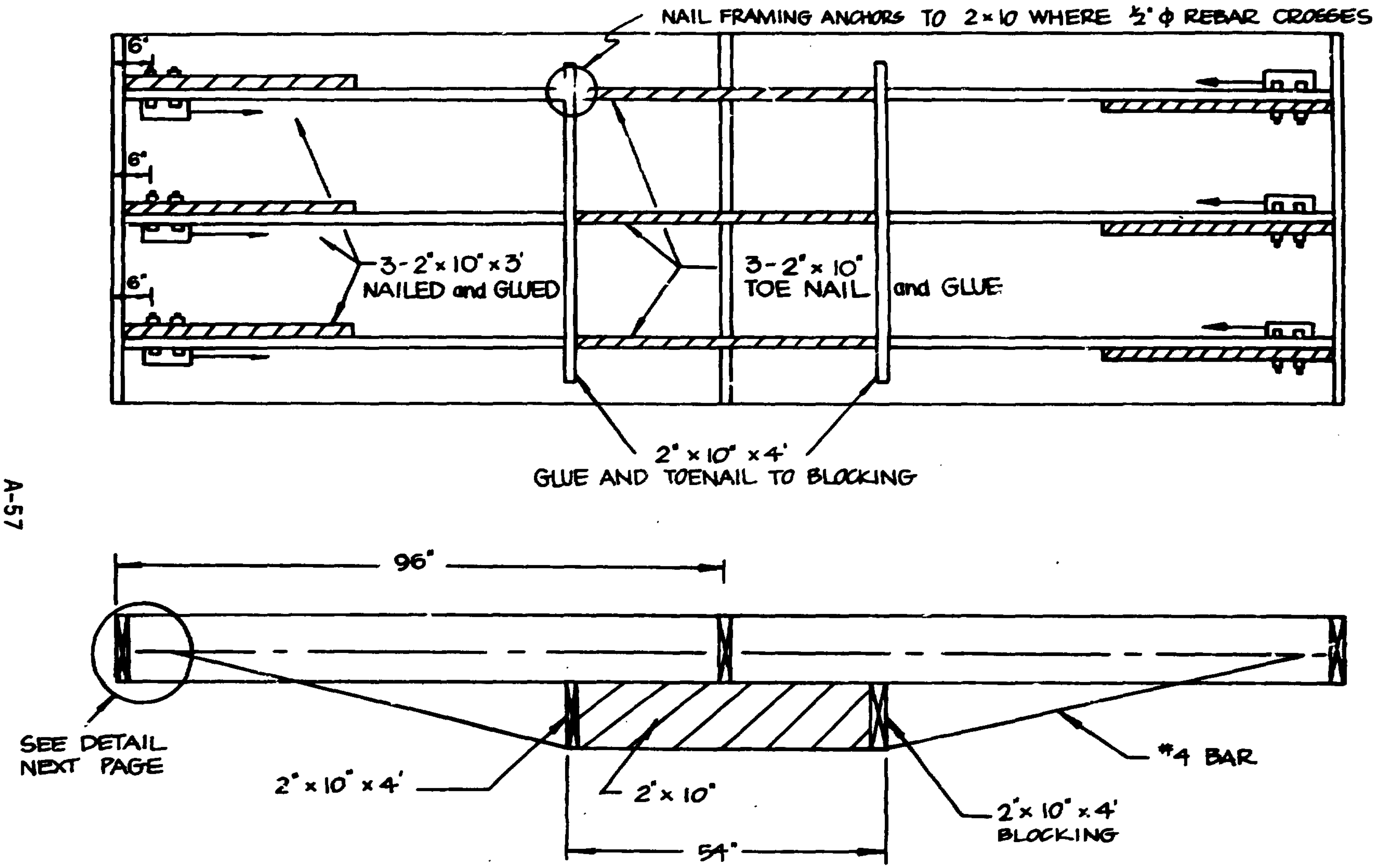

Fig. A-45. Construction Details, Floor Panels 7 and 8.

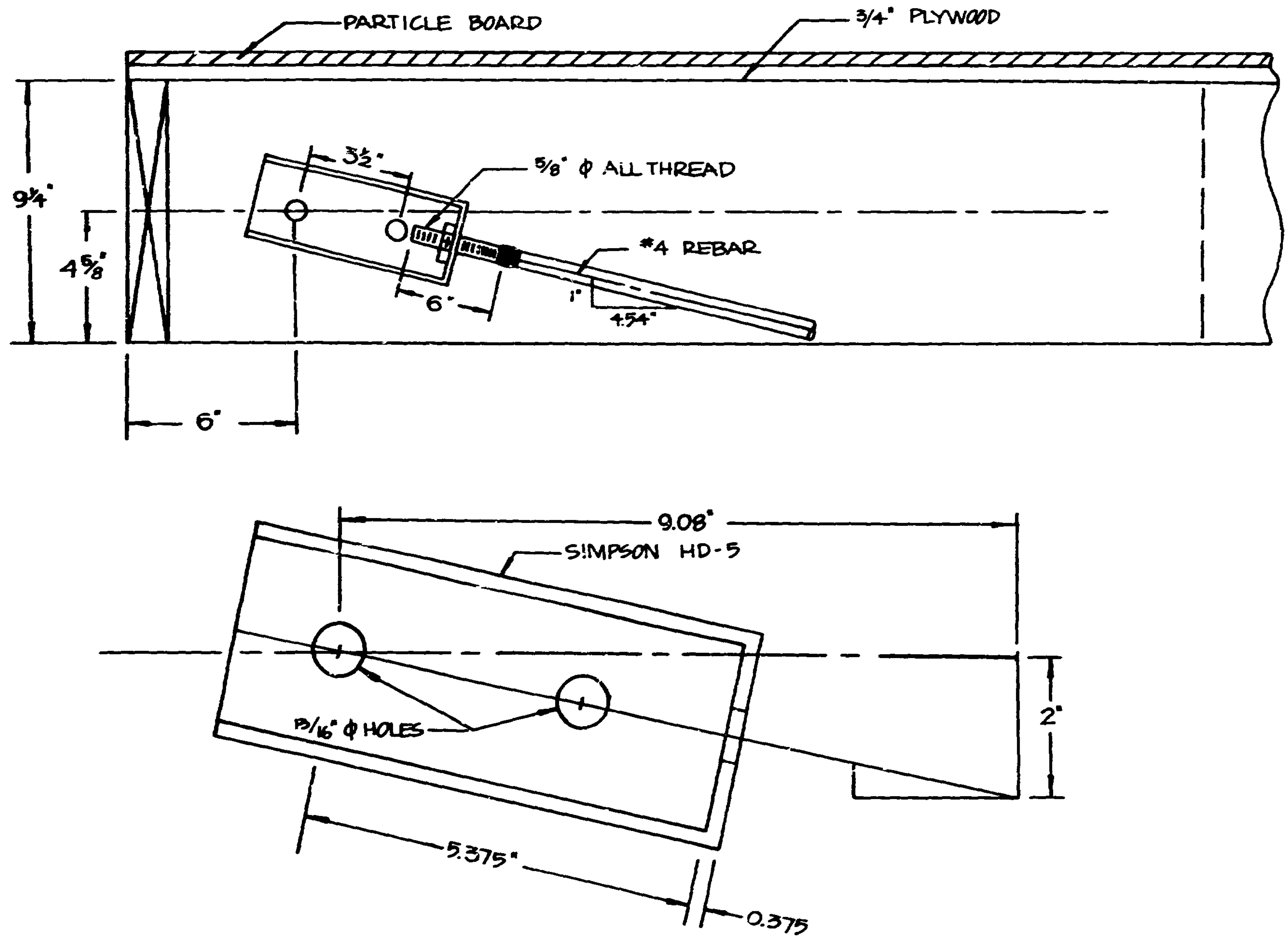

Fig. A-46. Construction Details — Rebar and Connections, Floor Panels 7 and 8.

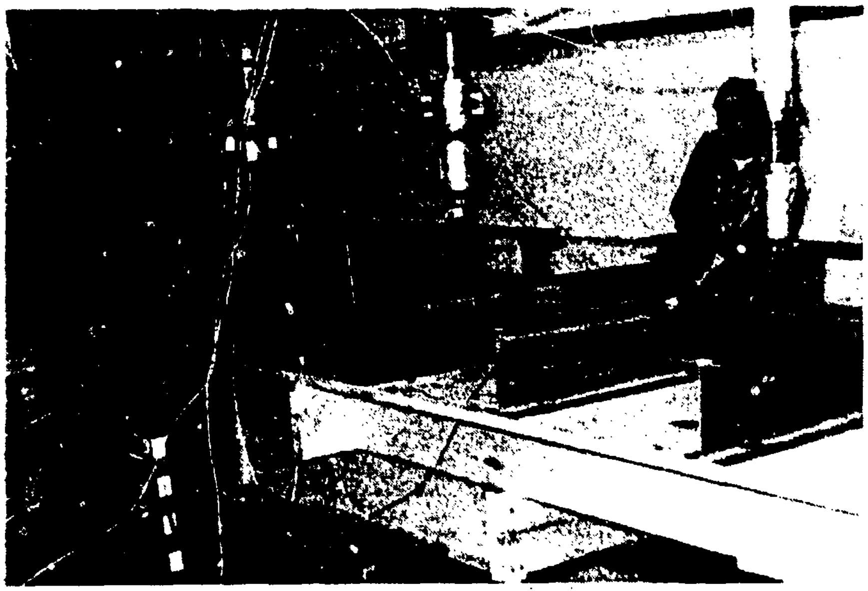

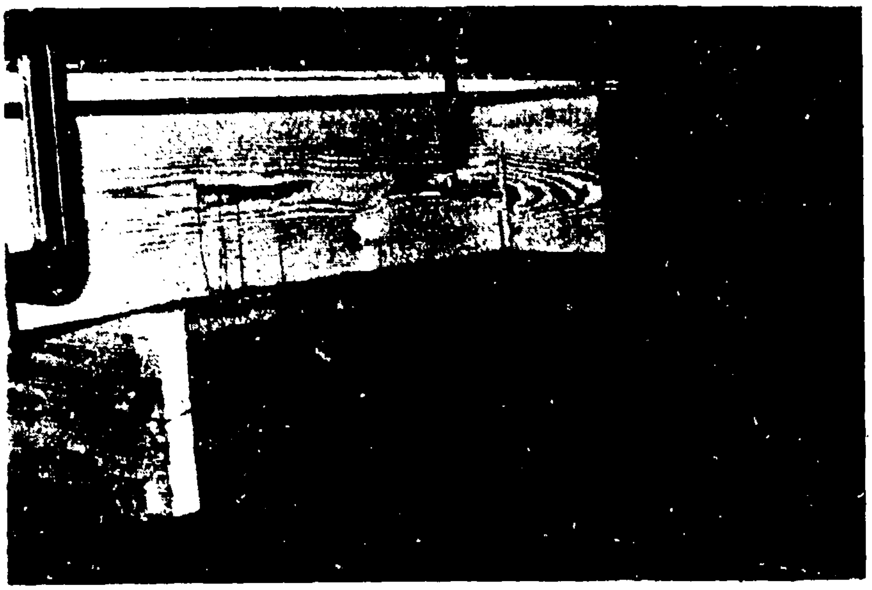

Fig. A-47. Pre-Test Photographs, Floor Panel 7.

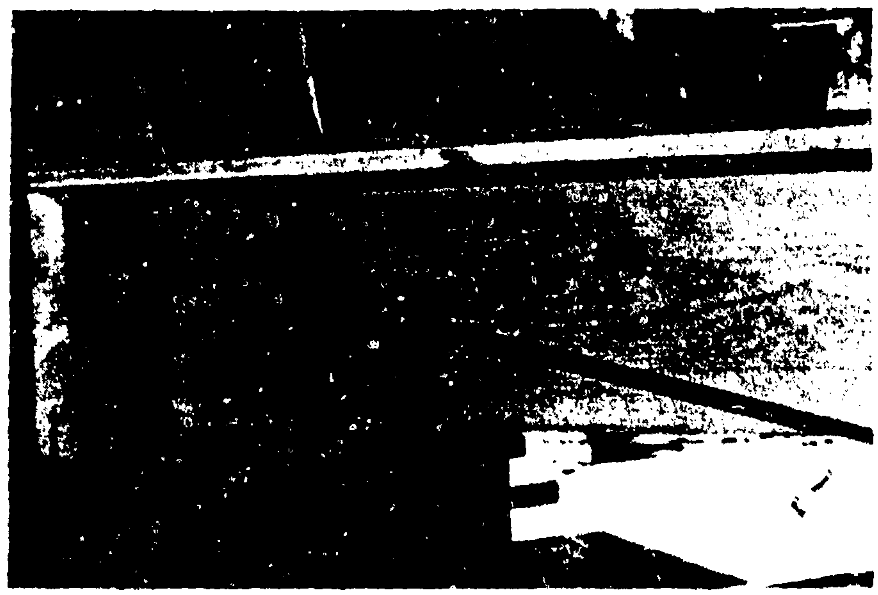

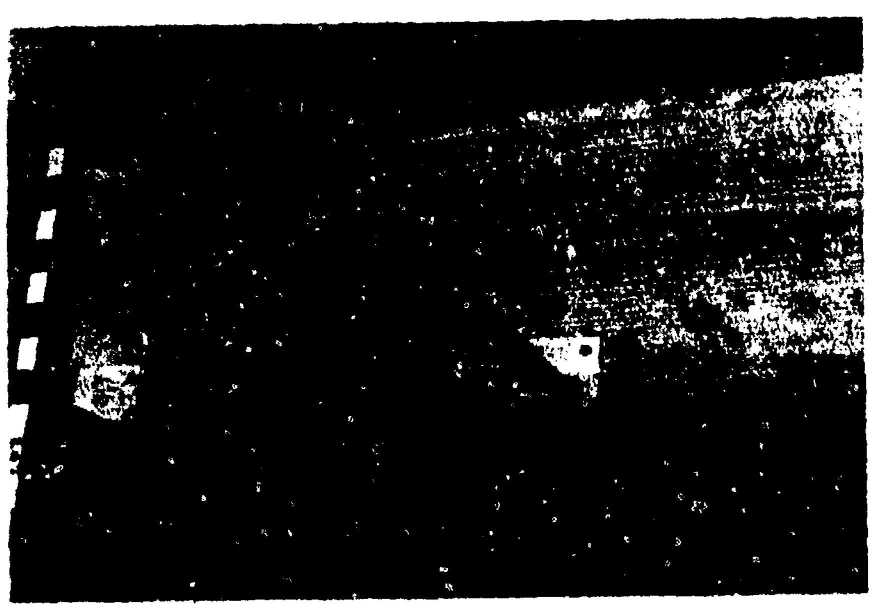

Fig. A-48. Photographs of Construction Details, Floor Panel 7.

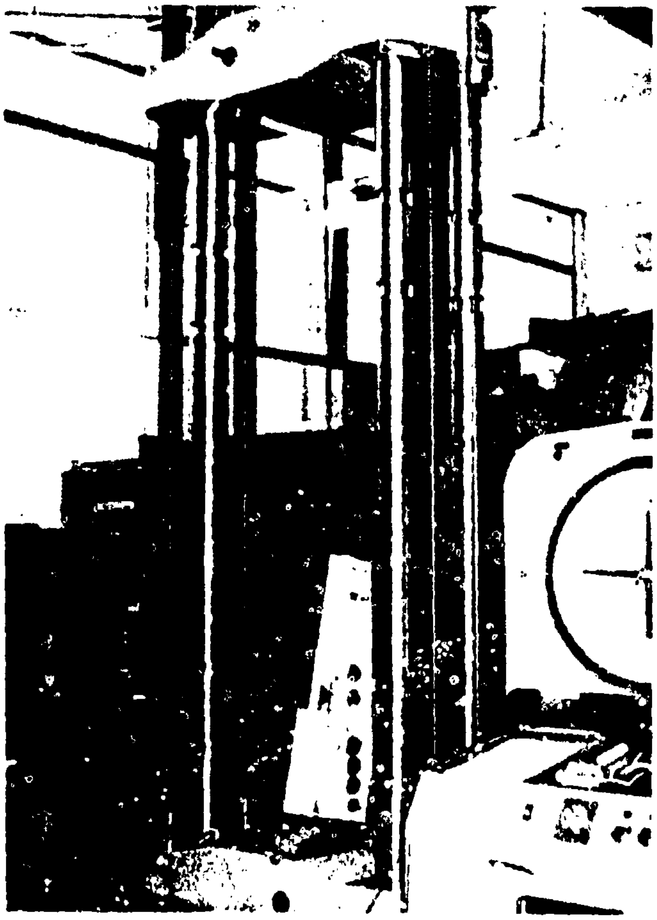

Fig. A-49. Test Arrangement — King Post Truss and Connection Test.

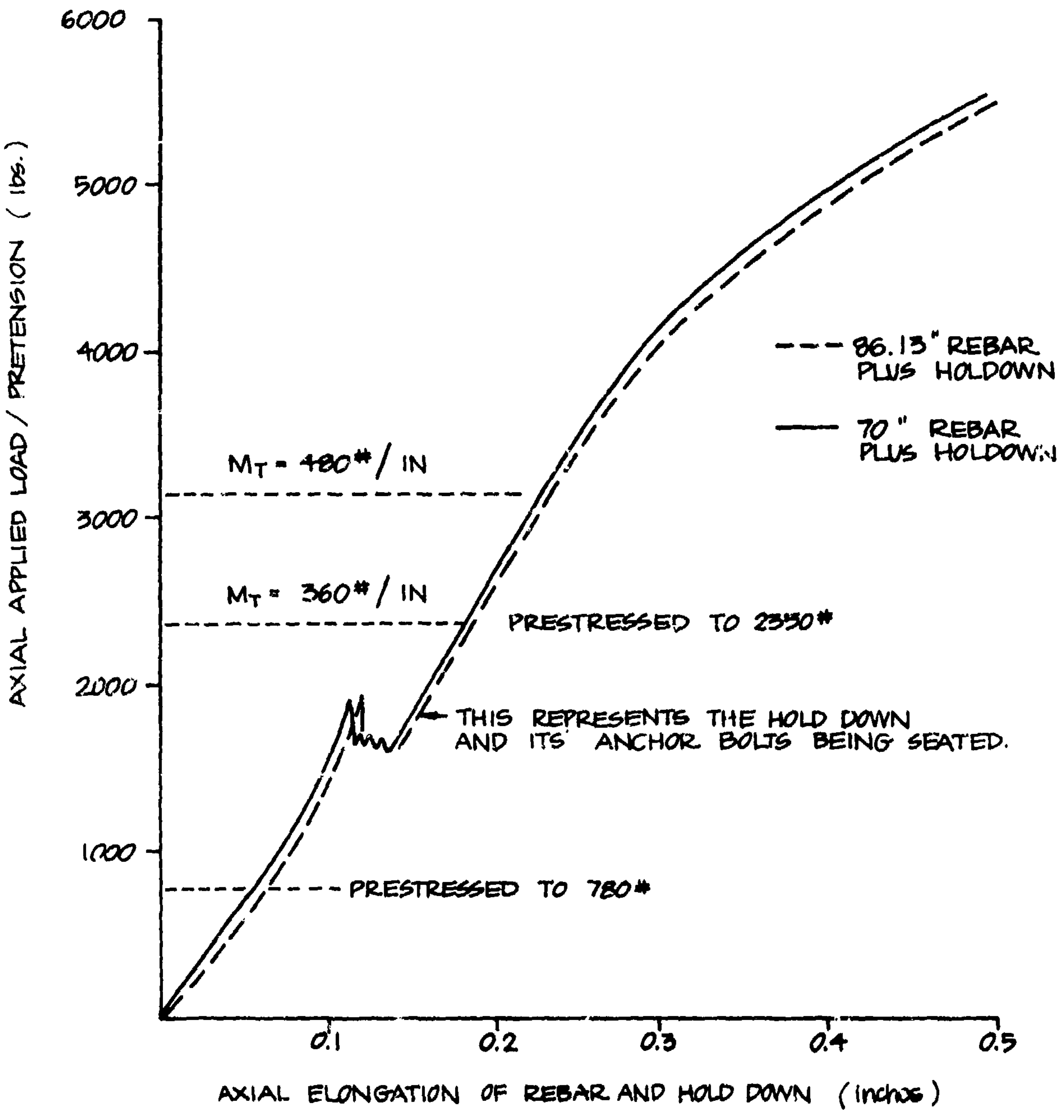

Fig. A-50. Load vs Deflection Data for King Post Truss and Connection Tests.

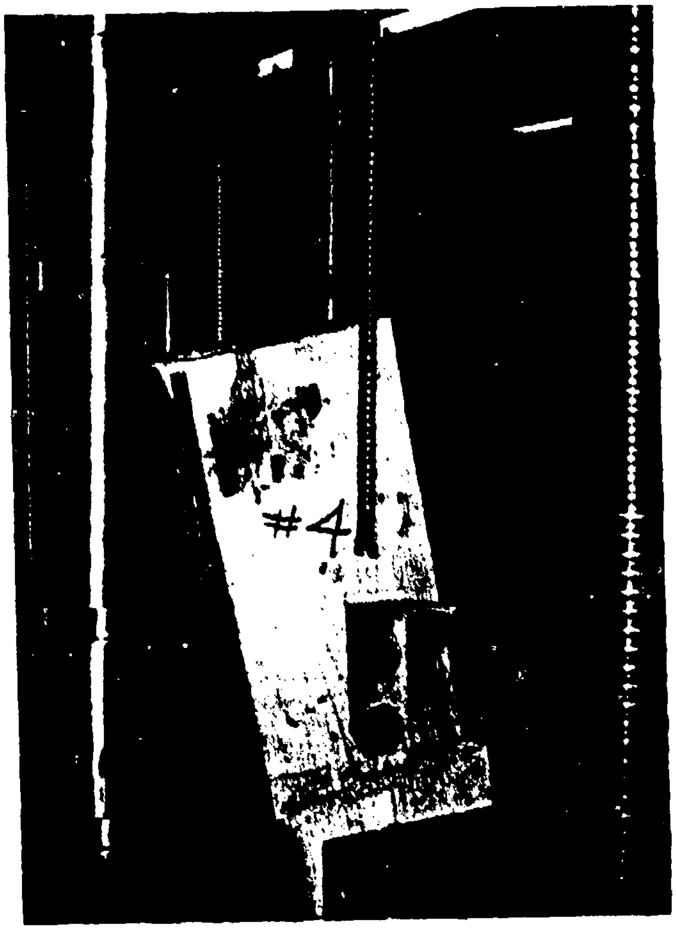

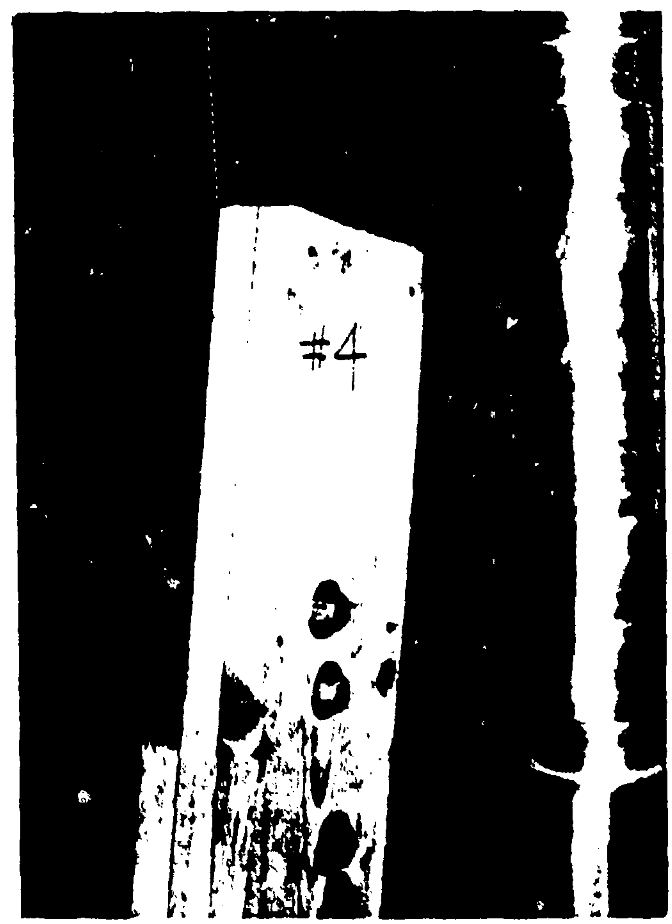

Fig. A-51. Post-Test Photographs, King Post Truss and Connection Tests.

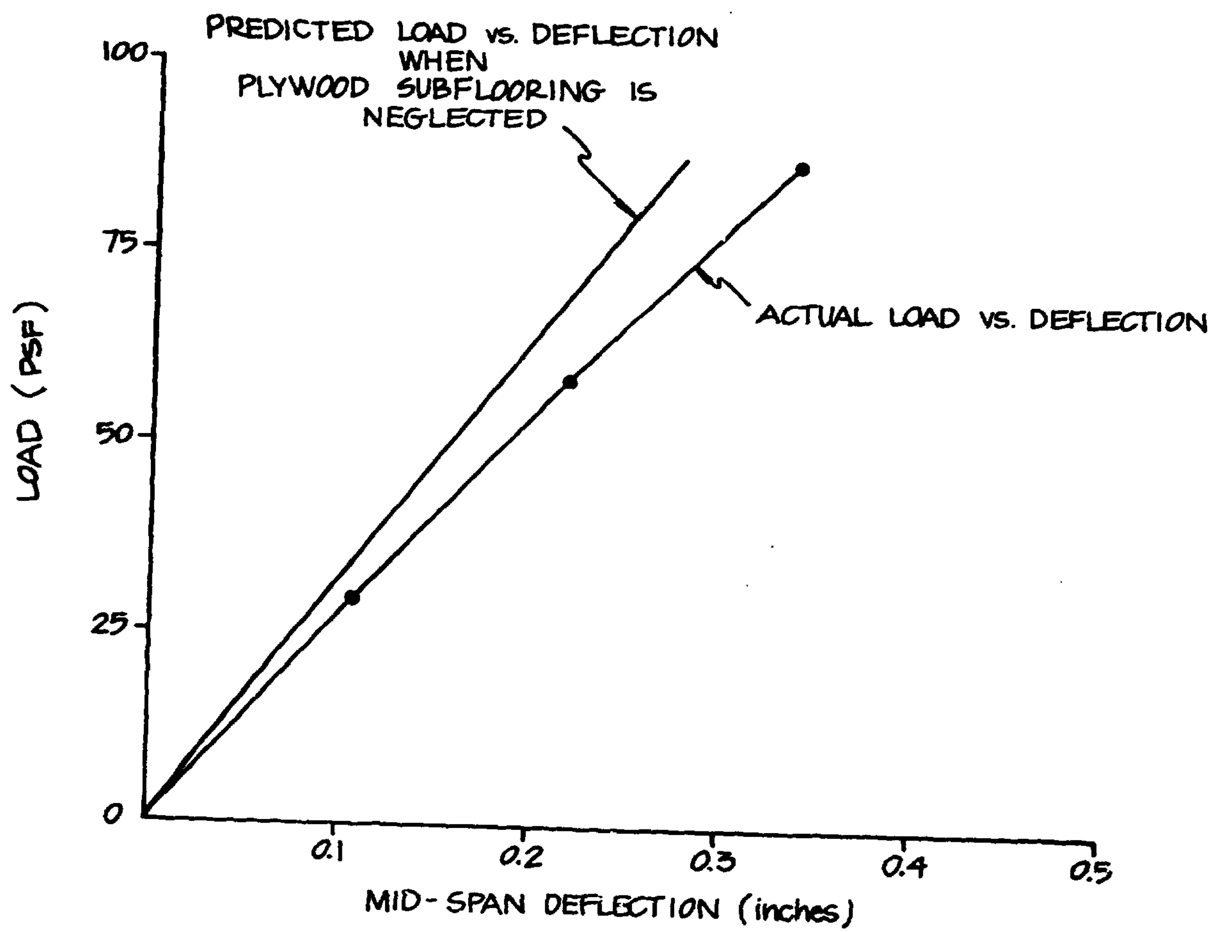

Fig. A-52. Load vs Deflection Data for Floor Panel 7 with Rebars Pre-Tensioned to 780 lbs Each.

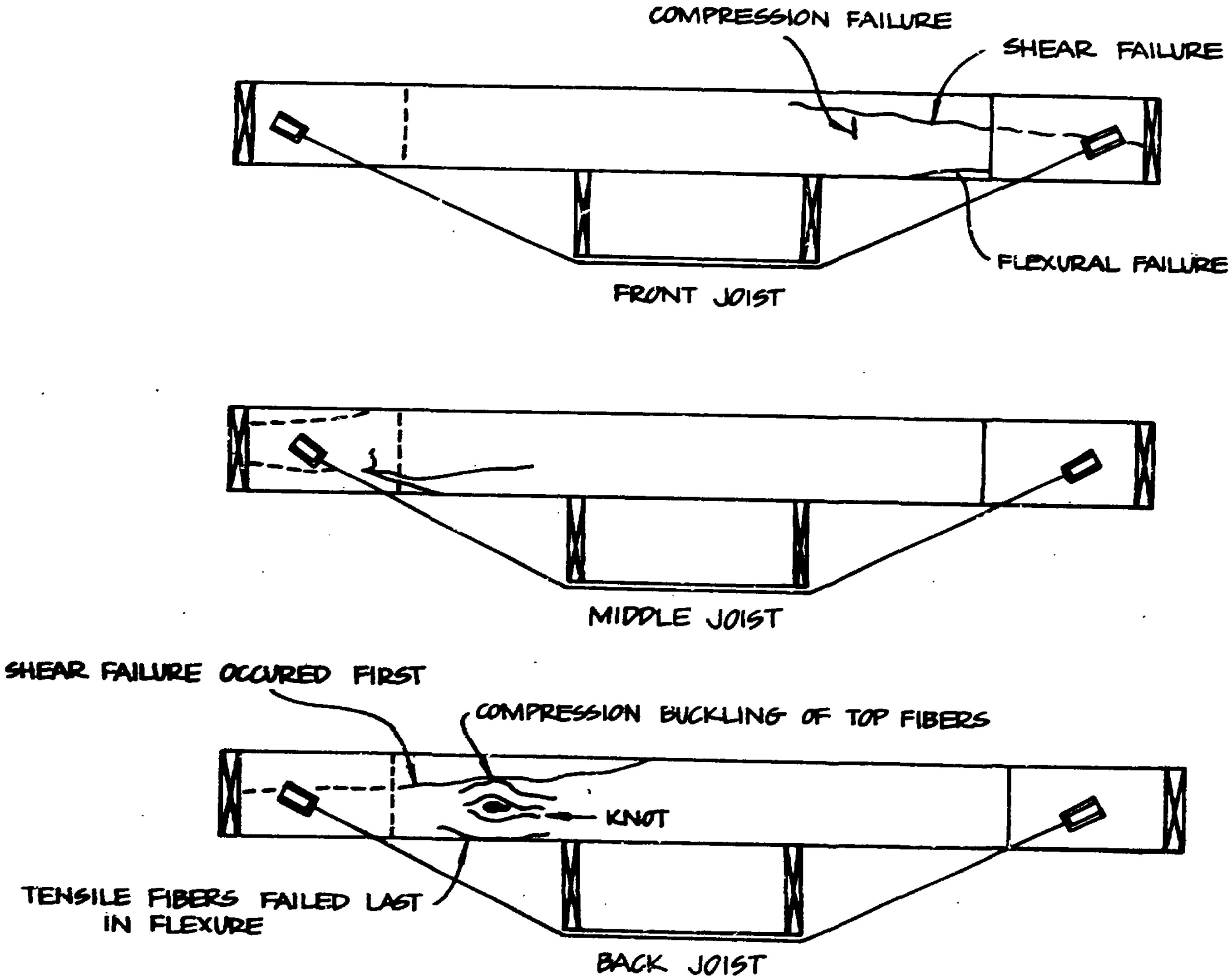

Fig. A-53. Sketch of Failures of Floor Panel 7.

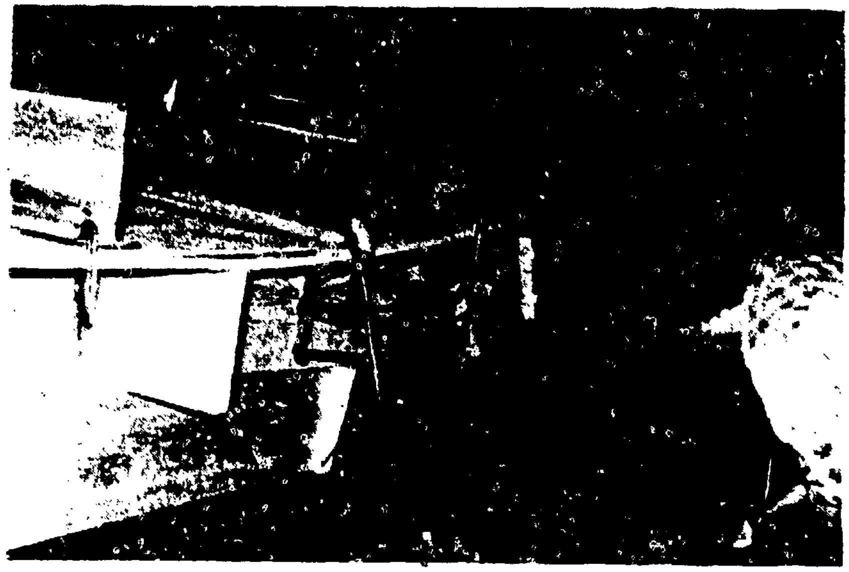

A. Back Joist

B. Back Left Support Joist

Fig. A-54. Post-Test Photographs, Floor Panel 7.

A. Back Joist, Left Support

B. Back Joist Center.

Fig. A-55. Post-Test Photographs, Floor Panel 7.

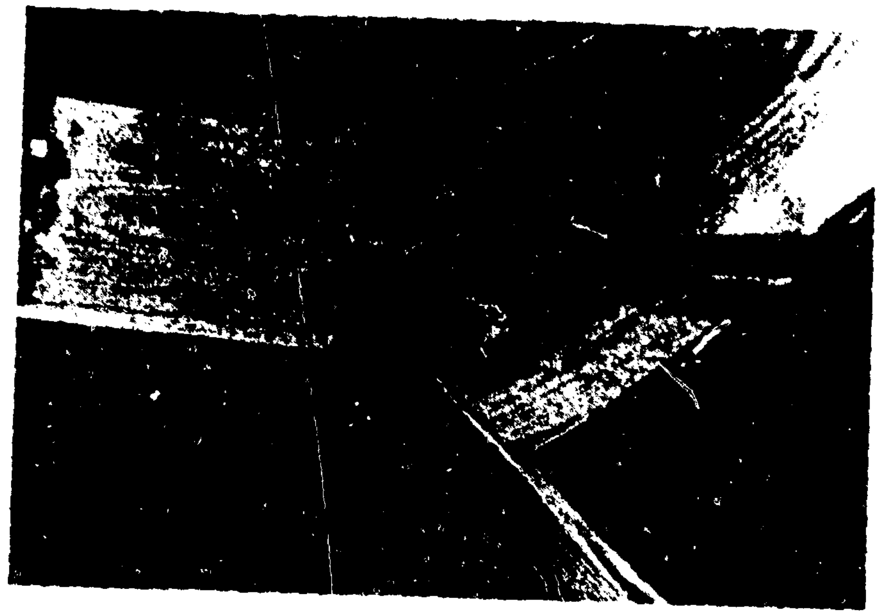

A. Middle Joist, Left Support

B. Front Joist, Right Support

Fig. A-56. Post-Test Photographs, Floor Panel 7.

Test Results - Floor Panel 8

Panel 8 differed from Panel 7 only in the amount of pre-tension applied to the rebar at the holddown. Panel 7 was tested with 780 lb of pre-tension and Panel 8 was statically tested at 1,560 lb, 2,180 lb, and 3,140 lb of pre-tension. The load-deflection data for this last test are presented in Fig. A-57; 3,140 lb was then used for the ultimate load test.

The ultimate failure load of this panel was 636 psf, or about 16 times design live load. The rear joist failed at a knot-weakened section, as shown in the photographs in Fig. A-58. There was also a bearing failure at the right support of the rear joist and the holddown bracket was distorted. The rear joist also had a localized flexural failure to the left of midspan. These failures are shown in Fig. A-59. The middle joist failed most dramatically at the right support, as shown in Fig. A-60A. Only minor cracks appeared on the front joist, as shown in Fig. A-60B.

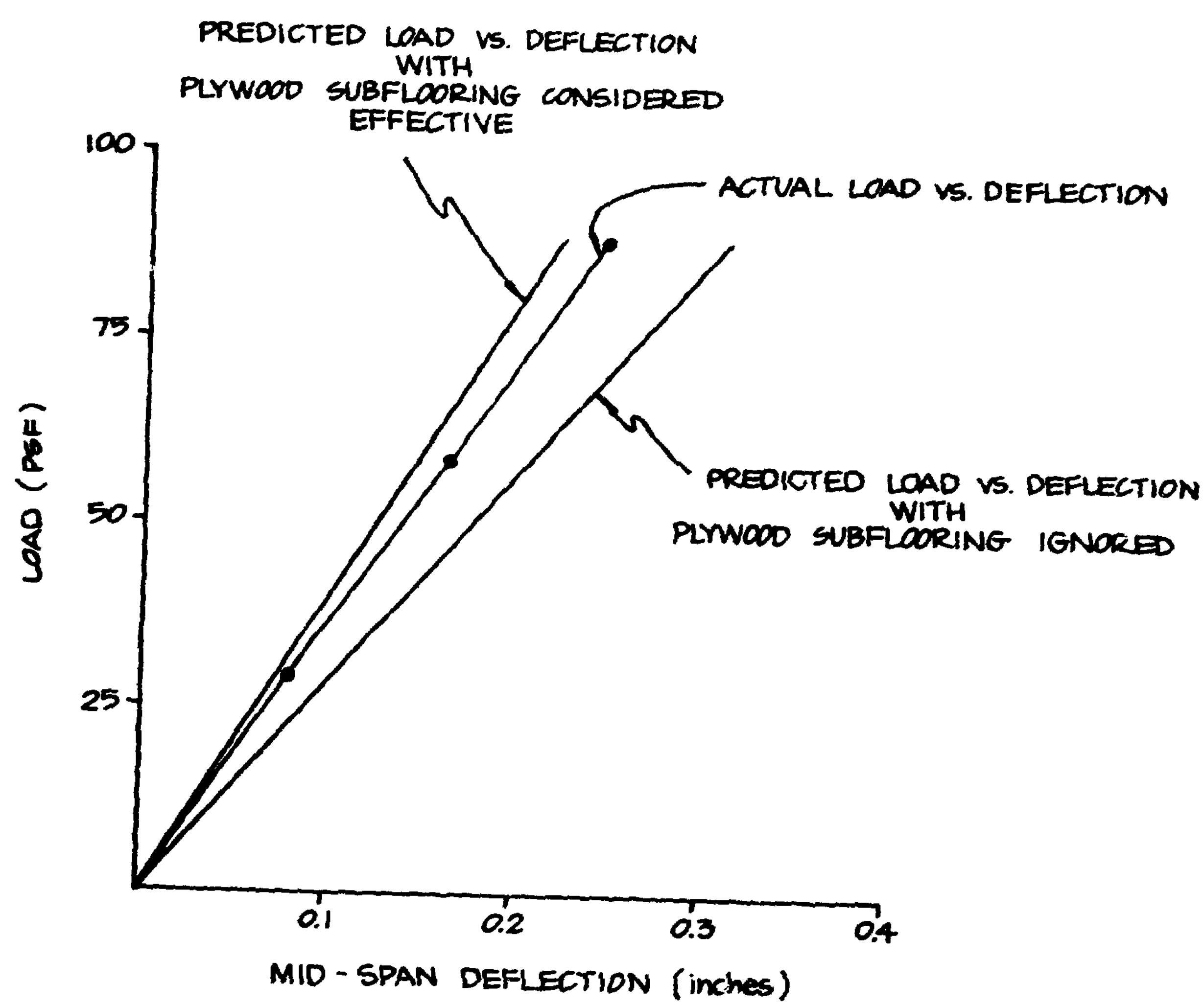

Fig. A-57. Load vs Deflection Data for Floor Panel 8, with the Rebar Pre-Tensioned to 3,140 lb/Rebar.

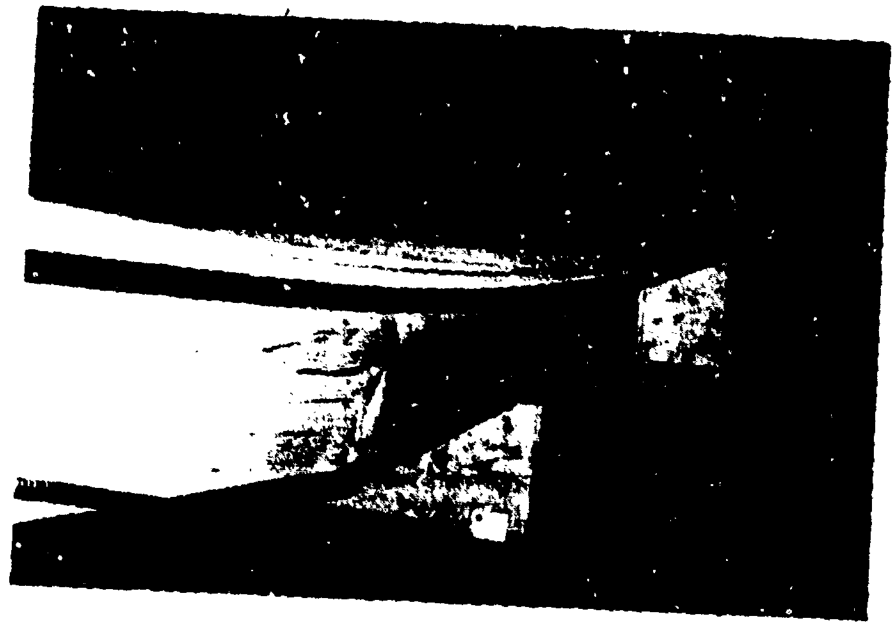

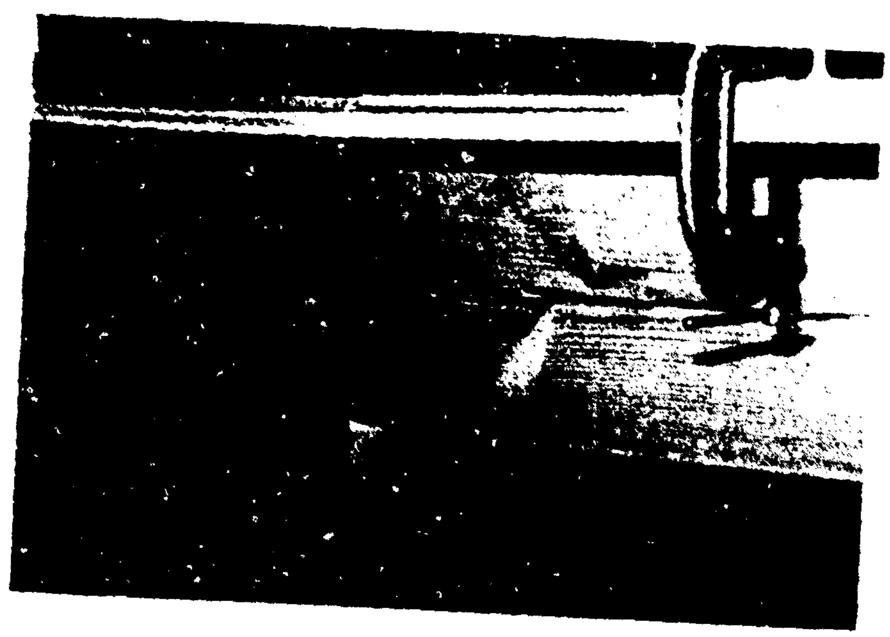

Fig. A-58. Post-Test Photographs, Floor Panel 8.

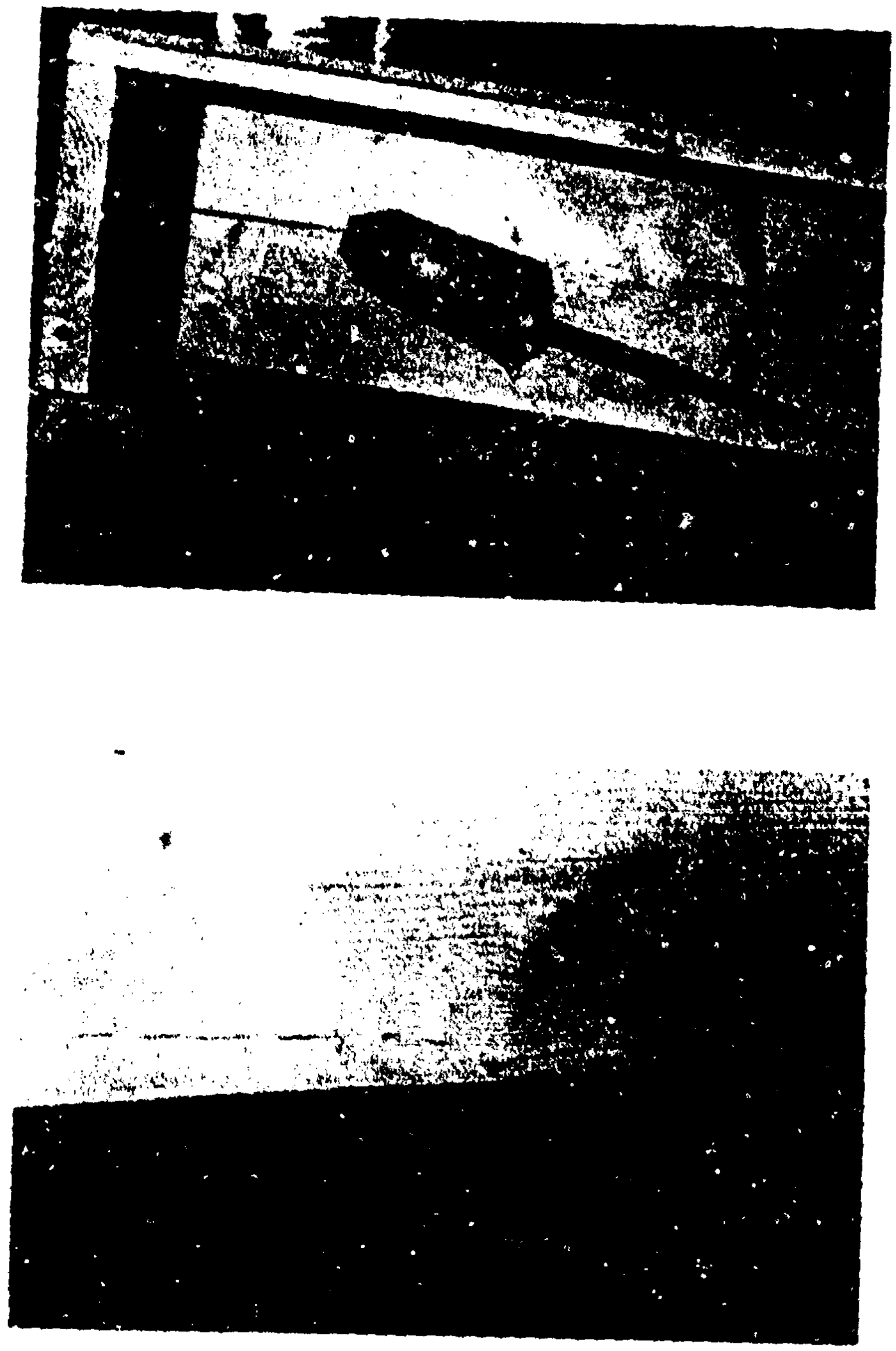

Fig. A-59. Post-Test Photographs, Floor Panel 8.

A

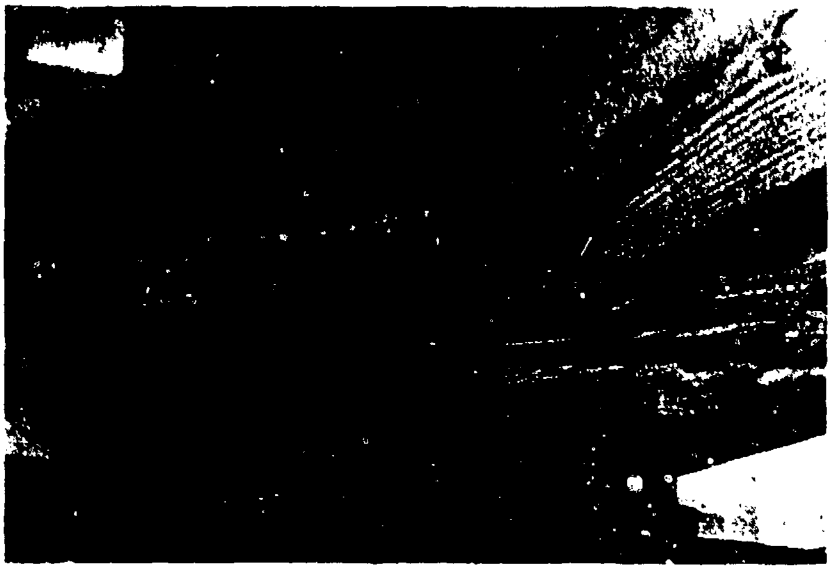

B

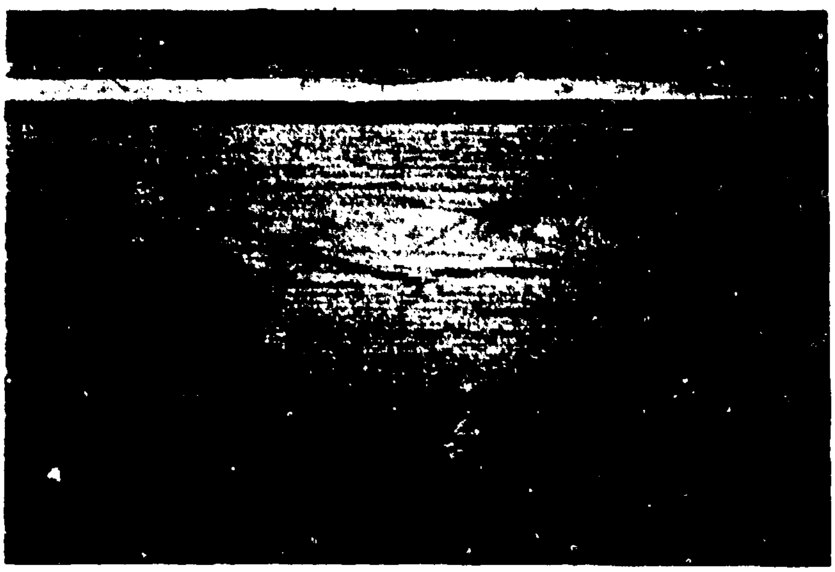

Fig. A-60. Post-Test Photographs, Floor Panel 8.

Construction Details Floor Panel 11

Floor Panel 11 was constructed similar to Panels 7 and 8. The reinforcing bars, however, were replaced with 1/2-in. wire cables which were connected to 1-1/2 in. pipes. Construction details and photographs of this floor system are shown in Figs. A-61 through A-65.

Test Results

The cable supports for floor Panel 11 were pretensioned to 500 lbs. This panel behaved as predicted under static loading as shown in the load vs deflection plot, Fig. A-66.

The ultimate failure load for this panel was 527 psf, or about 13 times the design live load.

The front joist failed in flexure just to the left of the king post frame. A glue line failure also occurred between the king post frame and the floor joist. In addition, two localized failures occurred — a bearing failure at the supports, and at the bearing plates at the end blocks.

Post-test photographs are presented in Fig. A-67.

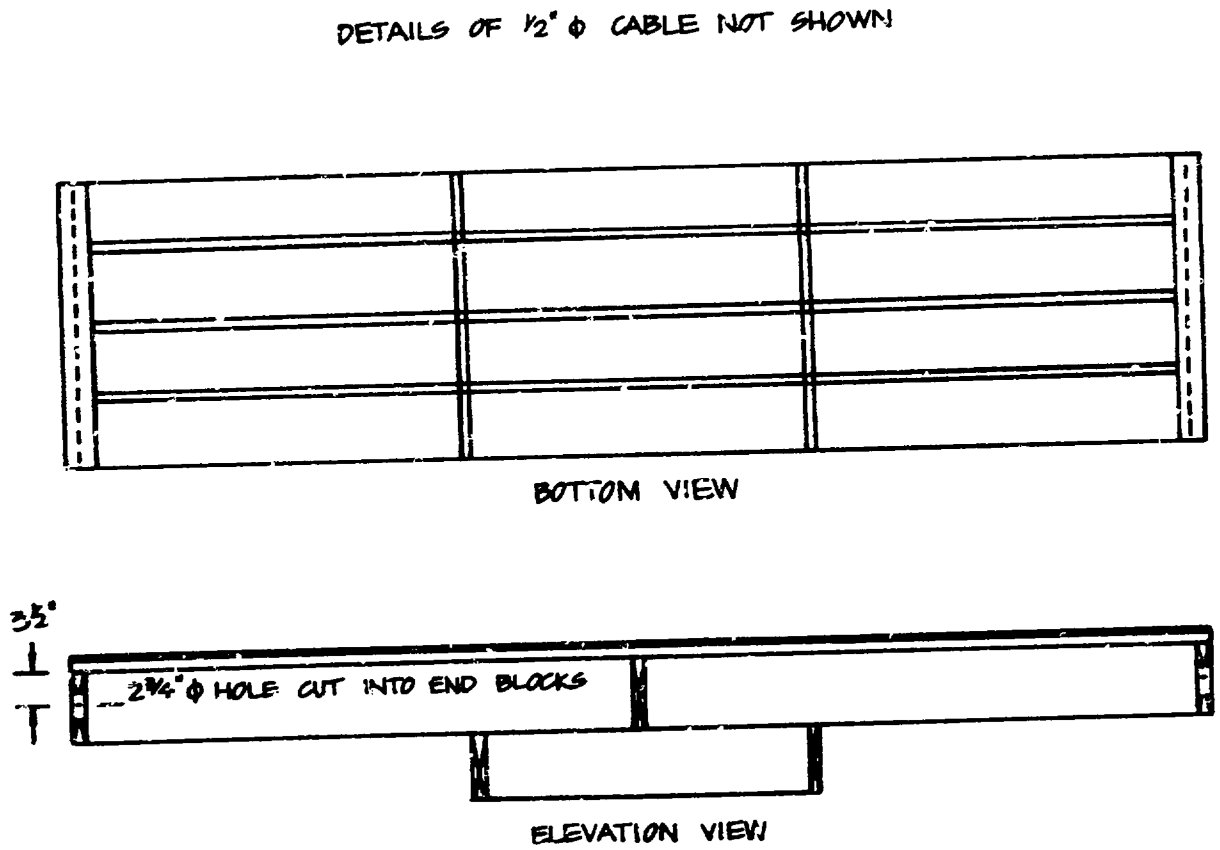

Fig. A-61. Construction Details Floor Panel 11

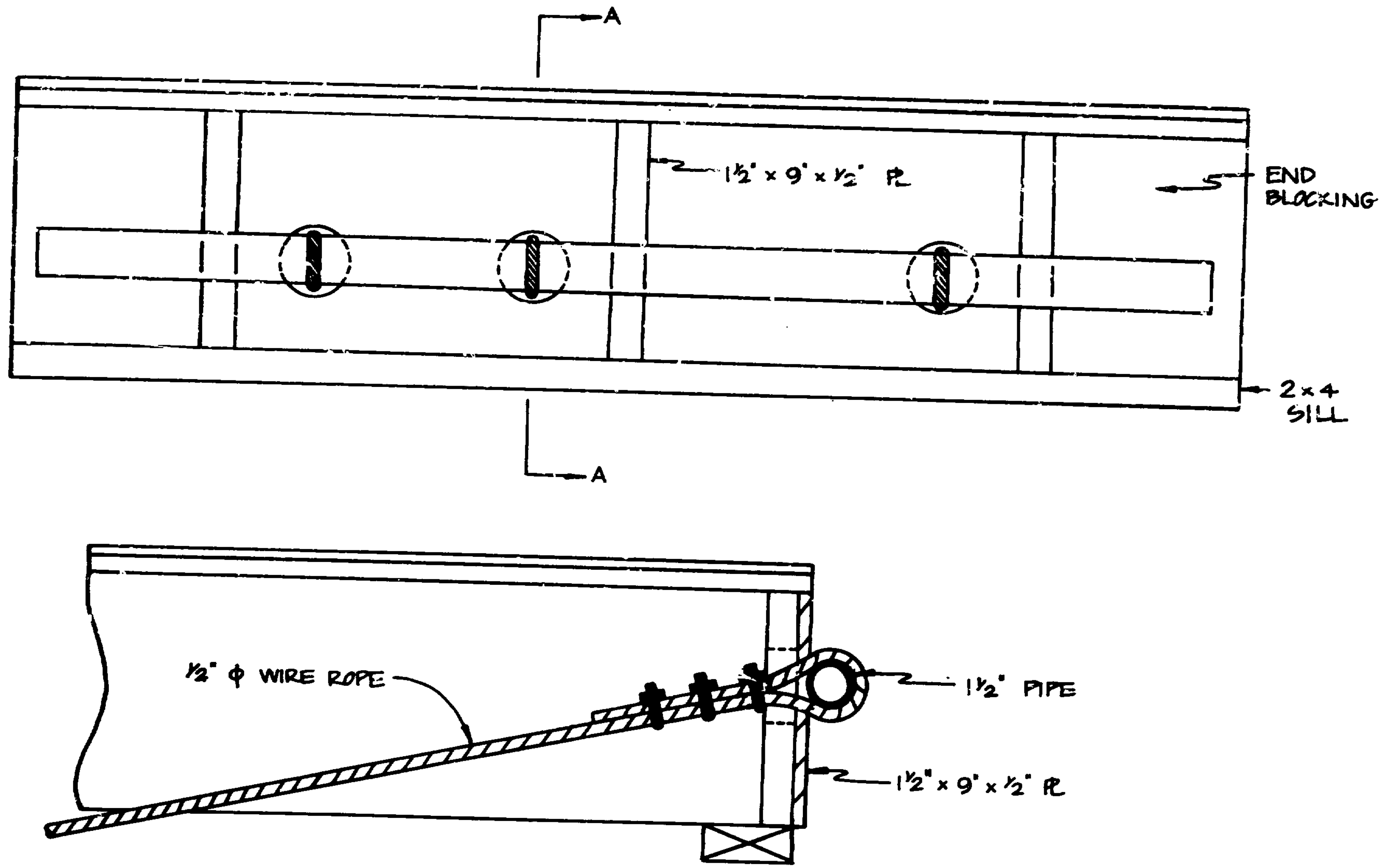

Fig. A-62. Construction Details Floor Plan 11.

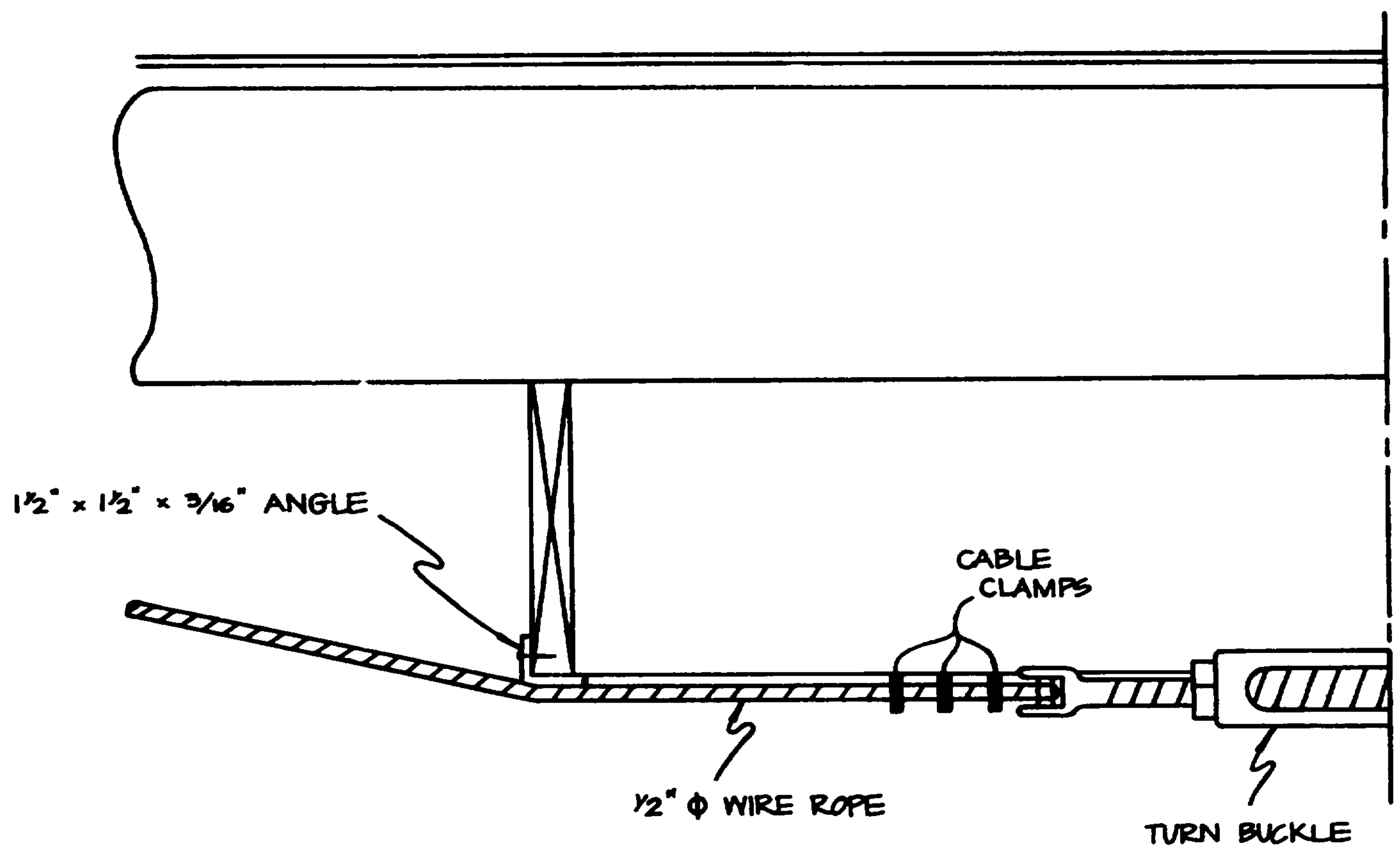

Fig. A-63. Construction Details Floor Plan 11.

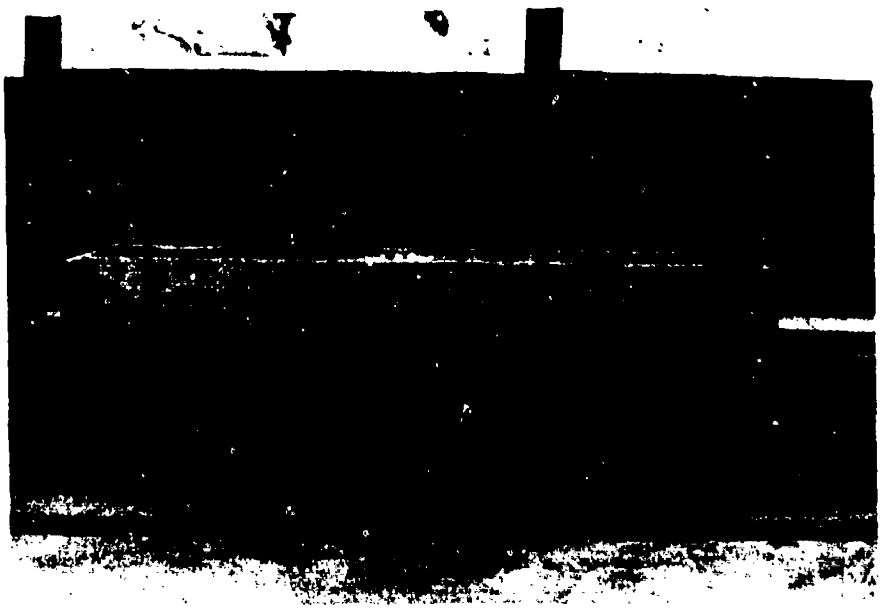

Fig. A-64. Construction Photographs Floor Panel 11.

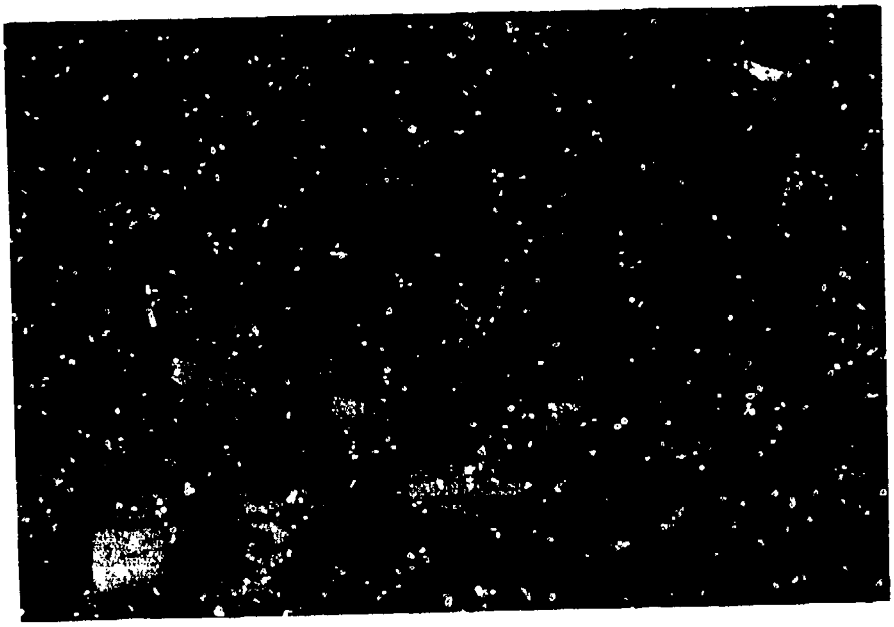

A. King Post Frame Showing Wire Rope Under Floor Panel

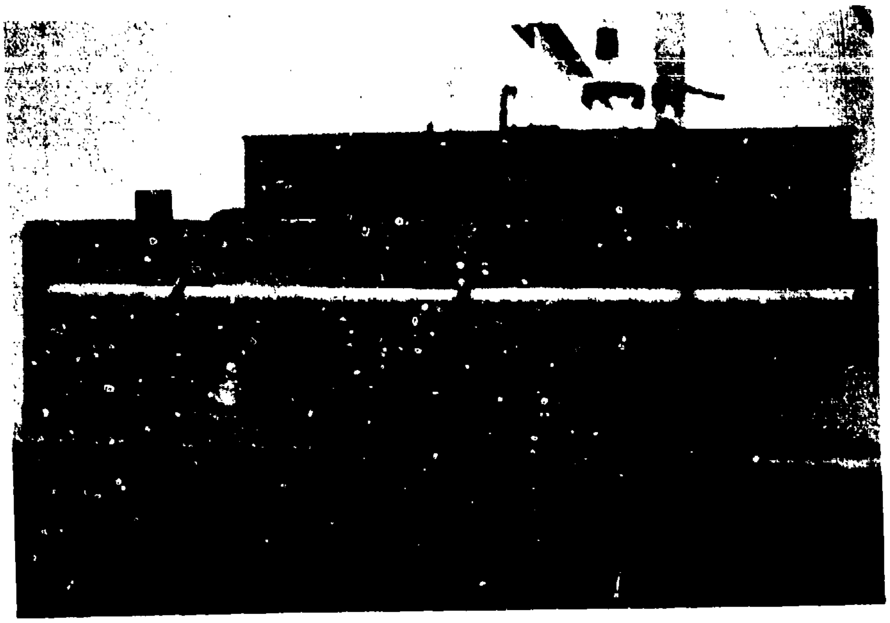

B. King Post Frame, End Connection

Fig. A-65. Construction Photographs Floor Panel 11.

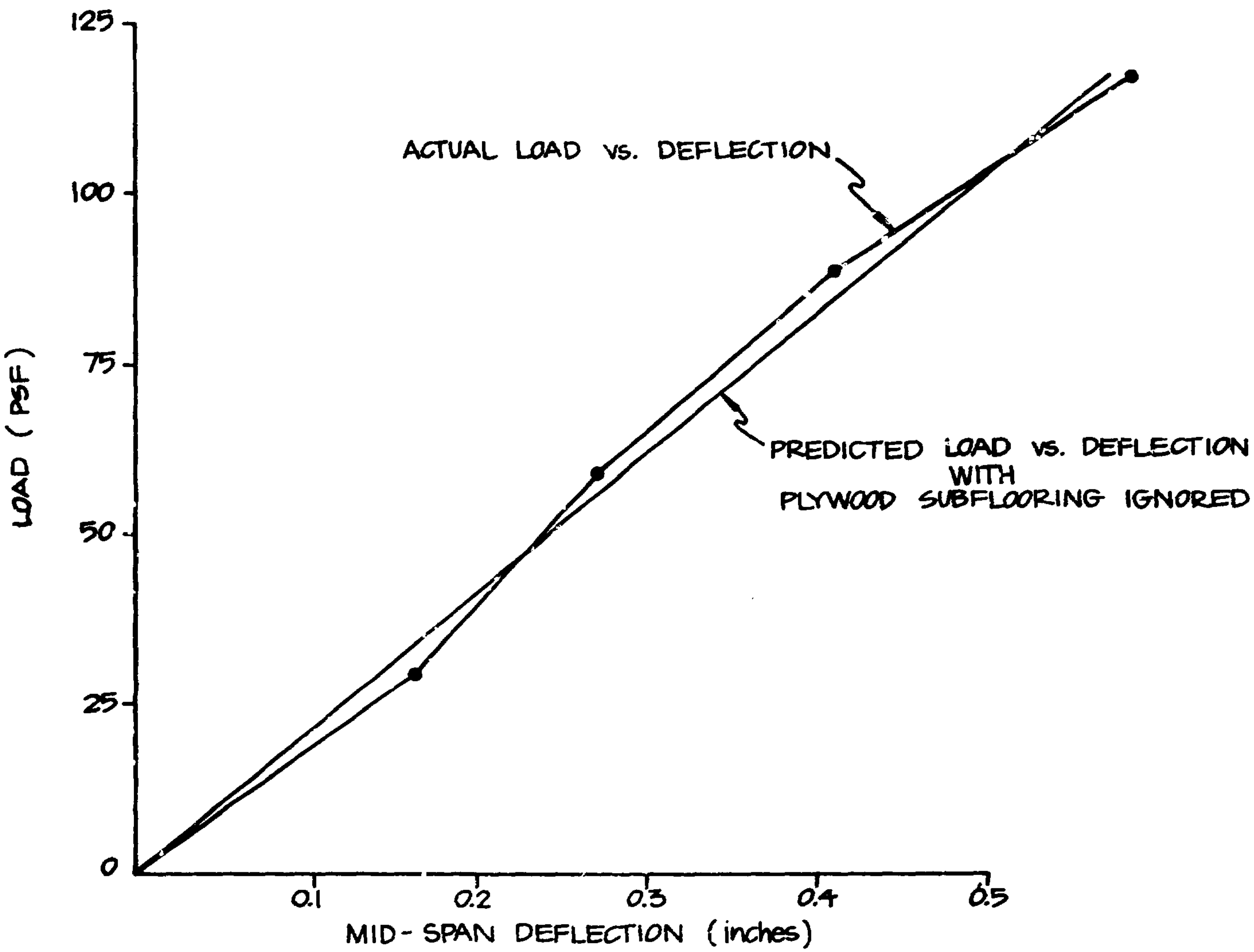

Fig. A-66. Load vs. Deflection Data for Floor Panel 11 with the 1/2" ϕ Cables Postioned to 500 lb each.

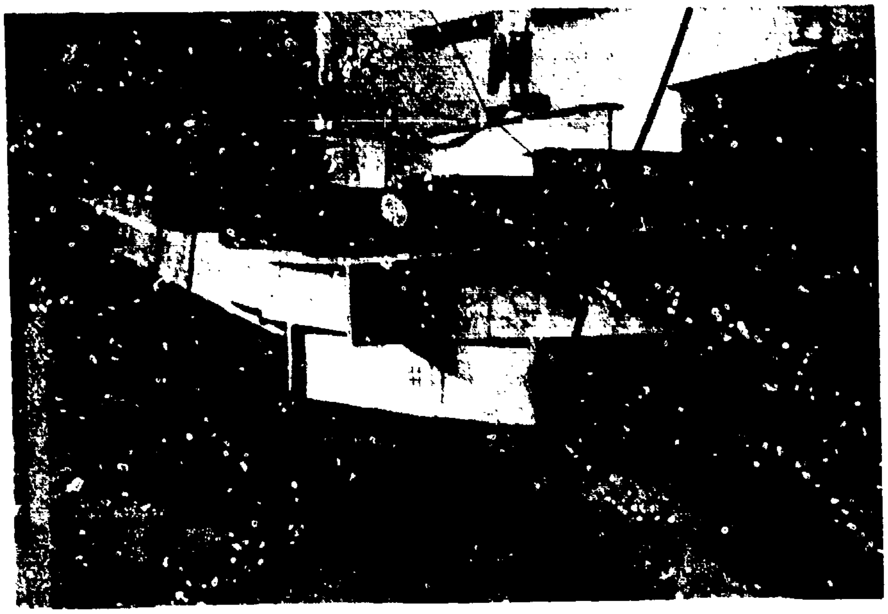

Fig. A-67. Post-Test Photographs Floor Panel 11.

DISTRIBUTION LIST

(one copy each unless otherwise specified)

Defense Civil Preparedness Agency
Research
Attn: Administrative Officer
Washington, D.C. 20301 (50)

Assistant Secretary of the Army (R&D)
Attn: Assistant for Research
Washington, D.C. 20301

Chief of Naval Research
Washington, D.C. 20360

Commander, Naval Supply Systems
Command (0421G)
Department of the Navy
Washington, D.C. 20376

Commander
Naval Facilities Engineering Command
Research and Development (Code 0322C)
Department of the Navy
Washington, D.C. 20390

Defense Documentation Center
Cameron Station
Alexandria, Virginia 22314 (12)

Civil Defense Research Project
Oak Ridge National Laboratory
Attn: Librarian
P.O. Box X
Oak Ridge, Tennessee 37830

Chief of Naval Personnel
(Code Pers M12)
Department of the Navy
Washington, D.C. 20360

U.S. Naval Civil Engineering
Laboratory
Attn: Document Library
Port Hueneme, California 93041

Director, Civil Effects Branch
Division of Biology and Medicine
Atomic Energy Commission
Attn: Mr. L.J. Deal
Washington, D.C. 20545

Air Force Special Weapons Laboratory
Attn: Technical Library
Kirtland Air Force Base
Albuquerque, New Mexico 87117

AFWL/Civil Engineering Division
Kirtland AFB, New Mexico 87117

Civil Engineering Center/AF/PRECET
Wright-Patterson AFB, Ohio 45433

Chief of Engineers
Department of the Army
Attn: ENGME-RD
Washington, D.C. 20314

Office of the Chief of Engineers
Department of the Army
Attn: Mr. Tomassoni
Washington, D.C. 20314

Director, U.S. Army Engineer
Waterways Experiment Station
P.O. Box 631
Vicksburg, Mississippi 39180

Director, U.S. Army Engineer
Waterways Experiment Station
P.O. Box 631
Attn: Nuclear Weapons Effects Branch
Vicksburg, Mississippi 39180

Director, Defense Nuclear Agency
Attn: Technical Library
Washington, D.C. 20305

Director, Defense Nuclear Agency
Attn: Mr. Tom Kennedy
Washington, D.C. 20305

Director, U.S. Army Ballistic
  Research Laboratories
Attn: Document Library
Aberdeen Proving Ground, MD 21005

Director, U.S. Army Ballistic
  Research Laboratories
Attn: Mr. William Taylor
Aberdeen Proving Ground, MD 21005

Agbabian Associates
250 N. Nash Street
El Segundo, California 90245

The Rand Corporation
1700 Main Street
Santa Monica, California 90401

The Dikewood Corporation
1009 Bradbury Drive, S.E.
University Research Park
Albuquerque, New Mexico 87106

Mr. J.W. Foss
Supervisor, Buildings Studies Group
Bell Telephone Laboratories, Inc.
Whippany Road
Whippany, New Jersey 07981

Dr. William J. Hall
University of Illinois
111 Talbot Laboratory
Urbana, Illinois 61801

Mr. Samuel Kramer, Chief
Office of Federal Building
  Technology
Center for Building Technology
National Bureau of Standards
Washington, D.C. 20234

Mr. Anatole Longinow
IIT Research Institute
10 West 35 th Street
Chicago, Illinois 60616

Dr. Stanley B. Martin
Stanford Research Institute
333 Ravenswood Avenue
Menlo Park, California 94025

Mr. H.L Murphy
Stanford Research Institute
333 Ravenswood Avenue
Menlo Park, California 94025

Research Triangle Institute
P.O. Box 12195
Research Triangle Park
North Carolina 27709

Mr. George N. Sisson
Research Directorate
RE(HV)
Defense Civil Preparedness Agency
Washington, D.C. 20301

Dr. Lewis V. Spencer
National Bureau of Standards
Room C313 - Building 245
Washington, D.C. 20234

Mr. Thomas E. Waterman
IIT Research Institute
Technology Institute
Technology Center
10 West 35th Street
Chicago, Illinois 60616

Stanford Research Institute
333 Ravenswood Avenue
Menlo Park, California 94025

Mr. Eugene F. Witt
Bell Telephone Laboratories, Inc.
Whippany Road
Whippany, New Jersey 07981

Mr. Milton D. Wright
Research Triangle Institute
P.O. Box 12194
Research Triangle Park
North Carolina 27709

Mr. Paul Zigman
Environmental Science Associates
1291 E. Hillsdale Blvd
Foster City, California 94404

Dr. F.J. Agardy
c/o URS Research Company
155 Bovet Road
San Mateo, California 94402

Mr. J.R. Janney
c/o Wiss, Janney, Elstner & Associates
330 Pfinston Road
Northbrook, Illinois 60062

Mr. Chuck Wilton
Scientific Service, Inc.
1536 Maple Street
Redwood City, California 94063

BLAST UPGRADING OF EXISTING STRUCTURES
SSI 7719-4
Scientific Service, Inc., Redwood City, California
January 1979 270 pages
Contract No. DCPA01-77-C-0205, Work Unit No. 1127G

UNCLASSIFIED

A major facet of preparedness is the upgrading of structures to provide shelter from nuclear weapons effects. This report describes some upgrading concepts, develops practical techniques for predicting structural failure, and verifies the failure prediction methodology by comparing the analysis with structural failure test data developed under this program and available in the literature.

The analyses and prediction techniques were applied to wood, steel, and concrete roof and floor specimens; and to static, dynamic, and combined loadings. The prediction methodology is founded on engineering mechanics, limit theory, and a statistical approach to failure analysis that enables realistic assessment of failure probabilities based on the combined effects of statistical variation in materials, structural elements and construction processes.

The upgrading techniques tested improved structural resistance to failure by factors of 2 to 30. The greatest improvement was developed by simple shoring. In a wood structure shored at the third points, the improvement was ten fold, and in the single shored reinforced concrete slab, the improvement was three fold. Failure loads of the concrete test specimens were predicted within 10% by the analytical techniques. Further, the concrete tests clearly indicate potential for achieving 30 to 40 psi shelter spaces in risk areas with standard concrete floor systems.

BLAST UPGRADING OF EXISTING STRUCTURES
SSI 7719-4
Scientific Service, Inc., Redwood City, California
January 1979 270 pages
Contract No. DCPA01-77-C-0205, Work Unit No. 1127G

UNCLASSIFIED

A major facet of preparedness is the upgrading of structures to provide shelter from nuclear weapons effects. This report describes some upgrading concepts, develops practical techniques for predicting structural failure, and verifies the failure prediction methodology by comparing the analysis with structural failure test data developed under this program and available in the literature.

The analyses and prediction techniques were applied to wood, steel, and concrete roof and floor specimens; and to static, dynamic, and combined loadings. The prediction methodology is founded on engineering mechanics, limit theory, and a statistical approach to failure analysis that enables realistic assessment of failure probabilities based on the combined effects of statistical variation in materials, structural elements and construction processes.

The upgrading techniques tested improved structural resistance to failure by factors of 2 to 30. The greatest improvement was developed by simple shoring. In a wood structure shored at the third points, the improvement was ten fold, and in the single shored reinforced concrete slab, the improvement was three fold. Failure loads of the concrete test specimens were predicted within 10% by the analytical techniques. Further, the concrete tests clearly indicate potential for achieving 30 to 40 psi shelter spaces in risk areas with standard concrete floor systems.

BLAST UPGRADING OF EXISTING STRUCTURES
SSI 7719-4
Scientific Service, Inc., Redwood City, California
January 1979 270 pages
Contract No. DCPA01-77-C-0205, Work Unit No. 1127G

UNCLASSIFIED

A major facet of preparedness is the upgrading of structures to provide shelter from nuclear weapons effects. This report describes some upgrading concepts, develops practical techniques for predicting structural failure, and verifies the failure prediction methodology by comparing the analysis with structural failure test data developed under this program and available in the literature.

The analyses and prediction techniques were applied to wood, steel, and concrete roof and floor specimens; and to static, dynamic, and combined loadings. The prediction methodology is founded on engineering mechanics, limit theory, and a statistical approach to failure analysis that enables realistic assessment of failure probabilities based on the combined effects of statistical variation in materials, structural elements and construction processes.

The upgrading techniques tested improved structural resistance to failure by factors of 2 to 30. The greatest improvement was developed by simple shoring. In a wood structure shored at the third points, the improvement was ten fold, and in the single shored reinforced concrete slab, the improvement was three fold. Failure loads of the concrete test specimens were predicted within 10% by the analytical techniques. Further, the concrete tests clearly indicate potential for achieving 30 to 40 psi shelter spaces in risk areas with standard concrete floor systems.

BLAST UPGRADING OF EXISTING STRUCTURES
SSI 7719-4
Scientific Service, Inc., Redwood City, California
January 1979 270 pages
Contract No. DCPA01-77-C-0205, Work Unit No. 1127G

UNCLASSIFIED

A major facet of preparedness is the upgrading of structures to provide shelter from nuclear weapons effects. This report describes some upgrading concepts, develops practical techniques for predicting structural failure, and verifies the failure prediction methodology by comparing the analysis with structural failure test data developed under this program and available in the literature.

The analyses and prediction techniques were applied to wood, steel, and concrete roof and floor specimens; and to static, dynamic, and combined loadings. The prediction methodology is founded on engineering mechanics, limit theory, and a statistical approach to failure analysis that enables realistic assessment of failure probabilities based on the combined effects of statistical variation in materials, structural elements and construction processes.

The upgrading techniques tested improved structural resistance to failure by factors of 2 to 30. The greatest improvement was developed by simple shoring. In a wood structure shored at the third points, the improvement was ten fold, and in the single shored reinforced concrete slab, the improvement was three fold. Failure loads of the concrete test specimens were predicted within 10% by the analytical techniques. Further, the concrete tests clearly indicate potential for achieving 30 to 40 psi shelter spaces in risk areas with standard concrete floor systems.